Advances in Clinical and Experimental Medicine

MONTHLY ISSN 1899-5276 (PRINT) ISSN 2451-2680 (ONLINE) www.advances.umed.wroc.pl

2019, Vol. 28, No. 12 (December)

Impact Factor (IF) – 1.227
Ministry of Science and Higher Education – 40 pts.
Index Copernicus (ICV) – 155.19 pts.

Wroclaw Medical University

Advances
in Clinical and Experimental
Medicine

Advances
in Clinical and Experimental Medicine

ISSN 1899-5276 (PRINT) ISSN 2451-2680 (ONLINE) www.advances.umed.wroc.pl

MONTHLY 2019
Vol. 28, No. 12
(December)

Advances in Clinical and Experimental Medicine is a peer-reviewed open access journal published by Wroclaw Medical University. Its abbreviated title is Adv Clin Exp Med. Journal publishes original papers and reviews encompassing all aspects of medicine, including molecular biology, biochemistry, genetics, biotechnology, and other areas. It is published monthly, one volume per year.

Editorial Office
ul. Marcinkowskiego 2–6
50-368 Wrocław, Poland
Tel.: +48 71 784 11 36
E-mail: redakcja@umed.wroc.pl

Publisher
Wroclaw Medical University
Wybrzeże L. Pasteura 1
50-367 Wrocław, Poland

Online edition is the original version of the journal

Editorial Policy

Advances in Clinical and Experimental Medicine (Adv Clin Exp Med) is an independent multidisciplinary forum for exchange of scientific and clinical information, publishing original research and news encompassing all aspects of medicine, including molecular biology, biochemistry, genetics, biotechnology and other areas. During the review process, the Editorial Board conforms to the "Uniform Requirements for Manuscripts Submitted to Biomedical Journals: Writing and Editing for Biomedical Publication" approved by the International Committee of Medical Journal Editors (www.ICMJE.org/). The journal publishes (in English only) original papers and reviews. Short works considered original, novel and significant are given priority. Experimental studies must include a statement that the experimental protocol and informed consent procedure were in compliance with the Helsinki Convention and were approved by an ethics committee.

For all subscription-related queries please contact our Editorial Office:
redakcja@umed.wroc.pl

For more information visit the journal's website:
www.advances.umed.wroc.pl

Pursuant to the ordinance No. 134/XV R/2017 of the Rector of Wroclaw Medical University (as of December 28, 2017) from January 1, 2018 authors are required to pay a fee amounting to 700 euros for each manuscript accepted for publication in the journal Advances in Clinical and Experimental Medicine.

„Podniesienie poziomu naukowego i poziomu umiędzynarodowienia wydawanych czasopism naukowych oraz upowszechniania informacji o wynikach badań naukowych lub prac rozwojowych – zadanie finansowane w ramach umowy 784/p-DUN/2017 ze środków Ministra Nauki i Szkolnictwa Wyższego przeznaczonych na działalność upowszechniającą naukę".

Indexed in: MEDLINE, Science Citation Index Expanded, Journal Citation Reports/Science Edition, Scopus,
EMBASE/Excerpta Medica, Ulrich's™ International Periodicals Directory, Index Copernicus

Typographic design: Monika Kolęda, Piotr Gil
DTP: Wydawnictwo UMW
Cover: Monika Kolęda
Printing and binding: EXDRUK

Advances
in Clinical and Experimental Medicine

MONTHLY 2019, Vol. 28, No. 12 (December)

ISSN 1899-5276 (PRINT)
ISSN 2451-2680 (ONLINE)
www.advances.umed.wroc.pl

Contents

Original papers

Reviews

Acknowledgements

We would like to express our gratitude to all reviewers who devoted their time and expertise to evaluate manuscripts in Advances in Clinical and Experimental Medicine. We sincerely appreciate all your hard work and dedication. It is due to your contribution that we can achieve the standard of excellence.

Editors

Reviewers in 2019:

Marcin Adamczak, Tomasz Adamowski, Wojciech Apoznański, Julia Bar, Alicja Bartkowska-Śniatkowska, Marzenna Bartoszewicz, Paweł Basta, Dariusz Biały, Rafał Białynicki-Birula, Anna Bizoń, Tomasz Błasiak, Krzysztof Błaszyk, Vladimir Bobek, Marek Bochnia, Krzysztof Boczar, Agnieszka Bojarska-Junak, Maria Borszewska-Kornacka, Anna Brzecka, Ligia Brzezińska-Wcisło, Shuyang Bu, Sławomir Budrewicz, Da-Zhong Cao, Limei Cao, Halina Cichoż-Lach, Roberto Cirocchi, Jacek Daroszewski, Bożena Dembowska-Bagińska, Katarzyna Derwich, Dorota Diakowska, Tadeusz Dobosz, Marzena Dominiak, Dorota Drożdż, Piotr Dzięgiel, Jerzy Florjański, Wojciech Fortuna, Marcin Frączek, Marian Gabryś, Jacek Gajek, Tomasz Gedrange, Hanna Gerber, Justyna Gil, Monika Gos, Grażyna Gościniak, Waldemar Goździk, Kinga Grzech-Leśniak, Bronisław Grzegorzewski, Teresa Grzelak, Yongqing Guo, Katarzyna Haczkiewicz-Leśniak, Nongyue He, Magdalena Hurkacz, Augustina Jankauskiene, Beata Jankowska-Polańska, Anna Janocha, Tomasz Kaczmarzyk, Katarzyna Kakareko, Dorota Kamińska, Paweł Karpiński, Bernarda Kazanowska, Jarosław Kaźmierczak, Radosław Kempiński, Bartosz Kempisty, Wojciech Kielan, Katarzyna Kiliś-Pstrusińska, Mariusz Klencki, Brygida Knysz, Tomasz Kolenda, Anna Kołodziej, Andrzej Konieczny, Tomasz Konopka, Wiesław Konopka, Marcin Kozakiewicz, Katarzyna Koziak, Dariusz Kozłowski, Wojciech Krajewski, Ewa Krzystanek, Eliza Kubicka, Julita Kulbacka, Ilona Kurnatowska, Mariusz Kusztal, Katarzyna Kuśmierska, Zhiqiang Liu, Elżbieta Łuczynska, Łukasz Łaczmański, Krystyna Łoboz-Grudzień, Katarzyna Madziarska, Joanna Maj, Agata Majos, Krzysztof Małyszczak, Mirosław Markiewicz, Andrzej Marszałek, Jolanta Masiak, Małgorzata Matusiewicz, Jacek Matys, Marcin Mikulewicz, Piotr Milejski, Błażej Misiak, Maciej Misiołek, Katarzyna Mizia-Stec, Agnieszka Młynarska, Piotr Morasiewicz, Witold Musiał, Jadwiga Nessler, Aleksandra Nowak, Michał Nowak, Marta Nowakowska-Kotas, Marta Obremska, Tomasz Ociepa, Mateusz Olbromski, Pawel Olczyk, Małgorzata Pańczyk-Tomaszewska, Konrad Pawełczyk, Edyta Pawlak-Adamska, Halina Pawlicka, Elżbieta Piątkowska, Jan Pietruski, Hanna Piotrowska-Kempisty, Andrzej Piotrowski, Agnieszka Piwowar, Anna Pokryszko-Dragan, Agnieszka Pollak, Elżbieta Poniewierka, Monika Prochorec-Sobieszek, Marcin Protasiewicz, Bartosz Puła, Krzysztof Reczuch, Paweł Reichert, Dylan Roi, Dagna Rukasz, Adam Rzechonek, Anna Sadakierska-Chudy, Marzena Samardakiewicz, Ela Sarnowska, Marek Sąsiadek, Paweł Siekierski, Teresa Sierpińska, Violetta Skrzypulec-Plinta, Jolanta Słowikowska-Hilczer, Agnieszka Sławuta, Jan Sobczyński, Ewa Straburzyńska-Migaj, Jan Styczyński, Pan Su, Aleksandra Szczepankiewicz, Tomasz Szczepański, Leszek Szenborn, Jacek Szepietowski, Andrzej Szuba, Tomasz Szydełko, Bartłomiej Szynglarewicz, Robert Śmigiel, Dariusz Timler, Krzysztof Tokarski, Anna Tomaszuk-Kazberuk, Grzegorz Trybek, Krzysztof Tupikowski, Anetta Undas, Wiktor Urbański, Lidia Usnarska-Zubkiewicz, Marek Ussowicz, Alberto Vazguez, Dominika Wcisło-Dziadecka, Jolanta Wierzba, Sławomir Wołczyński, Janusz Woytoń, Krzysztof Woźniak, Xun Xu, Shune Yang, Mieszko Zagrajek, Anna Zalewska, Katarzyna Zatońska, Jolanta Zawilska, Zygmunt Zdrojewicz, Jingyu Zhang, Qingfei Zheng, Jun Zhu Zhu, Marzena Zielińska, Anna Zimny, Krzysztof Zwierz, Danuta Zwolińska, Małgorzata Zwolińska-Wcisło, Dorota Zyśko

Obesity-induced insulin resistance via changes in the DNA methylation profile of insulin pathway genes

Małgorzata Małodobra-Mazur[1,A,C–F], Aneta Alama[1,B,C], Dorota Bednarska-Chabowska[2,B], Dorota Pawelka[3,B], Aneta Myszczyszyn[4,B], Tadeusz Dobosz[1,A]

[1] Molecular Techniques Unit, Department of Forensic Medicine, Wroclaw Medical University, Poland
[2] Department of Angiology, Hypertension and Diabetology, Wroclaw Medical University, Poland
[3] 1st Department and Clinic of General, Gastroenterological and Endocrinological Surgery, Wroclaw Medical University, Poland
[4] 1st Department and Clinic of Gynecology and Obstetrics, Wroclaw Medical University, Poland

A – research concept and design; B – collection and/or assembly of data; C – data analysis and interpretation; D – writing the article; E – critical revision of the article; F – final approval of the article

Advances in Clinical and Experimental Medicine, ISSN 1899–5276 (print), ISSN 2451–2680 (online) *Adv Clin Exp Med*. 2019;28(12):1599–1607

Address for correspondence
Małgorzata Małodobra-Mazur
E-mail: malgorzata.malodobra-mazur@umed.wroc.pl

Funding sources
Statutory activity – maintain the research capacity, Wroclaw Medical University, ST.A122.16.030

Conflict of interest
None declared

Received on April 23, 2019
Reviewed on May 7, 2019
Accepted on June 27, 2019

Published online on November 25, 2019

Abstract

Background. Obesity has been shown to play a key role in the development of insulin resistance (IR). Abundant data implicate obesity in DNA hypermethylation at global and site-specific levels, including genes regulating insulin sensitivity. Deregulation of epigenetic marks implicates gene expression and changes in cell metabolism.

Objectives. Our previous reports demonstrated that the strongest risk factor in the development of IR is BMI; accordingly, the objective of this study was to investigate the effect of obesity on DNA methylation and insulin sensitivity.

Material and methods. A study was carried out on lymphocytes (N-34) and visceral adipose tissue (VAT; N-35) of insulin-resistant subjects and healthy controls. Genetic material (DNA and RNA) was extracted from cells. Global and site-specific DNA methylation was analyzed with the use of restriction enzymes followed by real-time polymerase chain reaction (PCR). Gene expression was analyzed as relative mRNA level normalized to a housekeeping gene.

Results. Global DNA methylation increased in both types of tissue in obese and insulin-resistant individuals and correlated positively with IR. Two of the 3 investigated promoters of insulin pathway genes were hypermethylated, which correlated negatively with gene expression and positively with IR. The *DNMT3a* gene was upregulated in obese insulin-resistant individuals in both types of tissues and correlated positively with global DNA methylation.

Conclusions. DNA methylation profile changed depending on body mass index (BMI) and influenced glucose metabolism and insulin sensitivity in VAT.

Key words: obesity, insulin resistance, DNA methylation, insulin signaling pathway

Cite as
Małodobra-Mazur M, Alama A, Bednarska-Chabowska D, Pawelka D, Myszczyszyn A, Dobosz T. Obesity-induced insulin resistance via changes in the DNA methylation profile of insulin pathway genes. *Adv Clin Exp Med*. 2019;28(12):1599–1607. doi:10.17219/acem/110321

DOI
10.17219/acem/110321

Introduction

Overweight and obesity are among the leading problems of modern civilization. Obesity plays a key role in the development of insulin resistance (IR), leading to other metabolic disorders along with the consequent development of type 2 diabetes (T2D).[1] Insulin resistance is defined as a state in which a standard amount of insulin is insufficient to develop the physiological response of the cell, i.e., increasing glucose uptake, storage and oxidation.[2]

Population and family studies confirmed the genetic background of both obesity and IR, suggesting susceptible loci as one of the causes of both conditions. However, the impact of the genetic background on the induction of obesity and obesity-related disorders turned out to be relatively modest. In both conditions (obesity and IR), the key role is played by gene–environment interaction; accordingly, epigenetic changes in chromatin structures and gene function may be responsible for genetic susceptibility.[3] Epigenetic markers are believed to explain the link between gene–lifestyle interactions and the pathogenesis of numerous metabolic disorders and have even been proposed as specific biomarkers of metabolic disorders and possible therapeutic targets.[4]

Epigenetic modification is defined as the heritable and reversible modification of gene expression without changes in the DNA sequence, maintained over generations.[5] Epigenetic modifications include DNA methylation, the positioning of nucleosomes, and modifications in histones. All of these modifications are involved in establishing and maintaining the 2 major forms of chromosomal structure: the inactive heterochromatin and the transcriptionally active euchromatin.[6–10]

Indeed, abundant data implicate obesity in DNA hypermethylation at both global and site-specific levels, including genes regulating insulin sensitivity, such as *ADIPOQ*, *LPL*, or *PPARγ*.[11–13] Zheng et al. reported a link between obesity and methylation of mtDNA (mitochondrial DNA).[14] Analysis of DNA methylation carried out before and after weight loss revealed a differentially methylated region of the genome correlated with numerous genes, including 21 genes regulating insulin sensitivity.[15] A genome-wide DNA methylation study showed the differentially methylated profiles of numerous CpG sites in visceral adipose tissue (VAT) of insulin-resistant vs insulin-sensitive obese individuals.[16] On the other hand, caloric restriction was demonstrated to modulate chromatin function and increase genome stability mainly by reversing DNA methylation, which correlated with improving insulin sensitivity and whole-body weight reduction.[17,18]

The exact mechanism by means of which obesity influences insulin sensitivity via DNA methylation remains unclear. Some reports indicate the role of inflammatory cytokines.[19] Our report, along with others, demonstrated that the greatest risk factor in the development of IR is body mass index (BMI).[20,21] Accordingly, the effect of obesity on DNA methylation and its influence on insulin sensitivity was investigated in the present study.

Material and methods

The research protocols were approved by the ethical review board of Wroclaw Medical University, Poland (approval No. KB-556/2008).

Population characterization

All participants were informed about the purposes of the study and all subjects gave written consent for their participation in the study. The T2D patients were selected based on a diagnosis of T2D. Additionally, fasting glucose and insulin level, BMI, IR ratios (homeostatic model assessment of insulin resistance (HOMA-IR) or quantitative insulin sensitivity check index (QUICKI)), and lipid metabolism were assessed. Type 2 diabetic patients being treated with insulin were excluded. Lymphocytes (L) were collected from whole blood obtained from 13 types 2 diabetic patients (8 men and 5 women). The type 2 diabetic patients were inpatients of the Department of Angiology, Hypertension, and Diabetology, Wroclaw Medical University. Control lymphocytes were obtained from healthy subjects (11 men and 10 women) of similar age based on a fasting glucose level below 100 mg/dL, the absence of diabetes in family history, and, for women, no history of gestational diabetes.

Visceral adipose tissue biopsies were collected during abdominal surgeries from 9 patients with T2D (3 men and 6 women) and from 26 controls (17 men and 9 women) of similar age. Adipose tissue donors were inpatients of the First Department and Clinic of General, Gastroenterological, and Endocrinological Surgery, Wroclaw Medical University, and of the 1st Department and Clinic of Gynaecology and Obstetrics, Wroclaw Medical University. Controls were selected from patients without T2D undergoing abdominal surgery, based on a fasting glucose level below 100 mg/dL, the absence of diabetes in family history, and, for women, no history of gestational diabetes. The aims of abdominal surgeries were mainly cholecystectomy, surgical repair of an abdominal hernia, or gastric surgery.

Additional excluding criteria for all subjects were as follows: other systemic diseases such as sclerosis, thyroid dysfunction, hepatitis, chronic inflammatory or infective diseases, neurological diseases, and tumors. Heavy drinkers or those with a positive history were also excluded.

Body mass index and insulin resistance ratios

Body mass index was calculated as the patient's weight in kilograms divided by the square of their height in meters [kg/m^2]. Overweight was defined as BMI > 25 kg/m^2,

obesity as BMI > 30 kg/m^2. Insulin resistance rate was assessed using IR ratios calculated as follows[22]:
1) HOMA-IR [(glucose [mmol/L] * insulin [μU/mL])/22.5],
2) QUICKI [1/(log glucose [mg/dL] + log insulin [μU/mL])].

Insulin resistance was diagnosed on the basis of HOMA-IR > 2.5 and QUICKI < 0.321.

Lymphocyte preparation and visceral adipose tissue biopsy collection

Lymphocytes were isolated from whole blood collected on anticoagulant using centrifugation on Grandison L (AquaLab, Warszawa, Poland). Five milliliters of the whole blood was placed on 2 mL of Grandison L and centrifuged at 2,000 rpm for 20 min at 4°C. The lymphocytes ring was collected and washed twice with phosphate-buffered saline (PBS); the red blood cells were removed using a lysis buffer (HH_4Cl, $KHCO_3$, EDTA-Na_2). Lymphocytes were suspended in PBS and centrifuged at maximum speed for 2 min at 4°C; PBS was discarded and the pellet was frozen at –80°C pending analysis.

Visceral adipose tissue biopsies taken from patients undergoing abdominal surgery were immediately placed in RNA*Later* (Ambion), incubated at 4°C for 24 h. The RNA*Later* was discarded and the adipose tissue biopsies froze at –80°C pending analysis.

RNA extraction and gene expression study

RNA was isolated from peripheral lymphocytes using a mirVana miRNA Isolation Kit (Ambion, Carlsbad, USA) according to the manufacturers' protocol for total RNA. RNA from VAT biopsies was isolated using TriPure Isolation Reagent (Roche, Basel, Switzerland) according to the manufacturers' protocol. The tissues were homogenized using 2.0 mm zirconia beads (BioSpec Products, Inc., Bartlesville, USA). Following homogenization, the tissues were centrifuged at maximum speed for 2 min at 4°C in order to collect the fatty deposit at the top of the tube, which was then discarded. The homogenate was extracted with 200 μL of chloroform and centrifuged for 15 min at maximum speed at 4°C. The aqueous phase was collected and the RNA precipitated with 500 μL of isopropanol, centrifuged for 10 min at maximum speed, and washed with 1 mL of 70% ethanol. The RNA pellet was dissolved in RNase-Free Water and stored at –80°C.

Reverse transcription was performed with the use of a High-Capacity cDNA Reverse Transcription Kit (Applied Biosystems, Foster City, USA). *INSR, PIK3R1*, and *SLC2A4* gene expression levels were analyzed with real-time polymerase chain reaction (RT-PCR) with the use of TaqMan Gene Expression Assays (Applied Biosystems) and Real-Time PCR Universal Master Mix (Applied Biosystems). The following TaqMan Gene Expression Assays were used: *INSR*, Hs00961557_m1; *PIK3R1*, Hs00381459_m1; *SLC2A4*, Hs00168966_m1; *β-actin*, Hs00181698_m1.

The DNA methyltransferase (*DNMT1, DNMT3a*, and *DNMT3b*) expression rate was assessed via Real-Time PCR using a SensiFast SYBR Hi-ROX Kit (Bioline, London, UK). Primers were designed manually to span the exon-exon junction; specificity was checked using Primer-BLAST (NCBI); the secondary structures were analyzed using OligoAnalyzer 3.1 (IDT, Coralville, USA). Prior to Real-Time PCR, the efficiency of primers was analyzed using the standard curve method; specificity was checked based on the denaturation curve. The primer sequences used for measurements of *DNMT* expression are presented in Table 1.

Table 1. Primers sequences used for gene expression analysis (*DNMTs*) and promoters methylation analysis (insulin pathway genes)

Gene	Primer	Sequence (5′→3′)	Size (bp[1])	Location in gene	R^2
DNMT1	forward	AGGCGGCTCAAAGATTTG	57	1-2 exon	97.5%
	reverse	CTCCTTCACACATTCCTT			
DNMT3a	forward	CAGGATAGCCAAGTTCAGC	120	17-18 exon	97.0%
	reverse	GTGCACCATAAGATGTCCTC			
DNMT3b	forward	ATGCTCTGGAGAAAGCTAG	94	8-9 exon	95.8%
	reverse	CACTCCAACATGGGCTTCA			
β-actin	forward	GAGAAGATGACCCAGATCA	72	2-3 exon	99.9%
	reverse	TAGCACAGCCTGGATAGCAA			
PIK3R1	forward	AGACACTCGGATTAGAGACG	135	295-299 upstream TSS[2]	97.6%
	reverse	AGTGCTCTGGCTCTACACG			
INSR	forward	GGTAGAGAAAGGATCTGTG	73	628-632 upstream TSS	99.2%
	reverse	GAGTCTCCTCCAGTTTCAG			
SLC2A4	forward	TGAAAGACAGGACCAAGCAG	57	646-650 upstream TSS	97.4%
	reverse	CAGGAAATTCCGTTCCCAC			

[1]base pairs; [2]transcription start site; [3]efficiency assessed based on standard curve method.

DNA extraction and global and site-specific DNA methylation

The VAT was dissected and digested with Collagenase A (Roche) overnight at 37°C. DNA was then extracted with the use of a High Pure PCR Template Preparation Kit (Roche). DNA from lymphocytes was extracted using the same kit. The DNA concentration was assessed using NanoDrop ND1000 (Thermo Fisher Scientific, Waltham, USA).

Global DNA methylation in VAT and lymphocytes was measured using an EpiJET DNA Methylation Analysis Kit (Thermo Fisher Scientific) according to the manufacturers' protocol. Briefly, genomic DNA (500 ng from VAT and 200 ng from lymphocytes) was digested with 2 restriction enzymes: *HpaII* and *MspI*. Both enzymes recognized the same DNA sequence (5′-CCGG-3′); however, when the internal C within the recognized sequence was methylated, cleavage with *HpaII* was blocked, although unaffected with *MspI*. After digestion, the DNA treated with *HpaII*, *MspI*, and non-digested DNA was separated using 1.2% agarose gel stained with ethidium bromide. The bands of DNA digested with *HpaII* and non-digested DNA were analyzed using ImageJ (National Institutes of Health, Bethesda, USA). Global methylation was calculated as a percentage of non-digested DNA. Site-specific DNA methylation was analyzed using an EpiJET DNA Methylation Analysis Kit (Thermo Scientific). Real-time PCR was run following the digestion of enzymes using a SensiFast SYBR Hi-ROX Kit (Bioline). Primers were designed manually to hybridize within promoters of investigated genes flanking the recognition sequence (5′-CCGG-3′). Designed primers were analyzed according to specificity (Primer-BLAST, NCBI) and secondary structure formation (OligoAnalyzer 3.1; IDT). A CpG islands prediction was done using MethPrimer with CG content > 60% and an Obs/Exp ratio > 0.6. Ct values were used to calculate the promoter methylation rate using the formula

$$\% \text{ of } 5 - mC = 100/(1+E)^{Cq2-Cq1}$$

[E – PCR efficiency; Cq1 – threshold cycle of undigested DNA; Cq2 – threshold cycle of *HpaII*-digested DNA]

The sequences of primers used for promoters methylation analysis are presented in Table 1.

Cytokine levels measurements

Two inflammatory cytokine levels were measured in the plasma of the investigated subjects using commercial enzyme-linked immunosorbent assay (ELISA) kits: the PeliKine human IL-6 ELISA and PeliKine human TNF-alpha ELISA Kits (Sanquin, Amsterdam, the Netherlands).

Statistical analyses

Statistical analyses were performed with the use of STATISTICA (StatSoft, Inc., Tulsa, USA). Statistical significance was set at $p < 0.05$. Differences between the clinical features of tested groups were assessed using Student's t-test. Correlation between gene expression level and biochemical parameters was done using Pearson's coefficient of correlation. The power of the study was assessed using STATISTICA. The gene expression level was analyzed as relative gene expression normalized to *β-actin* using the ΔΔCt quantification model.[23]

Results

Characterization of study groups

The characterization of enrolled patients was carried out according to the type of biological material (patients from whom lymphocytes or adipose tissues samples were collected). Type 2 diabetic patients in both analyses were characterized by increased BMI and glucose and insulin levels, as well as by IR resistance ratios (HOMA-IR and QUICKI). Moreover, an increase in adiponectin and HDL levels were observed in control patients. However, when dividing enrolled patients according to BMI as lean (<25 kg/m^2) or obese (≥25 kg/m^2), in addition to the above changes, increased TG and IL-6 levels were observed, while HDL and adiponectin levels were decreased in obese subjects. A detailed characterization of the study cohort is presented in Table 2.

Global DNA methylation

Global DNA methylation was measured in the L and VAT of healthy subjects and T2D patients over a wide range of BMI. Global DNA methylation was increased in both types of tissue in T2D patients (VAT, $p = 0.1940$; L, $p = 0.0297$; Fig. 1A and 1F, respectively). The increase in VAT was not statistically significant. However, when categorizing enrolled subjects according to BMI (lean <25 kg/m^2, or overweight and obese ≥25 kg/m^2), a greater difference in global DNA methylation was observed (VAT, $p = 0.0026$; L, $p = 0.0001$; Fig. 1B and 1G, respectively), with higher global DNA methylation in overweight and obese subjects. What is more, a strong positive correlation was observed between global DNA methylation values measured in both types of tissue and BMI (VAT, $R = 0.53$, $p = 0.0143$; L, $R = 0.54$, $p = 0.0122$; Fig. 1C and 1H, respectively). These results suggest the strong influence of BMI on global DNA methylation.

Next, we were interested if global DNA methylation is changed between insulin-resistant vs insulin sensitive patients, Indeed, the global DNA methylation rate correlated positively with IR measured based on 2 IR ratios, HOMA-IR and QUICKI. A strong positive correlation was observed between global DNA methylation and HOMA-IR measured in VAT ($R = 0.61$, $p = 0.0048$, Fig. 1D) and in L ($R = 0.51$, $p = 0.0183$, Fig. 1I). On the other hand,

Table 2. Characterization of clinical and biochemical features enrolled between (A – visceral adipose tissue; B – lymphocytes)

A

Biochemical feature	Control group (mean ±SD)	T2DM (mean ±SD)	p-value (t-test)	Lean (<25 kg/m^2) (mean ±SD)	Obese (≥25 kg/m^2) (mean ±SD)	p-value (t-test)
Sex [F/M][1]	9/17	6/3	–	6/8	9/12	–
Age [years]	47 ±15	52 ±10	NS	47 ±17	51 ±10	NS
BMI [kg/m^2]	**24.4 ±5.1**	**31.8 ±6.2**	**0.0012**	**22.5 ±2.4**	**30.2 ±3.4**	**<0.0000**
Glucose [mg/dL]	**95 ±14**	**146 ±33**	**<0.0001**	105 ±31	122 ±64	NS
Insulin [uU/mL]	**7.2 ±8**	**25.7 ±22**	**0.0295**	**10 ±19**	**42.5 ±27**	**0.0368**
CHOL [mg/dL]	173 ±38	169 ±81	NS	209 ±22	222 ±32	NS
TG [mg/dL]	160 ±48	174 ±59	NS	**104 ±50**	**228 ±103**	**0.0126**
LDL [mg/dL]	120 ±33	81 ±40	NS	122 ±14	146 ±30	NS
HDL [mg/dL]	46 ±11	41 ±11	NS	**62.5 ±26**	**43.3 ±12**	**0.0382**
HOMA-IR	**1.6 ±1.8**	**8.9 ±11.7**	**0.0236**	**1.03 ±1**	**5.05 ±7**	**0.0500**
QIUCKI	**0.382 ±0.04**	**0.318 ±0.03**	**0.0019**	**0.399 ±0.04**	**0.336 ±0.05**	**0.0029**
IL-6 [pg/uL]	18.18 ±10.5	22.23 ±16	NS	**19.9 ±6.7**	**29.5 ±27**	**0.0426**
TNF-α [pg/uL]	2.5 ±0.67	1.7 ±1.15	NS	2.4 ±0.8	2.11 ±0.99	NS
Adiponectin [pg/uL]	**16.5 ±7.3**	**11.5 ±6.9**	**0.0299**	**16.2 ±5.3**	**10.5 ±3.6**	**0.0276**

B

Biochemical feature	Control group (mean ±SD)	T2DM (mean ±SD)	p-value (t-test)	Lean (<25 kg/m^2) (mean ±SD)	Obese (≥25 kg/m^2) (mean ±SD)	p-value (t-test)
Sex [F/M]	10/11	5/8	–	6/5	11/12	–
Age [years]	50 ±7	50 ±6	NS	46 ±3.7	51 ±6.8	NS
BMI [kg/m^2]	**27.6 ±3.8**	**31.7 ±3.4**	**0.0261**	**23 ±1.1**	**31 ±3.2**	**0.0008**
Glucose [mg/dL]	**89 ±7.9**	**182 ±70**	**0.0019**	92 ±6.8	151 ±72	NS
Insulin [uU/mL]	**4.0 ±0.8**	**8.2 ±2.3**	**0.0009**	5.3 ±2.8	6,22 ±3.15	NS
CHOL [mg/dL]	200 ±38	190 ±49	NS	214 ±62	222 ±112	NS
TG [mg/dL]	111 ±45	202 ±130	NS	65 ±35	175 ±112	NS
LDL [mg/dL]	143 ±42	120 ±54	NS	114 ±57	135 ±48	NS
HDL [mg/dL]	**68 ±18**	**43 ±7**	**0.0009**	**86 ±12**	**49 ±13**	**0.0003**
HOMA-IR	**1.3 ±1.4**	**3.6 ±1.3**	**0.0012**	1.9 ±1.99	2.5 ±1.82	NS
QIUCKI	**0.395 ±0.04**	**0.318 ±0.01**	**<0.0000**	0.372 ±0.04	0.346 ±0.05	NS
IL-6 [pg/uL]	16.2 ±5.6	22.2 ±3.1	NS	8.0 ±1.6	16.1 ±3.1	NS
TNF-α [pg/uL]	2.8 ±0.35	3.6 ±0.6	NS	2.7 ±0.3	2.7 ±0.6	NS
Adiponectin [pg/uL]	11.4 ±5	11.5 ±4.9	NS	13.9 ±9.4	12.8 ±3.8	NS

F – female; M – male; BMI – body mass index; CHOL – cholesterol; TG – triglicerydes; LDL – low-density lipoprotein; HDL – high-density lipoprotein; HOMA-IR – homeostatic insulin resistance; QIUCKI – quantitative insulin sensitivity check index; IL-6 – interleukin 6; TNF-α – tumor necrosis factor α; NS – statistically not important; bold text – statistically significant.

a negative correlation was observed between global DNA methylation and QUICKI measured in VAT (R = −0.41, p = 0.0475, Fig. 1E) and in L (R = −0.51, p = 0.0191, Fig. 1J).

DNA methyltransferase expression

Faced with differentially methylated DNA within the investigated groups, the expression rate of 3 main DNA methyltransferases was analyzed in both types of tissue in order to determine which DNA methyltransferase is responsible for various profiles of global DNA methylation. In both types of tissue, *DNMT3a* was upregulated in obese T2D patients compared to controls, with no differences in the expression rate of the other 2 methyltransferases, *DNMT1* and *DNMT3b*. In VAT the expression rate of *DMNT3a* was 1.92 times higher (p = 0.0204) in T2D patients compared to controls (Fig. 2A). In L the expression rate of *DNMT3a* was 1.59 times higher (p = 0.0052)

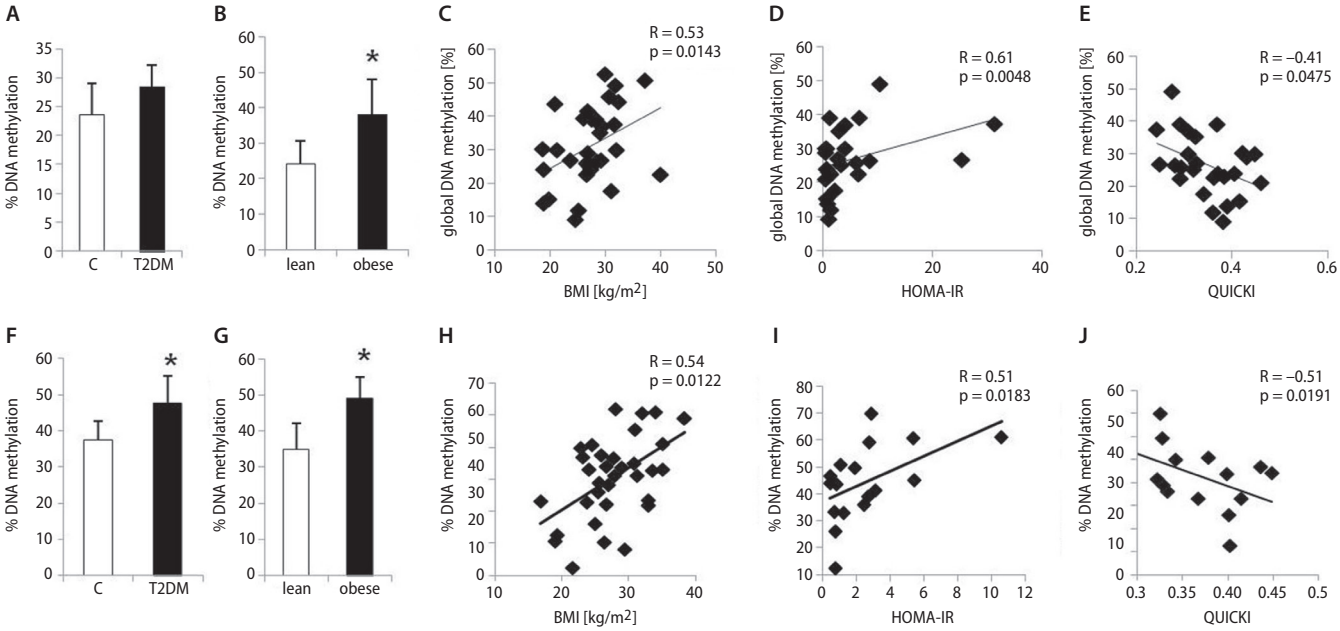

Fig. 1. Effect of global DNA methylation on insulin sensitivity

Comparison of global DNA methylation in VAT (A and B) and in L (F and G) between T2D and controls and between lean and obese patients. Correlation between global DNA methylation in VAT and BMI (C), HOMA-IR (D) and QUICKI (E); global DNA methylation in L and BMI (H), HOMA-IR (I) and QUICKI (J).

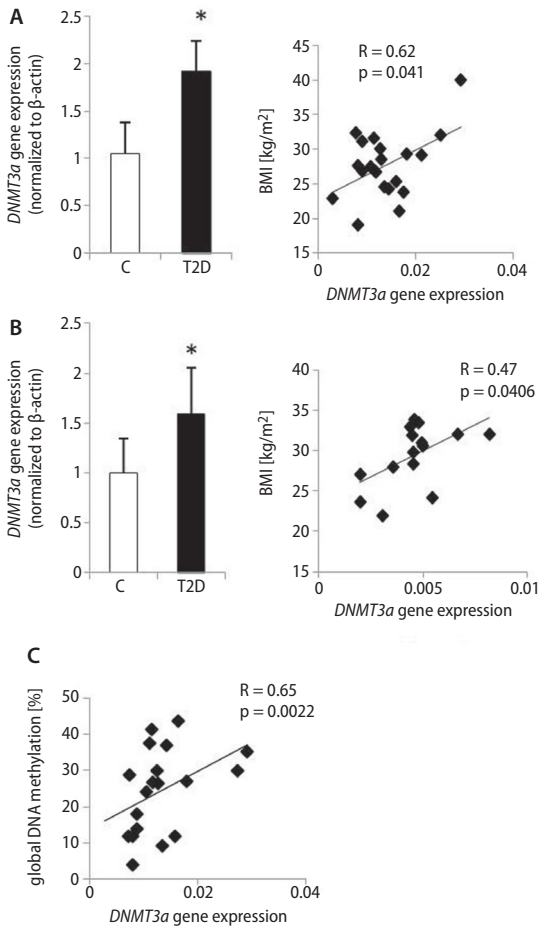

Fig. 2. The expression rate of *DNMT3a* methyltransferase

The expression of *DNMT3a* gene in VAT (A) and in L (B) of enrolled patients and its correlation with BMI. Correlation between expression of *DNMT3a* gene and global DNA methylation observed in VAT (C).

in T2D patients compared to controls (Fig. 2B), again with no changes detected in the gene expression of the other 2 DNA methyltransferases. Moreover, *DNMT3a* showed a positive correlation with BMI within investigated individuals in both types of tissue (VAT, R = 0.62, p = 0.0041, Fig. 2A; L, R = 0.47, p = 0.0406, Fig. 2B). Furthermore, the *DNMT3a* expression rate correlated positively with global DNA methylation in VAT (R = 0.65, p = 0.0022, Fig. 2C); however, a relatively weak positive correlation was observed in L.

In order to evaluate the influence of increased *DNMT3a* on insulin sensitivity, we investigated the correlation the mRNA level of *DNMT3a* measured in both VAT and L with IR ratios. The mRNA level of *DNMT3a* correlated positively with HOMA-IR (VAT, R = 0.59; L, R = 0.52) and negatively with QUICKI (VAT, R = −0.48; L, R = −0.46); however, correlations were close to being significant with the p-value slightly exceeding the limit value of 0.05. No correlation between IR ratios and other *DNMTs* were observed.

These results link obesity with overexpression of *DNMT3a* as a possible reason for global DNA hypermethylation in obesity and a possible reason for IR development.

Insulin pathway gene expression and promoter methylation

Global DNA methylation was shown to strongly correlate with IR in both types of tissues; accordingly, the gene expression rate and promoter methylation status of 3 main genes belonging to the insulin signaling pathway were investigated, namely the *INSR* (insulin receptor),

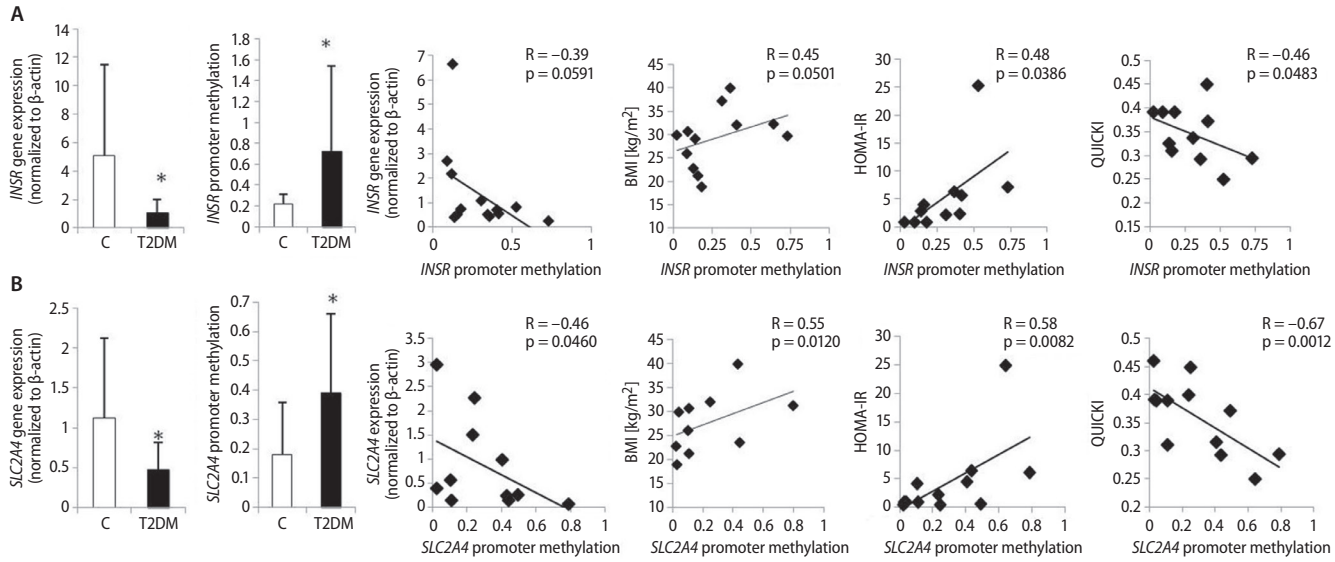

Fig. 3. Promoter methylation of insulin pathway genes

The differences in expression and methylation profile of promoters of 2 genes belonging to insulin signaling pathway: *INSR* gene (A) ad *SLC2A4* gene (B) in VAT along with correlation of promoter methylation with gene expression, BMI and IR.

PIK3R1 (phosphoinositide-3-kinase regulatory subunit 1), and *SLC2A4* genes (solute carrier family 2, facilitated glucose transporter, member 4). First, the gene expression rate was analyzed in both the L and VAT of the enrolled individuals. There was no difference in the expression rate of analyzed genes in L between the studied groups. *SLC2A4* gene expression was slightly reduced and *PIK3R1* gene expression slightly increased in T2D patients, though without statistical significance. Nor were there any statistically significant differences in promoter methylation between study groups of analyzed genes in L, although the global DNA methylation rate in L was increased in T2D patients.

All 3 examined genes displayed a reduced expression rate in the VAT of T2D patients when compared to control subjects.

The *INSR* gene was downregulated in the VAT of T2D patients (p = 0.0355, Fig. 3A); on the other hand, the promoter methylation rate of this gene was increased (p = 0.0206). What is more, the promoter methylation rate negatively correlated with *INSR* gene expression (R = −0.39, p = 0.0591, Fig. 3A); however without statistical significance. An interesting positive correlation was observed between *INSR* promoter methylation and the BMI of the investigated subjects (R = 0.45, p = 0.05, Fig. 3A). Subjects with BMIs under 30 kg/m^2 were characterized by a relatively low *INSR* promoter methylation rate, as opposed to subjects with BMIs over 30 kg/m^2, characterized by a significantly increased *INSR* promoter methylation rate. Furthermore, *INSR* promoter methylation correlated with IR in investigated individuals. A positive correlation between the methylation of *INSR* promoter and HOMA-IR (R = 0.48, p = 0.0386, Fig. 3A) and a negative correlation between the methylation of *INSR* promoter and QUICKI (R = −0.46, p = 0.0483, Fig. 3A) were observed.

The *PIK3R1* gene also showed decreased expression rate in T2D patients when compared to healthy individuals (p = 0.0199), along with a slightly increased rate of *PIK3R1* promoter methylation measured in this group (p = 0.0581). However, no correlation was observed between *PIK3R1* promoter methylation and gene expression, BMI or IR.

The *SLC2A4* gene encoding glucose transporter type 4 (GLUT4) was downregulated (p = 0.0569, Fig. 3B) and *SLC2A4* promoter methylation upregulated (p = 0.0158) in the VAT of T2D patients compared to controls. Furthermore, the expression rate was negatively correlated with promoter methylation (R = −0.46, p = 0.0460, Fig. 3B). Interestingly, the promoter methylation of the *SLC2A4* gene positively correlated with BMI within investigated individuals (R = 0.55, p = 0.012, Fig. 3B). What is more, *SLC2A4* promoter methylation displayed a positive correlation with HOMA-IR (R = 0.58, p = 0.0082, Fig. 3B) and a negative correlation with QUICKI (R = −0.67, p = 0.0012, Fig. 3B) in investigated subjects.

Discussion

In the present study, we investigated the influence of obesity on IR development through epigenetic mechanisms. We have shown that global DNA methylation increased in cases of obesity and correlated positively with IR. It was found that in obese individuals the expression of *DNMT3a* was increased, which could be the reason for the subsequent increase in global and site-specific DNA methylation, including promoters of main genes belonging to the insulin pathway (*INSR, SLC2A4*).

The global DNA methylation rate is tissue-specific; therefore, 2 different types of tissue were investigated in the present study in order to better assess their association with obesity and IR. Peripheral lymphocytes have been widely studied by many researchers, with various outcomes. In some studies, there was no association between BMI and global DNA methylation[24–26], while others showed results contradictory to ours, in which global DNA methylation negatively correlated with BMI.[27] In the present study, we showed increased global DNA methylation in the lymphocytes of obese individuals, which corresponds to other studies.[28,29] What is more, global DNA methylation measured in lymphocytes showed associations with IR (assessed based on HOMA-IR and QUICKI). Similar results were obtained by others who showed a positive association between global DNA methylation and fasting glucose levels[30,31] or HOMA-IR[32] in those cells. Although a positive correlation between global DNA methylation and IR has been shown in the present study, no significant changes, either in gene expression or in the promoter methylation profile of insulin pathway genes, were observed. Further research needs to be done in order to draw specific conclusions, especially on a larger number of investigated subjects. It is also possible that different patterns of DNA methylation in insulin-resistant subjects influence other pathways or genes important for proper lymphocytes metabolisms, like cytokine or inflammatory markers secretion, which might as well influence insulin sensitivity. Indeed, an inverse relationship between methylation of leptin and adiponectin promoters in peripheral blood samples and IR was observed by García-Cardona et al.[33] Similarly, a GWAS study performed by Su et al.[34] also showed a correlation between the methylation status of the lymphocyte antigen 86 (LY86) gene and obesity, IR, and inflammatory markers, which provides further evidence of the influence of epigenetic regulation on IR and obesity-related disorders.

Peripheral blood lymphocytes constitute relatively good study material with respect to their easy collection and isolation methods; however, the proper cells for the evaluation of IR are adipocytes or skeletal muscles, because these tissues utilize the greatest amount of glucose provided along with food in an insulin-dependent manner. Therefore, global DNA methylation and associations with IR were investigated in VAT samples collected from patients undergoing abdominal surgery. Similarly to lymphocytes, positive associations between DNA methylation, BMI and IR were shown. We have shown that, in both types of investigated tissue, global DNA methylation differed between lean and obese subjects, despite a relatively low number of investigated subjects. Furthermore, we observed a positive association between global DNA methylation and IR among enrolled subjects. The implication of epigenetic regulation in IR pathogenesis was also confirmed when analyzing the *DNMT3a* expression rate within enrolled individuals. *DNMT3a* correlated positively with BMI and IR ratios. The correlation with IR ratios (HOMA-IR and QUICKI) did not reach significance; however, the overall relationship was noticed. For sure, by increasing the number of investigated subjects we would obtain statistical significance.

Taking everything together, obesity influences global DNA methylation level in VAT and in lymphocytes by stimulating the expression rate of DNA methyltransferases, mainly *DNMT3a*. We have concluded that if there is a positive correlation between DNA methylation and IR, some insulin pathway genes must be epigenetically regulated by promoter methylation. Indeed, 2 of the 3 investigated genes were shown to be differentially methylated at the promoter sites; moreover, the methylation status correlated positively with BMI and IR ratios and negatively with gene expression. Other researchers, such as Barajas-Olmos et al.,[35] provided further evidence that an altered DNA methylation rate of numerous genes (mainly glucose metabolism, lipid metabolism and cell-cycle regulation genes) is a mechanism that may be involved in the pathogenesis of obesity-related disorders, including T2D.

To the best of the author's knowledge, there are only a few reports concerning the epigenetic regulation of insulin pathway genes. Jones et al.[36] demonstrated a decreased *INSR* expression rate in the subcutaneous adipose tissue of women with the influence of obesity, not of PCOS, on the expression of the *INSR* gene. The *IRS1* and *SLC2A4* genes exhibited a decreased expression rate, which correlated with an increase in promoter methylation in the skeletal muscle of adult rats which had been undernourished during the fetal stage.[37] The greatest difference in gene expression and promoter methylation of both genes was seen in the 20th week of postnatal life, which correlated with increased body weight and IR in those rats.

The relationship between DNA methylation and IR has been shown by other researchers, who described promoter methylation of other genes regulating IR, such as the adiponectin[19], leptin and *PPARγ* genes, etc.[11–13] The potential mechanism regulating the methylation status of the adiponectin gene was related to increased expression of *DNMT1*, stimulated by TNF-α.[19] In our study, we have shown altered expression of *DNMT3a* in both types of tissues, as the potential reason for differently methylated global and site-specific DNA methylation, especially insulin signaling pathway genes. *DNMT3a* was previously implicated with obesity-induced IR development, as *Dnmt3a* knock-out mice are protected from diet-induced IR.[38] Our results confirm the implication of *DNMT3a* with epigenetic regulation of IR in humans. There was no association between 2 other DNA methyltransferases (*DNMT1* and *DNMT3b*) and insulin resistance; therefore, *DNMT3a* was selectively shown to play a key role in obesity-related IR pathogenesis.

Summarizing all of the data described above (ours and others[19,11–13,33–35]), we suggest that IR is epigenetically regulated and thus potentially could be reversed. However, this statement has not been confirmed to date.

ORCID iDs

Małgorzata Małodobra-Mazur https://orcid.org/0000-0002-9864-5928
Aneta Alama https://orcid.org/0000-0001-8428-1089
Dorota Bednarska-Chabowska https://orcid.org/0000-0002-8920-7571
Dorota Pawelka https://orcid.org/0000-0003-2077-7629
Aneta Myszczyszyn https://orcid.org/0000-0003-3138-7554
Tadeusz Dobosz https://orcid.org/0000-0003-0413-9109

References

1. Nguyen DM, El-Serag HB. The epidemiology of obesity. *Gastroenterol Clin North Am.* 2010;39(1):1–7.
2. Brady MJ, Saltiel AR. Closing in on the cause of insulin resistance and type 2 diabetes. *J Clin Invest* 1999;104(6):675–676.
3. Drong AW, Lindgren CM, McCarthy MI. The genetic and epigenetic basis of type 2 diabetes and obesity. *Clin Pharmacol Ther.* 2012;92(6): 234–237.
4. Hamilton JP. Epigenetics: Principles and practice. *Dig Dis*. 2011;29(2): 130–135.
5. Londono Gentile T, Lu C, Lodato PM, et al. DNMT1 is regulated by ATP-citrate lyase and maintains methylation patterns during adipocyte differentiation. *Mol Cell Biol*. 2013;33(19):3864–3878.
6. Deaton AM, Bird A. CpG islands and the regulation of transcription. *Genes Dev.* 2011;25(10):1010–1022.
7. Zhang Q, Ramlee MK, Brunmeir R, Villanueva CJ, Halperin D, Xu F. Dynamic and distinct histone modifications modulate the expression of key adipogenesis regulatory genes. *Cell Cycle.* 2012;11(23):4310–4322.
8. Anamika K, Krebs AR, Thompson J, Poch O, Devys D, Tora L. Lessons from genome-wide studies: An integrated definition of the coactivator function of histone acetyl transferases. *Epigenetics Chromatin.* 2010;3(1):18–28.
9. Riccio A. New endogenous regulators of class I histone deacetylases. *Sci Signal.* 2010;3(103):pe1. doi:10.1126/scisignal.3103pe1
10. Gregoretti IV, Lee YM, Goodson HV. Molecular evolution of the histone deacetylase family: Functional implications of phylogenetic analysis. *J Mol Biol*. 2004;338(1):17–31.
11. Pietiläinen KH, Ismail K, Järvinen E, et al. DNA methylation and gene expression patterns in adipose tissue differ significantly within young adult monozygotic BMI-discordant twin pairs. *Int J Obes (Lond).* 2016;40(4):654–661.
12. Arner P, Sinha I, Thorell A, Rydén M, Dahlman-Wright K, Dahlman I. The epigenetic signature of subcutaneous fat cells is linked to altered expression of genes implicated in lipid metabolism in obese women. *Clin Epigenetics*. 2015;7:93.
13. Drogan D, Boeing H, Janke J, et al. Regional distribution of body fat in relation to DNA methylation within the LPL, ADIPOQ and PPARγ promoters in subcutaneous adipose tissue. *Nutr Diabetes.* 2015;5(7):e168.
14. Zheng LD, Linarelli LE, Liu L, et al. Insulin resistance is associated with epigenetic and genetic regulation of mitochondrial DNA in obese humans. *Clin Epigenetics*. 2015;7:60.
15. Benton MC, Johnstone A, Eccles D, et al. An analysis of DNA methylation in human adipose tissue reveals differential modification of obesity genes before and after gastric bypass and weight loss. *Genome Biol*. 2015;16:8.
16. Crujeiras AB, Diaz-Lagares A, Moreno-Navarrete JM, et al. Genome-wide DNA methylation pattern in visceral adipose tissue differentiates insulin-resistant from insulin-sensitive obese subjects. *Transl Res.* 2016;178:13–24.e5.
17. Vaquero A, Reinberg D. Calorie restriction and the exercise of chromatin. *Genes Dev.* 2009;23(16):1849–1869.
18. Wheatley KE, Nogueira LM, Perkins SN, Hursting SD. Differential effects of calorie restriction and exercise on the adipose transcriptome in diet-induced obese mice. *J Obes.* 2011;2011:265417.
19. Kim AY, Park YJ, Pan X, et al. Obesity-induced DNA hypermethylation of the adiponectin gene mediates insulin resistance. *Nat Commun*. 2015;3:585.
20. Malodobra M, Pilecka A, Gworys B, Adamiec R. Single nucleotide polymorphisms within functional regions of genes implicated in insulin action and association with the insulin resistant phenotype. *Mol Cell Biochem.* 2011;349(1–2):187–193.
21. Kelley DE, Thaete FL, Troost F, Huwe T, Goodpaster BH. Subdivision of subcutaneous abdominal adipose tissue and insulin resistance. *Am J Physiol Endocrinol Metab.* 2000;278(5):941–948.
22. Ruano M, Silvestre V, Castro R, et al. HOMA, QUICKI and MFfm to measure insulin resistance in morbid obesity. *Obes Surg.* 2006;16(5):549–553.
23. Pfaffl MW. A new mathematical model for relative quantification in real-time RT-PCR. *Nucleic Acids Res.* 2001;29(9):2002–2007.
24. Zhang FF, Cardarelli R, Carroll J, et al. Significant differences in global genomic DNA methylation by gender and race/ethnicity in peripheral blood. *Epigenetics.* 2011;6(5):623–629.
25. Gomes MVM, Toffoli LV, Arruda DW, et al. Age-related changes in the global DNA methylation profile of leucocytes are linked to nutrition but are not associated with the MTHRF C677T genotype or to functional capacities. *PLoS One.* 2012;7(12):52570.
26. Ulrich CM, Toriola AT, Koepl LM, et al. Metabolic, hormonal and immunological association with global DNA methylation among postmenopausal women. *Epigenetics.* 2012;7(9):1020–1028.
27. Zhang F, Santell R, Wolff M. White blood cell global methylation and IL-6 promoter methylation in association with diet and lifestyle risk factors in a cancer-free population. *Epigenetics.* 2012;7(6):606–614.
28. Kim M, Long TI, Arakawa K, Wang R, Yu MC, Laird PW. DNA methylation as a biomarker for cardiovascular disease risk. *PLoS One.* 2010; 5(3):9692.
29. Cash HL, McGarvey ST, Houseman EA, et al. Cardiovascular disease risk factors and DNA methylation at the LINE-1 repeat region in peripheral blood from Samoan Islanders. *Epigenetics*. 2011;6(10):1257–1264.
30. Oggiioni C, Lara J, Wells JCK, Soroka K, Siervo M. Shifts in population dietary patterns and physical inactivity as determinants of global trends in the prevalence of diabetes: An ecological analysis. *Nutr Metab Cardiovasc Des*. 2014;24(10):1105–1111.
31. Uusitupa M. Gene-diet interaction in relation to the prevention of obesity and type 2 diabetes: Evidence from the Finnish Diabetes Prevention Study. *Nutr Metab Cardiovasc Dis.* 2005;15(3):225–233.
32. Bernstein BE, Stamatoyannopoulos JA, Costello JF, et al. The NIH roadmap epigenomics mapping consortium. *Nat Biotechnol.* 2010; 28(10):1045–1048.
33. García-Cardona MC, Huang F, García-Vivas JM, et al. DNA methylation of leptin and adiponectin promoters in children is reduced by the combined presence of obesity and insulin resistance. *Int J Obes (Lond).* 2014;38(11):1457–1465.
34. Su S, Zhu H, Xu X, et al. DNA methylation of the LY86 gene is associated with obesity, insulin resistance, and inflammation. *Twin Res Hum Genet*. 2014;17(3):183–191.
35. Barajas-Olmos F, Centeno-Cruz F, Zerrweck C, et al. Altered DNA methylation in liver and adipose tissues derived from individuals with obesity and type 2 diabetes. *BMC Med Genet.* 2018;19(1):28.
36. Jones MR, Brower MA, Xu N, et al. Systems genetics reveals the functional context of PCOS loci and identifies genetic and molecular mechanisms of disease heterogeneity. *PLoS Genet.* 2015;11(8):e1005455.
37. Liu HW, Mahmood S, Srinivasan M. Developmental programming in skeletal muscle in response to overnourishment in the immediate postnatal life in rats. *J Nutr Biochem.* 2013;24(11):1859–1869.
38. You D, Nilsson E, Tenen DE, et al. Dnmt3a is an epigenetic mediator of adipose insulin resistance. *Elife.* 2017;6:e30766.

Aged garlic extract and S-allylcysteine increase the GLUT3 and GCLC expression levels in cerebral ischemia

Carlos Daniel Gomez[1,B,C,F], Penélope Aguilera[2,B,C,F], Alma Ortiz-Plata[3,B,F], Felipe Nares López[2,C,D,F], María Elena Chánez-Cárdenas[2,D,E,F], Eugenia Flores-Alfaro[4,C,F], Martha Eugenia Ruiz-Tachiquín[5,C,F], Monica Espinoza-Rojo[6,A,B,D,F]

[1] Department of Physiology and Pharmacology, University of Calgary, Canada
[2] Laboratory of Cerebral Vascular Pathology, National Institute of Neurology and Neurosurgery "Manuel Velasco Suárez", Mexico City, Mexico
[3] Laboratory of Experimental Neuropathology, National Institute of Neurology and Neurosurgery, Mexico City, Mexico
[4] Laboratory of Clinical and Molecular Epidemiology, Faculty of Biological and Chemical Sciences, Universidad Autónoma de Guerrero, Chilpancingo, Mexico
[5] Medical Research Unit on Human Genetics, Pediatrics Hospital, Mexican Institute of Social Security (IMSS), Mexico City, Mexico
[6] Laboratory of Molecular and Genomic Biology, Faculty of Biological Chemical Sciences, Universidad Autónoma de Guerrero, Chilpancingo, Mexico

A – research concept and design; B – collection and/or assembly of data; C – data analysis and interpretation;
D – writing the article; E – critical revision of the article; F – final approval of the article

Advances in Clinical and Experimental Medicine, ISSN 1899–5276 (print), ISSN 2451–2680 (online) *Adv Clin Exp Med*. 2019;28(12):1609–1614

Address for correspondence
Mónica Espinoza-Rojo
E-mail: monicaespinozarojo2014@gmail.com

Funding sources
Carlos Daniel Gómez was financed by CONACyT (scholarship No. 12296) and by Movilidad Santander Universia.

Conflict of interest
None declared

Acknowledgements
We thank Travis Ashworth for his contribution to the revision of English grammar in the manuscript, and Juan Miguel Mendoza Bello for his technical assistance.

Received on February 6, 2018
Reviewed on March 6, 2018
Accepted on June 27, 2019

Published online on December 16, 2019

Cite as
Gomez CD, Aguilera P, Ortiz-Plata A, et al. Aged garlic extract and S-allylcysteine increase the GLUT3 and GCLC expression levels in cerebral ischemia. *Adv Clin Exp Med.* 2019;28(12):1609–1614. doi:10.17219/acem/110328

DOI
10.17219/acem/110328

Abstract

Background. During cerebral ischemia, energy restoration through the regulation of glucose transporters and antioxidant defense mechanisms is essential to maintain cell viability. Antioxidant therapy has been considered effective to attenuate brain damage; moreover, the regulation of transcription factors that positively regulate the expression of glucose transporters is associated with this therapy. Recently, it has been reported that the use of antioxidants such as S-allylcysteine (SAC), a component of aged garlic extract (AGE), improves survival in experimental models of cerebral ischemia.

Objectives. The aim of this study was to determine the effect of AGE and SAC on the level of mRNA expression of the main neuronal glucose transporter (GLUT3) and the glutamate cysteine ligase catalytic subunit (GCLC) in rats with transient focal cerebral ischemia.

Material and methods. Cerebral ischemia was induced in male Wistar rats by middle cerebral artery occlusion (MCAO) for 2 h. The animals were sacrificed after different reperfusion times (0–48 h). Animals injected with AGE (360 mg/kg, intraperitoneally (i.p.)) and SAC (300 mg/kg, i.p.) at the beginning of reperfusion were sacrificed after 2 h. The mRNA expression level was analyzed in the fronto-parietal cortex using quantitative polymerase chain reaction (qPCR).

Results. Two major increases in GLUT3 expression at 1 h and 24 h of reperfusion were found. Both treatments increased GLUT3 and GCLC mRNA levels in control and under ischemic/reperfusion injury animals.

Conclusions. This data suggests that SAC and AGE might induce neuroprotection, while controlling reactive oxygen species (ROS) levels, as indicated by the increase in GCLC expression, and regulating the energy content of the cell by increasing glucose transport mediated by GLUT3.

Key words: antioxidants, cerebral ischemia, glucose transporters

Damage induced by cerebral ischemia and restoration of blood flow (reperfusion) has been linked to mitochondrial dysfunction and the concomitant production of noxious levels of reactive oxygen species (ROS).[1] Reactive oxygen species are released during mitochondrial respiration, causing tissue injury and cellular dysfunction.[2,3] Therefore, the reduction of ROS by antioxidants has been considered as a potential therapeutic method that, through the regulation of the cellular redox state, might ameliorate ischemic injury.[4–6]

Interestingly, antioxidant agents activate the hypoxia inducible factor-1α (HIF-1α) in cultured brain endothelial cells, astrocytes and neurons subjected to normoxia, hypoxia or ischemia.[7–9] This factor increases anaerobic glycolysis through the upregulation of glucose transporters (GLUTs), which possess hypoxia response elements (HRE) in their promoters,[10,11] and this upregulation facilitates cell survival by maintaining adenosine triphosphate (ATP) production.[9,12] Glucose transporters are essential for an adequate supply of energy in neurons, principally under conditions where the energy demand is high as occurs in hypoxia and brain ischemia.[13] The glucose transporter 3 (GLUT3) is the main transporter in neurons with the highest affinity for glucose (K_m 1.4 mmol/L),[10,11] its expression increases at the onset of cerebral ischemia, and its subsequent decline is followed by neuronal death.[14] On the other hand, treatment with antioxidant agents also increases expression levels of proteins involved in cellular redox regulation.[9,15] The glutamate cysteine ligase catalytic subunit (GCLC) is an enzyme that participates in the production of glutathione, an important endogenous antioxidant peptide.[16] The glutamate cysteine ligase catalytic subunit is increased in brain slices subjected to oxygen-glucose deprivation,[17] and in vitro models of chemical hypoxia-induced neurotoxicity.[18] Therefore, regulation of GLUT and GCLC are 2 potential mechanisms by which antioxidants might prevent the deleterious effects of ROS in cerebral ischemia.

In line, some antioxidant agents, such as aged garlic extract (AGE), and its main active component, S-allylcysteine (SAC), have been shown to prevent brain cell death and to improve neurologic deficit induced in experimental models of cerebral ischemia/reperfusion.[5,6,19,20] The effects of AGE and SAC in brain ischemia have been associated with their high antioxidant potential; nevertheless, their complete mechanism of action is not well understood. We assume that these antioxidants act in association with the regulation of GLUT3 expression to increase the entrance of glucose to the cell to augment ATP concentration, but are also associated with the regulation of GCLC mRNA to achieve a reduced cellular redox state, which is characterized by a high glutathione concentration. Therefore, we have determined the temporal expression patterns of GLUT3 induced by cerebral ischemia/reperfusion and the possible changes following reperfusion in the presence of AGE and SAC. We also have evaluated the effect of these antioxidants on GCLC expression in our model of cerebral ischemia/reperfusion. Our purpose was to identify a possible mechanism by which antioxidants participate in neuroprotection in the middle cerebral artery occlusion (MCAO) model of ischemia/reperfusion.

Material and methods

Reagents

Aged garlic extract Kyolic® was obtained from Wakunaga of America Co., Ltd. (Mission Viejo, USA), and SAC was synthesized by the reaction of L-cysteine with allylbromide and purified by recrystallization from ethanol-water, according to a previous report.[21] TRIzol Reagent, SuperScript® III First Strand Synthesis SuperMix and ramdom hexamer primers were obtained from Invitrogen Life Technologies (Carlsbad, USA); commercial predesigned TaqMan Probes system was performed in a 7500 Real-time PCR System (Applied Biosystems, Foster City, USA) using specific assay GLUT3 (Rn00567331_M1) and GCLC (Rn00563101_M1) (Applied Biosystem). 18S ribosomal RNA (18S rRNA, assay ID: Hs99999901_s1, Applied Biosystems). All other reagents were obtained from known commercial sources.

Experimental animals

Adult male Wistar rats weighing 280–320 g were included in this study. The mRNA expression encoding for GLUT3 and GCLC was studied in 3–8 animals per group. Nine animal groups were subjected to transient focal cerebral ischemia induced by MCAO during 2 h,[22] and then were sacrificed by decapitation after different times (0, 1, 2, 3, 4, 6, 10, 24, and 48 h) of reperfusion (n = 4). Briefly, animals were anaesthetized with isoflurane (2.5–3.0%). The left common carotid artery was exposed at the level of the external and internal carotid artery bifurcation. A 3-0 nylon monofilament was inserted into the external carotid artery and advanced into the internal carotid artery at a depth of about 17 mm to block the origin of the middle cerebral artery (MCA). Body temperature was kept at 37 ±0.5°C during the procedure. Two hours after the induction of ischemia, the filament was removed to allow reperfusion. The animals were returned to their cages and monitored until they recovered from anesthesia. Neurological deficit was determined 30 min before reperfusion and was scored on a 2-point scale: failure to extend right paw fully = 1; circling to right (more than 5 turns over a period of 30 s) = 1. Animals that presented neurological deficits <2 were exclude from the study.[5,22] An animal control group was subjected to surgery without MCAO. Another 3 control groups were injected intraperitoneally (i.p.) with a single dose of the antioxidant agents, AGE (360 mg/kg), SAC (300 mg/kg) or with their vehicles consisting in 20% ethanol in sterile water (control group). Finally, the last 3 animal groups were subjected to MCAO,

and then received a single i.p. injection of one of the above antioxidant agents at the beginning of reperfusion. All animal groups administered with the antioxidant agents were sacrificed by decapitation 2 h after the treatment injection. Experimental procedures were carried out in accordance with the National Institutes of Health (NIH) Guidelines for the Care and Use of Laboratory Animals, and with the ethical guidelines established by the National Institute of Neurology and Neurosurgery "Manuel Velasco Suárez" in Mexico City, Mexico (approved project No. 20/11 (624)).

Quantitative polymerase chain reaction

Total RNA extraction was performed on the whole fronto-parietal cortex, using TRIzol Reagent (Invitrogen Life Technologies) according to the manufacturer's instructions, and the amount and purity were determined using a spectrophotometer. cDNA was synthesized from 5 µg total RNA, using the kit SuperScript® III First Strand Synthesis SuperMix (Invitrogen Life Technologies). Quantitative polymerase chain reaction (qPCR) was performed in a 7500 Real-time PCR System (Applied Biosystems), using specific assay GLUT3 (Rn00567331_M1) and GCLC (Rn00563101_M1) (Applied Biosystem). 18S ribosomal RNA (18S rRNA, assay ID: Hs99999901_s1, Applied Biosystems) was used as a control to normalize the relative mRNA amount of the amplified genes. Reactions were done in triplicate and consisted of a denaturation cycle at 95°C for 10 min, followed by 40 cycles of denaturation at 92°C for 15 s and of annealing/extension at 60°C for 1 min. Values of cycle threshold (Ct) were determined through automated threshold analysis using SDS v. 1.3.1. software (Applied Biosystems, Waltham, USA). This software uses the comparative Ct method of relative quantification to determine relative gene expression levels.

Statistical analysis

Data analysis was performed using SPSS v. 13.0 (SPSS Inc., Chicago, USA) statistical software package. The results are presented as mean and standard deviation (mean ±SD). The statistical significance of differences between groups was analyzed using analysis of variance (ANOVA) and post hoc Tukey analysis was used for statistical evaluations. A value of $p < 0.05$ was considered significant.

Results

Effects of cerebral ischemia/reperfusion on GLUT3 mRNA expression levels in fronto-parietal cortex

Considering that major alterations in cerebral glucose concentration during ischemic injury have been reported,[23–25] temporal expression of glucose transporters induced by cerebral ischemia/reperfusion in the fronto-parietal cortex was evaluated. Figure 1 shows that focal cerebral ischemia (MCAO group) increased the GLUT3 mRNA expression level by 224% compared with control rats (1.41 ±0.24-fold; $p < 0.0001$). In the case of animals subjected to 2 h of MCAO followed by different times of reperfusion, 2 major increases in the GLUT3 mRNA expression were observed. After 1 h of reperfusion, the GLUT3 mRNA expression level remained elevated and reached 31% (0.8 ±0.08-fold) more than in the MCAO group ($p < 0.0001$). After 2, 3 and 4 h of reperfusion, the GLUT3 expression level was reduced to 52.4%, 67.7%, and 50%, respectively (2 h reperfusion = –1.21 ±0.08-fold; 3 h of reperfusion = –0.82 ±0.17-fold; 4 h of reperfusion = –1.27 ±0.17-fold; reperfusion group vs MCAO, $p < 0.0001$) reaching the baseline levels of expression (control group). After 6 and 10 h of reperfusion, the levels of GLUT3 were even lower that baseline reaching 22.1% and 14.6% (6 h of reperfusion = –1.98 ±0.01-fold; 10 h of reperfusion = –2.17 ±0.05-fold; reperfusion group vs MCAO, $p < 0.0001$). A more pronounced increase was found after 24 h of reperfusion, when the GLUT3 mRNA expression level was increased to 163% (1.62 ±0.26, 24 h of reperfusion vs MCAO $p < 0.0001$). Finally, after 48 h of reperfusion, GLUT3 mRNA decreased again 33% compared to the MCAO group (–1.68 ±0.14, $p < 0.0001$).

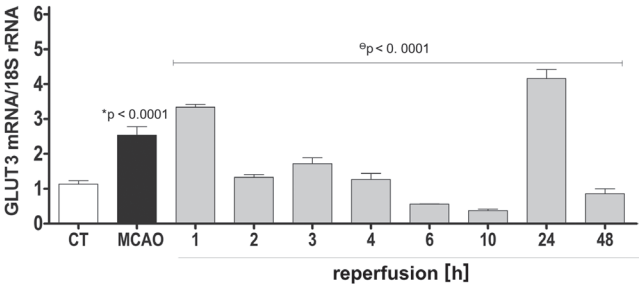

Fig. 1. Effect of cerebral ischemia/reperfusion on GLUT3 mRNA expression level in fronto-parietal cortex. Rats were subjected to middle cerebral artery occlusion (MCAO) for 2 h, and were, thereafter, sacrificed at different times of reperfusion: 0, 1, 2, 3, 4, 6, 10, 24, and 48 h. cDNA was synthesized using 5 µg of total RNA. The qPCR was performed to determine the expression level of GLUT3 mRNA, and ΔCt method was used to quantify the relative expression level. The changes in GLUT3 mRNA expression level (dark bars) are expressed as relative GLUT3 expression normalized to 18S ribosomal RNA. Results are the mean ±SD values of 4 animals included in each group. Statistical differences were calculated using ANOVA and post hoc Tukey analysis. Differences are indicated above each bar. *$p < 0.0001$ vs CT; $^{\theta}p < 0.0001$ vs MCAO

Effects of AGE and SAC on GLUT3 mRNA expression levels in cerebral ischemia/reperfusion

Recent evidence suggests a key role of GLUT3 as a potential therapeutic target in the treatment of cerebral ischemia/reperfusion.[26,27] Therefore, a possible effect of the AGE and its principal component SAC on GLUT3

Table 1. Single and combined effects of cerebral ischemia/reperfusion and antioxidant agents on GLUT-3 mRNA levels in brain cortex

Experimental condition	§ GLUT-3 levels	p-value between the indicated experimental conditions	
Control (a)	1.13 ±0.10		
MCAO/2R (b)	1.33 ±0.08	(b) vs (a) NS	
Aged garlic extract (c)	6.38 ±0.36	(c) vs (a) 0.00002	
Aged garlic extract + MCAO/2R (d)	4.43 ±0.38	(d) vs (a) 0.0002	(d) vs (b) 0.0002
SAC (e)	4.82 ±0.85	(e) vs (a) 0.002	
SAC + MCAO/2R (f)	3.51 ±0.59	(f) vs (a) 0.005	(f) vs (b) 0.008

§ main neuronal glucose transporter (GLUT3) levels are expressed in arbitrary units of GLUT-3 mRNA/18S rRNA
Results are the mean ±SD (n = 3–8).
Middle cerebral artery occlusion (MCAO)/2R – animals subjected to middle cerebral artery occlusion were sacrificed after 2 h of reperfusion.
NS – not statistically significant difference between the indicated experimental conditions.
Aged garlic extract (AGE) and S-allylcysteine (SAC) doses were 360 mg/kg and 300 mg/kg body wt, respectively.
AGE and SAC were administered at the beginning of reperfusion and animals were sacrificed after 2 h of reperfusion.

Table 2. Single and combined effects of cerebral ischemia/reperfusion and antioxidant agents on GCLC mRNA levels in brain cortex

Experimental condition	§ GCLC levels	p-value between the indicated experimental conditions	
Control (a)	1.00 ±0.03		
MCAO/2R (b)	1.09 ±0.13	(b) vs (a) NS	
Aged garlic extract (c)	3.06 ±0.38	(c) vs (a) 0.006	
Aged garlic extract + MCAO/2R (d)	2.92 ±0.45	(d) vs (a) 0.01	(d) vs (b) 0.02
SAC (e)	2.92 ±0.16	(e) vs (a) 0.001	
SAC + MCAO/2R (f)	2.25 ±0.22	(f) vs (a) 0.005	(f) vs (b) 0.02

§ glutamate cysteine ligase catalytic subunit (GCLC) levels are expressed in arbitrary units of GCLC mRNA/18S rRNA.
Results are the mean ±SD (n = 3–8).
Middle cerebral artery occlusion (MCAO)/2R – animals subjected to middle cerebral artery occlusion were sacrificed after 2 h of reperfusion.
NS – not statistically significant difference between the indicated experimental conditions.
Aged garlic extract (AGE) and S-allylcysteine (SAC) doses were 360 mg/kg and 300 mg/kg body wt, respectively.
AGE and SAC were administered at the beginning of reperfusion and animals were sacrificed after 2 h of reperfusion.

mRNA expression level in cerebral ischemia/reperfusion was tested here. Table 1 shows that both treatments increased the baseline expression of the mRNA encoding for GLUT3 (AGE and SAC groups). In the control rats, AGE increased GLUT3 mRNA expression level by 564.6% over basal conditions ($p < 0.0001$), while SAC increased the GLUT3 mRNA expression level by 426.5% ($p = 0.002$) (Table 1, row c and e vs a). On the other hand, AGE and SAC administration to the animals subjected to 2 h of ischemia and 2 h of reperfusion increased the GLUT3 mRNA expression level by 333% ($p = 0.0002$) in the MCAO/2R+AGE group and 263.9% in the MCAO/2R+SAC group (Table 1, row d and f vs b; $p = 0.008$).

Effects of AGE and SAC on GCLC mRNA expression levels in cerebral ischemia/reperfusion

Considering that oxidative stress generated during the ischemia/reperfusion process aggravates the damage, we evaluated the effect of AGE and SAC on GCLC mRNA expression level to determine a possible mechanism by which antioxidant molecules function as regulators in neuroprotection. Table 2 shows that both AGE and SAC administration induced a significant increase in the expression level of GCLC mRNA over control values in physiological conditions. The AGE treatment increased GCLC mRNA expression level by 306% ($p = 0.006$) in the control group + AGE, and by 292% ($p = 0.001$) in the control group + SAC (Table 2, row c and e vs a). In another observation, the increase induced by AGE and SAC on GCLC expression level was still present in animals subjected to brain ischemia, in the MCAO/2R+AGE group, the GLUT3 mRNA increased expression level 268% ($p = 0.02$), and 206% ($p = 0.02$) in the MCAO/2R+SAC group vs the MCAO/2R group (Table 2, row d and f vs b)

Discussion

The present study shows that in the fronto-parietal cortex dissected from animals exposed to transitory focal cerebral ischemia, the expression level of GLUT3 mRNA is increased after 2 h of injury and continued until 1 h of reperfusion period. We found that early transient increase in GLUT3 mRNA expression is presumably an acute response to brain ischemia, which could be explained by the activation of the HIF-1α, a potent inducer of GLUTs expression under hypoxia/ischemia situations. The HIF-1α mediates transcriptional regulation of glycolytic genes that possess hypoxia-response elements (HRE) in their promoters, including GLUT3.[11] During ischemia, deficiency of energy substrates induces the activation of cAMP response element-binding protein (CREB), which is also an important transcriptional factor of the GLUT3 gene.[10,27,28] Coupled to this, CREB is activated by the PI3K/Akt pathway,[29] a mechanism of neuroprotection in cerebral ischemia/reperfusion injury.[30]

In addition to neurons, it is possible that astrocytes contribute to the increase in GLUT3 expression. It has been demonstrated that in cultured astrocytes, under ischemic/reperfusion conditions, the ischemic stress increased

the expression levels of GLUT3, in order to enhance intracellular glucose storage during reperfusion, apparently as a protective mechanism against lethal ischemic stress.[27–31] Possibly, this transcriptional activation generates a prolonged protective effect. Interestingly, from 2 h to 10 h of reperfusion, the level GLUT3 decreased, and of 2 h to 4 h had normalized relative to the control, possibly through HIF inactivation, since HIF-1α under normoxic conditions is rapidly hydroxylated by prolyl hydroxylase and degraded.[32] Furthermore, during early reperfusion, the sudden increase in glucose might induce a decrease in GLUT expression, as a compensatory mechanism due to the excess supply of glucose that occurs with blood flow recovery.[27]

The second increase in GLUT3 mRNA expression observed at 24 h of reperfusion may be associated with the need for glucose to maintain the energy demands for cell repair, since during reperfusion there is an increase of ROS that induces damage and neuronal necrosis.[5] It has been shown that the increase in GLUT3 expression is related to increased glucose utilization.[10,14,25,27]

This data also shows that antioxidant agents such as SAC and possibly other components that have been identified in AGE are effective in enhancing GLUT3 and GCLC mRNA expression under ischemic and 2 h reperfusion. Previous studies have reported that AGE and SAC delays the appearance of neuronal damage and prevents cognitive impairments in some models of cerebral ischemia/reperfusion, possibly associated with their antioxidant potential.[4–6,19] Supporting this hypothesis in cultures of brain cells, some antioxidant agents increased the expression of GLUTs associated with a reduced redox state.[7–9] The increase of GLUT3 mRNA induced by AGE and SAC may be explained by the ability of some antioxidants to regulate signaling pathways. Antioxidants such as resveratrol induce Akt phosphorylation; this protein kinase is also involved in the activation of CREB.[33] Thus, it is likely that GLUT3 plays a key neuroprotective role in brain ischemia as an endogenous mechanism and as antioxidant's mechanism of action.

Comparison of the effect exerted by AGE and SAC on the mRNA baseline levels of GLUT3 shows that AGE is the most effective. The fact that AGE possesses a major effect suggests that components of the extract besides SAC are contributing to the outcome. Previously, we showed that AGE scavenges $O2^{\cdot-}$, $ONOO^{-}$, $OH^{\cdot}$, and $ROO^{\cdot}$.[34] Although several studies have suggested that SAC, the major compound in AGE, is the principal compound responsible for the inhibition of oxidative damage in the ischemic brain,[35] a wide variety of other potential antioxidant compounds present on AGE, such as sulfur compounds,[36] may be responsible for the upregulation of GLUT3 observed in our study.

Brian ischemia is known to induce oxidative stress that ultimately may lead to brain cell death. One strategy to slow the progression of brain damage is to prevent the formation and action of free radicals. To this end, maintenance of the reduced glutathione pool, which is the main intracellular antioxidant, is critical to cell survival during brain ischemic injury.[37] Interestingly, we found that AGE and SAC showed a positive inductive effect on the expression of the GCLC in the fronto-parietal cortex during focal cerebral ischemia and 2 h of reperfusion. This result could be explained by the activation of Nrf2, since it has been shown that some antioxidants increase the activity of the Nrf2 pathway in animal models of stroke and induce protection against ischemia injury.[2] Nrf2 activates a number of Nrf2-dependent genes encode antioxidant proteins, as GCLC and GCLM (glutamate-cysteine ligase), both enzymes involved in the synthesis of glutathione.[2,16,38]

Therefore, the present findings show the temporal course of GLUT3 mRNA expression in brain cortex during cerebral ischemia/reperfusion. This study also determined that the treatment with AGE and SAC increased the baseline expression of GLUT3, which may significantly account for their protective effect during brain ischemia. Furthermore, our results suggest that, in addition to the intrinsic antioxidant capability of AGE and SAC, the mechanism by which these antioxidants exert their neuroprotective effect may be by enhancing cellular antioxidant systems expression and facilitating the GLUT3 activity after an ischemic/reperfusion.

References

1. Starkov A, Chinopoulos C, Fiskum G. Mitochondrial calcium and oxidative stress as mediators of ischemic brain injury. *Cell Calcium*. 2004; 36(3–4):257–264.
2. Zhang R, Xu M, Wang Y, Xie F, Zhang G, Qin X. Nrf2: A promising therapeutic target for defensing against oxidative stress in stroke. *Mol Neurobiol*. 2017;54(8):6006–6017.
3. Fraser PA. The role of free radical generation in increasing cerebrovascular permeability. *Free Radic Biol Med.* 2011;51(5):967–977.
4. Numagami Y, Sato S, Ohnishi ST. Attenuation of rat ischemic brain damage by aged garlic extracts: A possible protecting mechanism as antioxidants. *Neurochem Int*. 1996;29(2):135–143.
5. Aguilera P, Chánez-Cardenas ME, Ortiz-Plata A, et al. Aged garlic extract delays the appearance of infarct area in a cerebral ischemia model, an effect likely conditioned by the cellular antioxidant systems. *Phytomedicine*. 2010;17(3–4):241–247.
6. Ashafaq M, Khan MM, Raza SS, et al. S-allyl cysteine mitigates oxidative damage and improves neurologic deficit in a rat model of focal cerebral ischemia. *Nutr Res*. 2012;32(2):133–143.
7. Wilson WJ, Poellinger L. The dietary flavonoid quercetin modulates HIF-1α activity in endothelial cells. *Biochem Biophys Res Commun*. 2002;293(1):446–450.
8. Zhang B, Tanaka J, Yang L, et al. Protective effect of vitamin E against focal brain ischemia and neuronal death through induction of target genes of hypoxia-inducible factor-1. *Neuroscience.* 2004;126(2): 433–440.
9. Doung TT, Chami B, McMahon AC, et al. Pre-treatment with the synthetic antioxidant T-butyl bisphenol protects cerebral tissues from experimental ischemia reperfusion injury. *J Neurochem.* 2014;130(6): 733–747.
10. Simpson IA, Dwyer D, Malide D, Moley KH, Travis A, Vannucci SJ. The facilitative glucose transporter GLUT3: 20 years of distinction. *Am J Physiol Endocrinol Metab.* 2008;295(2):E242–E253.
11. Barron CC, Bilan PJ, Tsakiridis T, Tsiani E. Facilitative glucose transporters: Implications for cancer detection, prognosis and treatment. *Metabolism.* 2016;65(2):124–139.

12. Wu F, Wu J, Nicholson AD, Echeverry R, et al. Tissue-type plasminogen activator regulates the neuronal uptake of glucose in the ischemic brain. *J Neurosci.* 2012;32(29):9848–9858.
13. Park SM, Lee JC, Chen BH, et al. Difference in transient ischemia induced neuronal damage and glucose transporter-1 immunoreactivity in the hippocampus between adult and young gerbils. *Iran J Basic Med Sci.* 2016;19(5):521–528.
14. Vannucci SJ, Seaman LB, Vannucci RC. Effects of hypoxia-ischemia on GLUTI and GLUT3 glucose transporters in immature rat brain. *J Cereb Blood Flow Metab.* 1996;16(1):77–81.
15. Ide N, Lau BH. Garlic compounds minimize intracellular oxidative stress and inhibit nuclear factor-kappa b activation. *J Nutr.* 2001; 131(3s):1020S–1026S.
16. Chen Y, Dong H, Thompson DC, Shertzer HG, Nebert DW, Vasiliou V. Glutathione defense mechanism in liver injury: Insights from animal models. *Food Chem Toxicol*. 2013;60:38–44.
17. Rawal AK, Muddeshwar MG, Biswas SK. *Rubia cordifolia*, *Fagonia cretica linn* and *Tinospora cordifolia* exert neuroprotection by modulating the antioxidant system in rat hippocampal slices subjected to oxygen glucose deprivation. *BMC Complement Altern Med.* 2004;4:11.
18. Guan D, Su Y, Li Y, et al. Tetramethylpyrazine inhibits CoCl2-induced neurotoxicity through enhancement of Nrf2/GCLc/GSH and suppression of HIF1α/NOX2/ROS pathways. *J Neurochem.* 2015;134(3): 551–565.
19. Numagami Y, Ohnishi ST. S-allylcysteine inhibits free radical production, lipid peroxidation and neuronal damage in rat brain ischemia. *J Nutr.* 2001;131(3s):1100S–1105S.
20. Qu Z, Mossine VV, Cui J, Sun GY, Gu Z. Protective effects of AGE and its components on neuroinflammation and neurodegeneration. *Neuromol Med.* 2016;18(3):474–482.
21. Maldonado PD, Alvarez-Idaboy JR, Aguilar-Gonzalez A, et al. Role of allyl group in the hydroxyl and peroxyl radical scavenging activity of S-allylcysteine. *J Phys Chem B.* 2011;115(45):13408–13417.
22. Longa EZ, Weinstein PR, Carlson S, Cummins R. Reversible middle cerebral artery occlusion without craniectomy in rats. *Stroke.* 1989; 20(1):84–91
23. Yager JY, Brucklacher RM, Vannucci RC. Cerebral energy metabolism during hypoxia-ischemia and early recovery in immature rats. *Am J Physiol.* 1992;262(3 Pt 2):H672–H677.
24. Thoren AE, Helps SC, Nilsson M, Sims NR. The metabolism of ^{14}C-glucose by neurons and astrocytes in brain subregions following focal cerebral ischemia in rats. *J Neurochem.* 2006;97(4):968–978.
25. Vannucci RC, Yager JY, Vannucci SJ. Cerebral glucose and energy utilization during the evolution of hypoxic-ischemic brain damage in the immature rat. *J Cereb Blood Flow Metab.* 1994;14(2):279–288.
26. Espinoza-Rojo M, Iturralde-Rodriguez KI, Chanez-Cardenas ME, Ruiz Tachiquin ME, Aguilera P. Glucose transporters regulation on ischemic brain: Possible role as therapeutic target. *Cent Nerv Syst Agents Med Chem.* 2010;10(4):317–325.
27. Patching SG. Glucose transporters at the blood-brain barrier: Function, regulation and gateways for drug delivery. *Mol Neurobiol.* 2017; 54(2):1046–1077.
28. Rajakumar A, Thamotharan S, Raychaudhuri N, Menon RK, Devaskar SU. Trans-activators regulating neuronal glucose transporter isoform-3 gene expression in mammalian neurons. *J Biol Chem.* 2004;279(25): 26768–26779.
29. Pugazhenthi S, Nesterova A, Sable C, et al. Akt/Protein kinase B upregulates Bcl-2 expression through cAMP-response element-binding protein. *J Biol Chem.* 2000;275(15):10761–10766.
30. Ma Y, Lu C, Li C, et al. Overexpression of HSPA12B protects against cerebral ischemia/reperfusion injury via a PI3K/Akt-dependent mechanism. *Biochim Biophys Acta.* 2013;1832(1):57–66.
31. Iwabuchi S, Kawahara K. Inducible astrocytic glucose transporter-3 contributes to the enhanced storage of intracellular glycogen during reperfusion after ischemia. *Neurochem Int.* 2011;59(2):319–325.
32. Bruick RK, McKnight SL. A conserved family of prolyl-4-hydroxylases that modify HIF. *Science.* 2001;294(5545):1337–1340.
33. Shin JA, Lee KE, Kim HS, Park EM. Acute resveratrol treatment modulates multiple signaling pathways in the ischemic brain. *Neurochem Res.* 2012;37(12):2686–2696.
34. Cervantes MI, de Oca Balderas PM, Gutierrez-Baños J, et al. Comparison of antioxidant activity of hydroethanolic fresh and aged garlic extracts and their effects on cerebral ischemia. *Food Chem.* 2013; 140(1–2):343–352.
35. Colin-Gonzalez AL, Santana RA, Silva-Islas CA, Chanez-Cardenas ME, Santamaria A, Maldonado PD. The antioxidant mechanisms underlying the aged garlic extract- and S-allylcysteine-induced protection. *Oxid Med Cell Longev.* 2012;2012:907162.
36. Bayan L, Koulivand PH, Gorji A. Garlic: A review of potential therapeutic effects. *Avicenna J Phytomed.* 2014;4(1):1–14
37. Zimmermann C, Winnefeld K, Streck S, Roskos M, Haberl RL. Antioxidant status in acute stroke patients and patients at stroke risk. *Eur Neurol.* 2004;51(3):157–161.
38. Sethy NK, Singh M, Kumar R, Ilavazhagan G, Bhargava K. Upregulation of transcription factor NRF2-mediated oxidative stress response pathway in rat brain under short-term chronic hypobaric hypoxia. *Funct Integr Genomics.* 2011;11(1):119–137.

Clinical outcomes of non-alcoholic fatty liver disease: Polish-case control study

Radosław Kempiński[1,A–F], Agata Łukawska[2,B,D–F], Filip Krzyżanowski[2,B,D–F], Dominika Ślósarz[2,B,D–F], Elżbieta Poniewierka[1,A,D–F]

[1] Department of Gastroenterology and Hepatology, Wroclaw Medical University, Poland
[2] Gastroenterology Student Organization, Wroclaw Medical University, Poland

A – research concept and design; B – collection and/or assembly of data; C – data analysis and interpretation; D – writing the article; E – critical revision of the article; F – final approval of the article

Advances in Clinical and Experimental Medicine, ISSN 1899–5276 (print), ISSN 2451–2680 (online) *Adv Clin Exp Med*. 2019;28(12):1615–1620

Address for correspondence
Radosław Kempiński
E-mail: radoslaw.kempinski@umed.wroc.pl

Funding sources
None declared

Conflict of interest
None declared

Received on February 28, 2019
Reviewed on March 15, 2019
Accepted on April 4, 2019

Published online on April 23, 2019

Abstract

Background. Non-alcoholic fatty liver disease (NAFLD) is becoming the most common cause of chronic liver disease worldwide, affecting up to 30% of population. Non-alcoholic fatty liver disease can lead to non-alcoholic steatohepatitis (NASH), fibrosis, cirrhosis, and hepatocellular carcinoma. Age, obesity, insulin resistance, type 2 diabetes, and dyslipidemia are important risk factors for developing hepatic steatosis. Concomitant diseases, especially cardiovascular, are discussed as important causes of death in NAFLD patients.

Objectives. The objective of this study was to conduct a retrospective comparison of the frequency of concomitant diseases in NAFLD patients and controls, especially metabolic syndrome and cardiovascular disease (CVD).

Material and methods. A total of 1,058 (558 NAFLD patients and 500 controls). Diagnosis of NAFLD was established with ultrasound examination in the absence of other causes of fatty liver. The control group included patients with no history of liver disease, normal liver image in ultrasound examination and normal liver laboratory tests.

Results. Overweight and/or obesity were diagnosed in 80.8% of patients in the study group and 40.8% in the controls ($p < 0.001$). Metabolic syndrome was present in 48.7% patients in the study group compared with 14.4% controls, ($p < 0.001$). In the study group, we found higher prevalence of hypertension (56.1% vs 37%; $p < 0.001$), type 2 diabetes mellitus (24.4% vs 8.6%; $p < 0.001$), decreased concentration of serum HDL (35.1% vs 19.5%; $p < 0.001$), elevated serum triglycerides (36.5% vs 15.4%; $p < 0.001$). Cardiovascular disease was found in 13.6% of individuals in the study group and in 15% controls (NS, $p = 0.32$). The most frequent concomitant gastrointestinal disease present in the study group was gastroesophageal reflux disease (GERD) (31.9% vs 22.8%; $p < 0.001$) followed by colonic diverticulosis (23.7% vs 15.8%; $p < 0.005$).

Conclusions. Metabolic syndrome with its components is more common in NAFLD patients compared to matched controls. Additionally, NAFLD patients are more often affected by GERD and colonic diverticulosis but not by CVD.

Key words: metabolic syndrome, cardiovascular disease, concomitant diseases, non-alcoholic fatty liver disease

Cite as
Kempiński R, Łukawska A, Krzyżanowski F, Ślósarz D, Poniewierka E. Clinical outcomes of non-alcoholic fatty liver disease: Polish-case control study. *Adv Clin Exp Med*. 2019;28(12):1615–1620. doi:10.17219/acem/106173

DOI
10.17219/acem/106173

Introduction

Non-alcoholic fatty liver disease (NAFLD) recently has become the predominant cause of chronic liver disease in many parts of the world.[1] The spectrum of the disease ranges from simple liver steatosis through non-alcoholic steatohepatitis (NASH) with possible fibrosis leading to cirrhosis. Furthermore, hepatocellular carcinoma is the complication of liver cirrhosis in patients with NAFLD. In the last decade, NAFLD was revealed to be multisystem disease, affecting also extra-hepatic organs.[2] Non-alcoholic fatty liver disease is diagnosed in approx. 30–40% of men and 15–20% of women.[3] In certain subgroups, like type 2 diabetes mellitus (T2DM) individuals, it occurs even in up to 70% of this group of patients.[4] Increasing incidence rates of NAFLD are related to the growing prevalence of obesity that is associated with a wide range of complications, including metabolic syndrome (MetS). Non-alcoholic fatty liver disease is strongly connected with metabolic syndrome and its components. Many cross-sectional studies have demonstrated that NAFLD is significantly associated with MetS.[5–8] Recent data showed that NAFLD increased the overall mortality by 57%, mainly from liver-related and cardiovascular disease (CVD) causes, and the risk of T2DM was increased approx. twofold.[9] Cardiovascular disease is the most common cause of death globally, with an estimated 17.9 million people dying from CVD in 2016. Emerging evidence shows that NAFLD is also connected to other chronic diseases, such as endocrinopathies (e.g., hypothyroidism, polycystic ovary syndrome, hypogonadism), colorectal cancer, sleep apnea, osteoporosis, and psoriasis.[10] Recent meta-analysis reported that NAFLD was associated with a twofold increased risk of chronic kidney disease.[11] As colonic diverticulosis shares the same pathways with NAFLD (obesity, hypertension, dyslipidemia)[12] and its risk is higher in patients with visceral fat accumulation.[13] The possible connection between NAFLD and colonic diverticulosis is additionally investigated.

Liver biopsy is still a gold standard for the diagnosis of NAFLD and its stage (simple steatosis, steatohepatitis, fibrosis, cirrhosis). It is an invasive procedure, requiring most often hospital admission. Therefore, non-invasive methods were recently implemented, especially to identify the patients with liver fibrosis. Abdominal ultrasound is a simple method to diagnose liver steatosis, but, unfortunately, like computed tomography or magnetic resonance techniques, it is not accurate in defining fibrosis in the liver. Transient elastography estimates liver tissue stiffness in ultrasound method and is a novel imaging technique to evaluate patients with liver fibrosis. Serum cytokeratin-18 is a promising and accurate non-invasive marker of non-alcoholic steatohepatitis (NASH). The staging of liver fibrosis with simple serum marker panels is still a challenge, the most accurate are FIB-4 test and NAFLD fibrosis score.[14] A novel method of fibrosis detection in NAFLD is ^{13}C-methacetin breath test.[15]

The objective of our study was a retrospective evaluation of patients with NAFLD and a comparison of the frequency of concomitant diseases in NAFLD patients and controls, especially metabolic syndrome with its components and CVD.

Material and methods

Study group

A total of 2,309 consecutive hospital charts of patient hospitalized in the Department and Clinic of Gastroenterology and Hepatology of Wroclaw Medical University between 2017–2018 were meticulously searched. Four hundred twenty-two individuals were excluded due to secondary causes of liver injury: viral hepatitis, autoimmune hepatitis, hemochromatosis, Wilson's disease, α-1 antitrypsin deficiency, drug-induced hepatic injury, cholestatic liver disease, and alcohol consumption higher than 30 mg/day for men and 20 mg/day for women.

One thousand eighty-seven patients were left for analysis. The study NAFLD group consisted of 558 consecutive patients with liver steatosis. Five hundred individuals with no history of liver disease, normal liver laboratory tests and normal image of liver on ultrasound examination were matched for age and sex with the study group and served as controls. Flowchart for patient inclusion was shown in Fig. 1.

Diagnosis of type 2 diabetes mellitus (T2DM) was defined as a registered diagnosis in patient charts, a non-fasting glucose value ≥180 mg/dL or a fasting glucose value ≥126 mg/dL, or having treatment for diabetes. Hypertension was diagnosed when there was a registered diagnosis in the patient's chart, a resting blood pressure ≥140/90 mm Hg or if the patient had any anti-hypertensive drug prescription. Dyslipidemia was defined

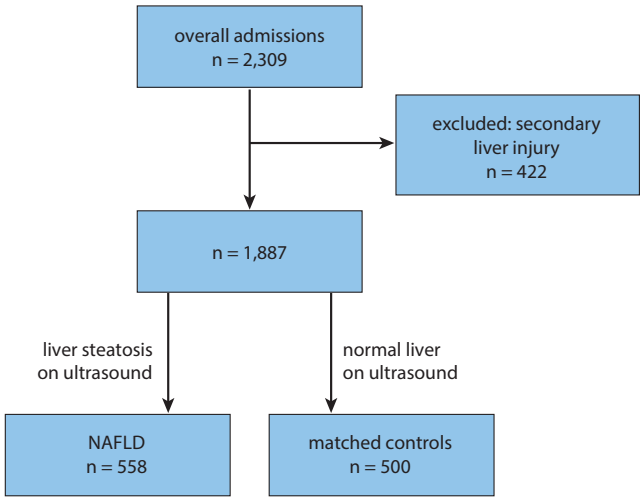

Fig. 1. Flowchart for patient inclusion

when the patient had a fasting triglyceride concentration value ≥150 mg/dL or HDL-cholesterol value <40 mg/dL (male), <50 mg/dL (female). Body mass index (BMI) was calculated as (weight [kg]/height [m]^2). The diagnosis of metabolic syndrome was established according to Adult Treatment Panel III criteria.[16] Cardiovascular disease was defined as one of the following: coronary heart disease, cerebrovascular disease, peripheral arterial disease, rheumatic heart disease, congenital heart disease, deep vein thrombosis, or pulmonary embolism. The diagnosis of colonic diverticulosis was based on an endoscopy and/or radiological examination.

Laboratory parameters extracted from patients' charts were blood morphology, AST, ALT, HDL-cholesterol, triglycerides, and glucose. Other parameters were incomplete and not included in the study.

The diagnosis of liver steatosis was defined in ultrasound examination. Patients were examined in the supine and left lateral decubitus position under fasting conditions. A gastroenterologist with over 10 years of abdominal ultrasound experience evaluated the echogenicity of the liver and the right kidney. Increased hepatorenal echogenicity, bright hepatic echoes, and vascular blurring of portal or hepatic vein were classified as exclusive features of NAFLD.

Statistical analysis

Continuous, normally distributed variables were summarized as mean ± standard deviation (SD). Student's t-test was performed to compare the means in groups with normally distributed data. In groups with non-normal distribution, the Mann–Whitney U-test was used. To compare mean prevalence differences between groups, the χ^2 test (categorical variables) was performed. Statistical analysis was performed using STATISTICA v. 13.3 software (StatSoft Inc., Tulsa, USA).

Ethical considerations

The study protocol was approved by local ethics committee in accordance with the Helsinki Declaration.

Results

Five hundred fifty-eight consecutive patients with liver steatosis and 500 controls were enrolled into the study. According to the absence of other causes of liver steatosis, all the patients in the study group were classified as NAFLD. Twenty-four patients (4.3%) in this group were diagnosed with liver cirrhosis. The mean age of the patients was 58.1 years in NAFLD group and 57.5 years in the controls, respectively. Individuals in the 7th decade of life were most often represented. A total of 50.4% of the patients in the study group were male. The mean age and the sex distribution in both groups did not differ statistically significantly. We tried to estimate the prevalence of NAFLD in all the patients admitted to the gastroenterology department: 558 cases out of 2,309 overall admissions = 24.2%. Selected clinical data of patients in NAFLD patients and controls is shown in Table 1.

The mean BMI was significantly higher in the study group compared to controls (29.2 vs 24.4, p < 0.001). Patients with NAFLD had significantly higher serum TG and lower HDL concentration.

The prevalence of metabolic syndrome and its components in NAFLD patients and controls were estimated (Table 2, number of patients in the brackets in cases where the missing data made it impossible to complete the calculation). Not surprisingly, MetS with components (hypertension, T2DM, dyslipidemia) was strongly correlated with NAFLD. The concomitant diseases in NAFLD and controls were evaluated. We managed to estimate the prevalence of consecutive diseases with odd ratios (Table 3). The concomitant diseases connected with NAFLD were: overweight/obesity, gastroesophageal reflux disease (GERD), colonic diverticulosis and cholecystolithiasis. Functional gastrointestinal diseases were less common in NAFLD than in the controls. The prevalence of other diseases was not significantly different in the study group and controls.

We chose FIB-4 scoring system to estimate the possibility of coexisting fibrosis.[17] In 348 patients (62.4%), the FIB-4 score was lower than 1.45, suggesting no advanced fibrosis present. These patients will not require

Table 1. Selected clinical data of NAFLD patients and controls

Clinical data	NAFLD	Controls	p-value
Age [years][a]	58.1 ±14.1	57.5 ±16.2	0.73
Sex (female/male)	277/281	252/248	0.81
BMI [kg/m^2][a]	29.2 ±5.5	24.4 ±3.9	<0.001
ALT [U/L][a]	33.5 ±32.5	26.2 ±16.5	<0.001
AST [U/L][a]	31.8 ±24.0	22.5 ±16.8	<0.001
Glucose [mg/dL][a]	108.5 ±30.6	103.6 ±32.2	0.35
TG [mg/dL][a]	147.1 ±86.8	108.4 ±60.5	<0.001
HDL (male: >40 mg/dL, female: >50 mg/dL)[a]	50.1 ±14.4	56.6 ±16.7	<0.001

ALT – alanine transaminase; AST – aspartate transaminase; HDL – high-density lipoprotein; BMI – body mass index; TG – triglycerides; [a] mean, standard deviation (SD).

Table 2. The prevalence of metabolic syndrome and its components in NAFLD patients and controls

Components of metabolic syndrome	NAFLD	[%]	Controls	[%]	p-value
Metabolic syndrome	268 (n = 550)	48.7	72 (n = 487)	14.4	<0.001
Hypertension	313	56.1	185	37	<0.001
Type 2 diabetes mellitus	136	24.4	43	8.6	<0.001
Hyperlipidemia (hypertriglyceridemia)	195 (n = 534)	36.5	75 (n = 487)	15.4	<0.001
Hyperlipidemia (decreased HDL)	183 (n = 522)	35.1	91 (n = 467)	19.5	<0.001

NAFLD – non-alcoholic fatty liver disease; HDL – high-density lipoprotein

Table 3. Concomitant diseases in NAFLD patients and controls

Concomitant diseases	NAFLD (n = 558)	[%]	Controls (n = 500)	[%]	p-value	Odds ratio
Overweight/obesity	451	80.8	204	40.8	<0.0001	6.12
GERD	178	31.9	114	22.8	0.0009	1.59
Colonic diverticulosis	132	23.7	79	15.8	0.0014	1.65
CVD	76	13.6	75	15	0.32	0.89
Cholecystolithiasis	74	13.3	36	7.2	0.0013	1.97
Hypothyroidism	60	10.8	50	10	0.69	1.08
Crohn's disease	60	10.8	38	7.6	0.078	1.46
Ulcerative colitis	53	9.5	54	10.8	0.48	0.87
Cardiac dysrhythmia	43	7.7	30	6.0	0.27	1.31
Pancreatitis	43	7.7	32	6.6	0.41	1.22
Neoplasm	38	6.8	37	7.4	0.71	0.91
Functional GI diseases	20	3.6	47	9.4	0.0001	0.36
Asthma	17	3.0	14	2.8	0.81	1.09
Chronic kidney disease	12	2.1	12	2.4	0.79	0.89
COPD	11	2.0	10	2.0	0.97	0.99

COPD – chronic obstructive pulmonary disease; CVD – cardiovascular disease; GERD – gastroesophageal reflux disease; GI – gastrointestinal.

further diagnostic procedure. Fifteen patients with FIB-4 score above 3.25 are likely to have advanced liver fibrosis. One hundred ninety-one (34.2%) patients with intermediate score 1.45–3.25 require additional diagnostic procedures (Fig. 2). These patients were sent for ambulatory transient elastography.

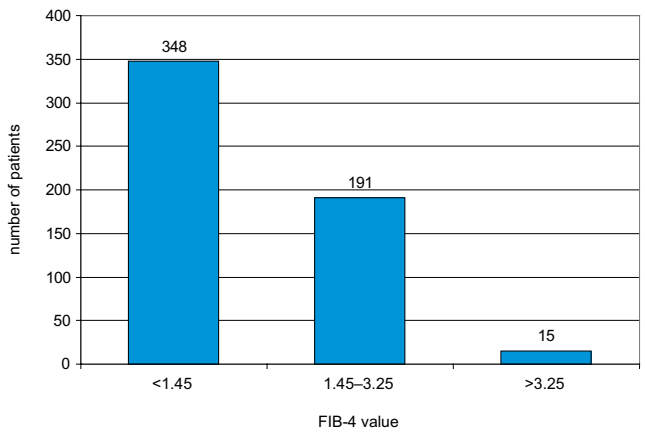

Fig. 2. FIB-4 score in patients with NAFLD

Discussion

Non-alcoholic fatty liver disease, a chronic condition of the liver related to hepatic steatosis, was recently recognized as the most common chronic liver disease. Increasing prevalence rates of the risk factors for NAFLD are the following: obesity, diabetes and metabolic syndrome will most probably result into further increasing incidence rates of NAFLD all over the world.

The mean age of the patients in the study group was 58.1. Non-alcoholic fatty liver disease was found slightly more often in men than in women (not statistically significant difference in our study group). This is consistent with the results of the epidemiological studies performed in the USA. The frequency of hepatic steatosis varies significantly with ethnicity (45% in Hispanics; 33% in Whites; 24% in Blacks).[3] Our study group was monoethnical – 100% individuals were White. We can only estimate the prevalence of hepatic steatosis in all the patients admitted to the gastroenterology department as approx. 25% (558 out of 2,309).

Non-alcoholic fatty liver disease afflicts overweight and obese people and presents the coexistence with

the MetS-associated disorders, like T2DM, hypertension and dyslipidemia.[18] These comorbidities have a negative impact on the natural course of NAFLD.[19] In fact, progression to fibrosis in NAFLD is highly influenced by the presence of T2DM and obesity.[20,21] In a very recent review, authors have mapped shared gene/protein interaction networks and performed gene-disease analysis.[18] Shared mechanisms among NAFLD and the MetS diseases were revealed and provided evidence that NAFLD and especially NASH, requires taking multi-target approaches, rather than focusing on single mechanisms of disease. Indeed, in our study we have confirmed strong connections between either MetS itself or its components and NAFLD. The prevalence of MetS was 48.7%, overweight/obesity was 80.8%, atrial hypertension 56.1%, T2DM 24.4%, hypertriglyceridemia 36.5%, and decreased HDL 35.1%, respectively. The difference in all the cases was significantly different from the corresponding rates in the control group.

Unexpectedly, the frequency of CVD was almost the same in the study group compared to controls (13.6% vs 15%). As patients with NAFLD have features of MetS, they also have important clinical implications for the development of future CVD. Many studies have addressed this issue before, finding the prevalence of CVD significantly higher in NAFLD patients.[22] Recently, a vast European study has been performed in Sweden[23] and its authors claim that it is the largest ever study of biopsy-proven NAFLD. Over 600 patients were followed up during a mean of 20 years. The authors found that death rates due to cardiovascular reasons did not differ statistically in NAFLD group compared to controls. The most common gastrointestinal disease in NAFLD group was GERD. It was statistically more common compared to controls. Large cohort study (over 34,000 participants) showed that NAFLD is not independently associated with the risk of the development of reflux esophagitis after adjusting for BMI and other metabolic factors.[24] The authors suggest that reflux esophagitis is primarily the consequence of increased BMI commonly associated with NAFLD. Probably for the same reason, cholecystolithiasis appeared more often in NAFLD patients, as both diseases share the same main risk factor: overweight and obesity. Moreover, this association is more strongly seen in females than in males.[25]

In the literature there is lacking evidence on connection between NAFLD and colonic diverticulosis. Only 1 case-control study claimed that diverticulosis in the elderly (>65 years) was a negative predictor of liver steatosis.[26] Our findings in the younger group were different. In NAFLD patients, the prevalence of diverticulosis was much higher compared to controls.

We have evaluated the FIB-4 score that is simple and easy to calculate and to estimate the risk of fibrosis in the liver. In our study group, most cases were classified as not having fibrosis, whereas only 1/3 of patients required additional examinations (for instance transient elastography).

Conclusions

Overweight and obesity as well as metabolic syndrome with its components: hypertension, type 2 diabetes mellitus, and dyslipidemia are more common in NAFLD patients compared to matched controls. No significant difference between the study group and controls was found in the frequency of CVD. Additionally, NAFLD patients are more often affected by GERD, colonic diverticulosis and cholecystolithiasis.

ORCID iDs

Radosław Kempiński https://orcid.org/0000-0002-6030-2700
Agata Łukawska https://orcid.org/0000-0002-3766-3073
Filip Krzyżanowski https://orcid.org/0000-0002-7571-7925
Dominika Ślósarz https://orcid.org/0000-0002-8159-1660
Elżbieta Poniewierka https://orcid.org/0000-0002-2074-976X

References

1. Masuoka HC, Chalasani N. Nonalcoholic fatty liver disease: An emerging threat to obese and diabetic individuals. *Ann N Y Acad Sci.* 2013; 1281:106–122.
2. Armstrong MJ, Adams LA, Canbay A, Syn WK. Extrahepatic complications of nonalcoholic fatty liver disease. *Hepatology.* 2014;59(3): 1174–1197.
3. Browning JD, Szczepaniak LS, Dobbins R, Nuremberg P, Horton JD, Cohen JC. Prevalence of hepatic steatosis in an urban population in the United States: Impact of ethnicity. *Hepatology.* 2004;40(6):1387–1395.
4. Blachier M, Leleu H, Peck-Radosavljevic M, Valla DC, Roudot-Thoraval F. The burden of liver disease in Europe: A review of available epidemiological data. *J Hepatol*. 2013;58(3):593–608.
5. Hamaguchi M, Kojima T, Itoh Y, et al. The severity of ultrasonographic findings in nonalcoholic fatty liver disease reflects the metabolic syndrome and visceral fat accumulation. *Am J Gastroenterol.* 2007; 102(12):2708–2715.
6. Musso G, Gambino R, Bo S, et al. Should nonalcoholic fatty liver disease be included in the definition of metabolic syndrome? A cross-sectional comparison with Adult Treatment Panel III criteria in non-obese nondiabetic subjects. *Diabetes Care.* 2008;31(3):562–568.
7. Kwon YM, Oh SW, Hwang SS, Lee C, Kwon H, Chung GE. Association of nonalcoholic fatty liver disease with components of metabolic syndrome according to body mass index in Korean adults. *Am J Gastroenterol*. 2012;107(12):1852–1858.
8. Speliotes EK, Massaro JM, Hoffmann U, et al. Fatty liver is associated with dyslipidemia and dysglycemia independent of visceral fat: The Framingham heart study. *Hepatology.* 2010;51(6):1979–1987.
9. Musso G, Gambino R, Cassader M, Pagano G. Meta-analysis: Natural history of non-alcoholic fatty liver disease (NAFLD) and diagnostic accuracy of noninvasive tests for liver disease severity. *Ann Med.* 2011;43(8):617–649.
10. Musso G, Cassader M, Olivetti C, Rosina F, Carbone G, Gambino R. Association of obstructive sleep apnoea with the presence and severity of non-alcoholic fatty liver disease. A systematic review and meta-analysis. *Obes Rev.* 2013;14(5):417–431.
11. Musso G, Gambino R, Tabibian JH, et al. Association of non-alcoholic fatty liver disease with chronic kidney disease: A systematic review and meta-analysis. *PLoS Med.* 2014;11(7):e1001680.
12. Kopylov U, Ben-Horin S, Lahat A, Segev S, Avidan B, Carter D. Obesity, metabolic syndrome and the risk of development of colonic diverticulosis. *Digestion*. 2012;86(3):201–205.
13. Nagata N, Sakamoto K, Arai T, et al. Visceral abdominal obesity measured by computed tomography is associated with increased risk of colonic diverticulosis. *J Clin Gastroenterol*. 2015;49(10):816–822.
14. Festi D, Schiumerini R, Marzi L, et al. Review article: The diagnosis of non-alcoholic fatty liver disease – availability and accuracy of non-invasive methods. *Aliment Pharmacol Ther.* 2013;37(4):392–400.
15. Kempiński R, Neubauer K, Wieczorek S, Dudkowiak R, Jasińska M, Poniewierka E. 13C-methacetin breath testing in patients with non-alcoholic fatty liver disease. *Adv Clin Exp Med.* 2016;25(1):77–81.

16. Executive Summary of The Third Report of The National Cholesterol Education Program (NCEP) Expert Panel on Detection, Evaluation And Treatment of High Blood Cholesterol In Adults (Adult Treatment Panel III). *JAMA*. 2001;285(19):2486–2497.
17. Sterling RK, Lissen E, Clumeck N, et al. Development of a simple noninvasive index to predict significant fibrosis in patients with HIV/HCV coinfection. *Hepatology*. 2006;43(6):1317–1325.
18. Sookoian S, Pirola CJ. Review article: Shared disease mechanisms between non-alcoholic fatty liver disease and metabolic syndrome – translating knowledge from systems biology to the bedside. *Aliment Pharmacol Ther*. 2019;49(5):516–527.
19. Rinella ME. Nonalcoholic fatty liver disease: A systematic review. *JAMA*. 2015;313(22):2263–2273.
20. Friedman SL, Neuschwander-Tetri BA, Rinella M, Sanyal AJ. Mechanisms of NAFLD development and therapeutic strategies. *Nat Med*. 2018;24(7):908–922.
21. Noureddin M, Rinella ME. Nonalcoholic fatty liver disease, diabetes, obesity, and hepatocellular carcinoma. *Clin Liver Dis*. 2015;19(2):361–379.
22. Targher G, Byrne CD, Lonardo A, Zoppini G, Barbui C. Non-alcoholic fatty liver disease and risk of incident cardiovascular disease: A meta-analysis. *J Hepatol*. 2016;65(3):589–600.
23. Hagström H, Nasr P, Ekstedt M, et al. Fibrosis stage but not NASH predicts mortality and time to development of severe liver disease in biopsy-proven NAFLD. *J Hepatol*. 2017;67(6):1265–1273.
24. Min YW, Kim Y, Gwak GY, et al. Non-alcoholic fatty liver disease and the development of reflux esophagitis: A cohort study. *J Gastroenterol Hepatol*. 2018;33(5):1053–1058. doi:10.1111/jgh.14042
25. Jia L, Haiyan L, Chengqi Z, et al. Non-alcoholic fatty liver disease associated with gallstones in females rather than males: A longitudinal cohort study in Chinese urban population. *BMC Gastroenterol*. 2014;14:213.
26. Sahin A, Tunc N, Demirel U, Poyrazoglu OK, Yalniz M, Bahcecioglu IH. Relationship between diverticulosis and nonalcoholic fatty liver disease in elderly patients. *J Int Med Res*. 2018;46(4):1545–1554.

Distribution of polymorphisms in the *CYP2C19* and *ABCB1* genes among patients with acute coronary syndrome in Lower Silesian population

Tomasz Wójcik[1,A,D], Paweł Szymkiewicz[1,A,D], Jerzy Wiśniewski[2,B,C], Arleta Lebioda[3,B,C], Anna Jonkisz[3,B,C], Andrzej Gamian[2,C,E], Wiktor Kuliczkowski[1,A,E], Krzysztof Ściborski[1,D], Andrzej Mysiak[1,A,E], Marcin Protasiewicz[1,A,D–F]

[1] Department and Clinic of Cardiology, Wroclaw Medical University, Poland
[2] Department and Section of Biochemistry, Wroclaw Medical University, Poland
[3] Section of Molecular Techniques, Wroclaw Medical University, Poland

A – research concept and design; B – collection and/or assembly of data; C – data analysis and interpretation; D – writing the article; E – critical revision of the article; F – final approval of the article

Advances in Clinical and Experimental Medicine, ISSN 1899–5276 (print), ISSN 2451–2680 (online) *Adv Clin Exp Med*. 2019;28(12):1621–1626

Address for correspondence
Tomasz Wójcik
E-mail: t.k.woojcik@gmail.com

Funding sources
None declared

Conflict of interest
None declared

Received on December 11, 2018
Reviewed on March 27, 2019
Accepted on June 27, 2019

Published online on November 28, 2019

Abstract

Background. Dual antiplatelet therapy (DAPT) with aspirin and clopidogrel administered to treat patients with acute coronary syndrome (ACS) is still being used. However, despite the proven efficacy of this treatment regimen, thromboembolic complications have been observed in some individuals. The reason for this phenomenon is linked to the so-called increased responsiveness of platelets despite high platelet resistance (HPR). A significant role in HPR is attributed to genetically determined differences in the absorption and activation of clopidogrel.

Objectives. The aim of the study was to assess the incidence of polymorphisms of the *ABCB1* and *CYPC19* genes that encode proteins involved in the absorption and metabolism of clopidogrel.

Material and methods. The analysis was performed in 199 consecutive patients from Lower Silesian voivodeship (Poland) who underwent coronary angioplasty with stenting for ACS. The single nucleotide polymorphism of the *CYP2C19* and *ABCB1* genes was performed using a mini sequencing or restriction fragment length polymorphism method.

Results. The results of this study revealed the high incidence of patients who may be unresponsive to antiplatelet treatment due to genetic causes. The CYPC19*2 allele in the form of homozygote or mutation heterozygote appeared in 26.1% of the study population. ABCB1 (C3435C> T) polymorphism was associated with 84% of patients. The total incidence of allelic disorders of low drug absorption and metabolism reached 14.6%.

Conclusions. The data obtained should prompt clinicians to use more recent antiplatelet agents (ticagrelor or prasugrel) first, instead of clopidogrel.

Key words: *ABCB1*, clopidogrel, Lower Silesia, polymorphism, *CYP2C9*

Cite as
Wójcik T, Szymkiewicz P, Wiśniewski J, et al. Distribution of polymorphisms in the *CYP2C19* and *ABCB1* genes among patients with acute coronary syndrome in Lower Silesian population. *Adv Clin Exp Med*. 2019;28(12):1621–1626. doi:10.17219/acem/110322

DOI
10.17219/acem/110322

Introduction

Dual antiplatel therapy (DAPT) with aspirin and clopidogrel has until recently been the gold standard for the treatment of acute coronary syndrome (ACS) patients. Nevertheless, despite the proven efficacy of this treatment regimen, thromboembolic complications continue to be observed in some patients.[1,2] The reason for this phenomenon is associated with a so-called sustained increase in platelets activity, in spite of DAPT. This phenomenon may be due to an impaired aspirin response, but it is mainly associated with an ineffective treatment with clopidogrel.

A number of factors contribute to increased platelet reactivity. The lack of expected effects of DAPT is most likely due to non-compliance to treatment recommendations. However, the complexity of genetically conditioned absorption and activation of clopidogrel is also important. The action of clopidogrel is conditioned by the efficacy of the pro-drug conversion into its active form. This process largely depends on intestinal absorption and complex hepatic metabolism. The first step of clopidogrel activation takes place in the gastrointestinal tract. The *ABCB1* gene expression product, P-GP (glycoprotein), plays a key role here. It is a membrane protein of the gastrointestinal tract, which acts to regulate xenobiotics concentrations in the human body, including clopidogrel. Spot mutations in the *ABCB1* gene type C3435C> T, resulting in the emergence of mutation homozygotes (TT) or mutation heterozygotes (CT) in place of proper homozygotes (CC), imply (TT) increased P-GP activity. This activity causes an excessive rejection of clopidogrel, hindering its attainment of adequate plasma concentrations. The polymorphism of this gene has a negative influence on the clinical effects of clopidogrel treatment and may cause high platelet resistance (HPR). An even greater association with individual differences in response to clopidogrel treatment is attributed to cytochrome P450. Its proper functioning allows for the final conversion of clopidogrel to its active metabolite.

Genetic studies are particularly difficult due to the numerous polymorphisms in the genes encoding CYP. CYP2C19, CYP3A4/5 and CYP1A2 are the most well-studied genetic variants. CYP2C19 alleles of type *2–*8 are these that impair the metabolism of clopidogrel. It was observed that having even 1 allele of CYP2C19*2 was associated with worse prognosis in a long-term follow-up of myocardial infarction with respect to the incidence of subsequent myocardial infarction, stroke and death. There have also been more cases of stent thrombosis in these patients.[3,4] The effect of the allele *17 in laboratory conditions is expressed by lower values for maximum platelet aggregation, better platelet inhibition and higher plasma concentrations of the active metabolite.[5] The clinical effect of increased transcriptional activity of this polymorphism was associated with more bleeding. There have been no significant benefits noticed in terms of ischemic events and stent thrombosis.[6]

In our research work, we evaluated the prevalence of polymorphism of major absorption genes (*ABCB1*) and clopidogrel metabolism (CYPC19 *2, *3, *17) in patients treated with coronary angioplasty with stent implantation due to ACS.

Material and method

A total of 199 patients (133 males and 63 females), mean age 65.2 ±11.9 years, randomized to the prospective study, were hospitalized for acute myocardial infarction, including unstable angina, with non ST-elevation myocardial infarction (NSTEMI), and ST-elevation myocardial infarction (ST-elevation MI). All patients engaged in the research were treated according to European Society of Cardiology (ESC) recommendations using coronary angioplasty with stent implantation. The study was approved by the appropriate research ethics committee, and all patients included in the study gave written informed consent. The basic demographic data of patients are presented in Table 1.

Table 1. Demographics

Study group	199
Sex, n (%) male female	 133 (66.8) 66 (33.2)
Age [years]	65.2 ±11.9
Caucasian race, n (%)	199 (100)
Residents of Lower Silesia, n (%)	183 (91.9)
STE-ACS, n (%)	110 (55.3)
NSTE-ACS/UA, n (%)	89 (44.7)
BMI [kg/m^2]	27.7 ±4.0
Diabetes, n (%)	40 (20.1)
Hypertension, n (%) 1st grade 2nd grade 3rd grade	 33 (16.6) 68 (34.1) 37 (18.6)
Serum creatinine concentration [mg/dL]	1.09 ±0.26
eGFR [mL/min/m^2]	70.69 ±18.81
Serum cholesterol [mg/dL]	203.74 ±48.76
LDL serum [mg/dL]	128.52 ±41.08
Smokers, n (%)	69 (34.6)
PLT [1,000/µL]	238.68 ±56.62
MPV [fL]	11.52 ±1.40
Hb [g/dL]	14.42 ±1.76

STE-ACS – ST-elevation acute coronary syndrome; NSTE-ACS – non ST-elevation acute coronary syndrome; UA – unstable angina; BMI – body mass index; eGFR – estimated glomerular filtration; LDL – low-density lipoprotein; PLT – platelet count; MPV – mean platelet volume; Hb – hemoglobin level.

Genetic research

In order to identify genetic polymorphism identification, genetic material was extracted from 200 µL of whole blood

samples of each patient using the High Pure PCR Template Preparation Kit (Roche Diagnostics, Warszawa, Poland). Using the ability of the DNA to bind under certain conditions with silica, centrifugation of the lysate was carried out in a mini column containing the silica membrane, which was then rinsed twice with washing buffer. Finally, the membrane was given a mini column elution buffer to recover the purified DNA. Amplified polymerase chain reaction (PCR) was the next step with the use of 4 pairs of specific primers, respectively for: CYP2C19*17 (-3402C> T), CYP2C19*3, *ABCB1* (C3435C> T) and CYP2C19 *2, as well as Multiplex PCR Kit (Qiagen, Hilden, Germany), according to the manufacturer's instructions. Single-nucleotide (DNA) polymorphism of the CYP2C19*2, *3 and *ABCB1* genes was performed using a mini-sequencing technique, a PCR modification. The SNaPshot Multiplex Kit (Applied Biosystems – Thermo Fisher Scientific, Gdańsk, Poland) was used for the analysis according to the manufacturer's instructions. Purification of the duplicated genetic material was carried out with alkaline phosphatase digestion and exonuclease to eliminate primers and deoxynucleotides that were not consumed in PCR. The mini-sequencing reaction was performed with specific primers designed to hybridize to the template, ending before the designated polymorphic site. Dideoxynucleotide triphosphates (ddNTP), or fluorescent labeled terminators, were involved in the reaction. Product detection was performed with capillary electrophoresis on a 3130 Genetic Analyzer (Applied Biosystems – Thermo Fisher Scientific). The results were analyzed with the use of the GeneMapper ID v. 3.2 program (Applied Biosystems, Foster City, USA) against the internal GeneScan™ LIZ 120 standard. To assess the polymorphism of CYP2C17*17 (locus -3402 C>T), a restriction fragment length polymorphism (RFLP) technique was used.

Division into absorption and metabolic phenotypes

The study population was divided into the group of "good absorbers" (GA), which included the wild-type homozygote (CC), which lacked the C3435C> T spot mutation in the *ABCB1* gene, and the "poor absorbers" group (PA), which included the mutation heterozygotes (CT) and mutation homozygotes (TT) of the *ABCB1* gene.

Alleles that negatively affect clopidogrel metabolism (CYP2C *2, *3), and thus contribute to higher platelet reactivity in laboratory tests, have been assigned to the so-called loss-of-function (LoF) group. In contrast, alleles promoting the effects of clopidogrel (CYP2C *17), thus decreasing platelet aggregation, were given GoF (gain-of-function) name. For the purposes of the present work, patients were eligible for 2 metabolic groups, due to the polymorphism and the onset of the LoF or GoF allele:

– poor metabolizers (PM) – *2 or *3 carriers/non-*17 carriers – individuals with at least 1 LoF allele and no GoF allele;

– not poor metabolizers (NPM) – without the presence of any LoF allele (i.e., *2 and *3) and simultaneously having at least 1 GoF allele (i.e., *17) or patients without LoF (i.e., *2 and *3) and GoF (i.e., *17) or carriers simultaneously with both opposing alleles (*2 or *3 and simultaneously *17).

Patients with both PA and PM (PA + PM) phenotype were also isolated from the study group. The rest of the patients were referred to as not PA + PM.

Results

The basic demographic data of the study population is presented in Table 1. The data is typical of the population with ischemic heart disease.

Genetic research

The incidence of *ABCB1* polymorphism in the study group is shown in Fig. 1. The largest percentage of subjects were heterozygous (57.9%). The minority of the patients were identified as wild-type homozygotes (CC). The incidence of CYP2C19 *2 gene polymorphism is shown in Fig. 2. Most of the variants studied were patients with alleles coding for normal protein activity, but 26.1% of them had at least 1 mutation. No CYP2C19 *3 allele was observed in the study population to reduce the activity of clopidogrel metabolism. A relatively high percentage of heterozygotes and wild-type homozygotes in the CYP2C19*17 allele were found in the study group (Fig. 3).

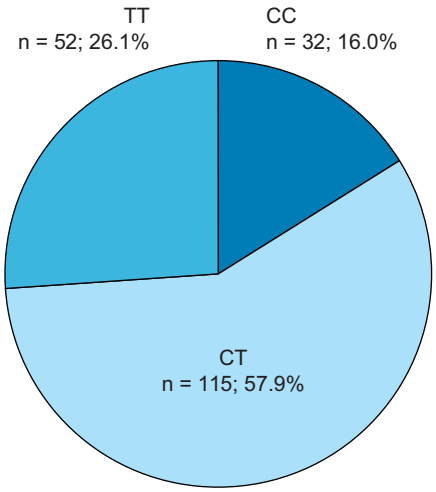

Fig. 1. Frequency of polymorphism of the *ABCB1* gene

CC – wild-type homozygote; CT – mutation heterozygote; TT – mutation homozygote.

Division into absorption and metabolic phenotypes

The incidence of clopidogrel GA and PA patients in the study population is shown in Fig. 4. The majority of the group were PA. Figure 5 shows the percentages

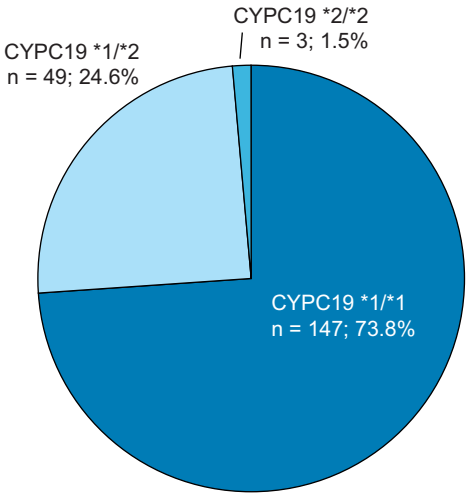

Fig. 2. Frequency of CYPC19*2 polymorphism

*1 – allele of normal CYP2C19 protein function; * 2 – CYP2C19 protein allelic dysfunction; *1/*1 – wild-type homozygote; *1/2 – mutation heterozygote; *2 – mutation homozygote.

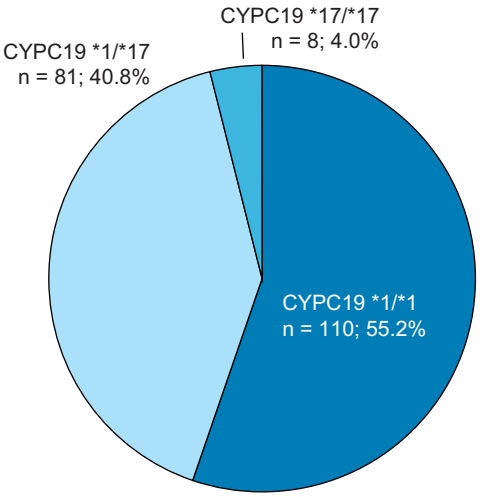

Fig. 3. Frequency of CYPC19 *17 polymorphism

*1 – allele of the normal function of the CYP2C19 protein, *17 – allele improving the function of the CYP2C19 protein, *1/*1 – wild-type homozygote, *17 – mutation heterozygote.

of individual metabolic phenotype in the study population. The relatively high proportion of patients (18%) was found to be PM patients. The simutaneous incidence of PA and PM phenotypes is shown in Fig. 6. As many as 29 patients in the study group were members of this group.

Discussion

In this work, genetic testing was performed in a homogeneous ethnic group of patients with ACS. An important element of the study was the high homogeneity of the study group. Each of the 199 categorized patients was Caucasian, and 92% of the study group were residents of Lower Silesia.

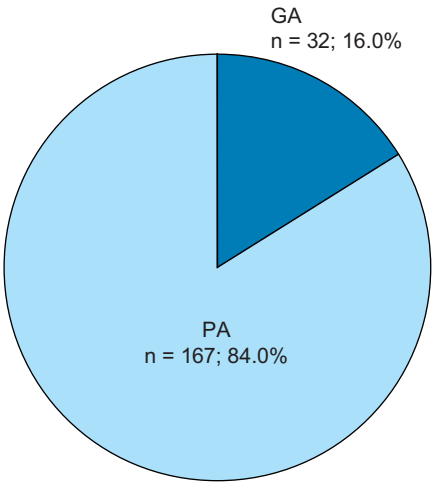

Fig. 4. Division into absorption phenotypes

PA – reduced absorption of clopidogrel; GA – good absorption of clopidogrel.

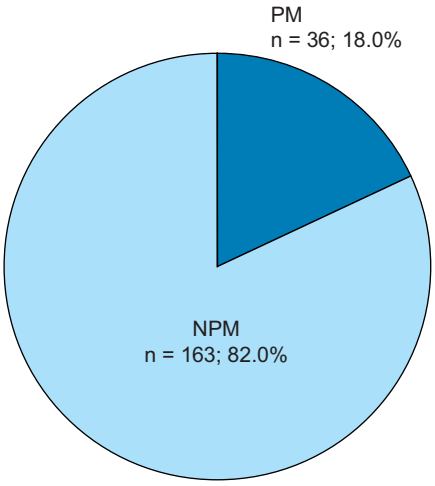

Fig. 5. Division into metabolic phenotypes

PM – poor metabolizers; NPM – not poor metabolizers.

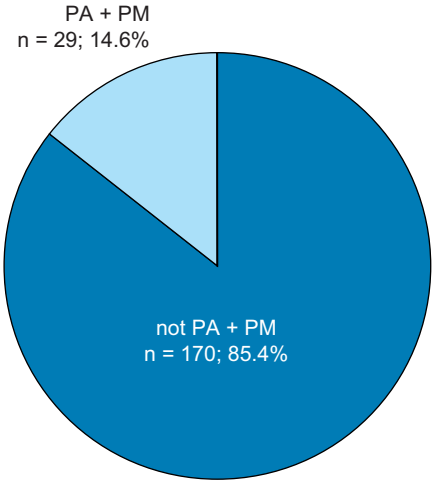

Fig. 6. Incidence of poor phenotype absorption and poor metabolism

PA + PM – reduced absorption plus poor metabolism.

The occurrence of *ABCB1* homozygous mutation polymorphism was demonstrated in 26.1% of the subjects (n = 52), which is comparable to the 27% of the carriers of the modified gene present within the large TRITON-TIMI 38 study, based on a population of nearly 3,000 patients.[7] Analyses concerning the variability of polymorphisms in various ethnic groups have revealed the prevalence of mutation homozygotes in the indigenous population of South America (27%), among Caucasians (20%) and Africans (13%).[8] The distribution of polymorphisms in *ABCB1* genes in the present study (CC 16.0%, CT 57.9%, TT 26.1%) is almost identical to that observed in large, randomized, multicenter studies. The obtained data correlates well with the analysis of genotypes of healthy volunteers in West Pomerania[9] and are slightly different with regards to wild-type homozygotes and heterozygotes among ACS patients in the population of Warszawa (CC 28%, CT 51%, TT 21%). However, the homozygous mutations percentage is very alike in different groups, as demonstrated in the study by Śpiewak et al.[10]

The incidence of particular polymorphisms of the CYP2C19 variant depends on the ethnic group under consideration. The differences apply to each of the alleles being analyzed.

One of the dysfunctional alleles, CYP2C19*2, has been found in the East Asian population in the amount of up to 55%. Among Africans, this polymorphism was observed in 40% of the subjects, and in the Caucasian population in Europe, the prevalence of CYP2C19 *2 was reported in 30% of the subjects.[11] In France, Collet et al. analyzed 259 patients with ACS episode. In their work, the wild-type homozygotes group of CYP2C19*1/*1 variant embraced 72% of the subjects, heterozygote *1/*2 25%, and mutation homozygote *2/*2 – only 2%.[4] Almost identical results were obtained in German and Portuguese populations, and only slightly different results – in Hungarian population.[12–14] As far as we know, the research on the prevalence of this polymorphism in the Polish population was conducted only once in a study by Malek et al.[15] The authors reported that wild-type homozygotes appear in 80% of the population, heterozygotes in 18% and mutation homozygotes in 2%. Our study has shown 73.9% of wild-type homozygotes, 24,6% of heterozygotes and 1,5% of mutation homozygotes; therefore, the data confirms the predecessors' observations.

The CYP2C19 *3 allele frequencies tend to vary across human populations. Most often this polymorphism is observed in East Asia. The incidence of *1/*3 genotype was reported by Jeong et al. at the level of 11%.[16] In Africa and Europe, this allele is much less frequent and sporadically exceeds 1%. In the Italian population, this percentage was reported at 1.6%[17] and in Russian population at 0.3%.[18] In our group of 188 patients, there was no single CYP2C19*3 mutation. To the best of our knowledge, our study is the first work which investigates the incidence of the CYP2C19*3 allele in the Polish population. The results confirm poor inspection of the discussed allele in this part of Europe.

Recently, CYP2C19*17 allele has been the most frequently reported polymorphism. In Europe, the heterozygous form of CYP2C19*17 allelic variant can be found in 31.7% of the population on average and the mutation homozygous – in 4.2%. Thus, the differences concern populations all over Europe. In Germany, the incidence of at least 1 allele *17 was reported at the frequency of 41%, in France 20% and in Sweden 18%.[5,6,11] In Poland, Kurzawski et al. analyzed the distribution of these polymorphisms in a group of 125 patients and found allele *17 in 27.2% of patients.[20] Widespread dissemination of the allele polymorphism in Africa is rarely reported in literature, but some reports indicate a frequency similar to that of the Caucasian population.[21] The incidence of the allele *17 in the Japanese population is estimated at 1.3%[22] and Chinese at 4%.[5] In our study on CYP2C19*17 polymorphisms, a higher incidence of this allele (40.8% heterozygous individuals and 4% homozygotes) was found, compared to the study by Kurzawski et al.[9] Nevertheless, when results obtained in this study are compared with those from a large group of over 1,500 German patients, one will find them to be very similar.[6] They also correspond to the results of studies conducted and published in Poland by Kubica et al.[23]

In the study, the prevalence of the phenotype absorption and metabolism was assessed for the first time in the Polish population. As many as 14.6% of patients showed a cumulative occurrence of the polymorphism of the investigated genes which condition the malabsorption of clopidogrel and its impaired metabolism. The use of clopidogrel in this group of patients may pose a particular risk of achieving an inadequate effect of the drug and, hence, the risk of thromboembolic complications with all clinical implications.

The reported variability in polymorphism frequency, with confirmation of increased platelet reactivity despite clopidogrel administration, is a serious clinical problem. The presence of these polymorphisms is an independent and contributing factor to HPR and thromboembolic complications following ACS. This data, confirming a relatively high level of penetration in the area of clopidogrel polymorphisms, should prompt Polish clinicians to recommend firstly the most recent antiplatelet drugs (ticagrelor or prasugrel), in spite of significantly higher costs of such pharmacotherapy for their patients.

ORCID iDs

Tomasz Wójcik https://orcid.org/0000-0001-9987-4872
Paweł Szymkiewicz https://orcid.org/0000-0002-8469-6871
Jerzy Wiśniewski https://orcid.org/0000-0003-2831-7643
Arleta Lebioda https://orcid.org/0000-0001-5802-2155
Anna Jonkisz https://orcid.org/0000-0001-6916-4212
Andrzej Gamian https://orcid.org/0000-0002-2206-6591
Wiktor Kuliczkowski https://orcid.org/0000-0001-6284-0820
Krzysztof Ściborski https://orcid.org/0000-0002-3922-2861
Andrzej Mysiak https://orcid.org/0000-0002-4728-2565
Marcin Protasiewicz https://orcid.org/0000-0003-0253-0585

References

1. Schomig A, Neumann FJ, Kastrati A, et al. A randomized comparison of antiplatelet and anticoagulant therapy after the placement of coronary-artery stents. *N Engl J Med*. 1996;334(17):1084–1089.
2. Claeys MJ. Antiplatelet therapy for elective coronary stenting: A moving target. *Semin Vasc Med*. 2003;3(4):415–418.
3. Mega JL, Close SL, Wiviott SD, et al. Cytochrome p-450 polymorphisms and response to clopidogrel. *N Engl J Med*. 2009;360(4): 354–362.
4. Collet JP, Hulot JS, Pena A, et al. Cytochrome P450 2C19 polymorphism in young patients treated with clopidogrel after myocardial infarction: A cohort study. *Lancet*. 2009;373(9660):309–317.
5. Sim SC, Risinger C, Dahl ML, et al. A common novel CYP2C19 gene variant causes ultrarapid drug metabolism relevant for the drug response to proton pump inhibitors and antidepressants. *Clin Pharmacol Ther.* 2006;79(1):103–113.
6. Sibbing D, Koch W, Gebhard D, et al. Cytochrome 2C19*17 allelic variant, platelet aggregation, bleeding events, and stent thrombosis in clopidogrel-treated patients with coronary stent placement. *Circulation*. 2010;121(4):512–518.
7. Murphy SA, Antman EM, Wiviott SD, et al; TRITON-TIMI 38 Investigators. Reduction in recurrent cardiovascular events with prasugrel compared with clopidogrel in patients with acute coronary syndromes from the TRITON-TIMI 38 trial. *Eur Heart J*. 2008;29(20): 2473–2479.
8. Santos PC, Soares RA, Santos DB, et al. CYP2C19 and *ABCB1* gene polymorphisms are differently distributed according to ethnicity in the Brazilian general population. *BMC Med Genet*. 2011;12:13.
9. Kurzawski M, Pawlik A, Czerny B, Domański L, Rózański J, Droździk M. Frequencies of the common promoter polymorphisms in cytokine genes in a Polish population. *Int J Immunogenet*. 2005;32(5):285–291.
10. Śpiewak M, Malek LA, Kostrzewa G, et al. Influence of C3435T multidrug resistance gene-1 (*MDR-1*) polymorphism on platelet reactivity and prognosis in patients with acute coronary syndromes. *Kardiol Pol*. 2009;67(8):827–834.
11. Desta Z, Zhao X, Shin JG, Flockhart DA. Clinical significance of the cytochrome P450 2C19 genetic polymorphism. *Clin Pharmacokinet*. 2002;41(12):913–958.
12. Sibbing D, Stegherr J, Latz W, et al. Cytochrome P450 2C19 loss-of-function polymorphism and stent thrombosis following percutaneous coronary intervention. *Eur Heart J*. 2009;30(8):916–922.
13. Teixeira R, Monteiro P, Marques G, et al. CYP2C19*2 and prognosis after an acute coronary syndrome: Insights from a Portuguese center. *Rev Port Cardiol.* 2012;31(4):265–273.
14. Rideg O, Haber A, Botz L, et al. Pilot study for the characterization of pharmacogenetically relevant CYP2D6, CYP2C19 and *ABCB1* gene polymorphisms in the Hungarian population. *Cell Biochem Funct*. 2011;29(7):562–568.
15. Malek LA, Przyluski J, Spiewak M, et al. Cytochrome P450 2C19 polymorphism, suboptimal reperfusion and all-cause mortality in patients with acute myocardial infarction. *Cardiology*. 2010;117(2):81–87.
16. Jeong YH, Tantry US, Kim IS, et al. Effect of CYP2C19*2 and *3 loss-of-function alleles on platelet reactivity and adverse clinical events in East Asian acute myocardial infarction survivors treated with clopidogrel and aspirin. *Circ Cardiovasc Interv*. 2011;4(6):585–594.
17. Scordo MG, Caputi AP, D'Arrigo C, Fava G, Spina E.Allele and genotype frequencies of CYP2C9, CYP2C19 and CYP2D6 in an Italian population. *Pharmacol Res*. 2004;50(2):195–200.
18. Gaikovitch EA, Cascorbi I, Mrozikiewicz PM, et al. Polymorphisms of drug metabolizing enzymes CYP2C9, CYP2C19, CYP2D6, CYP1A1, NAT2 and of P-glycoprotein in a Russian population. *Eur J Clin Pharmacol*. 2003;59(4):303–312.
19. Frere C, Cuisset T, Gaborit B, Alessi MC, Hulot JS. The CYP2C19*17 allele is associated with better platelet response to clopidogrel in patients admitted for non-ST acute coronary syndrome. *J Thromb Haemost*. 2009;7(8):1409–1411.
20. Kurzawski M, Gawrońska-Szklarz B, Wrześniewska J, Siuda A, Starzyńska T, Droździk M. Effect of CYP2C19*17 gene variant on *Helicobacter pylori* eradication in peptic ulcer patients. *Eur J Clin Pharmacol*. 2006;62(10):877–880.
21. Janha RE, Sisay-Joof F, Hamid-Adiamoh M, et al. Effects of genetic variation at the CYP2C19/CYP2C9 locus on pharmacokinetics of chlorcycloguanil in adult Gambians. *Pharmacogenomics*. 2009;10(9):1423–1431.
22. Sugimoto K, Uno T, Yamazaki H, Tateishi T. Limited frequency of the CYP2C19*17 allele and its minor role in a Japanese population. *Br J Clin Pharmacol*. 2008;65(3):437–439.
23. Kubica A, Kozinski M, Grzesk G, Fabiszak T, Navarese EP, Goch A. Genetic determinants of platelet response to clopidogrel. *J Thromb Thrombolysis*. 2011;32(4):459–466.

New colon anatomy-related ratios used to predict the course of colonoscopy in children

Sławomir Woźniak[1,A–E], Tomasz Pytrus[2,A–C,E,F], Marek Woynarowski[3,C,E,F], Bartosz Puła[4,C,E,F], Zygmunt Domagała[1,E,F], Barbara Iwańczak[2,C,E,F]

[1] Department of Human Morphology and Embryology, Division of Anatomy, Wroclaw Medical University, Poland
[2] 2nd Department and Clinic of Pediatrics, Gastroenterology and Nutrition, Wroclaw Medical University, Poland
[3] Department of Gastroenterology, Hepatology and Immunology. The Children's Memorial Health Institute, Warszawa, Poland
[4] Department of Hematology, Institute of Hematology and Transfusion Medicine, Warszawa, Poland

A – research concept and design; B – collection and/or assembly of data; C – data analysis and interpretation; D – writing the article; E – critical revision of the article; F – final approval of the article

Advances in Clinical and Experimental Medicine, ISSN 1899–5276 (print), ISSN 2451–2680 (online) *Adv Clin Exp Med*. 2019;28(12):1627–1632

Address for correspondence
Sławomir Woźniak
E-mail: slawomir.wozniak@umed.wroc.pl

Funding sources
None declared

Conflict of interest
None declared

Received on June 29, 2018
Reviewed on September 10, 2018
Accepted on February 18, 2019

Published online on April 19, 2019

Abstract

Background. In children, colonoscopy is a safe procedure, although it is more difficult to perform in patients whose body mass index (BMI) is under 25.

Objectives. The aim of the study was to establish the relationship between children's age, body mass and height and incomplete colonoscopies due to colon anatomy.

Material and methods. A retrospective evaluation of diagnostic endoscopies in 403 children aged 3–18 years (192 girls and 211 boys) was performed. New ratios were introduced: the incomplete colonoscopy anatomy-related ratio (ICAR) and the modified incomplete colonoscopy anatomy-related ratio (MICAR).

Results. The terminal ilium was not reached in 59 children: 27 girls and 32 boys (14.6% of patients). In 13 girls and 18 boys (comprising 7.69% of the study population) no pathological causes were found for the incomplete colonoscopy. There were statistically significant differences concerning colon anatomy-related incomplete colonoscopies in relation to the children's weight. No significance was found in relation to height or age. Incomplete examinations were more frequent in patients weighing less than 30 kg ($p = 0.0006$), both in boys ($p = 0.0090$) and girls ($p = 0.048$). The risk of incomplete colonoscopy (odds ratio – OR) in boys and girls weighing less than 30 kg was 3.995 (95% CI = 1.489–10.720) and 3.373 (95% CI = 1.078–10.560), respectively. For this group of patients, the ICAR ranged between 0.0309 and 0.1889, while the MICAR range was 0.0–0.1889.

Conclusions. Body mass is a statistically significant factor for evaluating the risk of incomplete colonoscopies in children. The lower the ICAR and MICAR values, the lower the risk of non-completion of a colonoscopy due to anatomical (i.e., disease-unrelated) causes.

Key words: pediatric colonoscopy, incomplete colonoscopy, colon anatomy-related incomplete colonoscopy

Cite as
Woźniak S, Pytrus T, Woynarowski M, Puła B, Domagała Z, Iwańczak B. New colon anatomy-related ratios used to predict the course of colonoscopy in children. *Adv Clin Exp Med*. 2019;28(12):1627–1632. doi:10.17219/acem/104547

DOI
10.17219/acem/104547

Introduction

The large intestine (LI) is evaluated using various diagnostic methods,[1] and data defining the colon provided by different authors can differ to a great degree.[2,3]

The number of flexures in the LI is usually 9–10, but it may be as high as 19.[2,4,5] The right colic flexures (RCF), left colic flexures (LCF) and the descending-sigmoid flexure (DSF) constitute sections with significantly limited mobility. Due to their attachment to the mesentery, the transverse colon (TC) and the sigmoid colon (SC) are the most movable sections. We refer to such segments as critical points (CPs). Previously published papers have provided a detailed assessment of the morphology of the entire LI, the mesentery and an analysis of position alterations of selected CPs (e.g., the RCF, LCF and DSF) in relation to the abdominal cavity, secondary to changes in body position.[6,7] The entire length of the LI is 56.5 ±2.7 cm in infants, 107.8 ±4.5 cm in 2-year-olds, 122.4 ±5.7 cm in 5-year-olds, and up to 180–190 cm in adults.[3,5,7]

Optical colonoscopy is the gold standard for the evaluation of the colon.[2,8] One of the quality parameters of endoscopy is intubation of the terminal ileum (TI) through the ileocecal valve.[9–12] Inserting the endoscope into the cecum is recommended in ≥90% of routine examinations and in ≥95% of screening examinations.[13,14] Difficulties associated with the insertion of the endoscope can be overcome by maneuvers such as changing the patient's position or pressing the patient's abdominal wall. If these techniques fail, another colonoscope or a gastroscope may be used.[15–17]

One of the indirect parameters related to insertion difficulties and the anatomic complexity of the LI is the time needed to reach the cecum.[18–20] Previous research has analyzed in particular the relationship between colonoscopic difficulties and the patients' gender, age, body mass and height, body mass index (BMI), waist circumference, and intra-abdominal fat.[6,15,18–21] Complications related to instrument insertion, including intestinal perforation, occur in only a minor percentage of patients.[22,23]

The aim of this study was to establish the relationships between the age, body mass and height of the children and incomplete colonoscopies due to colon anatomy-related difficulties.

Material and methods

The paper is based on a 5-year retrospective observational study (2012–2016), performed according to the Declaration of Helsinki and approved by the Wroclaw Medical University Bioethics Committee (resolution No. 667/2017). The colonoscopies were performed under general anesthesia at the 2nd Pediatrics, Gastroenterology and Nutrition Department at Wroclaw Medical University, Poland. The colonoscopic examinations were performed in the same conditions (between 8 a.m. and 2 p.m., in the same lab with the same personnel and equipment). All the examinations were performed by 2 specialists in gastroenterology with more than 10 years of experience in endoscopy, both holding the Polish Society of Gastroenterology Certificate of Advanced Skills in Colonoscopy.

The study included 403 children (192 girls and 211 boys) aged from 3 to 18 years. The body mass of the patients ranged between 12 kg and 92 kg, and the body height was between 92 cm and 188 cm. Every child's weight and height were measured on the day of colonoscopy. The preparation of the LI was either very good or good (8–9 points according to the Boston Bowel Preparation Scale).

Indications for the examination included inflammatory bowel disease (IBD) in 290 cases (199 follow-up examinations to assess current disease activity and 91 cases of suspected IBD), and gastrointestinal bleeding in the remaining 113 cases.

Written informed consent of the parent or legal guardian was obtained before the examination. The colonoscopies were performed with Olympus CFQ 165 L and PCF 160 AL colonoscopes (Olympus Corp., Tokyo, Japan) and the Pentax EC 3840MK2 colonoscope (Pentax Medical, Tokyo, Japan). The small number of examinations ensured that there was no wearing or tearing of scopes in the period analyzed. The patients' medical history was obtained, including past abdominal surgery. Typical pre-exam preparations involved purging with macrogol (Fortrans®; Ipsen Pharma, Paris, France), dosed according to body mass, orally or via a gastric tube; additionally, on the preceding day and the examination day, enemas were performed with solutions of hydrogen phosphates (Enema®; Laboratorium Galenowe Olsztyn, Olsztyn, Poland, or Rectanal®; Farmaceutyczno-Chemiczna Spółdzielnia Pracy Galenus, Warszawa, Poland). In the case of 24 children over the age of 15, an oral phosphate product was used (Fleet Phosphosoda®; Labarotorios Casen-Fleet S. L., Zaragoza, Spain).

An examination in which the colonoscope reached the TI was considered a complete colonoscopy (CC); if the colonoscope did not reach the TI, the examination was regarded as an incomplete colonoscopy (IC). The ICs were divided into 2 subgroups: incomplete pathological colonoscopies (IPCs) and incomplete anatomy-related colonoscopies (IACs). Incomplete pathological colonoscopies were primarily caused by major inflammatory changes in the LI, posing a risk of perforations; IACs were those involving unusual LI anatomy or unknown causes.

The data obtained were used to calculate 2 ratios that estimate the risk of performing an incomplete colonoscopy for non-pathological causes (anatomic or unknown) in children with specific characteristics, e.g., age, body mass or height. We retrospectively calculated these indices (i.a., related to complex bowel anatomy and the given technical scope of the examiner) for our study cohort in order to apply them in subsequent examinations of children with similar demographic parameters.

The incomplete colonoscopy anatomy-related ratio (ICAR)

$$ICAR = IAC : CC$$

where IAC is the number of incomplete colonoscopies with anatomical or unknown causes and CC is the number of complete colonoscopies. The smaller the value of the index, the higher the chance of performing a complete colonoscopy. For example, if a single IAC occurred in a group of 100 examined children aged X, the calculated index value would be 0.01. This value means that in a given lab, it is to be expected that an examination will fail for anatomical or unknown reasons in 1 future case out of 100.

The modified incomplete colonoscopy anatomy-related ratio (MICAR)

The second ratio refers to the reducing possibility of not completing the examination due to anatomical reasons after reaching subsequent CPs.

$$MICAR_{(CP)} = IACCP : CC$$

where IACCP is the number of incomplete colonoscopies (for anatomical or unknown reasons) that occurred before a particular analyzed CP, and CC is the number of complete colonoscopies. The IACCP is calculated by subtracting the number of examination interruptions at CPs already passed by the colonoscope from the total number of IACs. Assuming hypothetically that 100 examinations were performed in a cohort with certain demographic characteristics, of which 5 were ended at the splenic flexure and 4 at the hepatic flexure (a total of 9 incomplete exams), then as the scope approaches the splenic flexure the value of the index is 0.09; after it passes the LCF, the index drops to 0.04; after it passes the RCF, the index drops to 0.0. The index value indicates that in subsequent examinations, the risk of discontinuation at the LCF is 9 in 100, while after passing the LCF, it falls to 5 in 100, and after passing the RCF, there is no risk that the examination will be discontinued.

The ICAR is a fixed value for a given patient group, while the MICAR reflects the risk of non-completion decreasing as the scope passes subsequent bowel segments and flexures. We define difficult colon anatomy as a complicated 3D structure that causes an incomplete colonoscopy because of its flexures and/or atypical mesenteries.

Statistical analysis

The statistical analysis was carried out using STATISTICA v. 12 software (StatSoft Inc., Tulsa, USA). The χ^2 test and Fisher's exact test were used for qualitative data analysis. Relevant confidence intervals were estimated (95% CI). Relative risk (RR), sensitivity and specificity of the parameters studied were determined. The significance level for the study was $p < 0.05$.

Results

In 290 cases the examination confirmed IBD, while in the remaining 113 children the causes were as follows: 34 cases of gastrointestinal tract infections (among them *Campylobacter*, *Yersinia* or *Clostridium*); 10 cases of Meckel's diverticulum (the patients had isotope scans; 8 children underwent surgery, while the symptoms of the other 2 subsided with conservative management); 5 cases of isolated rectal ulcers; 8 cases of familial polyposis; 8 cases of polyps unrelated to polyposis; and in the remaining 48 cases, the cause of the presenting complaints remained unidentified. Some of these 48 children suffered from chronic constipation and we presume that the bleeding was related to lesions in the sphincter area (the bleeding coincided with the passing of stool). Some of the patients underwent magnetic resonance (MR) enterography due to suspected small bowel hemorrhage, but the examinations failed to provide a final diagnosis. The colonoscopy results are shown in Fig. 1.

In 15 of the IACs, the colonoscopy stopped at the RCF; in 13 at the LCF; and in 3 in the TC. None of the endoscopic examinations were interrupted in the SC or at the DSF. The detailed demographics of the children with IACs are shown in Table 1.

In the statistical analysis, the χ^2 test showed that ICs were more frequent in children weighing less than 30 kg ($p = 0.0006$), both in boys ($p = 0.009$) and in girls ($p = 0.048$).

The risk of an IC (the odds ratio – OR) in patients weighing less than 30 kg was 3.995 (95% CI = 1.489–10.720) and 3.373 (95% CI = 1.078–10.560) in boys and girls, respectively. There were no statistically significant relationships between the completion of the examination and the gender, height or age of the patients.

We used the ICAR and MICAR to explore the relationships between incomplete colonoscopies due to anatomical or unknown causes and the total number of colonoscopies in the examined groups. The calculated values of the ICAR

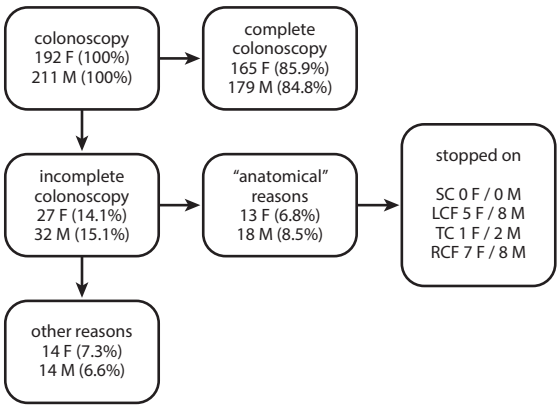

Fig. 1. Colonoscopy results

SC – sigmoid colon; LCF – left colic flexure; TC – transverse colon; RCF – right colic flexure.

Table 1. Incomplete colonoscopies in relation to the demographics of the children

Demographics		Number of patients	LCF		TC		RCF	
			F	M	F	M	F	M
Age [years]	≤6	47	2	3	0	0	0	0
	7–10	78	0	3	1	1	1	0
	11–14	127	2	1	0	1	2	3
	15–18	151	1	1	0	0	4	5
Body height [cm]	≤120	43	1	2	0	0	0	0
	121–130	55	1	2	1	0	1	1
	131–140	78	1	1	0	0	2	2
	141–150	108	1	1	0	1	2	2
	≥151	119	1	2	0	1	2	3
Body mass [kg]	≤30	109	4	6	1	2	2	2
	31–50	104	1	1	0	0	2	2
	51–70	108	0	1	0	0	1	1
	≥71	82	0	0	0	0	2	3

LCF – left colic flexure; RCF – right colic flexure; TC – transverse colon; F – female; M – male.

Table 2. Values of ICAR and MICAR in relation to the demographics of the children examined (both genders)

Demographics		Number of patients	ICAR	$MICAR_{DSF}$	$MICAR_{LCF}$	$MICAR_{TC}$	$MICAR_{RCF}$
Age [years]	≤6	47	0.1250	0.1250	0.1250	0.0	0.0
	7–10	78	0.0895	0.0895	0.0895	0.0448	0.0149
	11–14	127	0.0818	0.0818	0.0818	0.0545	0.0454
	15–18	151	0.0866	0.0866	0.0866	0.0709	0.0709
Body height [cm]	≤120	43	0.0857	0.0857	0.0857	0.0	0.0
	121–130	55	0.1304	0.1304	0.1304	0.0652	0.0435
	131–140	78	0.0882	0.0882	0.0882	0.0588	0.0588
	141–150	108	0.0737	0.0737	0.0737	0.0526	0.0421
	≥151	119	0.09	0.09	0.09	0.06	0.05
Body mass [kg]	≤30	109	0.1889	0.1889	0.1889	0.0778	0.044
	31–50	104	0.0652	0.0652	0.0652	0.0435	0.435
	51–70	108	0.0309	0.0309	0.0309	0.0206	0.0206
	≥71	82	0.0769	0.0769	0.0769	0.0769	0.0769

ICAR – incomplete colonoscopy anatomy-related ratio; MICAR – modified incomplete colonoscopy anatomy-related ratio; LCF – left colic flexure; RCF – right colic flexure; DSF – descending-sigmoid flexure; TC – transverse colon; F – female; M – male.

and MICAR in individual patient groups are presented in Table 2.

The ICAR and MICAR are shown in Fig. 2. We present only the data for children weighing no more than 30 kg, since the results for this group were statistically significant.

Discussion

The majority of the children examined suffered from IBD, which, paradoxically, may facilitate performing colonoscopies due to the rigidity of the gastrointestinal wall observed in such patients.

The ICAR and MICAR may be easier to understand for a child's parents than RR and OR. These ratios are easy to calculate and help evaluate the risk of IACs in the future on the basis of retrospective data. It is important to use these ratios together, i.e., to assess the combined risk of IACs for the age, body mass and height of a child. In our group of patients, the MICAR is equal to the ICAR up to the LCF, because none of the examinations were interrupted in the SC, which is in contrast with other studies, which describe the SC as being more complex from an anatomical point of view.[2,4]

In this paper we are reporting the ICAR and MICAR for the first time. Therefore, we do not suggest reference ranges. No prior study has attempted to estimate correlations between the assessed demographic parameters of pediatric subjects and the causes of incomplete colonoscopy unrelated to disease. Madiba et al. found that the SC is significantly

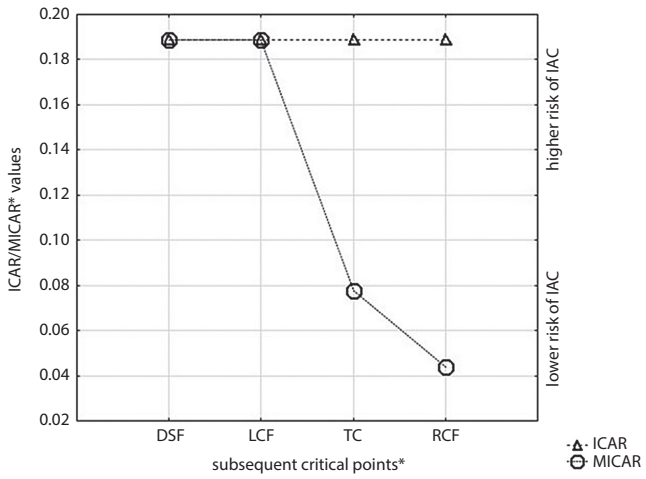

Fig. 2. ICAR/MICAR values at consecutive critical points

ICAR – incomplete colonoscopy anatomy-related ratio; MICAR – modified incomplete colonoscopy anatomy-related ratio; DSF – descending-sigmoid flexure; LCF – left colic flexure; TC – transverse colon; RCF – right colic flexure.

elongated in adults.[24,25] In our opinion, the SC may adapt its structure (length in particular) to the digestive lifestyle of the patients (for example, different defecation frequencies or stool volumes). The SC is longer in Africans, whereas their mesentery is comparatively narrower; older age is associated with an elongation of the entire colon, reduced elasticity of the colon wall and an increase in colon laxity.[26] However, in the present study, we cannot compare properties of the bowel (length and number of flexures) in the respective groups (defined by age, body mass and height) and their relationship with failed colonoscopies.

Elongation of the colon and/or complex colonic anatomy may be reflected in an increase in the time required to insert the colonoscope into the cecum. Hsieh et al. reported that time to be longer in women.[19] Sadahiro et al. demonstrated that elongation of the LI occurred along with increases in body mass and height; however, this correlation was not found in males.[26] This hypothesis was not confirmed by the results of our study. Other authors have also found no differences between the genders.[24,25,27]

Other authors have demonstrated a relationship between BMI and the duration of a colonoscopy.[28] There is more intra-abdominal fat in obese patients, which contributes to the rigidity of the mesentery; therefore, the possibility of the endoscope looping is reduced to a minimum. In addition, obese or overweight adults are reported to have shorter colons.[5] Our findings confirm this observation: In the present study there were more complete colonoscopies in heavier (>30 kg) patients than in lighter ones.

Our results may also confirm the observations of Hsieh et al., who indicated that waist circumference (larger waist circumference associated with a shorter insertion time) is the most important factor for a prognosis of difficulties with endoscope insertion.[19] Hanson et al. stated that ICs are more frequent in patients with BMIs <25.[4] Other authors agree with the idea of the significance of body fat for the performance of endoscopies.[2,18,20] In our group, a substantial proportion of patients demonstrated varying degrees of undernourishment due to their underlying disease, which also contributed to the incomplete examinations. Others authors' observations contradict these statements; Khashab et al. reported that a higher proportion of ICs can be attributed to relatively longer colons in patients whose BMIs are ≤25, and in women.[5]

Struijs et al. estimated the length of the LI as 122.4 cm in children aged 5, or with a body mass of 20 kg, or a body height of approx. 120 cm. The LI gradually increases in length up to the age of 5; from then on, LI length does not increase significantly. According to those authors, the height of a child is the best factor for estimating the length of the LI.[3]

We agree that a colonoscopist's experience is one of the most significant factors affecting the success of the examination.[29,30] We also share the prevailing view that the entire endoscopic team should exclusively perform pediatric endoscopies.[31] As far as complications are concerned, we observed only minor bleeding in individual cases. Other studies confirm that the examination is safe (a complication rate of less than 1%).[12,22,23] Previous papers have described difficulties associated with the examination in patients who have undergone prior surgery, especially in the lesser pelvis. These difficulties primarily resulted from SC immobilization and a higher number of SC flexures.[4] A small proportion of our patients had a history of surgery, usually involving partial resections of the ileocecal valve with end-to-end anastomosis, which had no significant effect on the examinations.

Thakkar et al. reported that up to 15% of colonoscopies do not reach the cecum.[12] Our results are similar.

Our study had certain limitations. There were difficulties associated with the analysis of ICs and IACs; we were unable to predict the course of a colonoscopy in subsequent LI segments (whether the examination would be complete or whether it would come to an end at the next CP). Also, the study was limited to a specific group of children; the majority of them suffered from IBD, but the examinations were not carried out during active phases of the disease.

Conclusions

Based on the results of our study, the following conclusions may be drawn: 1. Patients weighing up to 30 kg are highly prone to incomplete colonoscopies due to the specific anatomy of the LI. 2. Anatomy-related colonoscopy incompletion did not significantly correlate with the height and/or age of the patients. 3. The ICAR and MICAR are useful in predicting LI anatomy-related non-completion of colonoscopies and in presenting the risk to the patients' parents in an easily comprehensible way.

References

1. Bourgouin S, Bège T, Lalonde N, et al. Three-dimensional determination of variability in colon anatomy: Applications for numerical modeling of the intestine. *J Surg Res*. 2012;178(1):172–180.
2. Eickhoff A, Pickhardt PJ, Hartmann D, Riemann JF. Colon anatomy based on CT colonography and fluoroscopy: Impact on looping, straightening and ancillary maneuvers in colonoscopy. *Dig Liver Dis*. 2010;42(4):291–296.
3. Struijs M-C, Diamond IR, de Silva N, Wales PW. Establishing norms for intestinal length in children. *J Pediatr Surg*. 2009;44(5):933–938.
4. Hanson ME, Pickhardt PJ, Kim DH, Pfau PR. Anatomic factors predictive of incomplete colonoscopy based on findings at CT colonography. *AJR Am J Roentgenol*. 2007;189(4):774–779.
5. Khashab MA, Pickhardt PJ, Kim DH, Rex DK. Colorectal anatomy in adults at computed tomography colonography: Normal distribution and the effect of age, sex, and body mass index. *Endoscopy*. 2009;41(8):674–678.
6. Alazmani A, Hood A, Jayne D, Neville A, Culmer P. Quantitative assessment of colorectal morphology: Implications for robotic colonoscopy. *Med Eng Phys*. 2016;38(2):148–154.
7. Punwani S, Halligan S, Tolan D, Taylor SA, Hawkes D. Quantitative assessment of colonic movement between prone and supine patient positions during CT colonography. *Br J Radiol*. 2009;82(978):475–481.
8. Spada C, Hassan C, Barbaro B, et al. Colon capsule versus CT colonography in patients with incomplete colonoscopy: A prospective, comparative trial. *Gut*. 2015;64(2):272–281.
9. Brenner H, Chang-Claude J, Jansen L, Seiler CM, Hoffmeister M. Role of colonoscopy and polyp characteristics in colorectal cancer after colonoscopic polyp detection: A population-based case-control study. *Ann Intern Med*. 2012;157(4):225–232.
10. Kaminski M, Hassan C, Bisschops R, et al. Advanced imaging for detection and differentiation of colorectal neoplasia: European Society of Gastrointestinal Endoscopy (ESGE) Guideline. *Endoscopy*. 2014; 46(5):435–457.
11. Rees CJ, Rajasekhar PT, Rutter MD, Dekker E. Quality in colonoscopy: European perspectives and practice. *Expert Rev Gastroenterol Hepatol*. 2014;8(1):29–47.
12. Thakkar K, Holub JL, Gilger MA, et al. Quality indicators for pediatric colonoscopy: Results from a multicenter consortium. *Gastrointest Endosc*. 2016;83(3):533–541.
13. Niv Y, Hazazi R, Levi Z, Fraser G. Screening colonoscopy for colorectal cancer in asymptomatic people: A meta-analysis. *Dig Dis Sci*. 2008; 53(12):3049–3054.
14. Rathgaber SW, Wick TM. Colonoscopy completion and complication rates in a community gastroenterology practice. *Gastrointest Endosc*. 2006;64(4):556–562.
15. Gawron AJ, Veerappan A, McCarthy ST, Kankanala V, Keswani RN. Impact of an incomplete colonoscopy referral program on recommendations after incomplete colonoscopy. *Dig Dis Sci*. 2013;58(7): 1849–1855.
16. Morini S, Zullo A, Hassan C, Lorenzetti R, Campo SMA. Endoscopic management of failed colonoscopy in clinical practice: To change endoscopist, instrument, or both? *Int J Colorectal Dis*. 2011;26(1): 103–108.
17. Wehrmann T, Lechowicz I, Martchenko K, Riphaus A. Routine colonoscopy with a standard gastroscope. A randomized comparative trial in a Western population. *Int J Colorectal Dis*. 2008;23(4):443–446.
18. Chung GE, Lim SH, Yang SY, et al. Factors that determine prolonged cecal intubation time during colonoscopy: Impact of visceral adipose tissue. *Scand J Gastroenterol*. 2014;49(10):1261–1267.
19. Hsieh Y-H, Kuo C-S, Tseng K-C, Lin H-J. Factors that predict cecal insertion time during sedated colonoscopy: The role of waist circumference. *J Gastroenterol*. 2008;23(2):215–217.
20. Nagata N, Sakamoto K, Arai T, et al. Predictors for cecal insertion time: The impact of abdominal visceral fat measured by computed tomography. *Dis Colon Rectum*. 2014;57(10):1213–1219.
21. Shah HA, Paszat LF, Saskin R, Stukel TA, Rabeneck L. Factors associated with incomplete colonoscopy: A population-based study. *Gastroenterology*. 2007;132(7):2297–2303.
22. Iqbal CW, Askegard-Giesmann JR, Pham TH, Ishitani MB, Moir CR. Pediatric endoscopic injuries: Incidence, management, and outcomes. *J Pediatr Surg*. 2008;43(5):911–915.
23. Tringali A, Balassone V, De Angelis P, Landi R. Complications in pediatric endoscopy. *Best Pract Res Clin Gastroenterol*. 2016;30(5):825–839.
24. Madiba TE, Haffajee MR. Sigmoid colon morphology in the population groups of Durban, South Africa, with special reference to sigmoid volvulus. *Clin Anat*. 2011;24(4):441–453.
25. Madiba TE, Haffajee MR, Sikhosana MH. Radiological anatomy of the sigmoid colon. *Surg Radiol Anat*. 2008;30(5):409–415.
26. Sadahiro S, Ohmura T, Yamada Y, Saito T, Taki Y. Analysis of length and surface area of each segment of the large intestine according to age, sex and physique. *Surg Radiol Anat*. 1992;14(3):251–257.
27. Phillips M, Patel A, Meredith P, Will O, Brassett C. Segmental colonic length and mobility. *Ann R Coll Surg Engl*. 2015;97(6):439–444.
28. Krishnan P, Sofi AA, Dempsey R, Alaradi O, Nawras A. Body mass index predicts cecal insertion time: The higher, the better. *Dig Endosc*. 2012; 24(6):439–442.
29. Franciosi JP, Mascarenhas M, Semeao E, Flick J, Kelly J, Mamula P. Randomised controlled trial of paediatric magnetic positioning device assisted colonoscopy: A pilot and feasibility study. *Dig Liver Dis*. 2009; 41(2):123–126.
30. Holme Ö, Höie O, Matre J, et al. Magnetic endoscopic imaging versus standard colonoscopy in a routine colonoscopy setting: A randomized, controlled trial. *Gastrointest Endosc*. 2011;73(6):1215–1222.
31. Lightdale JR, Acosta R, Shergill AK, et al; ASGE Standards of Practice Committee; American Society for Gastrointestinal Endoscopy. Modifications in endoscopic practice for pediatric patients. *Gastrointest Endosc*. 2014;79(5):699–710.

Self-perception of smile attractiveness as a reliable predictor of increased patient compliance with an orthodontist

Michał Sarul[1,A–F], Joanna Antoszewska-Smith[1,A,C,E,F], Hyo-Sang Park[1,2,E,F]

[1] Department of Dentofacial Orthopedics and Orthodontics, Wroclaw Medical University, Poland
[2] Department of Orthodontics, Kyungpook National University, Daegu, South Korea

A – research concept and design; B – collection and/or assembly of data; C – data analysis and interpretation;
D – writing the article; E – critical revision of the article; F – final approval of the article

Advances in Clinical and Experimental Medicine, ISSN 1899–5276 (print), ISSN 2451–2680 (online) *Adv Clin Exp Med*. 2019;28(12):1633–1638

Address for correspondence
Michał Sarul
E-mail: michal.sarul@gmail.com

Funding sources
None declared

Conflict of interest
None declared

Received on October 10, 2018
Reviewed on November 20, 2018
Accepted on June 27, 2019

Published online on November 28, 2019

Abstract

Background. Predicting the cooperation of orthodontic patients seems to be of the utmost importance for successful results in treatment with removable appliances, especially if their cost is to be covered from public funding. Therefore, the issue of unbiased pre-treatment assessment of cooperation still calls for an investigation.

Objectives. The objective of this study was to check whether smile attractiveness and its importance, subjectively evaluated by the patients/their caregivers, are reliable predictors of a patient's compliance during treatment with removable appliances.

Material and methods. The study group comprised 97 patients aged 9–12 years, treated with active plates or twin-blocks, equipped with the TheraMon® system. Before treatment, the caregivers and the patients filled out the questionnaires ranking both of the investigated variables. After 9 months of treatment, we analyzed the correlations of the daily wear time (DWT) and other variables.

Results. The analysis revealed the following: no relevance of the DWT to the type of removable appliances; negative correlation between the DWT and smile attractiveness assessed by the children and their caregivers; evidently elongated DWT (up to 9.68 h in children), who, together with the caregivers, evaluated their smile attractiveness as poor; coherence of children's and their caregivers' responses evaluating smile attractiveness and its importance, as well as the lack of consistency when comparing responses provided separately by the children and their caregivers.

Conclusions. Application of the TheraMon® sensors objectively proved that the patient's smile attractiveness ranked subjectively as low predicts the orthodontic patient's irreproachable cooperation. Therefore, our easy-to-use questionnaire calls for changing the protocol regarding the wearing time of removable appliances during treatment and introducing an evidence-based policy of reimbursement for such therapy from public funds. Further investigation of the effectiveness of removable appliances worn shorter than previously presumed and of the motivation to continue treatment, once smile attractiveness has been improved, is necessary.

Key words: self-perception of smile attractiveness, orthodontic appliances, cooperative behavior

Cite as
Sarul M, Antoszewska-Smith J, Park H-S. Self-perception of smile attractiveness as a reliable predictor of increased patient compliance with an orthodontist. *Adv Clin Exp Med*. 2019;28(12):1633–1638. doi:10.17219/acem/110320

DOI
10.17219/acem/110320

Introduction

Nowadays, the alarming prevalence of malocclusions, which affect more than 90% of the population,[1,2] calls for interceptive orthodontic treatment, which improves the future general health status. Such early intervention is mostly realized with removable appliances, whose success is largely dependent on patient cooperation.[3–5] Monitoring patient cooperation has just recently been revolutionized due to microsensors, e.g., the TheraMon® system. These microsensors are almost imperceptible; they are imbedded in an acrylic plate, which does not affect comfort while wearing the orthodontic device. TheraMon® is also resistant to any interference from the patient, thus measuring wearing time accurately and reliably.[6,7]

Regrettably, studies using the electronic chips efficiently demonstrated considerably weaker patient cooperation than previously thought.[8] Therefore, many researchers focused on establishing factors that would enable us to predict patient cooperation before manufacturing an appliance.[9–12] Our previous studies,[13] similarly to those by Amado et al.,[14] have shown that the degree of compliance depends on the patients' and – more significantly – their caregivers' personality traits.

Such findings automatically gave rise to a question: is it possible to omit a complex psychological questionnaire and still predict cooperation reliably, especially that early orthodontic treatment is a part of the dental prophylaxis, which in many countries is reimbursed from public funds?

Bearing in mind that impaired smile attractiveness has been the main incentive to seek orthodontic treatment,[15–18] one might have presumed that the individuals who are dissatisfied with their smiles are likely to be the most compliant patients. However, since eager amenability to the regimen of treatment with removable appliances is an uncertain issue, and a strong relationship between poor smile esthetics and excellent patient cooperation has not yet been objectively verified, our hypothesis obviously remains a matter of controversy and debate.

Therefore, the purpose of our study was to provide evidence whether objectively, electronically monitored daily wear time (DWT) of removable devices correlates with self-perception of smile attractiveness assessed by patients and their caregivers. If so, we would have established an easy and reliable predictor of compliance, thus decreasing the orthodontic treatment cost/effectiveness ratio.

Material and methods

Study group

Ninety-seven healthy children (51 girls, 46 boys) without cleft palate or any oral disease, and qualified for interceptive or early orthodontic treatment with removable appliances, were enrolled in the study that received approval from the Ethical Review Committee of Wroclaw Medical University (approval No. KB-322/2014).

All patients met the following inclusion criteria: age 9–12 years, good health and no syndromes or clefts, malocclusion likely to improve with an active plate or twin block, i.e., mild or moderate crowding of the anterior maxillary teeth, Class II functional shift, or pseudo Class III or bilateral cross-bite due to narrowed maxillary dental arch.

Before treatment, the caregivers (79 females, 18 males), who declared future active supervision of the child's cooperation, signed the informed consent. Subsequently, all the caregivers and the patients responded to the questionnaires designed by a psychologist qualified in assessing pro-health behavior. The following factors were ranked:

– A1: children's self perception of smile attractiveness,
– A2: children's thoughts on the importance of smile attractiveness,
– B1: caregivers' perception of their children's smile attractiveness,
– B2: caregiver's thoughts on the importance of smile attractiveness.

Regarding the attractiveness of the patient's smile, the score was given from 1 to 5 as very poor, poor, fair, great, and excellent, respectively. Regarding the importance of smile attractiveness itself, the score was given from 1 to 5 as very indifferent, indifferent, barely important, important, and very important, respectively.

In each case, a psychologist participating in these studies explained to the patients are caregivers all the terms appearing in the form, which was completed only after the terminology of the questionnaire was understandable for the respondent.

Subsequently, 56 children (29 girls, 27 boys) received a twin block and 41 children (22 girls, 19 boys) received an active plate, all devices equipped with the TheraMon® electronic sensors of temperature fluctuation, measuring appliance wear time with an accuracy of 15 min. We asked the patients to wear their appliances at least 12–14 h per day and to report back every 6 weeks on the DWT measurements with the TheraMon® software. At that time, all patients appeared on designated appointments and none of the patients were excluded from the study.

In order to assess the accuracy of the TheraMon® sensors in vivo, prior to this study we applied the protocol described by Pauls et al.[19] To do so, we instructed 5 postgraduate students from our Department to wear Schwarz plates equipped with the TheraMon® sensors for 1 week, reading records provided by the sensors every day and noting every hour the device insertion and removal. The data analysis revealed insignificant mean discrepancy of 9.6 min per day between the recorded and the actual DWTs.

After 9 months, we subjected all the gathered data to a statistical analysis to answer the following research questions:

1. Is the DWT indifferent due to type of the removable device used in our study?
2. Does any of the 4 variables (A1–B2) affect the DWT and if yes, then how?
3. Is there any correlation between the 4 variables facilitating psychological evaluation process?

Statistical analysis

STATISTICA v. 12 software (StatSoft, Inc., Tulsa, USA) enabled us to answer our queries. The Shapiro–Wilk normality test results proved that the range of our data fell beyond the normal distribution pattern, so we applied a non-parametric analysis. All data was processed using the Mann–Whitney U test, Spearman's and Kendall's τ rank correlation coefficients and Dunn's multiple comparison test.[20–22] Power test analysis was performed with the Student's t-test, evaluating the significance of Spearman's R correlation coefficient. We established the significance level at $p < 0.05$ and the threshold of the power test analysis at the level of 0.95.

Results

Measurements of the daily wear time did not vary in the patients wearing twin block or an active plate (Table 1).

Figure 1 demonstrates percentage distributions of the ranks obtained in the questionnaires. As for statistics, all 4 variables significantly ($p < 0.05$) correlated with the DWT: A2 and B2 – positively, A1 and B1 – negatively.

Table 1. Statistical assessment of comparison of the daily wear time (DWT) in patients treated with twin blocks or active plates

Variable	Type of appliance		p-value
	twin block (M ±SD)	active plate (M ±SD)	
DWT [h]	7.37 ±2.76	7.88 ±3.49	0.41

M – median; SD – standard deviation.

Table 2. Statistical analysis of the relationship between the daily wear time (DWT) and evaluation of smile attractiveness/its importance

Variable	R coefficient	p-value	Power test analysis for α = 0.05
A1	−0.7680	<0.0001	1.0000
A2	0.4753	<0.0001	0.9976
B1	−0.9561	<0.0001	1.0000
B2	0.4418	<0.0001	0.9925

However, the negative correlation was twice stronger than the positive one (Table 2).

Table 3 demonstrates differentiation of the DWT depending on low (1–2 points) or high (3–5 points) scores from the questionnaires. Apparently, smile attractiveness evaluated as poor by children (A1, low) and their caregivers (B1, low) undoubtedly elongates the DWT to 9.64 h and 9.68 h respectively. So do the greater children's and the caregiver's concerns about importance of the smile attractiveness (A2, high and B2, high) – however, to a lesser extent: 7.90 h and 7.85 h, respectively.

Table 4 presents comparison in pairs of the caregivers' and children's judgments. We found statistically significant correlation ($r > 0.7$) only when comparing the A1 and B1

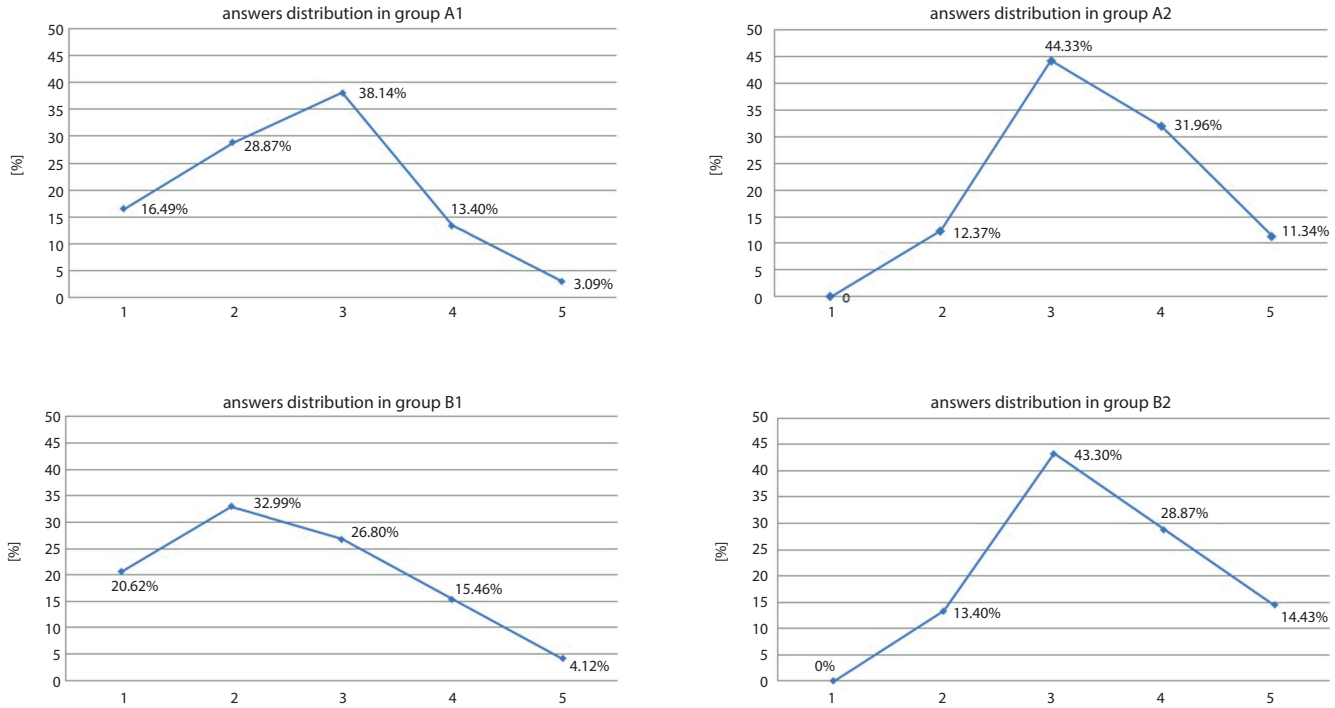

Fig. 1. Distribution of answers in each group

Table 3. Results of Mann–Whitney U test: intergroup comparisons between daily wear time (DWT) and subgroups

Variable	Admitted score	DWT [h]		p-value
		M	SD	
A1	low	9.64	2.77	0.0000
	high	5.92	2.28	
A2	low	5.57	2.68	0.0048
	high	7.90	3.09	
B1	low	9.68	2.58	0.0000
	high	5.22	1.63	
B2	low	6.06	3.11	0.0231
	high	7.85	3.07	

M – mean; SD – standard deviation.

Table 4. Statistical analysis of the variables (responses provided in the questionnaires) coherence

Pair of variables	R coefficient	p-value	Power test analysis for α = 0.05
A1 and B1	0.7971	0.0000	1.0000
A2 and B2	0.8754	0.0000	1.0000
A1 and A2	−0.3195	0.0000	1.0000
B1 and B2	−0.4827	0.0000	1.0000

or A2 and B2 variables. Interestingly, responses provided separately by the children (A1 and A2) and their caregivers (B1 and B2) turned out to present no correlation ($r > -0.5$).

Discussion

From a clinical point of view, it is particularly important to find a criterion that already at the stage of diagnosis would allow us to assess the future cooperation of young patients with regard to wearing their devices. And despite the fact the TheraMon® system was introduced in orthodontics a couple of years ago, such sensors have not been utilized to efficiently and reliably predict compliance instead of merely assessing it in-treatment.[19,23,24] That is why our entirely new and unique approach also has a scientific long-term goal. Namely, it opens the door for the objective verification of the efficiency and efficacy of removable appliances in complying patients selected prior to manufacturing the expensive orthodontic devices. This goal, however, requires the selection of criteria that best predict the degree of cooperation among patients. The authors have already made an attempt to objectively assess the effectiveness of some of these criteria in the published studies.[13,25] It is clear that conducting such a study would in the future create evidence-based treatment protocols regarding the DWT.

Sergl and Zentner[26] admittedly proved that the degree of compliance depends on the orthodontic appliance type; however, in their study the DWT was not verified objectively. Our outcome (Table 1), which is in accordance with that obtained by Schafer al.,[27] results from monitoring patients' cooperation with sensors, thus increasing reliability of the results. Therefore, we neglected the type of removable device in subsequent statistical analyses. Since we proved that the orthodontic patients do not prefer active plates to twin blocks, we assume that a therapeutic construction bite does not hamper the patients' acceptance of the removable apparatus and – afterwards – does not impair the cooperation level. Nevertheless, the inquiry as to whether other bite jumping devices, e.g., bionators, are tolerated equally well as the twin blocks, remains unanswered.

Dissatisfaction with one's facial appearance is commonly known as the main factor contributing to a patient seeking orthodontic treatment.[2,18,25,28,29] Therefore, in the literature from different decades reports can be found stating that esthetic impairment caused by malocclusion, as well as the caregivers' low rating of their child's occlusion support better cooperation during orthodontic therapy.[30–32] According to Lin et al.,[29] even the visual presentation of post-treatment esthetics deterioration and the ensuing non-cooperation during retention phase seems to increase patients' discipline with regard to wearing their Hawley's retainers. However, assessment of the virtual compliance in the quoted papers remains in a sphere of speculation due to lack of evidence, contrary to our findings (Table 2) based on reliable, objective measurements. The strong negative correlations of the DWT and poor smile attractiveness seen by the patients (A1, $r = -0.77$) or more importantly by their caregivers (B1, $r = -0.95$) evidently proved the role that perception of smile attractiveness plays in predicting adequate cooperation when wearing the removable appliances.

Positive, although not strong correlations of the DWT and declared children's (A2) or caregivers' (B2) attitude to the importance of a smile attractiveness (Table 2) demonstrated that the importance of smile esthetics is a more of an abstract issue than the smile esthetics itself, thus the prior cannon function as a reliable predictor of the DWT. In this way again we proved – indirectly – that aptly selected, one-question ranking self-perception of smile attractiveness is scientifically reliable as for an assessment of the young patient's future cooperation during treatment.

Orthodontic literature recommends that the wear time of removable appliances range from 12 h to 14 h per day. Regrettably, our study has proven that the discussed, objectively verified duration is less than 8 h on average. Furthermore, even if it reaches 10 h in the most cooperative patients, namely in children with a low rating of their smiles, 3 h of standard deviation (SD) occur (Table 3). This leaves no doubts that previous assumptions relating to treatment efficiency are overestimated, as the measured and monitored DWT were based on bias.[33] They are at odds with our highly reliable outcome, which evidently

justifies the necessity to evaluate the effectiveness of removable appliances, in order to modernize the apparently old fashioned recommendations regarding wearing time. Notwithstanding, such an assessment demands gathering only complying patients, whose simple selection is now possible, due to our presented study results.

Folger stated that parental acceptance is extremely important in orthodontic cooperation.[34] Furthermore, Albino[32] and Gross et al.[35] also proved that due to adolescents' likely negative perceptions of orthodontic appliances, parental support and control are critical to treatment success. Our results, obtained using an objective method of patients' cooperation evaluation, fully support these findings. We demonstrated that, due to a high correlation of answers to the same question (A1 and B1: r = 0.7971; A2 and B2: r = 0.8754), interviewing only the caregivers as to smile attractiveness efficiently and effectively predicts the children's cooperation (Table 4). This is how, based on our previous study results,[25] we are able to state that parental personality features, rather than their children's, mainly affect the future cooperation during orthodontic treatment with removable devices. Considering that neither children nor their caregivers separately are coherent in an assessment of smile attractiveness and its importance (Table 4), utilizing complex psychological questionnaires in order to predict the DWT seems to be fully justified, especially that self-perception of smile attractiveness is a reliable predictor of a young patients' compliance with an orthodontist.

As for the limitations of our study, the questionnaire we applied consisted of only 2 questions. However, such procedure of interviewing respondents is based on the data collected from the literature.[42,45,46]

Theoretically, the young age of the patients could also be a limiting factor. Nevertheless, numerous studies using questionnaires referencing similar issues among the peers of our patients[35–45] have already proven their adequacy among patient of that age group. It has also been confirmed by a psychologist participating in related studies that the age of the respondents did not influence their understanding of the questionnaire questions and, thus, the credibility of the given answers.

The smile esthetics was subjectively assessed only prior to the initiation of orthodontic treatment. It was done on purpose, as it prevented any influence of the therapy on the discussed parameter and, therefore, its significance for the patient cooperation prognosis. It should be remembered that, along with progress in treatment, even if the motivation is initially insufficient, a health habit related to wearing orthodontic device may be developed.[8,25] On the other hand, along with the improvement of smile esthetics – especially of the feature that was not initially accepted, regardless of whether it was defined or not – the commitment of the patient may decrease. Both phenomena could weaken the credibility of our result, if it had not been for the short duration of the study that made it impossible to obtain long-term effects of the treatment.

The final aspect that constitutes a limitation of the study is the fact that we have only proven the occurrence of strong correlations between the DWT and the subjective assessment of a child's smile. We have not proven, however, that there is a cause and effect relationship between these phenomena. Nonetheless, on the basis of the available literature on the subject,[13–18,29–34] it is well-founded to advocate the existence of such a dependence.

Conclusions

Our study reliably proved that the patient's smile attractiveness ranked subjectively as low on a 5-point scale survey predicts the orthodontic patient's irreproachable cooperation. What is important, we have achieved the results objectively, namely by applying the TheraMon® sensors. In other words, our easy-to-use questionnaire faciltates both: changing the protocol of removable appliances wearing time during treatment and introduction of an evidence-based policy of reimbursement of such therapy from the public funds.

In order to complete our findings, there is still a need to investigate the effectiveness of removable appliances worn shorter than previously presumed, in certain malocclusions. It would also be interesting to study whether the improved smile attractiveness negatively affects the motivation to continue treatment, thereby hindering the correction of severe malocclusions that are otherwise imperceptible to the patient.

ORCID iDs

Michał Sarul https://orcid.org/0000-0002-2518-0007
Joanna Antoszewska-Smith https://orcid.org/0000-0001-9192-1064
Hyo-Sang Park https://orcid.org/0000-0003-0227-4112

References

1. Tausche E, Luck O, Harzer W. Prevalence of malocclusions in the early mixed dentition and orthodontic treatment need. *Eur J Orthod*. 2004; 26(3):237–244.
2. Proffit WR, Fields HW Jr, Moray LJ. Prevalence of malocclusion and orthodontic treatment need in the United States: Estimates from the NHANES III survey. *Int J Adult Orthodon Orthognath Surg*. 1998; 13(2):97–106.
3. Witanowska J, Zadurska M. System solutions for orthodontic care across Europe, including world trends. *Forum Ortod*. 2012;8:207–214.
4. Żyła T, Kawala B, Antoszewska-Smith J, Kawala M. Black stain and dental caries: A review of the literature. *Biomed Res Int*. 2015;2015:469392.
5. Nimri K, Richardson A. Applicability of interceptive orthodontics in the community. *British J Orthod*. 1997;24(3):223–228.
6. Schott TC, Göz G. Wearing times of orthodontic devices as measured by the TheraMon® microsensor. *J Orofac Orthop*. 2011;72(2):103–110.
7. Stocker B, Jan H, Willmann JH, Wilmes B, Vasudavan S, Drescher D. Wear-time recording during early Class III facemask treatment using TheraMon chip technology. *Am J Orthod Dentofacial Orthop*. 2016; 150(3):533–540.
8. Kawala B, Antoszewska J, Sarul M, Kozanecka A. Application of microsensors to measure real wear time of removable orthodontic appliances. *Czas Stomatol*. 2013;66(3):321–330.

9. Schott TC, Ludwig B. Microelectronic wear-time documentation of removable orthodontic devices detects heterogeneous wear behavior and individualizes treatment planning. *Am J Orthod Dentofacial Orthop*. 2014;146(2):155–160.
10. Sergl H, Zentner A. Predicting patient compliance in orthodontic treatment. *Semin Orthod*. 2000;6(4):231–236.
11. Albino JE, Lawrence SD, Lopes CE, Nash LB, Tedesco LA. Cooperation of adolescents in orthodontic treatment. *J Behav Med*. 1991;14(1): 53–70.
12. Woolass KF, Shaw WC, Viader PH, Lewis AS. The prediction of patient co-operation in orthodontic treatment. *Eur J Orthod*. 1988;10(3): 235–243.
13. Sarul M, Kawala B, Kozanecka A, Łyczek J, Antoszewska-Smith J. Objectively measured cooperation during early orthodontic treatment: Do the treatment needs have an impact? *Adv Clin Exp Med*. 2017;26(1):83–87.
14. Amado J, Sierra AM, Gallon A, Alvarez C, Baccetti T. Relationship between personality traits and cooperation of adolescent orthodontic patients. *Angle Orthod*. 2008;78(4):688–691.
15. Shaw WC, Rees G, Dawe M, Charles CR. The influence of dentofacial appearance on the social attractiveness of young adults. *Am J Orthod*. 1985;87(1):21–26.
16. de Almeida AB, Leite ICG, Melgaço CA, Marques LS. Dissatisfaction with dentofacial appearance and the normative need for orthodontic treatment: Determinant factors. *Dental Press J Orthod*. 2014;19(3): 120–126.
17. Giraldo LMC, Rendón ACP, Londoño AG, Vásquez JMC. Perception of adolescent patients on cooperation during orthodontic treatment: A qualitative study. *Int J Odontostomat*. 2014;8(2):225–228.
18. Samsonyanová L, Broukal Z. A Systematic review of individual motivational factors in orthodontic treatment: Facial attractiveness as the main motivational factor in orthodontic treatment. *Int J Dent*. 2014;2014:938274.
19. Pauls A, Nienkemper M, Panayotidis A, Wilmes B, Drescher D. Effects of wear time recording on the patient's compliance. *Angle Orthod*. 2013;83(6):1002–1008.
20. Koronacki J, Mielniczuk J. *Statystyka dla kierunków technicznych i przyrodniczych*. Warszawa, Poland: WNT; 2001.
21. Colwell DJ, Gillett JR. Spearman versus Kendall. *The Mathematical Gazette*. 1982;66:307–309.
22. Zar JH. *Biostatistical Analysis*. 5th ed. DeKalb, IL: Northern Illinois University, Pearson Education Limited; 2010.
23. Schott TC, Meyer-Gutknecht H, Mayer N, Weber J, Weimer K. A comparison between indirect and objective wear-time assessment of removable orthodontic appliances. *Europ J Orthod*. 2017;39(2):170–175.
24. Kirshenblatt S, Chen H, Dieltjens M, Pliska B, Almeida FR. Accuracy of thermosensitive microsensors intended to monitor patient use of removable oral appliances. *J Can Dent Assoc*. 2018;84:i2.
25. Sarul M, Lewandowska B, Kawala B, Kozanecka A, Antoszewska-Smith J. Objectively measured patient cooperation during early orthodontic treatment: Does psychology have an impact? *Adv Clin Exp Med*. 2017;26(8):1245–1251.
26. Sergl HG, Zentner A. A comparative assessment of acceptance of different types of functional appliances. *Eur J Orthod*. 1998;20(5):517–524.
27. Schäfer K, Ludwig B, Meyer-Gutknecht H, Schott TC. Quantifying patient adherence during active orthodontic treatment with removable appliances using microelectronic wear-time documentation. *Eur J Orthod*. 2015;37(1):73–80.
28. Allan TK, Hodgson EW. The use of personality measures as a determinant of patient cooperation in an orthodontic practice. *Am J Orthod*. 1968;54(6):433–440.
29. Lin FO, Sun H, Ni ZY, Zheng ML, Yao LJ. A feasible method to improve adherence of Hawley retainer in adolescent orthodontic patients: A randomized controlled trial. *Patient Prefer Adherence*. 2015;9: 1525–1530.
30. Jie Y, Dan-Dan L, Yan-Qi Y, Colman P, McGrath J, Nikos M. What are patients' expectations of orthodontic treatment: A systematic review. *BMC Oral Health*. 2016;16:19.
31. Dion KK, Berscheid E. Physical attractiveness and peer perception among children. *Sociometry*. 1974;37(1):1–12.
32. Albino JEN. Factors influencing adolescent cooperation in orthodontic treatment. *Semin Orthod*. 2000;6(4):214–223.
33. Chen JY, Will LA, Niederman R. Analysis of efficacy of functional appliances on mandibular growth. *Am J Orthod Dentofacial Orthop*. 2002;122(5):470–476.
34. Folger J. Relationships of children's compliance to mothers' health beliefs and behavior. *J Clin Orthod*. 1988;22(7):424–426.
35. Gross AM, Samson G, Dierkes M. Patient cooperation in treatment with removable appliances: A model of patient noncompliance with treatment implications. *Am J Orthod*. 1985;87(5):392–397.
36. Shaw WC. The influence of children's dentofacial appearance on their social attractiveness judged by peers and lay adults. *Am J Orthod*. 1981;79(4):399–415.
37. Cross JF, Cross J. Age, sex, race, and the perception of facial beauty. *Develop Psych*. 1971;5(3):433–439.
38. Kleck R, Richardson S, Ronald L. Physical appearance cues and interpersonal attraction in children. *Child Develop*. 1974;45(2):305–310.
39. Lansdown R, Polak L. A study of the psychological effects of facial deformity in children. *Child Care Health Dev*. 1975;1(2):85–91.
40. Kjäldman I-O. *Self-Concept and School Achievement of Pupils with Cleft Lip, Cleft Palate or Both. A Longitudinal Study* [doctoral dissertation]. University of Helsinki, Finland; 2006.
41. Henson ST, Lindauer SJ, Gardner WG, Shroff B, Tufekci E, Best AM. Influence of dental esthetics on social perceptions of adolescents judged by peers. *Am J Orthod Dentofacial Orthop*. 2011;140(3):389–395.
42. Birkeland K, Bøe OE, Wisth PJ. Relationship between occlusion and satisfaction with dental appearance in orthodontically treated and untreated groups. A longitudinal study. *Europ J Orthod*. 2000;22(5): 509–518.
43. Planinšec J, Fošnarič S. Relationship of perceived physical self-concept and physical activity level and sex among young children. *Percept Mot Skills*. 2005;100(2):349–353.
44. Cavero MAB. Harter's Self-Perception Profile for Children: An adaptation and validation of the Spanish version. *Psych Rep*. 2014;115(2): 444–466.
45. Salih FN, Lindsten, Bågesund M. Perception of orthodontic treatment need among Swedish children, adolescents and young adults. *Acta Odontologica Scandinavica*. 2017;75(6):407–412.
46. Boeira GF, Salas MMS, Araújo DC, Masotti AS, Correa MB, Demarco FF. Factors influencing dental appearance satisfaction in adolescents: A cross-sectional study conducted in southern Brazil. *Braz J Oral Sci*. 2016;15(1):8–15.

Inhibition of eukaryotic initiation factor 3B suppresses proliferation and promotes apoptosis of chronic myeloid leukemia cells

Laiquan Huang[1,B,D], Kun He[1,B], Jianxin Wang[1,C], Jiawei Yan[1,C], Yizhi Jiang[1,C], Zhongling Wei[1,E], Jun Zhang[1,E], Guangxi Li[1,E], Lili Sheng[2,A,F]

[1] Department of Hematology, Yijishan Hospital, First Affiliated Hospital of Wannan Medical College, Wuhu, China
[2] Department of Oncology, Yijishan Hospital, First Affiliated Hospital of Wannan Medical College, Wuhu, China

A – research concept and design; B – collection and/or assembly of data; C – data analysis and interpretation; D – writing the article; E – critical revision of the article; F – final approval of the article

Advances in Clinical and Experimental Medicine, ISSN 1899–5276 (print), ISSN 2451–2680 (online) *Adv Clin Exp Med*. 2019;28(12):1639–1645

Address for correspondence
Lili Sheng
E-mail: 13605535185@163.com

Funding sources
Natural Science Research Project of Colleges and Universities in Anhui Province, China; grant No. KJ2017A263.

Conflict of interest
None declared

Received on December 1, 2018
Reviewed on December 23, 2018
Accepted on June 27, 2019

Published online on November 28, 2019

Abstract

Background. Eukaryotic translation initiation factor 3B (*eIF3b*) has been reported to be overexpressed in colon, bladder and prostate cancers as well as in glioblastoma. However, there is no report on any correlation of *eIF3b* gene expression with cell proliferation and apoptosis in chronic myeloid leukemia (CML).

Objectives. In this study, we evaluated the role of *eIF3b* in cell proliferation and apoptosis in CML.

Material and methods. Samples from patients with CML and CML cell lines were used. Quantitative RT-PCR, siRNA transfection, flow cytometry, and western blot analysis were performed.

Results. Quantitative RT-PCR revealed that the expression of eIF3b mRNA in CML patients was higher than that in the non-malignant controls. The proliferation of CML cells decreased after transfection of the cells with siRNA. The proportion of cells in the G1 and S phases in the experimental group decreased after transfection, while the number of cells in the G2/M phase increased, as compared with the control group. The total cell apoptosis percentage in the sheIF3b group (transduction with lentivirus-anti-eIF3b in K562 cells) was higher than the shCtrl group (transduction with empty-vector lentivirus in K562 cells) after transfection. Caspase 3/7 activity was higher and the expression of anti-apoptotic protein BCL-2 was lower in the sheIF3b group than in the shCtrl group after transfection.

Conclusions. Our results suggest that downregulation of eIF3b expression inhibits proliferation and induces apoptosis in CML cells.

Key words: cell proliferation, eukaryotic initiation factor 3b, chronic myeloid leukemia

Cite as
Huang L, He K, Wang J, et al. Inhibition of eukaryotic initiation factor 3B suppresses proliferation and promotes apoptosis of chronic myeloid leukemia cells. *Adv Clin Exp Med*. 2019;28(12):1639–1645. doi:10.17219/acem/110323

DOI
10.17219/acem/110323

Introduction

Chronic myeloid leukemia (CML) is a hematopoietic stem cell (HSC) malignancy that results from the formation of the Philadelphia chromosome due to reciprocal chromosomal translocation t(9;22)(q34.12;q11.23), and it accounts for 15–20% of all leukemias.[1] Patients with CML need to be treated for life; moreover, the prognosis of patients with blastic transformation of CML is extremely poor. Thus, there is an unmet need to find better treatments for CML.

Eukaryotic initiation factors (eIFs) are a large family of proteins that regulate the rate-limiting step of protein synthesis in the initiation stage.[2] To date, numerous eIFs have been identified and several of them consist of multiple subunits that determine their functions.[3,4] A growing number of studies illustrate that various eIFs are aberrantly expressed or activated in different types of human cancers.[5,6]

There is a growing interest in understanding the mechanisms of eIFs in modulating gene translation initiation and how they promote oncogenesis. Scientists have hypothesized that an increased rate of translation would affect the downstream mRNA synthesis and that a high level of eIFs could enhance the translation of these mRNAs. Preclinical studies have shown that overexpression of eIFs resulted in cells transforming into those with cancerous characteristics, as demonstrated by pervasive growth and increased proliferation.[7]

The largest group of these eIFs, eukaryotic translation initiation factor 3 (*eIF3*), consists of 13 subunits (eIF3a through eIF3m) with a total molecular mass of 700 kDa, and plays an essential role in the initiation of translation.[8] eIF3 mediates several steps of the translation initiation pathway, which includes recruiting the eIF2–GTP–MET–tRNA (iMet) ternary complex and other eIFs to the 40S ribosomal subunit to form the 43S preinitiation complex, mRNA recruitment and subsequent scanning of the 5' untranslated region (UTR) and starting codon.[9] eIF3b has been verified to be overexpressed in colon, bladder and prostate cancers as well as in glioblastoma due to its impact on the cellular activity of cancer cells.[10–12]

While several eIF proteins have been implicated in CML,[6,7] there is no study in the literature exploring the correlation of *eIF3b* expression with cell proliferation and apoptosis in CML. Therefore, that is precisely the aim of the current study.

Material and methods

Sample collection and eIF3b mRNA expression

A total of 16 CML patients were enrolled in this study at the Department of Hematology of Yijishan Hospital, First Affiliated Hospital of Wannan Medical College, Wuhu, China, from January 2015 to March 2017. As controls, 16 age- and gender-matched non-malignant patients who had undergone bone marrow biopsy (12 thrombocytopenic purpura, 3 infectious diseases and 1 healthy donor) were enrolled. During the bone marrow biopsy, 2 mL of bone marrow sample was obtained from each participant; mononuclear cells were then isolated. This was followed by total RNA extraction and eIF3b mRNA was detected with quantitative real-time reverse transcription polymerase chain reaction (qRT-PCR). This study was approved by the Ethics Committee of Yijishan Hospital, First Affiliated Hospital of Wannan Medical College Hospital. The participants provided written informed consent.

eIF3b expression in different leukemia cell lines

TK-6, K562 and Jurkat cell lines were purchased from the Shanghai Institutes for Biological Science (Shanghai, China). After resuscitation, these cells were maintained in RPMI-1640 medium (Gibco, Carlsbad, USA) containing 10% fetal bovine serum (Gibco) and 1% penicillin/streptomycin (Corning, Lowell, USA) at 37°C with a humidified atmosphere of 5% CO_2. Meanwhile, mononuclear cells were isolated from the bone marrow of 3 control subjects (patients without malignancies) and were defined as the control group. The expression of eIF3b mRNA was detected with qRT-PCR.

Detection of K562 cell transduction, proliferation and apoptosis

K562 cells were transduced with the lentivirus-anti-eIF3b vector (LVpGCSIL-004PSC2749-1; Shanghai Gemma, Shanghai, China) and identified as the sheIF3b group (the sequences of anti-eIF3b: 5′-GCUACAAGCUUGACAAGCAdTdT-3′ (F) and 5′- UGCUUGUCAAGCUUGUAGCdTdT-3′ (R)); those transduced with an empty vector (psc3741, Shanghai Gemma) served as the control group (shCtrl group, irrelevant sequence). The level of fluorescence was observed under a fluorescence microscope; all transduction rates were more than 90%. Briefly, qRT-PCR, western blotting, CCK-8 and fluorescence-activated cell sorting (FACS) were used to examine the eIF3b mRNA level, protein level, cell proliferation, cell cycles, and apoptosis in the K562 cells. For western blot analysis, the total protein was adjusted into equal amounts and subjected to sodium dodecyl sulfate polyacrylamide gel electrophoresis (SDS-PAGE). Specific antibodies were used to detect each corresponding protein. The antibodies used for western blotting analysis are listed in Table 1.

RNA extraction and qRT-PCR analysis

Total RNA samples from cells were extracted with TRIzol reagent (Invitrogen, Carlsbad, USA) according to the manufacturer's instructions. The extracted RNA

Table 1. Details of the antibodies used

Antibody name	Company	Country	Dilution ratio
Primary antibody Mouse Anti-Flag	 Sigma	 USA	 1:2000
Mouse anti-GAPDH	Santa-Cruz	USA	1:2000
Anti-BCL2	Abcam	USA	1:2000
Anti-GAPDH	Santa-Cruz	USA	1:2000
Secondary antibody Goat Anti-Mouse IgG Anti-Mouse IgG	 Santa-Cruz Santa-Cruz	 USA USA	 1:2000 1:2000

was pretreated with RNase-free DNase, and 1 μg of RNA from each sample was used for cDNA synthesis with random hexamers (RNA to cDNA EcoDry™ Premix; TAKARA, Kusatsu, Japan). The cDNA products were subjected to qRT-PCR with a SYBR FAST Mastermix kit (KAPA, Boston, USA). The following primer sequences were used:

– eIF3b forward primer:
  5'-CGGTGCCTTAGCGTTTGTG-3';
– eIF3b reverse primer:
  5'-CGGTCCTTGTTGTTCTTCTGC-3';
– GAPDH forward primer:
  5'-TGACTTCAACAGCGACACCCA-3';
– GAPDH reverse primer:
  5'-CACCCTGTTGCTGTAGCCAAA-3'.

The PCR amplification was performed as follows: 95°C for 5 min, followed by 40 cycles of 95°C for 4 s and 61°C for 30 s. The PCR amplification was performed in triplicate. The qRT-PCR results were calculated with the $2^{-\Delta\Delta}$Ct method.

Western blot analysis

Western blotting was performed for the detection of eIF3b and Bcl-2 expression. The total protein was extracted from cells lysed in RIPA buffer (Thermo Fisher Scientific, Waltham, USA) containing phosphatase and protease inhibitors. Then, 20 μg of protein samples were subjected to SDS-PAGE and transferred onto polyvinylidene fluoride membranes (Merck Millipore, Bedford, USA). After blocking with 5% skim milk for 2 h, the membranes were incubated with the corresponding primary antibodies overnight at 4°C. Then, the membranes were incubated with the appropriate HRP-conjugated secondary antibodies for 1 h at room temperature. The bands were visualized using an enhanced chemiluminescence (ECL) kit (Merck Millipore), followed by exposure to X-ray film. All of the antibodies used are listed in Table 1.

CCK-8 assay

After transduction, cells coupled with CCK-8 dye were incubated with 5% CO_2 at 37°C. The proliferation was evaluated at timepoints of 4 h, 24 h, 48 h, 72 h, and 96 h. The plates were tested and the fluorescence value was read once a day with a microplate reader (Biotek, Winooski, USA). The fluorescence values of each of the 5 days were collected and analyzed to create a proliferation curve.

FACS analysis of cell cycle and apoptosis

For the analysis of the cell cycle, cells were collected 48 h after transduction. The cells were washed 3 times with phosphate-buffered saline (PBS) and fixed in 70% pre-chilled ethanol at 4°C for 1 h. The cells were then suspended in 500 μL of PBS combined with 50 μg/mL of propidium iodide (PI) and 100 μg/mL of ribonuclease, and incubated at 4°C for 30 min in the dark. A 300-mesh nylon net was used to filter and separate the aggregated cells. The cell cycle was analyzed with flow cytometry on a FACScan (BD Biosciences, East Rutheford, USA).

For the analysis of apoptosis, 48 h after transduction, the cells were collected and washed 3 times with PBS, then suspended in 100 μL of PBS; 1 μL of PI was added to the cell suspension, which was incubated at 4°C for 5 min in the dark. The cells stained with PI were detected using flow cytometry on a FACScan. The analysis was performed with a BD FACSCanto II flow cytometer and BD FACSDiva software v. 6.1.3 (BD Biosciences).

Caspase-3/7 activity analysis

Three days after transduction, cells were harvested for caspase-3/7 activity analysis using an Amplite™ Colorimetric Caspase 3/7 Assay Kit (AAT Bioquest, Sunnyvale, USA). Caspase-3/7 activity was measured using 30 μg of lysate by detecting the chromophore p-nitroaniline, which was cleaved from the labeled substrate N-acetyl-Asp-Glu-Val-Asp p-nitroanilide.

Statistical methods

The statistical analysis was performed using SPSS software v. 22.0 (IBM Corp., Armonk, USA). Data was presented as mean ± standard deviation (SD). Comparisons between 2 groups were carried out with a t-test. A p-value <0.05 was considered statistically significant.

Results

Overexpression of eIF3b mRNA in CML

The results of qRT-PCR showed that the expression of eIF3b mRNA in the CML patients was higher than that of the control group ($p < 0.01$) (Fig. 1A). In addition, *eIF3b* was found to be overexpressed in the TK-6 ($p < 0.001$), K562 ($p < 0.001$) and Jurkat ($p < 0.05$) CML cells when compared with normal control cells (mononuclear cells isolated from the bone marrow of healthy individuals, Fig. 1B).

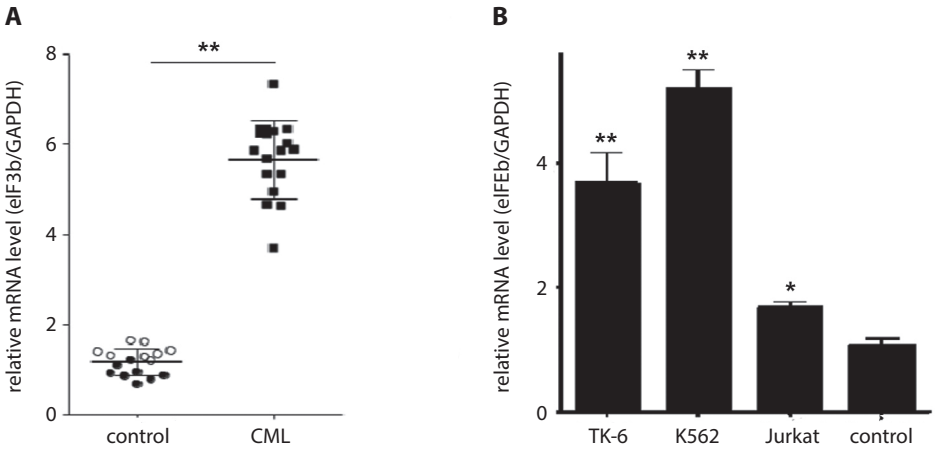

Fig. 1. Expression of eIF3b mRNA in CML cells, normal control cells (mononuclear cells of bone marrow) and different cell lines; A – expression of eIF3b mRNA in CML and controls; B – expression of eIF3b mRNA in TK-6, K562 and Jurkat CML cells, and control cells

*p < 0.05; **p < 0.01.

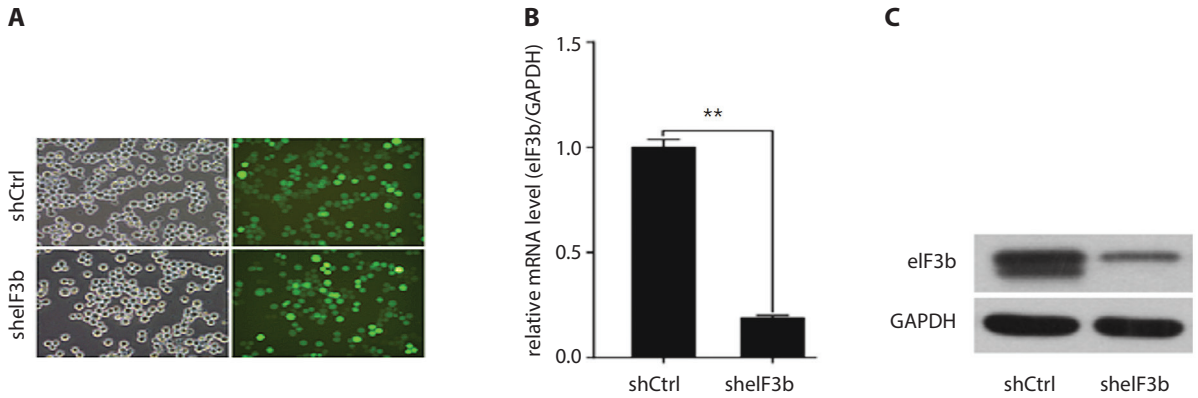

Fig. 2. Transduction of shRNA and the expression of eIF3b mRNA and protein; A – transduction efficiency of shRNA in K562 cells under fluorescence microscope; B – qRT-PCR of the relative mRNA level in the shCtrl and sheIF3b groups; C – western blotting of the level of eIF3b protein in the shCtrl and sheIF3b groups

**p < 0.01.

shRNA inhibits eIF3b mRNA and protein expression

After transduction with lentivirus-anti-eIF3b or empty-vector lentivirus in the K562 cells for 3 days, the fluorescence expression was observed under a fluorescence microscope, which showed that the transduction efficiency of both was over 90% (Fig. 2A). After 3 days, the expression of eIF3b mRNA and protein had both decreased markedly in the sheIF3b group compared with the shCtrl group (Fig. 2B,C).

Downregulation of eIF3b mRNA-inhibited proliferation of K562 cells

The CCK-8 assay showed no significant difference in baseline optical density (OD) between the sheIF3b and shCtrl groups. On days 3, 4 and 5 after transduction, the OD value of the sheIF3b group was lower than that of the shCtrl group (Fig. 3A,B), a finding which suggests that the inhibition of eIF3b mRNA suppresses the proliferation of K562 cells.

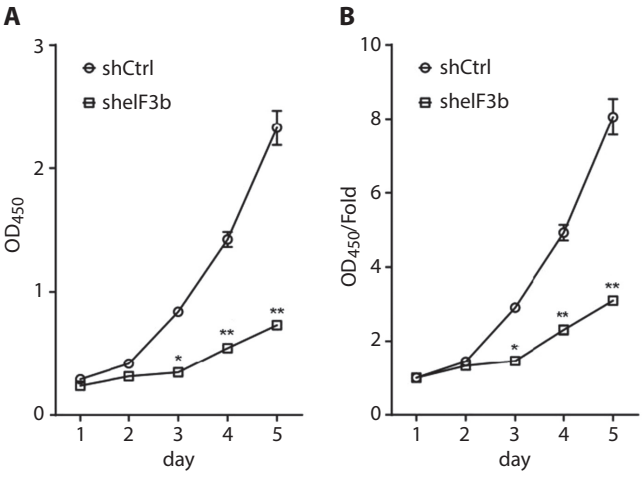

Fig. 3. Effect of eIF3b mRNA downregulation on the proliferation of K562 cells; A – OD_{450} value in the shCtrl and sheIF3b groups 5 days after transduction; B – OD_{450} value in the shCtrl and sheIF3b groups 5 days after transduction

*p < 0.05; **p < 0.01.

Effect of *eIF3b* gene downregulation on K562 cell cycles

Following transduction with shRNA lentivirus – on day 5 – the proportion of cells in the G1 ($p < 0.01$) and S phases ($p < 0.05$) of the sheIF3b group was lower than that of the shCtrl group, while the proportion of cells in the G2/M phase ($p < 0.01$) was higher than in the shCtrl group (Fig. 4A,B).

Effect of eIF3b mRNA downregulation on the apoptosis of K562 cells

On day 5 after transduction, the total cell apoptosis percentage in the sheIF3b group was substantially higher than that of the shCtrl group ($p < 0.01$, Fig. 5A,B). Caspase 3/7 activity in the sheIF3b group was remarkably higher ($p < 0.01$, Fig. 6A) than that of the control group, and the expression of anti-apoptotic protein Bcl-2 was markedly lower in the sheIF3b group than in the shCrtl group ($p < 0.01$, Fig. 6B), suggesting that eIF3b downregulation promoted the apoptosis of K562 cells.

Discussion

Chronic myeloid leukemia is a clonal HSC disorder resulting from a reciprocal translocation between the long arms of ch9 and ch22, t (9;22), which leads to the fusion of the *ABL1* proto-oncogene from ch9 with the *BCR*

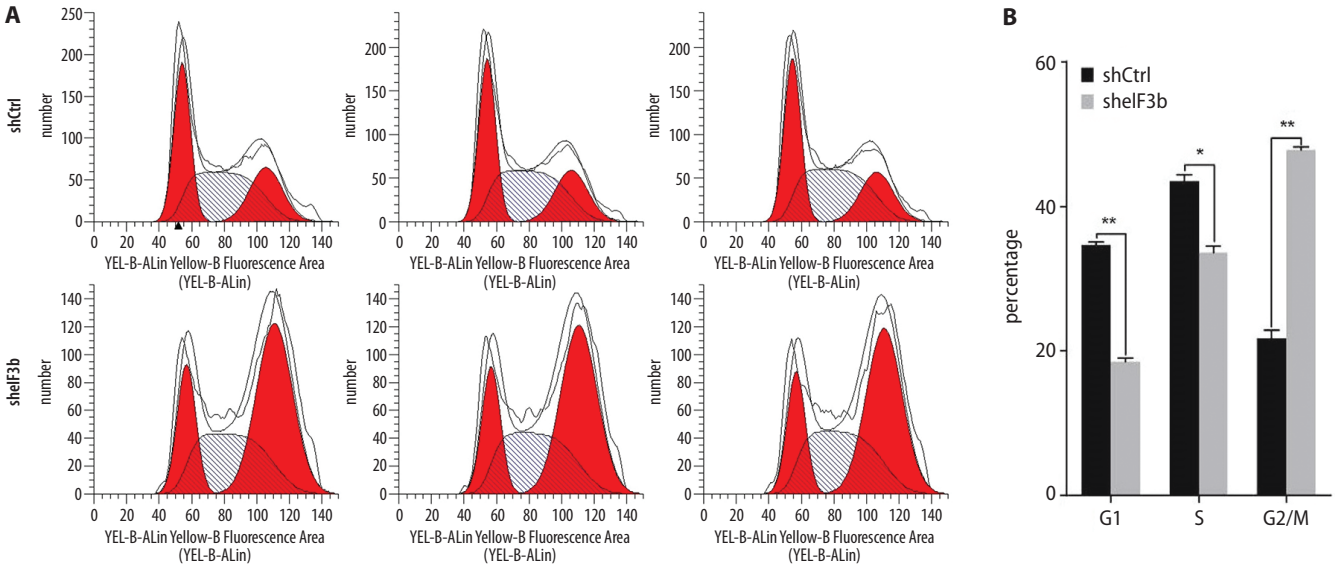

Fig. 4. Effect of *eIF3b* gene downregulation on the cell cycles of K562 cells; A – proportion of K562 cells in different phases in the shCtrl and sheIF3b groups; B – proportion of K562 cells in G1, S, and G2/M phases in the shCtrl and sheIF3b groups

*p < 0.01; **p < 0.01.

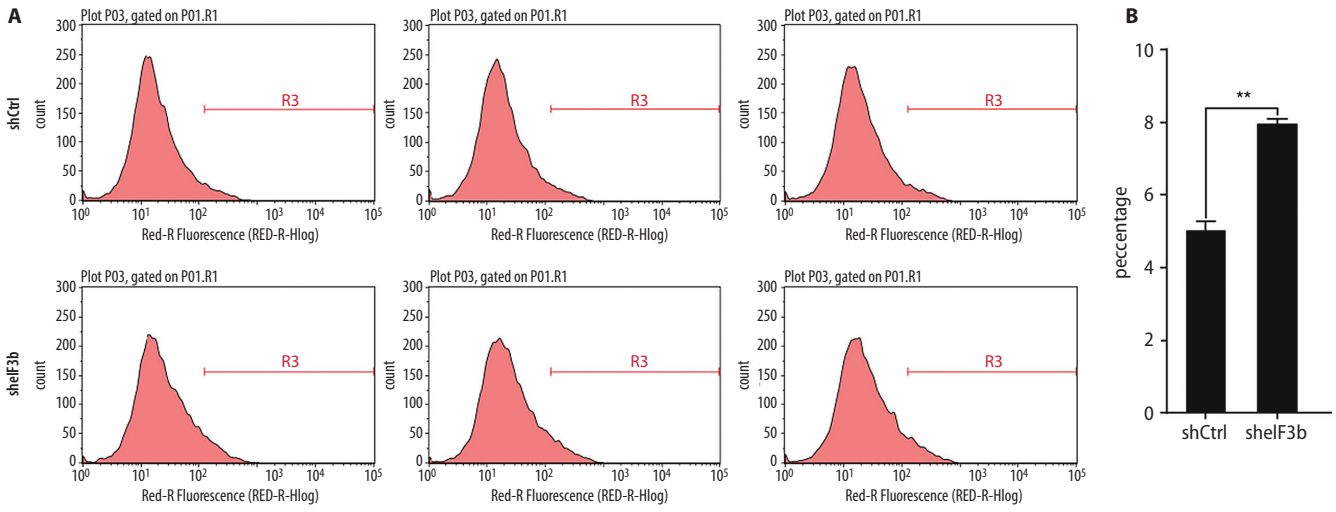

Fig. 5. Effect of *eIF3b* gene downregulation on the apoptosis of K562 cells; A – cell apoptosis of K562 cells in the shCtrl and sheIF3b groups; B – percentage of cell apoptosis in the shCtrl and sheIF3b groups

**p < 0.01.

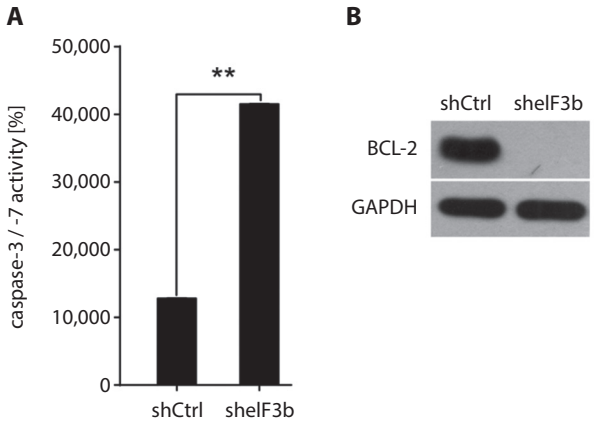

Fig. 6. Effect of *eIF3b* gene downregulation on apoptosis-related proteins; A – caspase 3/7 activity in the shCtrl and shelF3b groups; B – expression of anti-apoptotic protein BCL-2 in the shCtrl and shelF3b groups

**$p < 0.01$.

housekeeping gene on ch22 to produce the *BCR-ABL* gene.[13] This fusion gene is transcribed into BCR-ABL1 mRNA and translated into the BCR-ABL protein, which initiates the progression of CML.[14,15]

Dysregulation of mRNA translation leads to the aberrant activation of cellular pathways that promote cell proliferation, invasion and progression of leukemia. The main function of eIFs is in the interaction between the ribosome and mRNA, which takes part in the initial process of protein synthesis, affecting cell cycle, growth and apoptosis.[16,17]

eIF3b, a member of the eIF3 complex, is reported to be overexpressed in various tumor cells and acts as an oncogene. A study indicated that eIF3b mRNA is abundantly expressed in colon cancer cells, and that the downregulation of *eIF3b* inhibits cell proliferation, reduces the number of cells in the G1 phase and increases the number of cells in the S/G2 phases, as well as promotes cell apoptosis.[8] Another study investigating the role of *eIF3b* in esophageal squamous cell carcinoma (ESCC) also revealed that *eIF3b* expression is much higher in ESCC tissues and ESCC cell lines, while a reduction in *eIF3b* suppresses cell proliferation and stimulates cell apoptosis through the regulation of the β-catenin signaling pathway.[18] In bladder and prostate cancer cells, eIF3b deletion decreases cell growth and represses the G1/S cell cycle transition by regulating cyclin A, E, Rb, and p27Kip1 protein expression – but not mRNA expression – and it reduces migration as well as interrupting the actin cytoskeleton and focal adhesions.[11] A recently published study showed that knockdown of *eIF3b* decreases cell viability and promotes apoptosis in osteosarcoma cells due to the regulation of tumor necrosis factor receptor superfamily member 21 (TNFRSF21).[19] These findings indicate that *eIF3b* is involved in tumor development and progression by acting as a cancer-promoting gene.

In clinical research, Wang et al. examined the expression of eIF3b mRNA in patients with bladder cancer and prostate cancer, and reported that eIF3b mRNA expression is much higher in cancer patients than in controls. Interestingly, they also discovered that eIF3b mRNA is positively correlated with tumor grade and could predict unfavorable survival.[9] However, the role of *eIF3b* in CML remains unclear. In this study, we found that eIF3b mRNA expression was higher in CML patients and CML cell lines than in the controls. Downregulation of eIF3b expression suppressed CML cell proliferation, decreased G1/S-phase cells and induced cell apoptosis, which was in line with the oncogenic role of *eIF3b* in other studies. Reduced eIF3b mRNA expression inhibits proliferation and promotes apoptosis in K562 cells. The possible explanations could be as follows: 1) *eIF3b* could activate the β-catenin signaling pathway, including the downstream target gene cyclin D1 and c-Myc, thus inducing cell proliferation and invasion, as well as inhibiting cell apoptosis and interfering with the cell cycle[18] or; 2) *eIF3b* is involved in protein synthesis and *eIF3b* depletion can globally inhibit protein synthesis, which affects the proliferation and apoptosis of cancer cells.[9]

There were some limitations in this study. Firstly, the prognostic role of *eIF3b* expression in CML patients was not investigated. Secondly, we discovered the role of *eIF3b* in regulating CML cell proliferation and apoptosis, but the mechanism of how *eIF3b* affects cancer cell progression was not explored. This will be the focus of future research.

In conclusion, the downregulation of *eIF3b* inhibits proliferation and induces apoptosis in CML cells.

ORCID iDs

Laiquan Huang https://orcid.org/0000-0002-7139-9755
Kun He https://orcid.org/0000-0001-5843-2939
Jianxin Wang https://orcid.org/0000-0001-9548-1465
Jiawei Yan https://orcid.org/0000-0001-9887-503X
Yizhi Jiang https://orcid.org/0000-0002-4812-2547
Zhongling Wei https://orcid.org/0000-0002-2763-0964
Jun Zhang https://orcid.org/0000-0002-1759-2829
Guangxi Li https://orcid.org/0000-0002-4309-0611
Lili Sheng https://orcid.org/0000-0002-9579-7328

References

1. Gutierrez LG, Noriega MF, Laudicina A, Quatrin M, Bengio RM, Larripa I. An unusual translocation, t(1;11)(q21;q23), in a case of chronic myeloid leukemia with a cryptic Philadelphia chromosome. *Oncol Lett*. 2017;13(5):3159–3162.
2. Hinnebusch AG, Lorsch JR. The mechanism of eukaryotic translation initiation: New insights and challenges. *Cold Spring Harb Perspect Biol*. 2012;4(10). doi:10.1101/cshperspect.a011544
3. Pestova TV, Kolupaeva VG. The roles of individual eukaryotic translation initiation factors in ribosomal scanning and initiation codon selection. *Genes Dev*. 2002;16(22):2906–2922.
4. Sonenberg N, Hinnebusch AG. Regulation of translation initiation in eukaryotes: Mechanisms and biological targets. *Cell*. 2009;136(4):731–745.
5. Silvera D, Formenti SC, Schneider RJ. Translational control in cancer. *Nat Rev Cancer*. 2010;10(4):254–266.
6. Hagner PR, Schneider A, Gartenhaus RB. Targeting the translational machinery as a novel treatment strategy for hematologic malignancies. *Blood*. 2010;115(11):2127–2135.

7. Spilka R, Ernst C, Mehta AK, Haybaeck J. Eukaryotic translation initiation factors in cancer development and progression. *Cancer Lett*. 2013;340(1):9–21.
8. Mayeur GL, Fraser CS, Peiretti F, Block KL, Hershey JW. Characterization of eIF3k: A newly discovered subunit of mammalian translation initiation factor eIF3. *Eur J Biochem*. 2003;270(20):4133–4139.
9. Hinnebusch AG. eIF3: A versatile scaffold for translation initiation complexes. *Trends Biochem Sci*. 2006;31(10):553–562.
10. Wang Z, Chen J, Sun J, Cui Z, Wu H. RNA interference-mediated silencing of eukaryotic translation initiation factor 3, subunit B (eIF3b) gene expression inhibits proliferation of colon cancer cells. *World J Surg Oncol*. 2012;10:119.
11. Wang H, Ru Y, Sanchez-Carbayo M, Wang X, Kieft JS, Theodorescu D. Translation initiation factor eIF3b expression in human cancer and its role in tumor growth and lung colonization. *Clin Cancer Res*. 2013; 19(11):2850–2860.
12. Liang H, Ding X, Zhou C, et al. Knockdown of eukaryotic translation initiation factors 3B (eIF3b) inhibits proliferation and promotes apoptosis in glioblastoma cells. *Neurol Sci*. 2012;33(5):1057–1062.
13. Apperley JF. Chronic myeloid leukaemia. *Lancet*. 2015;385(9976): 1447–1459.
14. Kavalerchik E, Goff D, Jamieson CH. Chronic myeloid leukemia stem cells. *J Clin Oncol*. 2008;26(17):2911–2915.
15. Savona M, Talpaz M. Getting to the stem of chronic myeloid leukaemia. *Nat Rev Cancer*. 2008;8(5):341–350.
16. Pestova TV, Kolupaeva VG, Lomakin IB, et al. Molecular mechanisms of translation initiation in eukaryotes. *Proc Natl Acad Sci U S A*. 2001; 98(13):7029–7036.
17. Lee AS, Kranzusch PJ, Cate JH. eIF3 targets cell-proliferation messenger RNAs for translational activation or repression. *Nature*. 2015; 522(7554):111–114.
18. Xu F, Xu CZ, Gu J, et al. Eukaryotic translation initiation factor 3B accelerates the progression of esophageal squamous cell carcinoma by activating beta-catenin signaling pathway. *Oncotarget*. 2016;7(28): 43401–43411.
19. Choi YJ, Lee YS, Lee HW, Shim DM, Seo SW. Silencing of translation initiation factor eIF3b promotes apoptosis in osteosarcoma cells. *Bone Joint Res*. 2017;6(3):186–193.

Accuracy of digital dental models using the low-cost DAVID laser scanner

Raphael Olszewski[1,A–F], Joanna Szyper-Szczurowska[2,B–F], Maciej Opach[3,B–F], Piotr Bednarczyk[4,B–F], Jan Zapala[3,E,F], Stefan Szczepanik[4,A–F]

[1] Department of Oral and Maxillofacial Surgery, Cliniques universitaires Saint-Luc, Catholic University of Louvain, Brussels, Belgium
[2] Department of Orthodontics, Jagiellonian University Medical College, Kraków, Poland
[3] Department of Cranio-maxillofacial Surgery, Jagiellonian University Medical College, Kraków, Poland
[4] Department of Metal Forming, AGH University of Science and Technology, Kraków, Poland

A – research concept and design; B – collection and/or assembly of data; C – data analysis and interpretation; D – writing the article; E – critical revision of the article; F – final approval of the article

Advances in Clinical and Experimental Medicine, ISSN 1899–5276 (print), ISSN 2451–2680 (online) *Adv Clin Exp Med*. 2019;28(12):1647–1656

Address for correspondence
Raphael Olszewski
E-mail: raphael.olszewski@uclouvain.be

Funding sources
None declared

Conflict of interest
None declared

Received on December 21, 2018
Review on January 22, 2019
Accepted on June 27, 2019

Published online on November 28, 2019

Abstract

Background. Accurate laser scanning of plaster casts using validated, low-cost hardware represents a key issue in 3D orthodontics.

Objectives. The aim of this study was to compare the accuracy of measurements taken from plaster casts (gold standard) with digital models of those casts created with a low-cost structural light DAVID laser scanner.

Material and methods. Five different measurements were taken on each of 14 plaster casts by 2 independent observers with an electronic caliper. The measurements were repeated 10 times on all 14 plaster casts by each observer, with a 1-week interval between each set of measurements. All 14 plaster casts were digitized using a low-cost DAVID SLS 3 laser scanner. The same 5 measurements were performed on each of the 3D virtual surface models of the 14 plaster casts by 2 independent observers using MeshLab software in a manner similar to that used with the digital caliper. The measurements were repeated 10 times by the 2 observers with 1 week between each set of measurements.

Results. The laser-scanned models were more accurate than the plaster cast models in defining measurements based on simple tooth fissures. The accuracy of measurements based on complex tooth fissures were equivalent for the 2 types of model. For measurements based on interproximal dental contacts, the 2 methods of measurement were similar and both were notably poor in terms of accuracy.

Conclusions. Three-dimensional virtual models obtained from the low-cost DAVID laser scanner can be used clinically, but only for certain types of measurements and indications.

Key words: orthodontics, laser scanner, digital dental models, plaster cast

Cite as
Olszewski R, Szyper-Szczurowska J, Opach M, Bednarczyk P, Zapala J, Szczepanik S. Accuracy of digital dental models using the low-cost DAVID laser scanner. *Adv Clin Exp Med*. 2019;28(12):1647–1656. doi:10.17219/acem/110318

DOI
10.17219/acem/110318

Introduction

Digital dental models are used in orthodontics because they are easy to store, save time and space and facilitate the sharing of information with colleagues over the internet.[1] Digital models do not deteriorate over time.[1] Laser scanners are accessible to clinicians through a digitization service, such as OrtoCad (Align Technology Inc., San Jose, USA)[2,3] or "emodels" (GeoDigm Corp., Falcon Heights, USA),[2,3] through desktop laser scanners (i.e., 3Shape R500, 3Shape R700, 3Shape R1000, 3Shape R2000, Medianetx grande, Medianetx colori, DentaCore CS ULTRA, Dentaurum OrthoX, Maestro 3D, Imetric IScan D104i and GC Aadva Lab Scan[4]), through cone-beam computed tomography (CT)[5] and, recently, through intraoral laser scanners.[6] All of these technologies are still very expensive and limit the spread of digital orthodontics to the wealthiest clinical practices and private hospitals. Moreover, desktop laser scanners present sufficient accuracy, so further improvement would not provide additional benefit for use in orthodontics.[4] Nowak et al.[4] concluded that research on laser scanners in orthodontics and orthognathic surgery should focus primarily on reducing time and cost.[4]

With the advent of the low-cost three-dimensional (3D) printing era, a number of companies have also attempted to develop low-cost laser scanners. Among the 3 types of low-cost laser scans currently available on the market, only the DAVID SLS 3 laser scanner provides a maximum resolution of 0.05% of the scanned object at a price of 3,275 USD (www.aniwaa.com/comparison/3d-scanners). Therefore, our objective for this study was to compare the accuracy of measurements taken from plaster casts (gold standard) with digital models obtained from the low-cost DAVID laser scanner. The null hypothesis is that the digital model is as accurate as a plaster-cast model, and that the low-cost DAVID laser scanner could be used clinically.

The DAVID SLS 3 laser scanner uses structural light and consists of a light projector, 2 detectors and a rotary table. A calibration kit for the device is also provided by the manufacturer. The projector projects 48 light structures onto the object to be scanned and the detectors analyze the deformation of these light structures on the scanned object, which is rotated on the rotary table.

Material and methods

Initially, 31 plaster-cast models from patients treated with orthodontics and orthognathic surgery and presenting maxillomandibular Angle class III discrepancies were used. From the 31 plaster casts, we discarded 17 with missing teeth in the areas of further distance measurements and selected the remaining 14. The plaster casts were created in the same laboratory, and a similar length of time separated the alginate impression from casting.[2] Two calibrated observers participated in this study. Observer #1 was an experienced orthodontist, while observer #2 was a maxillofacial surgeon. The 2 examiners were calibrated by collaborating on 2 sample cases of plaster casts and 2 sample cases of laser-scanned casts.[2] The measurements were directly compared and discussed until final definition.[2]

Table 1. Definition of the measurements

Name	Definition
Measurement A	Anterior width of the upper dental arch: distance between the most lower points of the transversal groove of the first upper premolar teeth.
Measurement B	Posterior width of the upper dental arch: distance between the points of intersection of the transversal groove with the buccal groove of the first upper permanent molar teeth.
Measurement C	Palatal width: distance between the intersection points of the palatal groove with the gingival margin of first upper permanent molar teeth (Howe et al.[2]).
Measurement D	Anterior width of the lower dental arch: distance between the vestibular contact points of the first and the second lower premolars.
Measurement E	Posterior width of the lower dental arch: distance between the distal and lingual cusp tips of right and left mandibular permanent first molars.

Five measurements (A–E) (Table 1) were performed on each of the 14 plaster casts by the 2 independent observers using an electronic caliper (OTLT, Otelo, Saint-Ouen-l'Aumône, France) with a measurement error of 0.02 mm. The measurements were repeated on all 14 of the plaster casts 10 times each by the 2 observers, with a 1-week interval between each set of measurements.

All plaster casts (#1 to #14) were also digitized using a DAVID SLS 3 laser scanner v. 4.5.3 (DAVID; Antonius Köster, Meschede, Germany). The scanning angle was 36°. Each digitalized model was created from 10 measurements (a full rotation of the table is 360°). The cloud of points was then analyzed with DAVID SLS 3 software v. 4.5.3 (Antonius Köster). A 3D virtual surface model (.obj file) of each plaster cast was saved for further measurements by the 2 observers. Five measurements (A–E) (Table 1) were performed on each of the 3D virtual surface models of the 14 plaster casts by 2 independent observers with MeshLab software (v. 1.3.2) (Consiglio Nazionale delle Ricerche – CNR, Rome, Italy) in a manner analogous to that employed with the digital caliper. The measurements were repeated on all of the 3D virtual surface models of the 14 plaster casts 10 times by 2 independent observers. A 1-week period of time elapsed between each set of measurements. Measurement A on model #4 was impossible to perform because one of the premolars was missing on the plaster-cast model. Palatal width definition was proposed according to the study by Howe et al.[7]

Figure 1 shows the measurements performed on the plaster casts, while Fig. 2 and 3 illustrate the measurements performed on the laser-scanned virtual 3D models of the plaster casts.

Fig. 1. Measurements A–C performed on the plaster cast of the upper maxilla. Measurements D and E performed on the plaster cast of the mandible

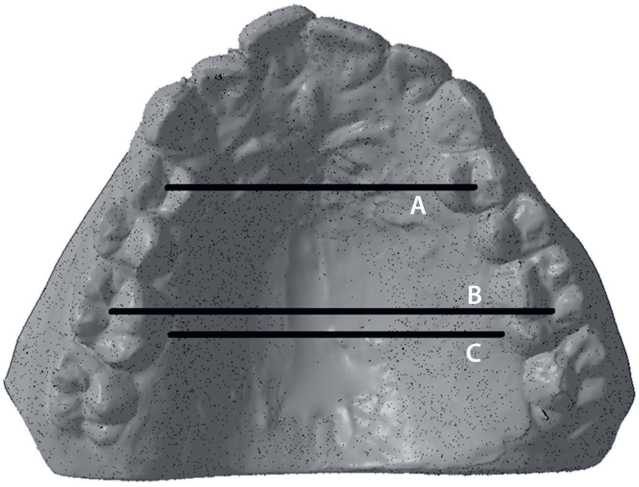

Fig. 2. Measurements A–C performed on the virtual 3D model of the laser-scanned upper maxilla plaster cast

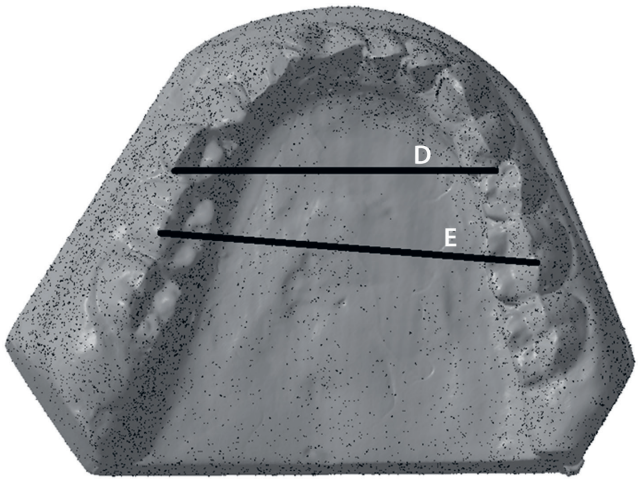

Fig. 3. Measurements D and E performed on the virtual 3D model of the laser-scanned mandibular plaster cast

Results

For statistical analysis, we assumed that the population presented a normal distribution. The populations represent 2 small groups of 14 elements, each consisting of measurements (Table 1) performed by observer #1 and observer #2. Table 2 (observer #1) and Table 3 (observer #2) show the pairs of measurements obtained from the 14 plaster casts with the minimum and maximum values, the difference between these values, the mean values, and their standard deviation (SD). Table 4 shows a comparison of the measurements taken by observers #1 and #2 and the confidence interval (95% CI) with $\alpha = 0.05$. Table 5 shows the CIs for the differences between the measurements observed by observer #1 and observer #2, according to the type of method (caliper vs 3D virtual model) and the type of measurement (A–E).

The CIs for the measurements performed by observer #1 (orthodontist) on the plaster casts and on the digital models are 0.069–0.196 mm and 0.057–0.329 mm, respectively. The CIs for the measurements performed by observer #2 (maxillofacial surgeon) on the plaster casts and on the digital models are 0.054–0.408 mm and 0.136–0.429 mm, respectively.

Measurement A was based on the anatomical definition of a simple tooth fissure. The laser-scanned models were more accurate than the plaster-cast models in defining measurement A (Table 5). Measurement B was based on the anatomical definition of a complex tooth fissure. Measurement C was based on the intersection between 2 different structures, such as a tooth fissure and the impression of the palatal gingiva on the tooth. The accuracy of measurements B and C was equivalent for the laser-scanned and the plaster models. Measurement D was based on interproximal dental contacts. Measurement E was based on the tips of cusps (curvature areas). Measurements D and E were equivalent and provided notably poor accuracy. Our findings related to measurements D and E were in accordance with the literature.[2]

Table 2. Measurements performed by observer #1

Measurement name	Caliper measurement plaster cast					3D virtual model measurement laser scanner				
	maximal value (max) [mm]	minimal value (min) [mm]	difference [max–min] [mm]	mean value [mm]	standard deviation [mm]	maximal value (max) [mm]	minimal value (min) [mm]	difference [max–min] [mm]	mean value [mm]	standard deviation [mm]
m01 A	33.02	32.44	0.58	32.81	0.17	33.35	32.58	0.77	32.92	0.30
m01 B	47.46	46.60	0.86	46.98	0.24	47.50	46.70	0.80	47.09	0.28
m01 C	34.76	33.50	0.26	34.43	0.37	35.60	34.77	0.83	35.27	0.23
m01 D	33.63	33.01	0.62	33.29	0.18	33.80	33.24	0.56	33.49	0.20
m01 E	43.62	42.39	1.23	42.93	0.37	43.63	42.76	0.87	43.20	0.26
m02 A	38.86	38.22	0.64	38.51	0.21	39.07	38.33	0.74	38.70	0.27
m02 B	51.97	51.19	0.78	51.78	0.22	53.11	52.11	1.00	52.46	0.28
m02 C	40.93	39.27	1.66	40.02	0.50	41.69	40.03	1.66	40.92	0.46
m02 D	37.59	36.39	1.20	37.00	0.34	38.77	37.97	0.80	38.44	0.26
m02 E	50.65	49.49	1.16	50.11	0.32	50.33	49.52	0.81	49.90	0.26
m03 A	36.28	35.62	0.66	36.05	0.22	37.05	35.73	1.32	36.52	0.36
m03 B	44.92	44.24	0.68	44.50	0.23	45.38	44.46	0.92	44.89	0.26
m03 C	32.53	31.02	1.51	32.09	0.42	33.94	33.22	0.72	33.50	0.24
m03 D	35.80	34.31	1.49	34.77	0.40	36.89	35.12	1.77	35.94	0.60
m03 E	45.88	44.91	0.97	45.36	0.31	46.52	45.05	1.47	45.53	0.43
m04 A	–	–	–	–	–	–	–	–	–	–
m04 B	46.88	45.51	1.37	46.26	0.40	47.00	45.99	1.01	46.43	0.29
m04 C	34.40	32.53	1.87	33.54	0.57	34.89	34.00	0.89	34.44	0.36
m04 D	35.66	34.11	1.55	34.88	0.44	36.89	36.14	0.75	36.41	0.19
m04 E	49.28	48.43	0.85	48.84	0.30	49.47	48.14	1.33	48.94	0.39
m05 A	29.90	29.04	0.86	29.48	0.29	29.75	29.01	0.74	29.54	0.22
m05 B	42.89	41.70	1.19	42.27	0.38	43.27	42.23	1.04	42.76	0.34
m05 C	32.90	31.74	1.16	32.29	0.36	33.87	32.83	1.04	33.36	0.32
m05 D	31.44	30.12	1.32	30.58	0.37	31.90	30.59	1.31	31.14	0.45
m05 E	41.84	40.64	1.20	41.24	0.41	42.26	41.36	0.90	41.70	0.32
m06 A	35.83	34.81	1.02	35.26	0.30	35.93	35.03	0.90	35.45	0.30
m06 B	51.75	51.11	0.64	51.41	0.20	52.07	51.32	0.75	51.68	0.27
m06 C	39.08	38.15	0.93	38.58	0.28	40.08	38.93	1.15	39.43	0.34
m06 D	37.58	36.36	1.22	37.07	0.33	38.92	37.72	1.20	38.22	0.40
m06 E	51.59	50.42	1.17	51.15	0.28	52.20	51.23	0.97	51.67	0.29
m07 A	30.04	29.68	0.36	29.93	0.10	31.47	30.08	1.39	30.56	0.45
m07 B	39.98	39.42	0.56	39.69	0.20	40.46	38.99	1.47	39.74	0.49
m07 C	30.32	28.84	1.48	29.49	0.44	31.68	30.54	1.14	31.06	0.33
m07 D	35.11	34.14	0.97	34.56	0.33	35.86	34.32	1.54	35.00	0.46
m07 E	46.66	45.98	0.68	46.33	0.26	48.29	47.07	1.22	47.58	0.43
m08 A	34.89	33.67	1.22	34.23	0.39	34.93	34.28	0.65	34.55	0.23
m08 B	44.75	43.86	0.89	44.39	0.29	45.01	44.09	0.92	44.52	0.22
m08 C	35.18	33.22	1.96	34.20	0.59	36.63	35.87	0.76	36.30	0.28
m08 D	32.45	31.26	1.19	32.13	0.32	33.83	32.08	1.75	32.84	0.55
m08 E	45.40	43.47	1.93	44.41	0.45	45.46	44.64	0.82	45.10	0.26
m09 A	37.05	36.09	0.96	36.42	0.26	37.20	35.63	1.57	36.47	0.38
m09 B	50.70	49.61	1.09	50.23	0.31	50.36	49.10	1.26	49.93	0.35

Table 2. Measurements performed by observer #1 – cont.

Measurement name	Caliper measurement plaster cast					3D virtual model measurement laser scanner				
	maximal value (max) [mm]	minimal value (min) [mm]	difference [max–min] [mm]	mean value [mm]	standard deviation [mm]	maximal value (max) [mm]	minimal value (min) [mm]	difference [max–min] [mm]	mean value [mm]	standard deviation [mm]
m09 C	38.23	37.46	0.77	37.87	0.26	39.49	38.57	0.92	39.11	0.32
m09 D	31.66	30.50	1.16	31.03	0.37	32.57	31.82	0.75	32.16	0.22
m09 E	42.08	40.69	1.39	41.38	0.41	44.97	44.10	0.87	44.51	0.26
m10 A	39.92	39.35	0.57	39.59	0.18	41.21	40.34	0.87	40.82	0.25
m10 B	49.83	49.17	0.66	49.44	0.20	51.08	49.96	1.12	50.38	0.29
m10 C	38.73	37.11	1.62	37.84	0.47	38.66	37.79	0.87	38.32	0.28
m10 D	35.21	33.08	2.13	34.11	0.62	36.42	34.91	1.51	35.43	0.44
m10 E	45.88	45.18	0.70	45.55	0.21	46.24	45.26	0.98	45.82	0.33
m11 A	34.85	33.37	1.48	33.95	0.40	34.94	33.98	0.96	34.39	0.35
m11 B	45.49	44.49	1.00	45.08	0.34	46.61	45.37	1.24	45.71	0.36
m11 C	32.48	31.51	0.97	31.92	0.29	33.44	31.81	1.63	32.27	0.47
m11 D	31.42	30.17	1.25	30.81	0.42	32.82	31.38	1.44	32.01	0.45
m11 E	44.42	43.13	1.29	43.78	0.46	44.02	43.02	1.00	43.56	0.37
m12 A	45.73	45.18	0.55	45.47	0.14	46.44	45.72	0.72	46.06	0.23
m12 B	55.73	54.95	0.78	55.29	0.24	56.32	55.49	0.83	55.84	0.26
m12 C	43.27	41.71	1.56	42.65	0.50	44.23	43.05	1.18	43.42	0.42
m12 D	42.83	41.35	1.48	42.16	0.42	43.17	41.98	1.19	42.58	0.31
m12 E	57.37	56.19	1.18	56.69	0.32	57.51	56.22	1.29	56.78	0.40
m13 A	32.34	31.43	0.91	31.73	0.27	32.52	30.81	1.71	31.78	0.51
m13 B	45.50	44.57	0.93	45.08	0.29	45.24	44.57	0.67	44.81	0.25
m13 C	33.04	31.91	1.13	32.29	0.31	34.33	32.95	1.38	33.73	0.34
m13 D	36.63	35.39	1.24	35.77	0.33	37.24	35.71	1.53	36.63	0.44
m13 E	53.15	51.96	1.19	52.48	0.33	53.62	52.06	1.56	52.92	0.53
m14 A	33.93	32.30	1.63	32.99	0.39	34.43	33.65	0.78	34.08	0.24
m14 B	45.39	44.30	1.09	44.81	0.31	45.57	44.74	0.83	45.15	0.25
m14 C	32.66	31.03	1.63	31.83	0.52	34.10	32.66	1.44	33.29	0.47
m14 D	35.89	34.70	1.19	35.41	0.36	37.51	36.22	1.29	36.67	0.42
m14 E	48.78	46.99	1.79	48.05	0.52	48.78	46.11	2.67	47.16	0.87

Discussion

The measurements taken by the orthodontist were more accurate than those taken by the maxillofacial surgeon, possibly because of personal experience and the clinical use of plaster casts in daily orthodontic practice. However, the mean values differ between the observers and the methods. The difference in measurements observed between both observers and both methods may be related to the observer's aptitude of correctly selecting landmarks which correspond to their theoretical definition. This selection may be influenced by 1) the subjective interpretation of the landmark's definition, 2) the quality of the occlusal surfaces and the interproximal contact points of the patient's teeth, 3) the quality of the impression obtained, 4) the type of material used for the plaster cast, 5) the color of the plaster cast, 6) the color of the 3D virtual rendering on the computer screen, and 7) 3D manipulation of the digital cast in the software (zooming, rotating and selecting views).[8] Measurements A–C performed on the digital models (Table 5) were included below the threshold difference of 1.5 mm which was suggested by Profitt as a limiting value for clinical significance.[9] The majority of measurements D and E were above the threshold difference of 1.5 mm for both methods (Table 5). Therefore, measurements D and E should be discarded from further comparative studies regarding the accuracy of laser-scanned and plaster-cast models.

Table 3. Measurements performed by observer #2

Measurement name	Observer #2									
	caliper measurement plaster cast					3D virtual model measurement laser scanner				
	maximal value (max) [mm]	minimal value (min) [mm]	difference (max–min) [mm]	mean value [mm]	standard deviation [mm]	maximal value (max) [mm]	minimal value (min) [mm]	difference [max–min] [mm]	mean value [mm]	standard deviation [mm]
m01 A	33.84	33.18	0.66	33.39	0.22	33.12	32.51	0.61	32.85	0.16
m01 B	47.48	46.94	0.54	47.22	0.19	47.69	47.24	0.45	47.46	0.18
m01 C	34.50	33.57	0.93	34.03	0.31	35.82	35.07	0.75	35.45	0.21
m01 D	35.33	34.22	1.11	34.78	0.39	35.35	34.72	0.63	35.12	0.18
m01 E	45.93	45.35	0.58	45.66	0.21	46.17	45.48	0.69	45.84	0.20
m02 A	40.94	39.18	1.76	40.04	0.45	39.45	38.56	0.89	38.86	0.28
m02 B	52.23	51.85	0.38	52.11	0.11	52.56	51.65	0.91	52.27	0.24
m02 C	40.41	39.83	0.58	40.17	0.18	41.72	40.77	0.95	41.33	0.25
m02 D	39.36	38.60	0.76	39.00	0.26	39.88	38.87	1.01	39.56	0.30
m02 E	53.93	52.17	1.76	52.92	0.52	53.48	52.30	1.18	52.99	0.35
m03 A	37.48	36.55	0.93	36.87	0.31	36.51	35.99	0.52	36.26	0.18
m03 B	45.96	45.17	0.79	45.62	0.28	45.64	44.78	0.86	45.00	0.25
m03 C	35.14	33.08	2.06	33.85	0.63	34.97	33.24	1.73	34.33	0.46
m03 D	37.59	36.18	1.41	37.19	0.45	38.02	37.30	0.72	37.60	0.22
m03 E	48.34	47.35	0.99	47.78	0.28	48.43	47.45	0.98	47.90	0.31
m04 A	–	–	–	–	–	–	–	–	–	–
m04 B	47.26	46.64	0.62	46.90	0.20	46.88	46.17	0.71	46.48	0.21
m04 C	35.52	33.34	2.18	34.07	0.62	35.41	34.38	1.03	34.81	0.32
m04 D	36.68	35.88	0.80	36.36	0.28	37.36	37.05	0.31	37.18	0.12
m04 E	52.75	51.89	0.86	52.37	0.26	53.62	53.00	0.62	53.28	0.21
m05 A	31.70	29.43	2.27	30.92	0.60	30.74	29.67	1.07	30.25	0.31
m05 B	42.88	42.23	0.65	42.53	0.22	43.35	42.34	1.01	42.71	0.32
m05 C	32.89	31.19	1.70	32.41	0.46	34.26	33.84	0.42	34.09	0.14
m05 D	34.00	32.09	1.91	33.45	0.57	34.58	33.73	0.85	34.19	0.25
m05 E	43.69	42.77	0.92	43.15	0.29	44.08	43.43	0.65	43.79	0.21
m06 A	37.70	36.31	1.39	36.86	0.49	36.08	35.33	0.75	35.80	0.22
m06 B	52.00	51.40	0.60	51.61	0.17	52.83	51.92	0.91	52.33	0.30
m06 C	38.71	38.26	0.45	38.43	0.55	39.55	38.31	1.24	38.78	0.37
m06 D	40.09	39.20	0.89	39.64	0.28	40.64	39.70	0.94	40.24	0.29
m06 E	53.89	53.51	0.38	53.69	0.12	54.95	53.87	1.08	54.26	0.32
m07 A	30.60	30.30	0.30	30.44	0.09	30.97	30.50	0.47	30.75	0.16
m07 B	40.17	39.02	1.15	39.69	0.34	40.01	39.36	0.65	39.71	0.24
m07 C	30.17	29.84	0.33	30.06	0.10	31.45	30.95	0.50	31.20	0.15
m07 D	36.42	34.80	1.62	35.73	0.54	36.52	35.72	0.80	36.06	0.31
m07 E	49.45	48.45	1.00	49.10	0.29	49.83	48.38	1.45	48.96	0.41
m08 A	35.06	34.64	0.42	34.86	0.14	34.54	33.81	0.73	34.23	0.21
m08 B	45.54	44.12	1.42	44.75	0.42	44.63	43.72	0.91	44.22	0.25
m08 C	35.44	34.91	0.53	35.10	0.19	37.81	37.34	0.47	37.52	0.16
m08 D	34.07	33.23	0.84	33.65	0.29	34.37	33.49	0.88	33.99	0.27
m08 E	47.38	46.10	1.28	46.84	0.43	48.19	37.81	10.38	46.65	3.12
m09 A	38.37	37.67	0.70	38.02	0.28	37.45	36.31	1.14	37.05	0.31
m09 B	50.48	49.75	0.73	50.24	0.23	50.93	49.89	1.04	50.42	0.38
m09 C	38.72	37.41	1.31	38.22	0.37	39.78	39.54	0.24	39.65	0.08
m09 D	35.02	33.63	1.39	34.30	0.47	34.86	34.07	0.79	34.47	0.24

Table 3. Measurements performed by observer #2 – cont.

Measurement name	Observer #2									
	caliper measurement plaster cast					3D virtual model measurement laser scanner				
	maximal value (max) [mm]	minimal value (min) [mm]	difference (max–min) [mm]	mean value [mm]	standard deviation [mm]	maximal value (max) [mm]	minimal value (min) [mm]	difference [max–min] [mm]	mean value [mm]	standard deviation [mm]
m09 E	44.21	43.38	0.83	43.93	0.27	44.38	43.89	0.49	44.12	0.15
m10 A	40.67	39.95	0.72	40.35	0.24	41.22	40.82	0.40	41.01	0.13
m10 B	50.38	49.68	0.70	50.06	0.21	50.95	50.31	0.64	50.60	0.22
m10 C	38.83	37.91	0.92	38.35	0.34	39.85	39.48	0.37	39.67	0.14
m10 D	38.50	38.00	0.50	38.30	0.16	37.93	37.65	0.28	37.77	0.08
m10 E	48.41	47.78	0.63	48.17	0.17	48.23	47.26	0.97	47.58	0.29
m11 A	36.04	35.00	1.04	35.28	0.31	35.54	34.90	0.64	35.22	0.24
m11 B	46.00	45.41	0.59	45.79	0.18	46.07	45.51	0.56	45.78	0.15
m11 C	32.00	31.52	0.48	31.78	0.17	34.10	33.58	0.52	33.87	0.16
m11 D	36.26	34.07	2.19	34.46	0.66	34.52	33.36	1.16	33.98	0.45
m11 E	46.32	45.68	0.64	45.99	0.18	46.53	45.89	0.64	46.18	0.23
m12 A	47.62	46.23	1.39	46.79	0.43	46.33	45.70	0.63	45.92	0.20
m12 B	56.67	55.87	0.80	56.40	0.25	56.81	56.00	0.81	56.50	0.26
m12 C	43.61	42.56	1.05	43.00	0.31	44.89	43.35	1.54	44.18	0.42
m12 D	45.77	44.85	0.92	45.27	0.39	45.21	44.81	0.40	45.07	0.12
m12 E	59.52	58.96	0.56	59.24	0.19	59.77	59.35	0.42	59.57	0.14
m13 A	33.36	31.41	1.95	32.76	0.55	32.94	32.34	0.60	32.60	0.17
m13 B	46.41	45.58	0.83	46.01	0.27	46.56	45.50	1.06	45.99	0.31
m13 C	32.37	31.90	0.47	32.14	0.14	34.42	33.78	0.64	34.17	0.20
m13 D	38.25	36.93	1.32	37.52	0.37	38.46	37.92	0.54	38.11	0.18
m13 E	56.02	55.34	0.68	55.61	0.22	56.39	55.44	0.95	55.80	0.27
m14 A	34.60	34.11	0.49	34.34	0.15	34.62	33.99	0.63	34.29	0.21
m14 B	45.93	45.53	0.40	45.73	0.13	45.75	45.21	0.54	45.42	0.16
m14 C	32.35	31.63	0.72	32.11	0.25	34.36	33.90	0.46	34.13	0.13
m14 D	38.43	37.45	0.98	37.93	0.32	38.46	37.61	0.85	37.98	0.25
m14 E	51.52	50.98	0.54	51.28	0.17	51.60	51.02	0.58	51.24	0.20

Our results were difficult to compare with reports in the literature because studies comparing plaster and digital dental models used considerably different methodologies, with variable numbers of observers, observations and repetitions of measurements, as well as using different types of digital calipers, laser scans, file formats, and software for reconstruction and analysis.[10] Better standardization is required in order to compare studies and to find stronger evidence for the accuracy of digital models. Moreover, even though measurement with caliper on a plaster cast is recognized as the gold standard, we also found errors in the measurements using this method, which follows the same pattern as those performed using digital models. A methodological alternative may be a comparison of measurements of digital models using a validated industrial laser scanner (gold standard) and a low-cost laser scanner using the same software for measurements.

In conclusion, the null hypothesis was partially accepted. Three-dimensional virtual models from the low-cost DAVID laser scanner can be used clinically, but only for certain types of measurements (types A, B and C). The low-cost DAVID laser scanner cannot be used clinically for measurements related to interproximal contact points. Therefore, the DAVID laser scanner is not suitable for analyses of teeth width, such as Bolton analysis.[11]

ORCID iDs

Raphael Olszewski https://orcid.org/0000-0002-2211-7731
Joanna Szyper-Szczurowska https://orcid.org/0000-0003-3354-1287
Maciej Opach https://orcid.org/0000-0003-0728-5945
Piotr Bednarczyk https://orcid.org/0000-0003-3725-5894
Jan Zapala https://orcid.org/0000-0002-5439-9614
Stefan Szczepanik https://orcid.org/0000-0001-8680-7750

Table 4. Comparison of the measurements between observers #1 and #2 and the confidence interval with α = 0.05

Measurement name	Difference of mean values observer #1 – observer #2 [mm]		Mean value [mm]			
			caliper measurement		3D virtual model measurement	
	caliper measurement	3D virtual model measurement	observer #1	observer #2	observer #1	observer #2
m01 A	0.58	−0.08	32.81 ±0.054	33.39 ±0.06	32.92 ±0.21	32.85 ±0.11
m01 B	0.23	0.37	46.98 ±0.07	47.22 ±0.06	47.09 ±0.20	47.46 ±0.12
m01 C	−0.40	0.18	34.43 ±0.11	34.03 ±0.09	35.27 ±0.16	35.45 ±0.15
m01 D	1.49	1.62	33.29 ±0.05	34.78 ±0.12	33.49 ±0.14	35.12 ±0.12
m01 E	2.73	2.64	42.93 ±0.11	45.66 ±0.06	43.20 ±0.18	45.84 ±0.14
m02 A	1.54	0.17	38.51 ±0.06	40.04 ±0.14	38.70 ±0.19	38.86 ±0.20
m02 B	0.33	−0.19	51.78 ±0.06	52.11 ±0.03	52.46 ±0.20	52.27 ±0.17
m02 C	0.15	0.41	40.02 ±0.15	40.17 ±0.05	40.92 ±0.32	41.33 ±0.17
m02 D	2.00	1.12	37.00 ±0.10	39.00 ±0.08	38.44 ±0.18	39.56 ±0.21
m02 E	2.81	3.09	50.11 ±0.10	52.92 ±0.16	49.90 ±0.18	52.99 ±0.25
m03 A	0.82	−0.27	36.05 ±0.10	36.87 ±0.09	36.52 ±0.25	36.26 ±0.12
m03 B	1.12	0.12	44.50 ±0.07	45.62 ±0.08	44.89 ±0.18	45.00 ±0.17
m03 C	1.76	0.83	32.09 ±0.30	33.85 ±0.19	33.50 ±0.17	34.33 ±0.32
m03 D	2.41	1.67	34.77 ±0.28	37.19 ±0.14	35.94 ±0.42	37.60 ±0.15
m03 E	2.43	2.36	45.36 ±0.22	47.78 ±0.08	45.53 ±0.30	47.90 ±0.22
m04 A	–	–	–	–	–	–
m04 B	0.64	0.05	46.26 ±0.28	46.90 ±0.06	46.43 ±0.20	46.48 ±0.15
m04 C	0.53	0.36	33.54 ±0.40	34.07 ±0.19	34.44 ±0.25	34.81 ±0.22
m04 D	1.48	0.77	34.88 ±0.31	36.36 ±0.08	36.41 ±0.13	37.18 ±0.08
m04 E	3.54	4.34	48.84 ±0.21	52.37 ±0.08	48.94 ±0.21	53.28 ±0.15
m05 A	1.45	0.71	29.48 ±9.20	30.92 ±0.18	29.54 ±0.15	30.25 ±0.22
m05 B	0.26	−0.06	42.27 ±0.27	42.53 ±0.01	42.76 ±0.24	42.71 ±0.22
m05 C	0.12	0.73	32.29 ±0.25	32.41 ±0.14	33.36 ±0.22	34.09 ±0.10
m05 D	2.87	3.06	30.58 ±0.26	33.45 ±0.18	31.14 ±0.32	34.19 ±0.17
m05 E	1.91	2.10	41.24 ±0.29	43.15 ±0.09	41.70 ±0.22	43.79 ±0.15
m06 A	1.60	0.35	35.26 ±0.21	36.86 ±0.15	35.45 ±0.21	35.80 ±0.15
m06 B	0.20	0.65	51.41 ±0.14	51.61 ±0.05	51.68 ±0.19	52.33 ±0.21
m06 C	−0.15	−0.64	38.58 ±0.20	35.43 ±0.00	39.43 ±0.24	38.78 ±0.26
m06 D	2.57	2.02	37.07 ±0.23	39.64 ±0.08	38.22 ±0.28	40.24 ±0.20
m06 E	2.54	2.59	51.15 ±0.20	53.69 ±0.03	51.67 ±0.22	54.26 ±0.22
m07 A	0.51	0.18	29.93 ±0.07	30.44 ±0.02	30.56 ±0.32	30.75 ±0.11
m07 B	−0.01	−0.03	39.69 ±0.14	39.69 ±0.10	39.74 ±0.28	39.71 ±0.17
m07 C	0.57	0.14	29.49 ±0.31	30.06 ±0.03	31.06 ±0.23	31.20 ±0.10
m07 D	1.17	1.06	34.56 ±0.23	35.73 ±0.17	35.00 ±0.32	36.06 ±0.22
m07 E	2.77	1.39	46.33 ±0.18	49.10 ±0.09	47.58 ±0.30	48.96 ±0.29
m08 A	0.63	−0.32	34.23 ±0.27	34.86 ±0.04	34.55 ±0.16	34.23 ±0.15
m08 B	0.37	−0.30	44.39 ±0.20	44.75 ±0.13	44.52 ±0.15	44.22 ±0.17
m08 C	0.89	1.21	34.20 ±0.44	35.10 ±0.06	36.30 ±0.20	37.52 ±0.11
m08 D	1.52	1.15	32.13 ±0.22	33.65 ±0.09	32.84 ±0.39	33.99 ±0.19
m08 E	2.42	1.55	44.41 ±0.32	46.84 ±0.13	45.10 ±0.18	46.65 ±0.23
m09 A	1.61	0.59	36.42 ±0.18	38.02 ±0.08	36.47 ±0.27	37.05 ±0.22
m09 B	0.01	0.49	50.23 ±0.22	50.24 ±0.07	49.93 ±0.25	50.42 ±0.27
m09 C	0.35	0.54	37.87 ±0.18	38.22 ±0.11	39.11 ±0.22	39.65 ±0.05
m09 D	3.28	2.31	31.03 ±0.26	34.30 ±0.14	32.16 ±0.15	34.47 ±0.17

Table 4. Comparison of the measurements between observers #1 and #2 and the confidence interval with α = 0.05– cont.

Measurement name	Difference of mean values observer #1 – observer #2 [mm]		Mean value [mm]			
			caliper measurement		3D virtual model measurement	
	caliper measurement	3D virtual model measurement	observer #1	observer #2	observer #1	observer #2
m09 E	2.55	−0.40	41.38 ±0.29	43.93 ±0.08	44.51 ±0.18	44.12 ±0.10
m10 A	0.76	0.19	39.59 ±0.12	40.35 ±0.07	40.82 ±0.17	41.01 ±0.09
m10 B	0.63	0.22	49.44 ±0.14	50.06 ±0.06	50.38 ±0.22	50.60 ±0.15
m10 C	0.51	1.35	37.84 ±0.33	38.35 ±0.06	38.32 ±0.20	39.67 ±0.10
m10 D	4.19	2.34	34.11 ±0.44	38.30 ±0.05	35.43 ±0.31	37.77 ±0.05
m10 E	2.62	1.76	45.55 ±0.15	48.17 ±0.05	45.82 ±0.23	47.58 ±0.26
m11 A	1.33	0.82	33.95 ±0.28	35.28 ±0.09	34.39 ±0.25	35.22 ±0.17
m11 B	0.70	0.07	45.08 ±0.02	45.79 ±0.05	45.71 ±0.25	45.78 ±0.10
m11 C	−0.14	1.59	31.92 ±0.20	31.78 ±0.05	32.27 ±0.33	33.87 ±0.11
m11 D	3.64	1.97	30.81 ±0.30	34.46 ±0.05	32.01 ±0.32	33.98 ±0.22
m11 E	2.20	2.63	43.78 ±0.32	45.99 ±0.20	43.56 ±0.26	46.18 ±0.16
m12 A	1.33	−0.13	45.47 ±0.10	46.79 ±0.13	46.06 ±0.16	45.92 ±0.14
m12 B	1.11	0.66	55.29 ±0.17	56.40 ±0.07	55.84 ±0.18	56.50 ±0.18
m12 C	0.35	0.76	42.65 ±0.35	43.00 ±0.09	43.42 ±0.30	44.18 ±0.30
m12 D	3.11	2.49	42.16 ±0.30	45.27 ±0.12	42.58 ±0.22	45.07 ±0.08
m12 E	2.55	2.79	56.69 ±0.22	59.24 ±0.06	56.78 ±0.28	59.57 ±0.10
m13 A	1.03	0.81	31.73 ±0.19	32.76 ±0.17	31.78 ±0.35	32.60 ±0.12
m13 B	0.93	1.18	45.08 ±0.20	46.01 ±0.08	44.81 ±0.17	45.99 ±0.22
m13 C	−0.15	0.44	32.29 ±0.22	32.14 ±0.04	33.73 ±0.24	34.17 ±0.14
m13 D	1.76	1.48	35.77 ±0.23	37.52 ±0.11	36.63 ±0.31	38.11 ±0.12
m13 E	3.14	2.88	52.48 ±0.23	55.61 ±0.06	52.92 ±0.37	55.80 ±0.19
m14 A	1.35	0.21	32.99 ±0.21	34.34 ±0.04	34.08 ±0.17	34.29 ±0.15
m14 B	0.92	0.27	44.81 ±0.22	45.73 ±0.04	45.15 ±0.17	45.42 ±0.11
m14 C	0.28	0.85	31.83 ±0.37	32.11 ±0.07	33.29 ±0.33	34.13 ±0.09
m14 D	2.52	1.31	35.41 ±0.25	37.93 ±0.10	36.67 ±0.30	37.98 ±0.17
m14 E	3.24	4.09	48.05 ±0.37	51.28 ±0.05	47.16 ±0.62	51.24 ±0.14

Table 5. Threshold differences of the measurements between the 2 observers and the 2 methods

Threshold [mm]	Method of measurement	Measurement A	Measurement B	Measurement C	Measurement D	Measurement E
<0.5	plaster cast	0	7	9	0	0
	laser scan	10	11	5	0	1
0.51–1.00	plaster cast	5	5	4	0	0
	laser scan	4	2	6	1	0
1.01–1.50	plaster cast	6	2	0	3	0
	laser scan	0	1	2	5	1
1.51–2.00	plaster cast	3	0	1	3	1
	laser scan	0	0	1	3	2
>2	plaster cast	0	0	0	8	13
	laser scan	0	0	0	5	10

References

1. Jiménez-Gayosso SI, Lara-Carrillo E, López-González S, et al. Difference between manual and digital measurements of dental arches of orthodontic patients. *Medicine (Baltimore)*. 2018;97(22):e10887.
2. Reuschl RP, Heuer W, Stiesch M, Wenzel D, Dittmer MP. Reliability and validity of measurements on digital study models and plaster models. *Eur J Orthod*. 2016;38(1):22–26.
3. Peluso MJ, Josell SD, Levine SW, Lorei BJ. Digital models: An introduction. *Semin Orthod*. 2004;10(3):226–238.
4. Nowak R, Wesemann C, Robben J, Muallah J, Bumann A. An in-vitro study comparing the accuracy of full-arch casts digitized with desktop scanners. *Quintessence Int*. 2017;20:667–676.
5. Robben J, Muallah J, Wesemann C, et al. Suitability and accuracy of CBCT model scan: An in vitro study. *Int J Comput Dent*. 2017;20(4):363–375.
6. Goracci C, Franchi L, Vichi A, Ferrari M. Accuracy, reliability, and efficiency of intraoral scanners for full-arch impressions: A systematic review of the clinical evidence. *Eur J Orthod*. 2016;38(4):422–428.
7. Howe RP, McNamara JA, Jr, O'Connor KA. An examination of dental crowding and its relationship to tooth size and arch dimension. *Am J Orthod*. 1983;83(5):363–373.
8. Horton HM, Miller JR, Gaillard PR, Larson BE. Technique comparison for efficient orthodontic tooth measurements using digital models. *Angle Orthod*. 2010;80(2):254–261.
9. Kim J, Lagravére MO. Accuracy of Bolton analysis measured in laser scanned digital models compared with plaster models (gold standard) and cone-beam computer tomography images. *Korean J Orthod*. 2016;46(1):13–19.
10. De Luca Canto G, Pachêco-Pereira C, Lagravere MO, Flores-Mir C, Major PW. Intra-arch dimensional measurement validity of laser-scanned digital dental models compared with the original plaster models: A systematic review. *Orthod Craniofac Res*. 2015;18(2):65–76.
11. Bailey E, Nelson G, Miller AJ, Andrews L, Johnson E. Predicting tooth-size discrepancy: A new formula utilizing revised landmarks and 3-dimensional laser scanning technology. *Am J Orthod Dentofacial Orthop*. 2013;143(4):574–585.

eGFR values and selected renal urine biomarkers in preterm neonates with uncomplicated clinical course

Monika Miklaszewska[1,A–D], Przemysław Korohoda[2,C–E], Dorota Drożdż[1,E,F], Katarzyna Zachwieja[1,B,E], Tomasz Tomasik[3,B], Anna Moczulska[1,B], Agata Korzeniecka-Kozerska[4,C,E], Przemko Kwinta[3,B–F]

[1] Department of Pediatric Nephrology and Hypertension, Jagiellonian University Medical College, Kraków, Poland
[2] Department of Electronics, Faculty of Computer Science, Electronics and Telecommunications, AGH University of Science and Technology, Kraków, Poland
[3] Department of Pediatrics, Faculty of Medicine, Jagiellonian University Medical College, Kraków, Poland
[4] Department of Pediatrics and Nephrology, Medical University of Białystok, Poland

A – research concept and design; B – collection and/or assembly of data; C – data analysis and interpretation; D – writing the article; E – critical revision of the article; F – final approval of the article

Advances in Clinical and Experimental Medicine, ISSN 1899–5276 (print), ISSN 2451–2680 (online) *Adv Clin Exp Med*. 2019;28(12):1657–1666

Address for correspondence
Monika Miklaszewska
mmiklasz@wp.pl

Funding sources
This work was supported by the Research Project Grant No. NN 407 45 97 38.

Conflict of interest
None declared

Received on August 13, 2018
Reviewed on January 28, 2019
Accepted on June 27, 2019

Published online on December 17, 2019

Abstract

Background. Diagnosing acute kidney injury (AKI) in preterm newborns, who are particularly susceptible to renal damage, is a serious challenge as there is no definite consensus about the diagnostic criteria.

Objectives. The objective of this study was to measure the values for selected urinary biomarkers and estimated glomerular filtration rate (eGFR) among a population of preterm infants with uncomplicated clinical course as well as to determine whether these markers depend on birth weight (BW), gestational age (GA), postnatal age (PNA), or gender.

Material and methods. The prospective study was carried out in neonatal intensive care unit (NICU). The evaluation included 57 children that were divided into 3 categories according to BW: low birth weight (LBW) – 1501–2500 g (22 infants); very low birth weight (VLBW) – 1000–1500 g (25 infants); and extremely low birth weight (ELBW) – 750–999 g (10 infants). Urine samples were collected daily between the 4th and 28th day of life for measurements of creatinine (Cr), neutrophil gelatinase-associated lipocalin (NGAL), osteopontin (OPN), and human kidney injury molecule 1 (hKIM1).

Results. The values of the 3 urine tubular biomarkers, serum creatinine and eGFR were taken in substantially healthy preterm infants with normal kidney function at 4 time intervals during the neonatal period. Their correlations were determined and a multivariable regression analysis was carried out with respect to BW, GA, PNA, and gender. Trends of the studied markers in terms of PNA and BW were also assessed with the Jonckheere–Terpstra test.

Conclusions. Glomerular and tubular function in preterm neonates during the 1st month of life is significantly influenced by BW, GA, PNA, and gender.

Key words: renal function, renal urine biomarkers, premature neonate

Cite as
Miklaszewska M, Korohoda P, Drożdż D, et al. eGFR values and selected renal urine biomarkers in preterm neonates with uncomplicated clinical course. *Adv Clin Exp Med*. 2019;28(12):1657–1666. doi:10.17219/acem/110317

DOI
10.17219/acem/110317

Introduction

Worldwide, approx. 6–10% of infants are born preterm. Preterm neonates are particularly susceptible to renal damage, as they are born before week 36 of gestation, when the complex process of nephrogenesis is still incomplete.[1,2]

Diagnosing acute kidney injury (AKI) in preterm newborns is a serious challenge because there is no definite consensus about the diagnostic criteria. Its true incidence among this age group is actually unknown, but the risk for this complication is considerably higher in more immature neonates.[3,4] Generally, AKI occurs in as many as 56% of neonates treated in neonatal intensive care units (NICU),[5] while the mortality rate among this population with AKI ranges from 33% to 78%.[6]

The search for new AKI markers is based on the poor prognosis of AKI in newborns, which is partially caused by the delay in diagnosis and therapeutic intervention. Diagnosis made only on the basis of serum creatinine (SCr) level in this specific population is made more complicated by several factors, including birth weight (BW), gestational (GA) and postnatal age (PNA), functional tubular immaturity, low glomerular filtration rate (GFR), high renal vascular resistance, high plasma renin activity, and decreased intercortical perfusion.[7,8] Furthermore, SCr is a measure of glomerular function – not of kidney damage.[9]

Advances in the field of clinical proteomics have greatly accelerated the discovery of novel urinary proteins which promptly increase in response to renal tubular injury.[10] Urine AKI biomarkers include neutrophil gelatinase-associated lipocalin (NGAL),[11] human kidney injury molecule 1 (hKIM1)[12,13] and osteopontin (OPN),[14] among many others. Plasma NGAL is freely filtered by the glomerulus and then largely reabsorbed by proximal tubular cells captured by megalin; thus, very little (0.1–0.2%) is found in the urine.[15] With renal tubular injury, NGAL reabsorption may be decreased, whereas its de novo synthesis in the epithelial cells of the loop of Henle and of distal tubule segments is strongly upregulated, after which it is found in high concentrations in the urine.[16] Neutrophil gelatinase-associated lipocalin has also been shown to play an important role in kidney development.[17] Osteopontin in the kidney is mainly found in the loop of Henle and distal nephrons, can be upregulated in all tubular and glomerular segments following kidney damage and may play a role in renal repair.[18] Human kidney injury molecule 1 is expressed in low levels in healthy proximal tubule cells; in case of kidney ischemia or toxicity, it is highly upregulated and shed into the extracellular space and the urine.[19]

According to the literature, these biomarkers are not only more sensitive than SCr for identifying AKI, but they can also indicate damage in a specific tubular region of the nephron.[20] Additionally, the ability to assay the markers noninvasively in the urine represents a significant advantage over current methods, especially for the neonatal population.[21] Still, despite the promising role of these novel urinary biomarkers in the early detection of AKI, a reference range for the preterm neonatal population has not yet been fully established. The inability of immature tubules to fully reabsorb these proteins in preterm infants may also lead to varying values in this heterogenic population.[8] Hence, the primary objective of this study was to determine the values for selected urinary tubular biomarkers in a population of preterm infants who have relatively uncomplicated clinical courses, and to determine whether these markers depend on BW, GA, PNA, or gender. To evaluate and characterize the glomerular function of the studied group, the estimated GFR (eGFR) values were calculated with the equation developed by Schwartz et al.,[22] which is easy to use bedside.

Material and methods

The prospective, observational study was carried out in the Neonatal Intensive Care Unit of the Department of Pediatrics at Jagiellonian University College of Medicine in Kraków, Poland. Prospective observations spanned the period from September 2010 to September 2012. The investigation was approved by the local Bioethical Committee (approval No. KBET/64/B/2009).

The inclusion criteria were as follows: informed consent of the parents (or legal guardians) and an age of up to 48 h upon the child's admission to the NICU. Ultimately, in the final analysis of data, only NICU survivors were included. The exclusion criteria consisted of a lack of informed consent, prenatal maternal angiotensin-converting enzyme (ACE) inhibitor or indomethacin therapy, congenital anomalies of the kidney and urinary tract (CAKUT), chromosomal aberrations, other severe, complex anomalies affecting an unfavorable late prognosis and complications such as acute renal failure, sepsis, suspicion of sepsis, urinary tract infection, tension pneumothorax, necrotizing enterocolitis, grade 3 and 4 intracranial hemorrhage, patent ductus arteriosus (PDA) requiring treatment, therapy with nonsteroidal anti-inflammatory drugs or amphotericin, or any type of surgery during the entire observation period.

The presence of AKI in a given child was determined based on the neonatal/pediatric (n/p) RIFLE and AKIN scales.[5,23] Serum creatinine was assessed at least every 48–72 h and whenever it seemed necessary. The normal ranges of SCr used for the studied population were taken from the study of Bateman et al.[24], while the eGFR values were calculated according to the one-marker equation developed by Schwartz et al.[22] The presence of sepsis in a given child was determined based on the gold standard, which continues to be a positive result of blood bacteriology, while a suspicion of sepsis was based on such clinical and laboratory criteria as apnea or deterioration of mechanical ventilation parameters, abnormalities of peripheral perfusion, abnormalities of arterial pressure, hepatomegaly and/

or splenomegaly, signs of feeding intolerance, leucopenia (<4,000/mL) or elevated white blood cell count (>10,000/mL), thrombocytopenia (<100,000/mL), immature granulocyte count (immature neutrophils/total neutrophils) >0.2, and elevated C-reactive protein (CRP) (>10 mg/L).

In the calculation process of the final results for urinary markers, only data from days without aminoglicoside (AG) administration, injury or 2nd stage of AKI according to the n/pRIFLE and AKIN scale, respectively, or signs or symptoms of sepsis were taken into consideration. The only AG used in our NICU was amikacin. The antibiotic was dosed under close serum level monitoring. Respiratory failure (RF) was recognized when the implementation of synchronized intermittent mandatory ventilation (SIMV) or continuous positive airway pressure (CPAP) was warranted. Nevertheless, in view of the fact that very low birth weight (VLBW) and extremely low birth weight (ELBW) children very often require respiratory support, either SIMV or CPAP, it was not considered an exclusion criterion.

Clinical observations were performed over the first 28 days of life (DOL). Urinary concentrations of the markers being studied were measured on a daily basis between the 4th and 28th DOL (25 days). A urine sample for creatinine (uCr), NGAL (uNGAL), OPN (uOPN), and hKIM1 assays was collected according to the schedule, once a day (at 7.00 a.m.) using a urine bag or a catheter. None of the children were specially catheterized to meet the purpose of the investigation; the insertion of a urinary catheter was dictated by the clinical status of the child. In order to obtain an appropriate volume of urine, in the case of catheterized children, the urine bags were emptied approx. 1 h prior to the planned urine collection, while in case of children without urinary catheters, a urine bag was fixed approx. 1 h before the planned urine collection. The values of the markers were analyzed in 4 time intervals: 4–7, 8–14, 15–21, and 22–28 DOL.

Description of laboratory methods

The collected urine was centrifuged and frozen at –80°C. Laboratory measurements of SCr and uCr were performed using the enzymatic method with a VITROS FS system (Ortho Clinical Diagnostics, Raritan, USA). The reading and recording of the results were automatic. The methods of analysis remained unchanged throughout the study period. Measurements of NGAL were performed employing a Human Lipocalin – 2/NGAL ELISA RD 191102200R kit (BioVendor, Brno, Czech Republic) and the immunoenzymatic method (enzyme-linked immunosorbent assay (ELISA)). The kit had the following parameters: intra-kit precision CV – 7.7%; inter-kit precision CV – 9.8%; and sensitivity of the method – <0.02 ng/mL. Determination of OPN was carried out using the Human Osteopontin Elisa BBT0482R kit (BioVendor) and the immunoenzymatic method (ELISA). The kit had the following parameters: intra-kit method precision CV – 3.7%; inter-kit precision CV – 5.8%; sensitivity of the method – <50 pg/mL; measurement range – 156–10,000 pg/mL. Measurements of human Kidney Injury Molecule-1 (hKIM1) were performed with an Elisa Kit for Human Kidney Injury Molecule 1 (Kim1) E0785HU kit (USCN Life Science Inc., Wuhan, China) and the immunoenzymatic method (ELISA). The kit had the following parameters: intra-kit method precision CV – <10%; inter-kit precision CV – <12%; sensitivity of the method – <0.038 ng/mL; and measurement range – 0.156–10 ng/mL. Sample absorbance was measured by the single-wave method using a 450-nm filter and the Universal Microplate Reader Elx800NB automatic microplate reader (BIO-TEK Instruments, Inc, Winooski, USA). Correction of urinary biomarker measurements with urine creatinine was performed to account for urine concentration.

Predefined comparisons

The children were divided into 3 categories according to their BW: low birth weight (LBW) infants with a BW of 1,501–2,500 g; VLBW infants with a BW of 1,000–1,500 g; and ELBW infants with a BW of 750–999 g.

Statistical methods

The following tests were used, as deemed appropriate: Kolmogorov–Smirnov test (KS), Student's t-test, rank sum Wilcoxon test, and Fisher's exact test. For normally distributed variables, the mean and standard deviation (SD) were calculated; otherwise, the median and interquartile range (IQR) range are presented. The significance level was 0.05 for all tests, apart from the KS test, where it was set to 0.1 in order to make it more restrictive for the null hypothesis. The values of the studied markers were preliminarily calculated by the common logarithm, as in the papers listed in References[10,17,25]; zero values – accounting for 10.8% of the results – were rejected. In this way, the log-norm distribution was achieved for all of the groups, as confirmed by the KS test. Having determined the parameters of the Gaussian model for the log-norm data, the authors defined 50% confidence intervals (CI50%), which – in the case of a Gaussian distribution – are equivalent to IQR. Subsequently, the mean values of the log-norm distributions and the CI50% range limits were converted to original values of the markers, thus arriving at respective geometric means and CI50% range limits. Statistical comparisons of data groups analyzed in this way were performed using Student's t-test for the logarithmic values. For the above values of the markers, the authors analyzed possible correlations with BBW, GA and DOL, also grouping by gender, and carried out a multivariable regression analysis in order to determine their dependence on the abovementioned variables. The Jonckheere–Terpstra test, a rank-based nonparametric test, was used to determine if there is a statistically significant trend between the ordinal independent variables (calendar-day intervals (4–7, 8–14, 15–21 and 22–28 DOL) and BW groups (ELBW,

VLBW and LBW)) and the continuous dependent variables: eGFR, SCr, uNGAL, uOPN, and hKIM1 concentrations. The STATISTICA v. 12.0 (StatSoft, Inc., Tulsa, USA) and MATLAB v. 2015a (Mathworks, Natick, USA) packages were used for all computations and to create the graphs.

Results

Fifty-seven infants were included in the study: 22 LBW, 25 VLBW and 10 ELBW newborns. All of the infants were of Caucasian race. The main diagnoses at admission in the LBW group were respiratory disorders (of various severity and origin) (n = 14) and prematurity (n = 8); in the VLBW group, it was respiratory disorders (of various severity and origin) (n = 6) and prematurity and severe prematurity (n = 19); and in the ELBW group, the diagnosis was severe prematurity with respiratory disorders (n = 10). None of the children enrolled in the study died during their NICU stay.

As shown in Table 1, which presents a clinical summary of the investigated population, the analyzed groups of children were comparable with respect to gender, delivery methods, fetal maturity, Apgar score, urine output (UO), and AG use. The infants from all study groups were generally in a good and stable condition throughout the entire observation period, as confirmed by their Score for Neonatal Acute Physiology II (SNAP II), which practically did not exceed the mean value of 5 points in any of the analyzed subgroups (a fact which predicts a good prognosis in a neonate) and showed no significant differences among the subgroups.[26] Similarly, the mean arterial pressure (MAP) values of the studied patient populations were within normal limits for their GA, at approx. the 50th percentile.[27]

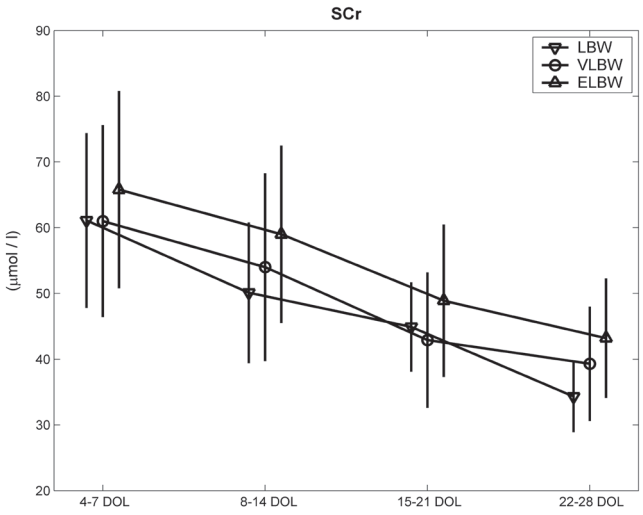

Fig. 1. Serum creatinine distribution parameters: mean ±SD, calculated from data collected in 4 weekly intervals in the study population

Table 1. Clinical summary of the study population (n = 57)

Variable	LBW (n = 22)	VLBW (n = 25)	ELBW (n = 10)	p-value (LBW vs VLBW)	p-value (LBW vs ELBW)	p-value (VLBW vs ELBW)
	Number (%)	Number (%)	Number (%)	p-value for Fisher's exact test		
Females/males	10 (45%)/12 (55%)	15 (60%)/10 (40%)	5 (50%)/5 (50%)	NS	NS	NS
Cesarean delivery	20 (91%)	19 (76%)	10 (100%)	NS	NS	NS
SGA/AGA	3 (14%)	1 (4%)	1 (10%)	NS	NS	NS
PDA	7 (31.8%)	8 (32%)	4 (40%)	NS	NS	NS
RF	11 (50%)	19 (76%)	9 (90%)	NS	0.0469	NS
AG	2 (9.1%)	8 (32%)	2 (20%)	NS	NS	NS
	Mean (SD)	Mean (SD)	Mean (SD)	p-value for Student t-test		
GA [weeks]	32.4 (2.1)	29.2 (1.7)	28.0 (2.4)	0.000	0.000	NS
BW [g]	1710.2 (166.2)	1244.8 (161.0)	947.5 (53.8)	0.000	0.000	0.000
Birth body length [cm]	43.4 (1.9)	38.9 (2.5)	36.6 (1.6)	0.000	0.000	0.011
	Median (IQR)	Median (IQR)	Median (IQR)	p-value for Wilcoxon test		
Apgar score 3/5	8 (2.0)	7 (4.0)	6.5 (2.0)	NS	NS	NS
SNAP II	5.0 (0.0)	5.0 (0.0)	5.0 (5.0)	NS	NS	NS
RF – number of days	2.0 (5.3)	4.0 (17.3)	24.0 (4.3)	NS	0.000	0.015
MAP [mm Hg]	49.7 (13.0)	46.0 (12.3)	44.3 (12.3)	0.000	0.000	0.008
AG administration – number of days	4.0 (2.0)	4.5 (4.00)		NS	NS	NS
UO [mL/kg/h]	2.9 (0.9)	3.1 (1.0)	2.9 (1.3)	NS	NS	NS
NICU hospitalization [days]	27.5 (16.0)	45.0 (24.8)	63.0 (21.0)	0.000	0.000	NS

RF – respiratory failure (number of days of CPAP and SIMV administration); AG – number of days of AG administration within the group that received an antibiotic; SL – spontaneous labor; CS – cesarean section; MAP – mean arterial pressure; UO – urinary output; SGA – small for gestational age; AGA – appropriate for gestational age; BW – body weight; LBW – low body weight; VLBW – very low body weight; ELBW – extremely low body weight; NICU – neonatal intensive care unit; SD – standard deviation.

Table 2. Serum creatinine (SCr) and estimated glomerular filtration rate (eGFR) distribution parameters calculated from data collected in 4 weekly intervals in the studied population; data is presented as mean (standard deviation (SD)); p-values were computed for the Jonckheere–Terpstra test for ordered alternatives

Variable	4–7 DOL	8–14 DOL	15–21 DOL	22–28 DOL	p-value
SCr [µmol/L]					
LBW	61.1 (13.3)	50.1 (10.7)	44.9 (6.8)	34.3 (5.4)	0.000
VLBW	61.0 (14.6)	54.0 (14.3)	42.9 (10.3)	39.3 (8.7)	0.01
ELBW	65.8 (15.0)	59.0 (13.5)	48.9 (11.6)	43.2 (9.1)	0.02
p-value	0.05	0.03	NS	0.01	
eGFR [mL/min/1.73 m^2]					
LBW	27.4 (7.1)	33.9 (9.70)	36.8 (5.3)	48.2 (7.9)	0.000
VLBW	24.6 (5.5)	28.4 (7.1)	36.4 (9.6)	39.6 (9.2)	0.003
ELBW	21.3 (6.1)	24.7 (7.9)	29.8 (8.9)	33.9 (9.7)	0.03
p-value	0.01	0.02	0.05	0.005	

DOL – days of life; LBW – low body weight; VLBW – very low body weight; ELBW – extremely low body weight.

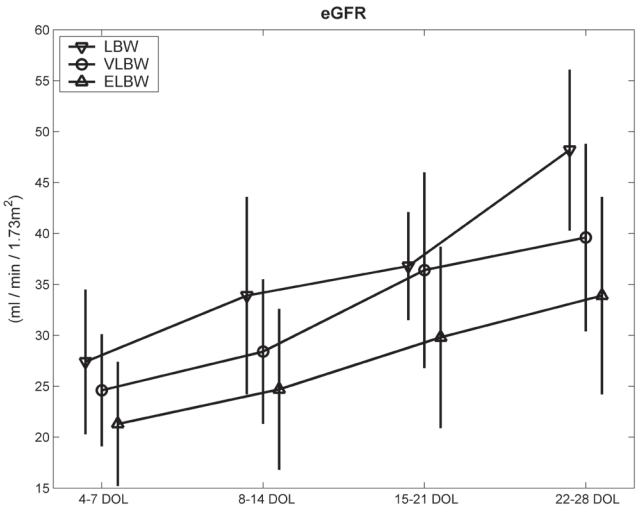

Fig. 2. Estimated glomerular filtration rate (eGFR) distribution parameters: mean ±SD, calculated from data collected in 4 weekly intervals in the study population

The number of days when a urine sample could potentially be collected was as follows: in the LBW group – 429; in the VLBW group – 623; and in the ELBW group – 251 (in total: 1,303 days). The final number of days included in the analysis – once days affected by the above interfering factors were excluded – was 1,126 (86.4%), with the following values for the selected population groups: LBW – 374 (87.2%), VLBW – 538 (86.4%) and ELBW – 214 (85.3%).

Table 3. Geometric mean and CI50% of uNGAL values calculated from data collected in 4 weekly intervals in the study groups; p-values were computed for the Jonckheere–Terpstra test for ordered alternatives

Variable	4–7 DOL	8–14 DOL	15–21 DOL	22–28 DOL	p-value
Females					
NGAL [ng/mL]					
LBW	11.1 (4.7–25.9)	6.7 (2.9–15.5)	4.7 (1.6–14.3)	15.8 (6.7–37.0)	NS
VLBW	24.0 (10.2–56.6)	14.3 (5.1–40.2)	11.2 (4.2–29.8)	9.4 (4.1–21.7)	<0.001
ELBW	19.3 (8.9–41.9)	15.2 (7.1–32.5)	12.4 (6.9–22.3)	18.5 912.5–27.3)	NS
p-value	0.02	0.01	0.02	NS	–
NGAL [ng/mgCr]					
LBW	69.7 (33.0–147.2)	46.9 (20.4–107.8)	36.8 (11.1–122.4)	120.7 (52.6–276.8)	NS
VLBW	217.1 (89.9–524.2)	120.0 (40.4–356.3)	89.4 (32.2–247.6)	78.7 (30.9–200.6)	<0.001
ELBW	173.3 (62.9–477.4)	116.7 (44.3–307.6)	94.0 (46.8–188.8)	155.4 (83.9–287.8)	NS
p-value	0.05	0.03	0.01	NS	–
Males					
NGAL [ng/mL]					
LBW	5.5 (2.3–13.10)	3.1 (1.2–8.0)	3.3 (1.1–10.1)	1.8 (0.9–3.5)	0.01
VLBW	14.7 (6.3–34.3)	9.0 (2.5–32.0)	5.8 (1.7–19.2)	3.9 (1.1–14.2)	<0.001
ELBW	23.0 (12.0–44.0)	23.6 (8.2–67.7)	8.7 (3.4–21.7)	7.5 (2.9–19.7)	0.03
p-value	<0.001	<0.001	0.02	0.01	–
NGAL [ng/mgCr]					
LBW	36.8 (15.4–87.8)	22.3 (8.3–59.9)	22.6 (7.7–66.8)	9.7 (4.6–20.4)	0.01
VLBW	110.7 (45.0–272.2)	81.2 (23.9–276.1)	51.0 (15.3–170.1)	33.1 (9.6–114.2)	<0.001
ELBW	208.6 (113.3–384.0)	172.7 (60.3–494.1)	78.1 (33.5–182.3)	65.4 (25.6–166.9)	0.02
p-value	<0.001	<0.001	0.01	0.003	–

DOL – days of life; LBW – low body weight; VLBW – very low body weight; ELBW – extremely low body weight; NGAL – neutrophil gelatinase-associated lipocalin; uNGAL – urine neutrophil gelatinase-associated lipocalin.

Table 2 and Fig. 1 and 2 present the values of SCr and eGFR calculated for the study groups. As it follows from the data and the Jonckheere–Terpstra test results for ordered alternatives, there is a statistically significant trend of lower SCr values and higher eGFR values in all BW groups with respect to PNA; simultaneously, there is a significant trend of higher SCr values and lower eGFR values with respect to lower BW (except for SCr values in the 3rd time interval).

Table 3 presents the geometric means and CI50% for the values of uNGAL, separated by gender, that were found in the 4 time intervals in the groups of children. As it follows from the data and the Jonckheere–Terpstra test results for ordered alternatives, there is a statistically significant trend of lower uNGAL values with respect to PNA (except LBW and ELBW females); likewise, there is a significant trend of higher uNGAL values with respect to lower BW (except for females in the 4th time interval). The analysis of logarithmic correlations of the uNGAL values performed both in girls and in boys demonstrated negative, average and high coefficients (R: –0.4––0.7; Table 6) for all of the uNGAL values, with respect to both BW and GA. Similarly, the analysis of the results of the multivariable linear regression for logarithmic uNGAL values with respect to BW, GA, PNA, and gender demonstrated a significant effect from all of these factors on the uNGAL values: they decreased by the percentage given in Table 7 with BW increasing by 100 g and GA increasing by 1 week and each subsequent DOL. Moreover, it was shown that the values of this marker were significantly (approx. by 40%) higher in girls than in boys (Table 7).

Table 4 presents the geometric means and CI50% for the values of uOPN, broken by gender, that were recorded in the study groups at the 4 time intervals. As it follows from the data and the Jonckheere–Terpstra test results for ordered alternatives, there is no trend of uOPN values with respect to PNA; however, there is a significant trend of higher uOPN values correlating with lower BW. The analysis of logarithmic correlations of the uOPN values showed negative, average and high coefficients (R: –0.4––0.7; Table 6) for most of the values with respect to BW and GA. There were no such correlations for the absolute uOPN correlation in girls with respect to GA or uOPN/mgCr in boys with respect to BW and GA. In turn, the analysis of the results of the multivariable linear regression for logarithmic uOPN values performed solely with respect to BW and gender showed a significant effect of these factors (the marker values were significantly higher – by approx. 40% – in boys than in girls); no significant effect of GA or PNA was observed on the uOPN values (Table 7).

Table 4. Geometric mean and CI50% of uOPN values calculated from data collected in 4 weekly intervals in the study groups; p-values were computed for the Jonckheere–Terpstra test for ordered alternatives

Variable	4–7 DOL	8–14 DOL	15–21 DOL	22–28 DOL	p-value
Females					
OPN [ng/mL]					
LBW	79.1 (36.8–170.2)	74.4 (32.2–172.0)	56.3 (19.4–163.3)	76.8 (31.6–186.4)	NS
VLBW	166.6 (77.9–356.20)	145.6 (57.8–366.3)	109.2 (34.1–349.80	164.6 (71.1–380.8)	NS
ELBW	180.5 (99.4–327.8)	139.8 (62.8–311.5)	149.6 (73.5–304.5)	173.1 (56.0–534.8)	NS
p-value	0.02	0.04	0.02	0.05	–
OPN [ng/mgCr]					
LBW	493.4 (234.4–1038.4)	527.3 (231.2–1202.6)	478.8 (174.2–1316.3)	665.4 (259.9–1703.7)	NS
VLBW	1478.9 (699.5–3126.8)	1158.3 (469.6–2857.1)	860.3 (297.4–2488.4)	1377.4 (610.4–3108.4)	NS
ELBW	1620.4 (662.7–3962.2)	1137.3 (489.2–2644.2)	1326.6 (720.7–2441.7)	1604.6 (752.3–3422.7)	NS
p-value	0.05	0.03	0.01	0.03	–
Males					
OPN [ng/mL]					
LBW	126.4 (73.8–216.5)	99.1 (44.8–219.3)	103.9 (36.0–299.6)	79.3 (19.5–323.3)	NS
VLBW	227.1 (99.5–518.3)	134.8 (58.1–312.5)	127.6 (65.4–248.8)	183.9 (100.4–336.7)	NS
ELBW	244.4 (104.2–573.1)	250.4 (114.3–548.6)	290.9 (130.5–648.3)	244.5 (107.0–558.5)	NS
p-value	0.05	0.01	0.02	0.01	–
OPN [ng/mgCr]					
LBW	897.7 (518.9–1553.1)	764.8 (366.9–1593.8)	614.2 (212.3–1776.7)	581.7 (167.6–2018.6)	NS
VLBW	1754.8 (787.8–3908.8)	1223.6 (524.1–2856.5)	1159.0 (621.5–2161.5)	1641.9 (976.0–2762.2)	NS
ELBW	2274.4 (1115.5–4637.4)	1815.2 (956.4–3445.1)	2611.5 (1087.5–6271.6)	2260.8 (983.9–5194.7)	NS
p-value	0.01	0.01	0.01	0.003	–

DOL – days of life; LBW – low body weight; VLBW – very low body weight; ELBW – extremely low body weight; OPN – osteopontin; uOPN – urine osteopontin.

Table 5. Geometric mean and CI50% of hKIM1 values calculated from data collected in 4 weekly intervals in the study groups; p-values were computed for the Jonckheere–Terpstra test for ordered alternatives

Variable	4–7 DOL	8–14 DOL	15–21 DOL	22–28 DOL	p-value
Females					
hKIM1 [pg/mL]					
LBW	74.6 (41.9–132.6)	130.4 (73.1–232.7)	88.8 (43.8–180.0)	69.6 (33.3–145.4)	NS
VLBW	73.6 (39.1–138.6)	84.3 (41.6–170.7)	112.4 (59.8–211.1)	115.3 (58.0–229.0)	0.05
ELBW	74.9 (23.9–234.5)	90.3 (41.3–197.6)	173.6 (92.8–324.5)	160.0 (71.6–357.5)	NS
p-value	NS	NS	0.02	0.05	–
hKIM1 [pg/mgCr]					
LBW	471.0 (279.0–795.1)	882.5 (489.8–1590.3)	658.7 (367.5–1180.7)	613.8 (337.1–1117.7)	NS
VLBW	679.0 (358.8–1285.0)	692.8 (325.2–1476.1)	912.9 (489.7–1701.7)	964.0 (466.6–1991.6)	0.05
ELBW	776.9 (186.9–3230.1)	774.5 (311.0–1928.7)	1347.5 (704.1–2578.8)	1124.2 (562.6–2246.4)	NS
p-value	NS	NS	0.01	0.03	–
Males					
hKIM1 [pg/mL]					
LBW	75.5 (32.9–173.3)	126.7 (60.7–264.4)	113.6 (59.1–218.6)	89.7 (49.3–163.4)	NS
VLBW	88.6 (42.7–183.5)	91.4 (46.3–180.3)	167.8 (92.2–305.3)	115.6 (59.0–226.7)	NS
ELBW	82.5 (41.1–165.8)	254.6 (166.0–390.4)	252.0 (151.3–419.8)	161.1 (80.5–322.4)	NS
p-value	NS	NS	0.02	0.01	–
hKIM1 [pg/mgCr]					
LBW	513.0 (230.7–1141.0)	995.7 (481.4–2059.1)	815.8 (402.8–1652.6)	619.1 (342.9–1117.9)	NS
VLBW	710.4 (321.6–1569.1)	802.6 (403.4–1596.7)	1536.3 (852.8–2767.7)	1031.0 (572.3–1857.4)	NS
ELBW	719.7 (354.6–1460.9)	1862.4 (1215.6–2853.2)	2369.4 (1338.3–4194.9)	1390.4 (743.3–2600.5)	NS
p-value	NS	NS	0.01	0.03	–

DOL – days of life; LBW – low body weight; VLBW – very low body weight; ELBW – extremely low body weight; hKIM1 – human kidney injury molecule 1.

Table 6. Pearson correlation coefficients (p-value) for the mean values of the investigated urine tubular biomarkers calculated for each patient from 4 to 28 DOL with reference to BW and GA and between the log-norm and PNA values

Biomarker	BW vs mean (log_{10}(marker))	GA vs mean (log_{10}(marker))	DOL vs log_{10}(marker)
Female			
NGAL [ng/mL]	−0.453 (0.012)	−0.403 (0.027)	−0.103 (0.011)
NGAL [ng/mgCr]	−0.484 (0.007)	−0.398 (0.029)	−0.086 (0.033)
Male			
NGAL [ng/mL]	−0.609 (0.000)	−0.619 (0.000)	−0.198 (0.000)
NGAL [ng/mgCr]	−0.437 (0.016)	−0.472 (0.008)	−0.181 (0.000)
Female			
OPN [ng/mL]	−0.385 (0.036)	−0.327 (NS)	−0.021 (NS)
OPN [ng/mgCr]	−0.477 (0.008)	−0.391 (0.032)	0.002 (NS)
Male			
OPN [ng/mL]	−0.514 (0.004)	−0.414 (0.023)	−0.005 (NS)
OPN [ng/mgCr]	−0.130 (NS)	−0.100 (NS)	0.030 (NS)
Female			
hKIM1 [pg/mL]	−0.152 (NS)	−0.171 (NS)	0.131 (0.002)
hKIM1 [pg/mgCr]	−0.270 (NS)	−0.238 (NS)	0.130 (0.002)
Male			
hKIM1 [pg/mL]	−0.084 (NS)	−0.045 (NS)	0.118 (0.009)
hKIM1 [pg/mgCr]	0.150 (NS)	0.128 (NS)	0.151 (0.001)

BW – body weight; GA – gestational age; PNA – postnatal age; NGAL – neutrophil gelatinase-associated lipocalin; OPN – osteopontin; hKIM1 – human kidney injury molecule 1.

Table 7. Multivariable linear regression for the log-norm data in reference to BW, GA, PNA, and gender. The table presents the change (increase/decrease) by a given percent of the marker expressed in the original values when the given parameter is changed by a set point value (negative values denote a decrease in the marker value at an increase of the given parameter)

Variable	BW [100g]	GA [week]	DOL [day]	G (from female to male)
NGAL [ng/mL] p-value	−11.2 (95 %CI = −14.4−−7.9) <0.001	−10.7 (95% CI = −14.7−−6.6) <0.001	−4.5 (95% CI = −5.6−−3.3) <0.001	−38.4 (95% CI = −47.9−−27.2) <0.001
NGAL [ng/mgCr] p-value	−13.4 (95% CI = −16.6−−10.1) <0.001	−11.3 (95% CI = −15.3−−7.1) <0.001	−4.4 (95% CI = −5.6−−3.2) <0.001	−37.8 (95% CI = −47.7−−26.2) <0.001
OPN [ng/mL] p-value	−8.6 (95% CI = −11.9−−5.1) <0.001	−1.5 (95% CI = −5.9–3.1) NS	−0.8 (95% CI = −1.9–0.4) NS	39.2 (95% CI = 17.7–64.8) <0.001
OPN [ng/mgCr] p-value	−10.4 (95% CI = −13.5−−7.2) <0.001	−2.2 (95% CI = −6.4–2.2) NS	−0.4 (95% CI = −1.5–0.8) NS	43.2 (95% CI = 22.0–68.1) <0.001
hKIM1 [ng/mL] p-value	−1.2 (95% CI = −4.0–1.7) 0.415 (NS)	−0.6 (95% CI = −4.2–3.0) NS	1.8 (95% CI = 0.9–2.7) <0.001	24.6 (95% CI = 9.5–41.7) <0.001
hKIM1 [ng/mgCr] p-value	−2.8 (95% CI = −5.6–0.1) 0.056 (NS)	−1.7 (95% CI = −5.2–2.0) NS	1.9 (95% CI = 1.0–2.8) <0.001	29.9 (95% CI = 14.1–48.0) <0.001

BW – body weight; GA – gestational age; PNA – postnatal age; NGAL – neutrophil gelatinase-associated lipocalin; OPN – osteopontin; hKIM1 – human kidney injury molecule 1; G – gender.

Table 5 presents the geometric means and CI50% for the values of hKIM1 by gender for the 4 time intervals in the groups of children studied. As it follows from the data and the Jonckheere–Terpstra test results for ordered alternatives, there is no trend of hKIM1 values with respect to PNA (except VLBW females); there is, however, a significant trend of higher hKIM1 values and lower BW, but only at the 3rd and 4th time intervals. The analysis of correlation coefficients of the logarithmic hKIM1 values did not demonstrate any correlations with BW, GA or PNA (Table 6); similarly, the multivariable linear regression performed for logarithmic marker values did not show BW or GA to exert a significant effect on the hKIM1 values; only in terms of PNA and gender did the regression demonstrate a significant effect of these factors on the marker values, as hKIM1 values were significantly (25–30%) higher in boys than in girls (Table 7).

Discussion

There are many urinary markers which are detectable in neonates, but in this heterogeneous population no clear neonatal reference ranges have been developed. Therefore, one of the main objectives of this study was to define appropriate values of uNGAL, uOPN and hKIM1 recorded in LBW, VLBW and ELBW infants with uncomplicated clinical course and with normal kidney function. Moreover, the majority of studies of modern AKI markers only include special neonatal populations, such as newborns presenting with post-neonatal asphyxia[28] or requiring cardiac surgery.[29]

Studies dedicated to AKI biomarkers in healthy preterm and term neonates are not only very scarce, but the results of such studies are also highly diverse and sometimes quite conflicting.[30] To illustrate this fact, it should be mentioned that there are reports where the uNGAL values are quite comparable with the results obtained in the current study,[17,25,30,31] while in other studies,[2,10,23,32–34] the values of uNGAL (and uNGAL/mgCr[10,20,33]) are higher than in this study. In turn, in the study by Askenazi et al.,[34] the values of uOPN are comparable, yet in a report published 5 years later by the same author, the values of uOPN and uOPN/mgCr are higher than in the current study.[33] Finally, in the studies by Askenazi et al.[10,34] and Genc et al.[35] addressing the hKIM1 and hKIM1/mgCr levels in preterm neonates, the values of these biomarkers are comparable to those found in this study, but there are also reports which published higher values.[36,37] Only in 1 study concerning term infants were the hKIM1 and hKIM1/mgCr values lower than the values found in the present study.[31] The causes of such disparities can mainly be found in the days of life in which the urine samples were collected from the newborns for measuring particular biomarkers. Only in some studies (by La Manna et al.,[2] Huynh et al.,[17] Parravicini et al.,[25] and Chi-Nien et al).[23] were the days of urine collection similar to the timespan used in the present study, and they included practically the entire neonatal period. In the remaining studies, the concentration values of the given biomarkers were determined within a much shorter timeframe – most often in the very first 7 days of life.[10,31–33,35–37]

Analyzing the importance and effect of gender on the values of the markers under discussion, one realizes that data from the subject literature are fairly scarce and ambiguous. There are reports stating that there is a higher level and increased variability of uNGAL in girls,[17] as well as other papers claiming that there is no significant association with gender.[23,25,30] The available literature is quite unambiguous in stating that there is no correlation and no effect of gender on the values of hKIM1.[35–37] In the present study, gender exerts a highly significant effect of several score percent on the values of the 3 investigated tubular markers.

Moreover, in the current literature there are various – sometimes discrepant – reports concerning the effect of GA, BW and PNA on the concentations of the urinary renal markers in question. According to a number of studies, uNGAL is inversely correlated with GA[1,10,17,38]; additionally, inverse correlations with BW[38] and PNA have been demonstrated.[17] Furthermore, according to Askenazi et al.,[10] uNGAL/mgCr also decreases with increasing GA, and there are detailed reports where uNGAL levels declined by 23.1%[10] or by 17.8%[17] for each week of increasing GA. However, there are also researchers who found no association between uNGAL and GA[23,25,30,39] and those who report no correlation with BW,[23,30,39] or PNA.[23,27,38] However, Huynh et al.[17] demonstrated that uNGAL levels declined by 1.33% for each day of PNA. In the present study, all of the uNGAL values in both genders were highly inversely correlated with BW and GA. Furthermore, statistically significant decreasing trends of uNGAL with respect to PNA and increasing trends with respect to lower BW were found. Moreover, in the linear regression, the above factors exerted a significant effect on uNGAL values, as did PNA. Gender also plays a significant role, since the values of uNGAL in girls were significantly higher.

Reports concerning correlations with uOPN are quite scarce, as only Askenazi et al.[10] showed that uOPN/mgCr decreased with increasing GA and that uOPN declined by 34.8% for each week of increasing GA. In the present study, most of the uOPN values were inversely correlated with BW and GA (which was also confirmed by a statistically significant increasing trend of uOPN values with respect to lower BW); nevertheless, an increase of GA by 1 week (similarly as is the case with PNA) did not exert a significant effect on the values of the marker when it was analyzed using linear regression. On the other hand, gender played a significant role, since the uOPN values in boys were significantly higher.

In the study by Askenazi et al.,[10] hKIM1 and hKIM1/mgCr were shown to decrease with increasing GA. The same correlation concerning only hKIM1 was found by Sarafidis et al.,[31] but this study was performed in term infants. Nevertheless, there are studies which proved no correlation between hKIM1 and GA[35,36]; likewise, BW has been reported not to correlate with this marker.[35,37] On the other hand, in a study that was performed in a population of term infants, GA correlated positively with hKIM1.[37] The present study did not demonstrate any correlation between hKIM1 and BW or GA (only in the 3rd and 4th time intervals is there a statistically significant inverse correlation between hKIM1 and BW). Postnatal age exerted a weak effect and gender had a significant effect on the marker value in the linear regression, since the hKIM1 values in boys were significantly higher.

Glomerular filtration rate in term (and particularly in preterm) infants is very low, and there is a wide distribution of normal SCr values, which vary greatly depending on the level of prematurity and PNA.[40] Depending on the degree of the neonate's prematurity, GFR steadily improves during the first months of life. Keeping this observation in mind, we additionally measured the ranges of SCr values and calculated eGFR values in the 3 BW groups of neonates with normal kidney function between 4 and 28 DOL.

We are aware of some limitations of this study, including the fact that the number of neonates – particularly in the ELBW group – is relatively small, but this issue stems from the considerable difficulty in forming a study group consisting of numerous, homogeneous and unquestionably healthy neonates without comorbidities. Nevertheless, a high number of days (214) in the analyzed ELBW children made the authors inclined to treat this group as a separate entity. Furthermore, analyzing the diagnoses (mostly prematurity and respiratory disorders), MAP values and SNAP scale, it may be concluded that the entire study population was in generally good clinical condition. Additionally, the confounding factors (AG) were also acknowledged in the statistical calculations.

The main advantage of the current study was its scrupulous collection of serum samples (every 48–72 h) for SCr, as well as urine samples (every 24 h) for urinary renal markers throughout the neonatal period in the LBW, VLBW and ELBW infants with normal kidney function, which allowed for a detailed background to define reference weekly ranges for SCr, eGFR and 3 AKI urinary tubular markers. Also, to minimize the variability related to urinary concentration, the correction with urine creatinine was adopted. However, due to the limited number of patients included in the study, there is a future need for validation and evaluation of the above data in larger groups of neonates to provide the most reliable reference values, ideally in multicenter studies.

In summary, the findings of this study demonstrate that tubular and glomerular function in preterm neonates during the 1st month of life is significantly affected by BW, GA and PNA. Furthermore, gender also exerts a significant effect on the values of the markers studied: the uNGAL values are significantly higher in girls, while uOPN and hKIM1 are higher in boys. Secondly, we determined the values of 3 urine tubular biomarkers (uNGAL, uOPN and hKIM1) recorded in a substantially healthy, preterm population of neonates with normal kidney function, along with any trends of these values with respect to PNA and BW, which should form a solid groundwork for rational interpretation of the results of future clinical trials using the same AKI biomarkers in very young children.

ORCID iDs

Monika Miklaszewska https://orcid.org/0000-0003-0776-4946
Przemysław Korohoda https://orcid.org/0000-0002-8768-012X
Dorota Drożdż https://orcid.org/0000-0002-1281-1164
Katarzyna Zachwieja https://orcid.org/0000-0002-1949-5096
Tomasz Tomasik https://orcid.org/0000-0003-2107-3607
Anna Moczulska https://orcid.org/0000-0002-8479-050X
Agata Korzeniecka-Kozerska https://orcid.org/0000-0001-6165-3302
Przemko Kwinta https://orcid.org/0000-0002-3017-0348

References

1. Gubhaju L, Sutherland MR, Horne R, et al. Assessment of renal functional maturation and injury in preterm neonates during the first month of life. *Am J Physiol Renal Physiol*. 2014;307(2):F149–F158.
2. La Manna G, Galletti S, Capelli I, et al. Urinary neutrophil gelatinase-associated lipocalin at birth predicts early renal function in very low birth weight infants. *Pediatr Res*. 2011;70(4):379–383.
3. Koralkar R, Ambalavanan N, Levitan EB, McGwin G, Goldstein S, Askenazi D. Acute kidney injury reduces survival in very low birth weight infants. *Pediatr Res*. 2011;69(4):354–358.
4. Jetton JG, Askenazi DJ. Update on acute kidney injury in the neonate. *Curr Opin Pediatr*. 2012;24(2):191–196.
5. Stojanović VD, Barišić NA, Vučković NM, Doronjski AD, Peco Antić AE. Urinary kidney injury molecule-1 rapid test predicts acute kidney injury in extremely low-birth-weight neonates. *Pediatr Res*. 2015; 78(4):430–435.
6. Akcan-Arikan A, Zappitelli M, Loftis LL, Washburn KK, Jefferson LS, Goldstein SL. Modified RIFLE criteria in critically ill children with acute kidney injury. *Kidney Int*. 2007;71(10):1028–1035.
7. Abitbol CL, Bauer CR, Montané B, Chandar J, Duara S, Zilleruelo G. Longterm follow-up of extremely low birth weight infants with neonatal renal failure. *Pediatr Nephrol*. 2003;18(9):887–893.
8. Libório AB, Pereira Castello Branco KM, Torres deMelo Bezerra C. Acute kidney injury in neonates: From urine output to new biomarkers. *BioMed Res Int*. 2014;2014:601568.
9. Greenberg JH, Parikh CR. Biomarkers for diagnosis and prognosis of AKI in children: One size does not fit all. *Clin J Am Soc Nephrol*. 2017;12(9):1551–1557.
10. Askenazi DJ, Koralkar R, Levitan EB, et al. Baseline values of candidate urine acute kidney injury biomarkers vary by gestational age in premature infants. *Pediatr Res*. 2011;70(3):302–306.
11. Mishra J, Ma Q, Prada A, et al. Identification of neutrophil gelatinase-associated lipocalin as a novel early urinary biomarker for ischemic renal injury. *J Am Soc Nephrol*. 2003;14(10):2534–2543.
12. Han WK, Bailly V, Abichandani R, Thadhani R, Bonventre JV. Kidney injury molecule-1 (KIM-1): A novel biomarker for human renal proximal tubule injury. *Kidney Int*. 2002;62(1):237–244.
13. Liangos O, Perianayagam MC, Vaidya VS, et al. Urinary N-acetyl-beta-(D)-glucosaminidase activity and kidney injury molecule-1 level are associated with adverse outcomes in acute renal failure. *J Am Soc Nephrol*. 2007;18(3):904–912.
14. Trof RJ, Di Maggio F, Leemreis J, Groeneveld AB. Biomarkers of acute renal injury and renal failure. *Shock*. 2006;26(3):245–253.
15. Nguyen MT, Devarajan P. Biomarkers for the early detection of acute kidney injury. *Pediatr Nephrol*. 2008;23(12):2151–2157.
16. Mori K, Lee HT, Rapoport D, et al. Endocytic delivery of lipocalin-siderophore-iron complex rescues the kidney from ischemia-reperfusion injury. *J Clin Invest*. 2005;115(3):610–621.
17. Huynh TK, Bateman DA, Parravicini E, et al. Reference values of urinary neutrophil gelatinase-associated lipocalin in very low birth weight infants. *Pediatr Res*. 2009;66(5):528–532.
18. Xie Y, Sakatsume M, Nishi S, Narita I, Arakawa M, Gejyo F. Expression, roles, receptors, and regulation of osteopontin in the kidney. *Kidney Int*. 2001;60(5):1645–1657.
19. Bailly V, Zhang Z, Meier W, Cate R, Sanicola M, Bonventre JV. Shedding of kidney injury molecule-1, a putative adhesion protein involved in renal regeneration. *J Biol Chem*. 2002;277(42):39739–39748.
20. Coca SG, Yalavarthy R, Concato J, Parikh CR. Biomarkers for the diagnosis and risk stratification of acute kidney injury: A systematic review. *Kidney Int*. 2008;73(9):1008–1016.
21. Thongboonkerd V, Malasit P. Renal and urinary proteomics: Current applications and challenges. *Proteomics*. 2005;5(4):1033–1042.
22. Schwartz GJ, Munoz A, Schneider MF, et al. New equations to estimate GFR in children with CKD. *J Am Soc Nephrol*. 2009;20(3):629–637.
23. Chi-Nien C, Chia-Hung C, Suh-Fang J, et al. Urinary neutrophil gelatinase-associated lipocalin levels in neonates. *Pediatr Neonatol*. 2016; 57(33):207–212.
24. Bateman DA, Thomas W, Parravicini E, Polesana E, Locatelli C, Lorenz JM. Serum creatinine concentration in very-low-birth-weight infants from birth to 34–36 week postmenstrual age. *Pediatr Res*. 2015;77(5): 696–702.
25. Parravicini E, Lorenz JM, Nemerofsky SL, O'Rourke M, Barasch J, Bateman D. Reference range of urinary neutrophil gelatinase-associated lipocalin in very low-birth-weight infants: Preliminary data. *Am J Perinatol*. 2009;26(6):437–440.
26. Noemi M, Ramirez M, Godoy LE, Barrientos EA. SNAP II and SNAPPE II as predictors of neonatal mortality in a pediatric intensive care unit: Does postnatal age play a role? *Int J Pediatr*. 2014;2014:298198.
27. Dionne JM, Abitbol CL, Flynn JT. Hypertension in infancy: Diagnosis, management and outcome. *Pediatr Nephrol*. 2012;27(1):17–32.
28. Selewski DT, Jordan BK, Askenazi DJ, Dechert RE, Sarkar S. Acute kidney injury in asphyxiated newborns treated with therapeutic hypothermia. *J Pediatr*. 2013;162(4):725–729.
29. Alabbas A, Campbell A, Skippen P, Human D, Matsell D, Mammen C. Epidemiology of cardiac surgery-associated acute kidney injury in neonates: A retrospective study. *Pediatr Nephrol*. 2013;28(7):1127–1134.
30. Elmas AT, Tabel Y, Ipek S. Determination of reference values for urinary neutrophil gelatinase-associated lipocalin in premature infants. *J Matern Fetal Neonatal Med*. 2014;27(2):187–191.
31. Sarafidis K, Tsepkentzi E, Agakidou E, et al. Serum and urine acute kidney injury biomarkers in asphyxiated neonates. *Pediatr Nephrol*, 2012;27(9):1575–1582.
32. Cangemi G, Storti S, Cantinotti M, et al. Reference values for urinary neutrophil gelatinase-associated lipocalin (NGAL) in pediatric age measured with a fully automated chemiluminescent platform. *Clin Chem Lab Med*. 2013;51(5):1101–1105.
33. Askenazi DJ, Koralkar R, Patil N, Halloran B, Ambalavanan N, Griffin R. Acute kidney injury urine biomarkers in very low-birth-weight infants. *Clin J Am Soc Nephrol*. 2016;11(9):1527–1535.
34. Askenazi DJ, Montesanti A, Hunley H, et al. Urine biomarkers predict acute kidney injury and mortality in very low birth weight infants. *J Pediatr*. 2011;159(6):907–912.
35. Genc G, Ozkaya O, Avci B, Aygun C, Kucukoduk. Kidney injury molecule-1 as a promising biomarker for acute kidney injury in premature babies. *Am J Perinatol*. 2013;30(3):245–252.
36. Youssef M, Abdelsalam M, Saeed R, Mohamed A. Urinary kidney injury molocule-1 level in preterm neonates with respiratory distress syndrome. *Open J Pediatr*. 2016;6(1):1–9.
37. Kamianowska M, Szczepański M, Kulikowska EE, Bebko B, Wasilewska A. Do serum and urinary concentrations of kidney injury molecule-1 in healthy newborns depend on birth weight, gestational age or gender? *J Perinatol*. 2017;37(1):73–76.
38. Lavery AP, Meinzen-Derr JK, Anderson E, et al. Urinary NGAL in premature infants. *Pediatr Res*. 2008;64(4):423–428.
39. Suchojad A, Tarko A, Smertka M, et al. Factors limiting usefulness of serum and urinary NGAL as a marker of acute kidney injury in preterm newborns. *Ren Fail*. 2015;37(3):439–445.
40. Aggarwal A, Kumar P, Chowdhary G, Majumdar S, Narang A. Evaluation of renal functions in asphyxiated newborns. *J Trop Pediatr*. 2005; 51(5):295–299.

Acute coronary syndrome in patients undergoing anticancer therapies: A single-center, controlled case study

Izabela Nabiałek-Trojanowska[1,2,B–D], Alicja Dąbrowska-Kugacka[2,E], Zuzanna Lewicka-Potocka[1,2,C–E], Yasmina Abdulaziz[2,B–D], Anna Szerszyńska[2,B–D], Grzegorz Raczak[2,E], Ewa Lewicka[2,A,E,F]

[1] First Department of Cardiology, Medical University of Gdańsk, Poland
[2] Department of Cardiology and Electrotherapy, Medical University of Gdańsk, Poland

A – research concept and design; B – collection and/or assembly of data; C – data analysis and interpretation; D – writing the article; E – critical revision of the article; F – final approval of the article

Advances in Clinical and Experimental Medicine, ISSN 1899–5276 (print), ISSN 2451–2680 (online) *Adv Clin Exp Med*. 2019;28(12):1667–1673

Address for correspondence
Ewa Lewicka
E-mail: elew@gumed.edu.pl

Funding sources
None declared

Conflict of interest
None declared

Received on January 1, 2019
Reviewed on April 20, 2019
Accepted on June 27, 2019

Published online on December 18, 2019

Abstract

Background. Anticancer therapies can be accompanied by cardiovascular complications, including acute coronary syndrome (ACS). In turn, the presence of cancer can influence therapeutic decisions if ACS occurs.

Objectives. The aim of the study was to analyze ACS treatment in patients with cancer.

Material and methods. The study consisted of a retrospective analysis based on the medical records of patients who were admitted due to ACS, with cancer diagnoses. Patients currently undergoing cancer treatment or having treatment which ended up to 6 months before the ACS were included. They were compared to a control group consisting of consecutive patients admitted for ACS during the same period, but who did not have a diagnosis of cancer; they were matched with the experimental group in terms of age, gender and clinical type of ACS.

Results. Thirty-two consecutive cancer patients (70 ±9 years; 53% men) met the inclusion criteria. In 22 of them (69%), ACS occurred during their cancer treatment, and in 10 (31%), it presented within 6 months of completing cancer treatment. Upon hospital admission, 19 (59%) cancer patients complained of dyspnea and 7 of typical angina, while in the control group 28, (87%) and 4 (13%) reported such symptoms, respectively.The clinical manifestation of ACS was NSTEMI in 16 patients (50%), UA in 10 (31%) and STEMI in 5 (15.6%). Coronary angiography was done in 25 (78%) of the cancer patients and in all members of the control group. Percutaneous coronary angioplasty (PCA) was performed in 17 (53%) and 23 (72%) of the patients from the respective groups. The median time to percutaneous coronary intervention (PCI) was 10 h (30 min–10 days) among the cancer patients and 7.5 h among the control group (30 min–6 days). There were no PCI-related complications or severe bleeding in both groups. In-hospital mortality was 6.25% in the cancer group and there were no reported hospital deaths in the control group.

Conclusions. Dyspnea is the most common symptom of ACS in cancer patients who are treated invasively too rarely: the presence of cancer and active anticancer treatment should not limit the management of ACS in accordance with current guidelines.

Key words: acute coronary syndrome, anticancer therapy, STEMI, NSTEMI, cancer disease

Cite as
Nabiałek-Trojanowska I, Dąbrowska-Kugacka A, Lewicka-Potocka Z. Acute coronary syndrome in patients undergoing anticancer therapies: A single-center, controlled case study. *Adv Clin Exp Med*. 2019;28(12):1667–1673. doi:10.17219/acem/110316

DOI
10.17219/acem/110316

Introduction

Anticancer therapies can be accompanied by cardiovascular complications, including acute coronary syndrome (ACS). A recently published registry has shown that cancer survivors, compared to the general population, are at a higher risk of cardiovascular morbidity and mortality and that they represent a large group of patients undergoing percutaneous coronary intervention (PCI): 1 in every 13 patients.[1] Cancer at various stages and treated with various anticancer therapies is reported in about 15% of patients with ACS.[2]

The association between cancer and ACS is complex and multifactorial. Many cancers have risk factors in common with coronary artery disease: older age, male sex, smoking and obesity.[3] Cancer itself leads to a prothrombotic state, oxidative stress and the progression of atherosclerosis.[4] Additionally, anticancer treatment may increase thrombotic risk and lead to cardiotoxic effects, since chemotherapy and radiotherapy exert pro-inflammatory and vasospastic effects.[5,6]

Optimal ACS treatment in cancer patients can be difficult, as these patients are at risk of both stent thrombosis and the bleeding that is often increased due to thrombocytopenia. In clinical practice, cancer reported in anamnesis can change the treatment plan due to the unknown prognosis of life length and the higher risk of bleeding, as well as to thrombotic events which may accompany the treatment.

The aim of our study was to analyze the treatment of ACS administered to patients with cancer during or soon after the end of their anticancer therapy.

Methods

Based on the hospital database, 3 investigators independently reviewed the discharge cards, medical history reports and all available medical documents of patients hospitalized in our Cardiology Departments because of ACS from January 2012 to December 2017. The keywords for the search were ACS, ST-elevation myocardial infarction (STEMI), non-ST-segment elevation myocardial infarction (NSTEMI), unstable angina (UA), cancer, and neoplasm, using ICD codes C0-C97, D37-D48 and I20-I22.

Next, we searched for patients in whom ACS presented during or soon after (up to 6 months after the end of anticancer therapy or treatment). The medical records of these patients were carefully screened to analyze the ACS treatment. The control group consisted of consecutive patients admitted for ACS during the same period, but without a diagnosis of cancer. They were matched with the study group in terms of age, gender and clinical type of ACS. The statistical analyses of continuous data were performed using a t-test in the case of normal distributions, and non-parametric tests (Mann–Whitney U test) in the case of non-normally distributed or ordinal data. P-values <0.05 were considered statistically significant.

Results

Overall, 8,327 records with ACS reported were retrieved from the hospital database, of which 441 records were of patients with a diagnosis of cancer. Finally, 32 records based on the inclusion criteria and deemed adequate for the purpose of our study were screened in detail. The control group consisted of 32 patients with a similar age and sex distribution and the same frequency of ACS types.

We analyzed the data obtained from 32 consecutive cancer patients at a mean age of 70 ±9 years (58–88 years) 17 of whom (53.1%) were men admitted from the emergency department due to ACS occurring a median of 7 months after their cancer diagnosis. In the cancer group, the most common disease was lung cancer, diagnosed in 9 patients (28.1%). From the remaining patients, breast cancer was in 6 (18.8%), prostate cancer in 4 (12.5%), colon cancer in 4 (12.5%), gastric cancer in 2, ovarian cancer in 2, head and neck cancer in 2, endometrial cancer in 1, non-Hodgkin lymphoma in 1, and chronic myeloid leukemia in 1. For 29 of the patients, it was a newly diagnosed tumor, while in the remaining 3 it was a recurrence of cancer. In 22 patients (69%), ACS occurred during anticancer treatment: chemotherapy in 15 patients, hormonotherapy in 4, combined radiation and chemotherapy in 2, and during immunotherapy in 1. In 10 patients (31%), ACS developed within 6 months of the end of anticancer treatment: in 5 patients who had previously undergone chemotherapy and after thorax radiation in the other 3 patients. Twenty-two patients (68.7%) had received chemotherapy, and the most commonly used anticancer drugs which could potentially affect coronary arteries or lead to arterial thrombosis were platinum compounds and fluoropyrimidines, administered in 31.2% and 18.6% of patients, respectively. Data on the chemotherapy agents which were administered is shown in Table 1. Thirteen patients (40.6%) had recently undergone radiotherapy. Of the 13, 7 (21.9%) had undergone thorax irradiation and in 2 patients the cancer recurred more than 10 years after radiotherapy. Seven patients (21.9%) received combined chemotherapy and radiotherapy.

Almost all cancer patients (30 (94%)) presented with at least 1 cardiovascular risk factor or comorbidity. Coronary artery disease was reported in 13 (40%) patients, and previous myocardial infarction in 3 patients. In the control group, all patients had at least 1 cardiovascular risk factor or comorbidity, and coronary artery disease was diagnosed in 14 (44%) patients, while previous myocardial infarction was found in 11 patients. The clinical characteristics of both groups are shown in Table 2.

Upon admission to the hospital, 19 patients (59%) from the control group presented with dyspnea, and 7 (22%) with typical angina. In the control group, the main ACS symptom was typical angina in 28 patients (87%), while dyspnea was reported by 4 patients (13%). The most common clinical ACS manifestation was NSTEMI, diagnosed

Table 1. Anticancer therapy in the study group of cancer patients

Chemotherapy agents	Number of patients
Platinum compounds	
cisplatin	5
carboplatin	4
oxaliplatin	1
Fluoropyrimidines	
5-fluorouracil	2
capecitabine	3
gemcitabine	1
Anthracyclines	
doxorubicin	3
Alkylating agents	
cyclophosphamide	2
Antimicrotubulale agents	
docetaxel	2
paclitaxel	1
VEGF inhibitors	
bevacizumab	1
Vinca alkaloids	
vincristine	1
vinorelbine	2
Hydroxycarbamide	1

VEGF – vascular endothelial growth factor.

Table 2. Clinical characteristics of patients with acute coronary syndrome and cancer (study group) and those without cancer (control group)

Parameter	Cancer group (n = 32)	Control group (n = 32)	p-value
Males, n (%)	17 (53)	17 (53)	p = 1.0
Age [years]	70 ±9	70 ±9	p = 1.0
Previous coronary artery disease, n (%)	13 (40)	14 (44)	p = 1.0
Arterial hypertension, n (%)	23 (72)	30 (94)	p = 0.1
Dyslipidemia, n (%)	12 (37.5)	30 (94)	p < 0.001
Diabetes, n (%)	10 (32)	18 (56)	p = 0.08
Smoking history, n (%)	15 (54)	10 (31)	p = 0.14
Obesity (BMI > 30 kg/m^2), n (%)	6 (19)	9 (28)	p = 0.7
STEMI, n (%)	5 (15.6)	5 (15.6)	p = 1.0
NSTEMI, n (%)	10 (31.3)	10 (31.3)	p = 1.0
Unstable angina, n (%)	16 (50)	16 (50)	p = 1.0
Type 2 myocardial infarction, n (%)	1 (3.1)	1 (3.1)	p = 1.0

BMI – body mass index; STEMI – ST-elevation myocardial infarction; NSTEMI – non-ST-segment-elevation myocardial infarction.

in 16 cancer patients (50%). Unstable angina (UA) had occurred in 10 patients (31.3%) and STEMI in 5 (15.6%). In 1 patient with severe anemia, a type 2 myocardial infarction (MI) had occurred. The incidence of the various clinical ACS types was the same as in the control group.

In the cancer group, coronary angiography was done in 25 patients (78%). Seventeen patients (53%) underwent percutaneous coronary angioplasty (PCA), with the implantation of a drug-eluting stent (DES) in 12 patients and a bare metal stent (BMS) in the remaining 5 patients. None of the patients were treated with balloon angioplasty (POBA) or referred for coronary artery bypass grafting (CABG). In 6 patients, a third-generation DES was implanted. In the control group, all patients were referred for coronary angiography. Twenty-three (72%) were treated with PCA: DES implantation in 21 patients and BMS implantation in 1, while 1 patient was treated with POBA. In 4 patients, a third-generation DES was implanted. As in the cancer group, none of the patients were referred for CABG. In the cancer group, PCA with stent implantation was performed in 3 patients (60%) with STEMI, 9 with NSTEMI and 5 with UA, while in the control group it was in 5 (100%), 12 and 6 patients, respectively.

The median time from hospital admission to PCA among the cancer patients was 10 h; it was 105 min in the patients with STEMI (ranging from 30 min to 10 h), 14.5 h in patients with NSTEMI (from 30 min to 10 days) and 13.5 h in those with UA (from 30 min to 4 days). In the control group, the median time between admission and PCA was 7.5 h (p = 0.6 vs the cancer group); it was 35 min in the patients with STEMI (ranging from 30 min to 8 h; p = 0.6), 11.5 h in the patients with NSTEMI (from 30 min to 6 days; p = 0.8) and 5 h in those with UA (from 60 min to 42 h; p = 0.1).

Coronary catheterization was performed using the radial approach in all but 1 cancer patient, in whom femoral access was used. There were no PCA-related complications or serious bleeding. In 2 patients, bleeding in the arterial puncture area was noted (1 patient with femoral access), which was self-limiting and did not require medical intervention. In the control group, coronary angiography was performed using the radial approach in 26 patients (81%), via a brachial artery in 2 and via a femoral artery in 4 (12%). No PCA-related complications or bleeding were reported in the control group. Data on the ACS treatment administered to individual patients are shown in Table 3.

Among the cancer patients, aspirin was administered to 29 (94%), clopidogrel to 23 (74%) and 22 (71%) patients obtained double antiplatelet therapy (DAPT). Nine patients did not receive antiplatelet treatment because they reported anemia or severe bleeding in anamnesis, and 1 was allergic to aspirin. Enoxaparine was administered to 16 patients (51.6%). A loading dose of 300 mg of aspirin was administered to 20 patients and 600 mg of clopidogrel to 23. Ticagrelor and prasugrel were not used in our patients. Triple antithrombotic therapy, involving aspirin, clopidogrel and enoxaparine, was used in 13 patients. None of the patients received a vitamin K antagonist (VKA) or a novel oral anticoagulant (NOAC). In 1 patient, data about antiplatelet and antithrombotic treatment was not obtained. Gastrointestinal bleeding occurred in 1 patient and nasal bleeding in another 1, but medical intervention or prolongation of hospitalization were not required. Statin

Table 3. Hematological data and treatment strategy in patients with acute coronary syndrome (ACS) and cancer (study group) and in those without cancer (control group)

Patient	Cancer group (n = 32)							Control group (n = 32)						
	Hb [mg/dL]	PLT [×10⁹/L]	ACS treatment	Aspirin daily in the long-term treatment [mg]	Clopidogrel daily in the long-term treatment [mg]	Anticoagulant therapy	Bleeding complication	Hb [mg/dL]	PLT [×10⁹/L]	ACS treatment	Aspirin daily in the long-term treatment [mg]	Clopidogrel daily in the long-term treatment [mg]	Anticoagulant therapy	Bleeding complication
1	13.0	217	PCA+DES	75*	75*	1	0	12.4	256	non-invasive	75*	0	0	0
2	10.3	313	PCA+DES	75*	75*	1	0	15.2	265	PCA+DES	75*	75*	0	0
3	11.8	244	PCA+DES	75*	75*	1	0	12.2	305	PCA+DES	75	75	0	0
4	12.8	230	PCA+DES	75*	75*	0	0	15.8	203	PCA+DES	75	0	0	0
5	13.5	159	PCA+DES	75	75*	0	1	12.8	219	PCA+DES	75*	75*	0	0
6	9.1	351	non-invasive	75	0	1	0	12.8	215	non-invasive	0	0	1	0
7	14.7	74	non-invasive	0	0	1	0	8.2	217	POBA	75	75	0	0
8	10.4	235	non-invasive	nd	nd	nd	0	11.3	179	non-invasive	75	75	0	0
9	11.7	207	PCA+DES	75*	75*	1	0	11.6	216	non-invasive	75	0	0	0
10	12.8	172	non-invasive	75*	75*	1	0	15.0	134	PCA+DES	75*	75*	0	0
11	12.8	121	non-invasive	75*	75*	1	0	13.3	211	non-invasive	75*	75*	0	0
12	11.0	277	PCA+DES	75*	75*	1	0	14.3	162	PCA+DES	75	75	0	0
13	13.9	228	non-invasive	75*	75*	0	0	9.9	255	PCA+DES	75*	75*	0	0
14	13.5	250	non-invasive	0#	75*	0	1	8.9	653	PCA+DES	75*	75*	1	0
15	13.7	273	non-invasive	75*	75*	1	0	14.4	194	PCA+DES	75*	75*	0	0
16	12.3	182	PCA+DES	75*	75*	0	0	13.7	269	PCA+DES	75*	75*	1	0
17	11.0	217	PCA+BMS	75*	75*	0	0	13.1	225	PCA+DES	75*	75*	0	0
18	10.6	139	non-invasive	75	0	0	0	15.1	229	PCA+DES	75*	75*	0	0
19	11.9	296	PCA+BMS	75*	75*	1	0	14.1	229	PCA+DES	75	75*	0	0
20	13.3	206	non-invasive	75	0	0	0	15.1	238	non-invasive	75	75*	0	0
21	13.8	202	non-invasive	75*	0	0	0	11.9	218	non-invasive	75	0	0	0
22	11.7	212	non-invasive	75	0	0	0	12.3	162	PCA+DES	75	75	1	0
23	10.6	394	non-invasive	75	75*	0	0	12.3	363	PCA+DES	75*	75*	0	0
24	11.7	119	PCA+BMS	75*	75*	1	1	16.0	298	non-invasive	75*	0	0	0
25	9.6	280	PCA+BMS	75*	75*	0	0	9.2	400	PCA+DES	75	75	0	1
26	10.5	421	PCA+DES	75*	75*	0	0	12.7	243	PCA+DES	75	75	0	0
27	11.4	145	PCA+DES	75	75*	1	0	15.5	180	PCA+DES	75*	75*	0	0
28	12.8	301	non-invasive	75	0	0	0	13.8	272	PCA+BMS	75*	75*	0	700
29	12.3	423	PCA+DES	75	75*	0	0	11.8	247	PCA+DES	75*	75*	0	0
30	12.2	313	PCA+BMS	75*	75*	1	0	15.1	253	PCA+DES	75	75*	0	0
31	8.7	189	non-invasive	75*	0	1	1	15.2	252	PCA+DES	75*	75*	0	0
32	14.0	147	PCA+DES	75*	75*	1	0	14.3	175	non-invasive	75*	0	0	0

Hb – hemoglobin concentration; PLT – platelet count; PCA – percutaneous coronary angioplasty; DES – drug-eluting stent; BMS – bare metal stent; nd – no data; 1 – 'Yes'; 0 –'No'; *application of a loading dose of 300 mg of aspirin and/or 600 mg of clopidogrel; # – aspirin allergy.

was administered to 25 patients (80.6%), β-blockers in 28 (87.1%) and an angiotensin converting enzyme inhibitor (ACEI) or angiotensin receptor blocker (ARB) was administered to 23 (74.2%).

In the control group, 31 (97%) patients received aspirin, 25 (78%) clopidogrel, 1 (3%) received ticagrelor, and 26 (81%) were given DAPT. A loading dose of 300 mg of aspirin was administered to 18 patients, and 600 mg of clopidogrel

to another 18 patients. One patient with type 2 myocardial infarction due to tachyarrhythmia was treated conservatively and received only anticoagulant therapy (enoxaparine). In 3 other patients, antithrombotic therapy was administered: warfarine in 2 patients and dabigatran in 1. One patient had nasal bleeding which was treated conservatively, with no significant drop in hemoglobin concentration. Thirty patients (94%) received statin, 25 (78%) β-blockers and 29 (91%) patients were administered ACEI or ARB.

None of the patients from either study group suffered from severe thrombocytopenia, and hemoglobin concentration in the 2 groups varied from 8.7 mg/dL to 14 mg/dL and from 8.2 mg/dL to 16.0 mg/dL, respectively. In echocardiographic examination performed before hospital discharge, the mean left ventricular ejection fraction was 55 ±12% (33–66%) in the cancer group and 50 ±10% (25–74%) in the control group (p = 0.16).

In-hospital mortality among all patients admitted to our cardiology departments due to ACS in the study period was 6.16%. In the cancer group, during a median of 5 days (3–31 days) of hospitalization 2 patients died (6.25%) due to sudden cardiac arrest and pulseless electrical activity. There were no more deaths from ACS during the following 30 days, though data regarding outcome were not collected on 2 patients. In the control group, the median duration of hospitalization was 6 days (2–22 days) and there were no hospital deaths or deaths from ACS during the following 30 days.

Discussion

The results of the study indicate that the majority of patients with ACS presenting during or soon after anticancer treatment can be treated according to the current ACS guidelines, without adversely affecting in-hospital prognosis or the duration of hospitalization. The vast majority of cancer patients received antiplatelet therapy, and even if DAPT or enoxaparine was used, it was not accompanied by an increased risk of bleeding during hospitalization. Most patients were given a β-blocker, ACEI or ARB and statin. However, coronary angiography was performed too rarely (in only 78% of the cancer patients) and only 53% underwent PCA with stent implantation.

The pathogenesis of ACS among cancer patients includes the impact of classic cardiovascular risk factors, as well as the influence of a prothrombotic state, oxidative stress and tumor-induced atherosclerosis.[4] The effects of anticancer treatment (i.e., chemotherapy, radiotherapy or surgery) must also be considered. The majority of our cancer patients presented with cardiovascular risk factors or comorbidities, with no significant differences in comparison with the controls (apart from dyslipidemia) which was more frequent among the control group. In addition, the median time from cancer diagnosis was 7 months, which may affect the occurrence of ACS. It has been reported that the incidence of ACS in patients with newly diagnosed cancer increases in the first 6 months from diagnosis and then decreases after a year to increase again in more advanced cancer stages.[6,7] In our patients, we must also consider the influence of recent anticancer therapy on the development of their ACS, as chemotherapy and radiotherapy can exert prothrombotic, pro-inflammatory and vasospastic effects.[5,6,8] We focused on an early cardiac manifestation of anticancer therapy complication, although 2 patients from our group presented with tumor recurrence years after thorax radiotherapy. In this case, the mechanism of ACS may differ, and it could be a result of fibrosis or calcification within the coronary arteries.

Many chemotherapeutic agents predispose one to ACS, as they may provoke coronary vasospasm, endothelial damage or arterial thrombosis and they may aggravate atherosclerosis.[9] A number of chemotherapeutic agents may lead to acute coronary events, mainly cisplatin, 5-fluorouracil, vincristine, rituximab, and BCR-ABL-directed tyrosine kinase inhibitors. Likewise, paclitaxel, capecitabine, VEGF inhibitors, erlotinib, nilotinib, and ponatinib have been reported to exert vascular toxicity, especially in coronary arteries. The time of ischemia onset varies widely. It may occur within hours of infusion or several days afterwards.[10] Cisplatin-related risk can persist even after the end of chemotherapy.[11]

Modern radiotherapy aims to focus the radiation beam on the invaded tissue; complications of such treatment are rarer than with the previously used methods. The mechanism of radiation-related damage to the coronary arteries is similar to chemotherapy, and it could be an effect of endothelial injury, coronary vasospasm, atherosclerotic plaque rupture or thrombosis.[9,12] Such injuries are usually located in the ostia and proximal segments of the coronary arteries.[13] The risk of radiation-related coronary artery disease depends on the radiation dosage and the volume of the irradiated heart.[9] It can manifest early, during or soon after the end of radiation, or with a delay, even after 10–15 years.

As opposed to patients from the control group, who reported angina as the main ACS symptom, many of the cancer patients presented with dyspnea at hospital admission, which is consistent with the observations of other authors.[14–16] Radio- and chemotherapy-related neurotoxicity can affect the ability to feel pain, so in effect patients after anticancer treatment complain of angina less often. The occurrence of ACS manifests as dyspnea in 44.3% of cancer patients, chest pain in 30.3% and hypotension in 22.7%.[16] As a result of either the higher prevalence of silent ischemia or the altered perception of angina after anticancer treatment, cancer patients seek emergency care after some delay. Emphasis should be placed on cardiac check-up before anticancer treatment with any cardiotoxicity potential and regularly after the end of the treatment in order to reveal complications of anticancer therapy at an early stage.

The most common clinical manifestation of ACS in our patients was NSTEMI. This finding is in accordance with other studies, which reported that in 85% of cancer patients the ACS manifested as NSTEMI and in 15% as STEMI.[17] Conservative treatment of ACS in cancer patients leads to poor survival rate.[18] An analysis of treatment in patients with metastatic cancer who developed STEMI or NSTEMI revealed that invasive treatment with PCI resulted in a 2- to 3-fold reduction in in-hospital mortality.[19] However, the results of one study indicated that cancer patients undergoing PCI due to STEMI had poorer survival after 1 year (10.7% vs 5.4%) and higher cardiac mortality, which especially pertained to those diagnosed up to 6 months before the onset of ACS.[20] The optimal treatment in this group remains indefinite, because there is no data available on cancer patients in the PCI registries. Formerly, cancer patients were excluded from most major randomized, controlled ACS trials. According to the available data, PCI offers a better prognosis in this group of patients, but the need for antiplatelet therapy after stenting should be taken into account in treatment planning. Double antiplatelet therapy can cause hemorrhagic complications and anemia, especially gastrointestinal and urinary bleeding.

It has been proven that early PCI improves outcomes in ACS independently from the patients' group.[21] In the general population, the frequency of PCI has increased during the last 2 decades, from 11.9% to 60.8% of patients admitted with STEMI. This corresponds with significantly lower 30-day mortality and overall mortality.[22] In Poland, according to a recent registry, PCI was performed in 96.2% of patients with STEMI, and in 76.3% of patients with NSTEMI or UA.[23] In our groups, 78% of cancer patients were referred for coronary angiography, and 53% were treated with PCA and stent implantation, while in the control group it was 100% and 72% of patients, respectively. Our data indicates that invasive treatment of ACS is less common in patients with cancer, despite current guidelines. Moreover, in STEMI patients with cancer, the median time from admission to PCI was 105 min, while it was 35 min in the control group. Guidelines recommend that the interval between arrival at the hospital and intracoronary balloon inflation (door-to-balloon time) during primary PCI should be 90 min or less. In the STEMI registry, the median door-to-balloon time was 83 min[24]; thus, it was too late in our patients.

A study comparing PCI outcomes in patients with and without cancer history proved that those reporting cancer in anamnesis received stents less often. Moreover, a delay in invasive treatment, assessed by the time between diagnosis and balloon inflation, was evident in the cancer group. In this study, higher early cardiac mortality was linked to anemia and cardiogenic shock during PCA, which occurred more frequently in cancer patients.[20]

In the majority of study patients, PCI was performed by the radial approach. One of 2 bleeding events at the puncture site in our group occurred in a cancer patient on whom PCI was performed via the femoral artery. According to the literature, femoral artery access is associated with a higher risk of bleeding, even with the use of vascular closure devices after coronary angiography.[25] The femoral approach should be used in patients with abnormal Allen's test results in both hands, with arterial lines, those who have had bilateral mastectomy or multiple radial procedures and in those on hemodialysis. Radial artery access is preferred for others.[26]

The small number of bleeding events in our patients, which were self-terminated and clinically insignificant, may be due to the fact that none of the patients had severe thrombocytopenia during the treatment of ACS. This fact allowed aspirin to be safely administered in 94% of cancer patients and DAPT to be used in 71%, similarly to the control group (97% and 78% of patients, respectively). There is no platelet count which limits coronary catheterization,[26] and the use of aspirin in ACS treatment among cancer patients with a platelet count below 100,000/μL was associated with a higher 7-day survival rate compared to those who did not receive aspirin (90% vs 6%).[27] Double antiplatelet therapy with clopidogrel can be used in patients with a platelet count of 30,000–50,000/μL. Ticagrelor and prasugrel should not be used in cancer patients due to the high risk of bleeding in this group.[17]

In 70% of cancer patients who underwent PCA, a drug-eluting stent was implanted, which is contrary to other studies reporting that BMSs are used more often in cancer patients.[13,20] The antiproliferative effects of chemotherapy may delay the normal endothelization process observed among non-cancer patients after stent implantation,[26] which may favor the use of DES in cancer patients with sufficient prognosis. Drug-eluting stent has lower rates of stent thrombosis[18] and with third-generation DES the duration of DAPT can be shortened to 3–6 months in ACS patients. However, in cancer patients with a platelet count from 10,000/μL to 30,000/μL or if DAPT cannot be used or in those demanding surgery or chemotherapy within the next 4 weeks, balloon angioplasty should be considered.[26] With balloon angioplasty, DAPT is required for at least 2 weeks.[26]

The vast majority of our patients were treated with a β-blocker, ACEI or ARB and statin. It was reported that not only aspirin use, but also β-blocker use, in cancer patients as in the general population, improves survival rates in ACS.[16] For unknown reasons, β-blockers are less likely to be administered to cancer patients.[20] Each cancer patient with ACS should be considered for optimal therapy with an antiplatelet drug or drugs, statin, ACEI or ARB and a β-blocker.

The most important limitation of our study is the small size of the cancer group and the lack of long-term observation after hospital discharge. Our data does not include the stage of cancer or planned further anticancer treatment, though this was not the focus of our study. The short

observation period may have resulted in the low frequency of bleeding complications in the time of recommended DAPT therapy after PCI. The data was collected from our hospital database based on the medical recognition on the information cards at hospital discharge. If a diagnosis of cancer was missing on this card, the patient may not have been included in the analysis. This may to some extent explain the small number of patients from our hospital database who met the inclusion criteria for the study. As our sample is small, conclusions regarding the population of cancer patients with ACS should only be drawn with special caution. We included data on in-hospital mortality among ACS patients without cancer who were treated in our cardiology departments, but no direct comparison was made with the cancer group.

Conclusions

Our data suggests that cancer patients with ACS should be treated according to the current guidelines for ACS in the general population, taking into consideration additional factors related to cancer. Data regarding ACS management in cancer patients is still lacking, as the current information is most often based on small population studies and expert consensus. According to our results, patients with ACS onset during or shortly after anticancer therapy are too rarely treated invasively. Moreover, those with STEMI are referred for coronary angiography too late after hospital admission. The presence of cancer and active anticancer treatment should not limit the effective and safe treatment of ACS.

ORCID iDs

Izabela Nabiałek-Trojanowska https://orcid.org/0000-0001-9986-2265
Alicja Dąbrowska-Kugacka https://orcid.org/0000-0002-5546-7818
Zuzanna Lewicka-Potocka https://orcid.org/0000-0002-7716-1190
Yasmina Abdulaziz https://orcid.org/0000-0002-2659-8245
Anna Szerszyńska https://orcid.org/0000-0002-4381-865X
Grzegorz Raczak https://orcid.org/0000-0001-8535-8658
Ewa Lewicka https://orcid.org/0000-0002-0162-2659

References

1. Landes U, Kornowski R, Bental T, et al. Long-term outcomes after percutaneous coronary interventions in cancer survivors. *Coron Artery Dis.* 2017;28(1):5–10.
2. Goldberg R, Chen H-Y, Saczynski J, et al. The impact of cardiac and noncardiac comorbidities on the short-term outcomes of patients hospitalized with acute myocardial infarction: A population-based perspective. *Clin Epidemiol.* 2013;5:439–448.
3. Hess CN, Roe MT. Treatment of coronary artery disease in cancer survivors. *Coron Artery Dis.* 2017;28(1):1–2.
4. Mozzini C, Garbin U, Fratta Pasini AM, Cominacini L. An exploratory look at NETosis in atherosclerosis. *Intern Emerg Med.* 2017;12(1):13–22.
5. Hasin T, Iakobishvili Z, Weisz G. Associated risk of malignancy in patients with cardiovascular disease: Evidence and possible mechanism. *Am J Med.* 2017;130(7):780–785.
6. Navi BB, Reiner AS, Kamel H, et al. Risk of arterial thromboembolism in patients with cancer. *J Am Coll Cardiol.* 2017;70(8):926–938.
7. Yeh ETH, Chang H-M. Cancer and clot: Between a rock and a hard place. *J Am Coll Cardiol.* 2017;70(8):939–941.
8. Caine GJ, Stonelake PS, Lip GYH, Kehoe ST. The hypercoagulable state of malignancy: Pathogenesis and current debate. *Neoplasia.* 2002;4(6):465–473.
9. Zamorano JL, Lancellotti P, Rodriguez Muñoz D, et al. 2016 ESC Position Paper on cancer treatments and cardiovascular toxicity developed under the auspices of the ESC Committee for Practice Guidelines. *Eur Heart J.* 2016;37(36):2768–2801.
10. Barac A, Murtagh G, Carver JR, et al. Cardiovascular health of patients with cancer and cancer survivors. *J Am Coll Cardiol.* 2015;65(25):2739–2746.
11. Herrmann J, Yang EH, Iliescu CA, et al. Vascular toxicities of cancer therapies: The old and the new. An evolving avenue. *Circulation.* 2016;133(13):1272–1289.
12. Wrona A, Dziadziuszko R, Jassem J, et al. Radioterapia a ryzyko powikłań ze strony układu sercowo-naczyniowego. In: Szymański F, Filipiak K, eds. Nieklasyczne Czynniki Ryzyka Chorób Układu Sercowo-Naczyniowego w Gabinecie Lekarza Praktyka. Warsaw: ITEM Publishing; 2017:137–158.
13. Lancellotti P, Nkomo VT, Badano LP, et al. Expert consensus for multi-modality imaging evaluation of cardiovascular complications of radiotherapy in adults: A report from the European Association of Cardiovascular Imaging and the American Society of Echocardiography. *Eur Heart J Cardiovasc Imaging.* 2013;14(8):721–740.
14. Munoz E, Iliescu G, Vejpongsa P, et al. Takotsubo stress cardiomyopathy: Good news in cancer patients? *J Am Coll Cardiol.* 2016;68(10):1143–1144.
15. Roffi M, Patrono C, Collet J-P, et al. 2015 ESC Guidelines for the management of acute coronary syndromes in patients presenting without persistent ST-segment elevation. *Eur Heart J.* 2016;37(3):267–315.
16. Yusuf SW, Daraban N, Abbasi N, et al. Treatment and outcomes of acute coronary syndrome in the cancer population. *Clin Cardiol.* 2012;35(7):443–450.
17. Banasiak W, Zymliński R, Undas A. Optimal management of cancer patients with acute coronary syndrome. *Polish Arch Intern Med.* 2018;128(4):244–253.
18. Iliescu C, Tsitlakidou D, Giza DE, Marmagkiolis K. Primary percutaneous coronary interventions in cancer patients. *Cancer Res Front.* 2017;3(1):64–71.
19. Guddati AK, Joy PS, Kumar G. Analysis of outcomes of percutaneous coronary intervention in metastatic cancer patients with acute coronary syndrome over a 10-year period. *J Cancer Res Clin Oncol.* 2016;142(2):471–479.
20. Velders MA, Boden H, Hofma SH, et al. Outcome after ST elevation myocardial infarction in patients with cancer treated with primary percutaneous coronary intervention. *Am J Cardiol.* 2013;112(12):1867–1872.
21. Gale CP, Allan V, Cattle BA, et al. Trends in hospital treatments, including revascularisation, following acute myocardial infarction, 2003–2010: A multilevel and relative survival analysis for the National Institute for Cardiovascular Outcomes Research (NICOR). *Heart.* 2014;100(7):582–589.
22. Puymirat E, Simon T, Steg PG, et al. Association of changes in clinical characteristics and management with improvement in survival among patients with ST-elevation myocardial infarction. *JAMA.* 2012;308(10):998–1006.
23. Wojtkowska I, Stępińska J, Stępień-Wojno M, et al. Current patterns of antithrombotic and revascularisation therapy in patients hospitalised for acute coronary syndromes. Data from the Polish subset of the EPICOR study. *Kardiol Pol.* 2017;75(5):445–452.
24. Rathore SS, Curtis JP, Chen J, et al. Association of door-to-balloon time and mortality in patients admitted to hospital with ST elevation myocardial infarction: National cohort study. *BMJ.* 2009;338(19):b1807–b1807.
25. Sciahbasi A, Fischetti D, Picciolo A, et al. Transradial access compared with femoral puncture closure devices in percutaneous coronary procedures. *Int J Cardiol.* 2009;137(3):199–205.
26. Iliescu CA, Grines CL, Herrmann J, et al. SCAI Expert consensus statement: Evaluation, management, and special considerations of cardio-oncology patients in the cardiac catheterization laboratory (endorsed by the Cardiological Society of India, and Sociedad Latino Americana de Cardiologıa Intervencion. *Catheter Cardiovasc Interv.* 2016;87(5):E202–223.
27. Sarkiss MG, Yusuf SW, Warneke CL, et al. Impact of aspirin therapy in cancer patients with thrombocytopenia and acute coronary syndromes. *Cancer.* 2007;109(3):621–627.

Evaluation of liver-type fatty acid binding protein (L-FABP) and interleukin 6 in children with renal cysts

Krzysztof Plesiński[1,A–D], Piotr Adamczyk[2,A,D,E], Elżbieta Świętochowska[3,C,E], Aurelia Morawiec-Knysak[4,C,F], Aleksandra Gliwińska[4,B,E], Wojciech Korlacki[5,B,E,F], Maria Szczepańska[2,A,E,F]

[1] Cardiological Outpatient Center "Medicor", Myszków, Poland
[2] Department of Pediatrics, School of Medicine with the Division of Dentistry in Zabrze, Medical University of Silesia in Katowice, Poland
[3] Chair and Department of Medical and Molecular Biology, School of Medicine with the Division of Dentistry in Zabrze, Medical University of Silesia in Katowice, Poland
[4] Pediatric Nephrology Ward, Public Clinical Hospital No. 1 in Zabrze, Poland
[5] Department of Children's Developmental Defects Surgery and Traumatology, School of Medicine with the Division of Dentistry in Zabrze, Medical University of Silesia in Katowice, Poland

A – research concept and design; B – collection and/or assembly of data; C – data analysis and interpretation; D – writing the article; E – critical revision of the article; F – final approval of the article

Advances in Clinical and Experimental Medicine, ISSN 1899–5276 (print), ISSN 2451–2680 (online) *Adv Clin Exp Med*. 2019;28(12):1675–1682

Address for correspondence
Maria Szczepańska
E-mail: mszczepanska@szpital.zabrze.pl

Funding sources
Grant KNW-102/N/6/K from the Medical University of Silesia in Katowice, Poland.

Conflict of interest
None declared

Received on March 26, 2019
Reviewed on May 29, 2019
Accepted on June 27, 2019

Published online on November 28, 2019

Abstract

Background. Renal cysts, according to their etiology, can be divided into genetic and acquired cysts. This is of great importance in patients with cystic kidney disease with a possible poor prognosis to identify markers of early kidney damage.

Objectives. The objective of this study was to evaluate the concentration of serum and urine liver-type fatty acid binding protein (L-FABP) and interleukin 6 (IL-6) in children with kidney cysts.

Material and methods. The study was conducted on a group of 39 children with kidney cysts including 20 subjects with autosomal dominant polycystic kidney disease (ADPKD).

Results. Serum and urine L-FABP concentration in children with renal cysts was significantly higher compared to the controls, regardless of the underlying type of cystic degeneration, number of cysts and gender. Also, serum and urinary IL-6 concentration was significantly higher than in the control group. There was a significant negative correlation between serum L-FABP concentration and standard deviation score (SDS) for diastolic blood pressure (DBP). A significant negative correlation was found between serum IL-6 concentration and systolic blood pressure (SBP), DBP and mean arterial pressure (MAP) values as well as SDS for SBP and DBP. In addition, a significant positive correlation was found between urinary IL-6 concentration and estimated glomerular filtration rate (eGFR).

Conclusions. Higher concentration of L-FABP in serum and urine in children with kidney cysts indicates the early damage to the renal parenchyma, detectable before the onset of hypertension and other organ damage. Significantly higher serum and urinary IL-6 levels in children with cystic kidney disease compared to healthy children may suggest the role of this cytokine in chronic kidney disease development.

Key words: children, interleukin 6, autosomal dominant polycystic kidney disease, liver-type fatty acid binding protein, kidney cysts

Cite as
Plesiński K, Adamczyk P, Świętochowska E, et al. Evaluation of liver-type fatty acid binding protein (L-FABP) and interleukin 6 in children with renal cysts. *Adv Clin Exp Med*. 2019;28(12):1675–1682. doi:10.17219/acem/110312

DOI
10.17219/acem/110312

Introduction

The kidney cyst is defined as a space filled with fluid of non-uniform size, which arises in various locations as a result of widening and changing of the structure of renal tubules. The most common are simple kidney cysts that can appear in kidneys not affected with any defined disease, and their number often increases with age. They usually do not cause clinical symptoms and, therefore, are detected accidentally during an ultrasound examination. In 1964, Osathanondh et al. classified renal cysts into 4 categories. Type I was identified with autosomal recessive polycystic kidney disease (ARPKD), type II was described as polycystic renal dysplasia, type III referred to autosomal dominant polycystic kidney disease (ADPKD), while type IV included pathologies associated with impaired urine outflow and the presence of hydronephrosis.[1]

Currently, the classification of diseases related to the presence of cysts in the kidneys is of an etiological basis and includes, apart from the family history, also the clinical picture, the location and morphology of the cysts as well as the presence of extrarenal symptoms.[2] Genetically caused cystic kidney diseases were systematized according to a new classification developed by Kim et al.[2] Of these, ADPKD is the most common.[3–6] Diagnosis of ADPKD due to the typical symptoms, initially before confirmation by genetic testing, is based on family history and imaging.[6–8] For the diagnosis of ADPKD, the ultrasound criteria according to Ravine are currently used.[6] The ADPKD is the most common genetically determined cause of end-stage renal failure in adults.[3,5,9] The reason for the development of ADPKD in 80–85% of cases is the mutation of the *PKD1* gene, which encodes the polycystine-1 protein, while in the remaining 15–20% of patients it is the *PKD2* gene encoding polycystin-2.[10] Incorrectly encoded proteins that arise as a result of mutations lead to the growth and proliferation of kidney tubules cells with the formation of cysts, then to their enlargement and secretion and collection of fluid inside them.[11] In patients with ADPKD, hypertension occurs much earlier than in the general population and often in childhood, which leads to left ventricular hypertrophy, followed by diastolic and later on systolic heart dysfunction.[12,15,16] In about 30–50% of patients with ADPKD, hematuria may occur. In children proteinuria or albuminuria may be present as well. In the course of ADPKD, concomitant cysts in the liver and other organs could be present as well as intracerebral aneurysms, which carry the risk of subarachnoid hemorrhage.[13,17]

Fatty acid binding proteins (FABPs) are low molecular weight cytoplasmic proteins of 14–15 kDa. The physiological role of these proteins is to bind free long chain fatty acids and transfer them to intracellular sites of utilization or storage in the cytoplasmic reticulum and cytoplasm.[18,19]

We currently know 9 types of these proteins with their names derived from the organ or tissue in which they were identified for the first time. Liver fatty acid binding protein (L-FABP) was first detected in hepatocytes, but it is also synthesized in the small and large intestine, lungs and kidneys.[19–21] It binds fatty acids and transports them to mitochondria and peroxisomes, where they are metabolized by beta-oxidation and in that manner provide energy to the epithelial cells.[19,21,22] It has a high affinity to fatty acid peroxidation products, participating in the urinary excretion process, which makes L-FABP an endogenous antioxidant.[19] In recent years, attention has been paid to the prognostic value of L-FABP in kidney disease. Liver fatty acid binding proteins circulating in the blood are filtered in the glomeruli and then reabsorbed at the proximal renal tubules, which explains the increase in their concentration in the urine in the case of damage to the proximal tubules.[19,22,23]

Interleukin 6 (IL-6) is one of the main factors regulating defense mechanisms of the body. Formerly, IL-6 was determined as factor 2 stimulating B lymphocytes, β2 interferon or the growth and differentiation factor of T cytotoxic lymphocytes. It is secreted primarily by macrophages and monocytes, but also by endothelial cells, fibroblasts, chondrocytes, and T and B lymphocytes.[24] The most important role of IL-6 is its participation in the immune response and inflammatory processes by stimulating the differentiation of B lymphocytes into plasma cells, production of acute phase proteins and activation of T lymphocytes.[24–26] Interleukin 6 also participates in hematopoiesis by stimulating hematopoietic stem cells and inducing differentiation of megakaryocytes into platelets. Interleukin 6 produced in excess leads to the development of chronic inflammatory reaction, conducive to the development of autoreactive immune response, leading to the destruction of tissues and organs. Elevated levels of IL-6 have been confirmed in multiple myeloma, chronic lymphocytic leukemia, Alzheimer's disease, systemic lupus erythematosus, rheumatoid arthritis, Castelman's disease, connective tissue diseases, as well as hypertension.[25–27] Chronic inflammatory process, mediated by IL-6 among others, contributes to the increase in blood pressure (BP). Interleukin 6 also affects the growth and development of hypertension by stimulating the sympathetic nervous system and controlling the expression of angiotensinogen, resulting in an increase in angiotensin II. In addition to the direct effect on BP, the increase in IL-6 concentration is associated with obesity, coronary heart disease and diabetes, the last of which also contributes to the development of hypertension and enhances the progression of chronic kidney disease (CKD).[28]

Recently, new markers have been proposed for the diagnosis of early kidney damage in the course of cystic kidney disease. This could help to identify children whose disease progresses faster, with a higher risk of developing organ complications and end-stage renal failure in adolescence or young adulthood.

The hypothesis of our work is the statement that such markers may include the following: protein binding fatty

acids of liver origin (L-FABP) and IL-6. The aim of the study was to assess the usefulness of determining protein-FABP and IL-6 concentrations in serum and urine in children with kidney cysts of various etiologies and their relationship to the underlying cystic kidney disease, the number of cysts found, gender, and hypertension.

Material and methods

The study group consisted of 39 children and adolescents (23 girls and 16 boys) between 1.9 and 20 years of age (mean age 10.9 ±5.0 years) with renal cysts. In all children, we confirmed the presence of cysts in the renal parenchyma on the basis of an ultrasound examination. After conducting family history and evaluation of ultrasounds according to Ravine's criteria,[7] we identified in the study group the following subgroups of children: with ADPKD (20 children – 51%) and without diagnosis of this disease – non-ADPKD (19 children – 49%). Analyzing the number of cysts found on the basis of ultrasound, we identified children with single cysts – less than 10 cysts (29 children – 74%) and multiple cysts (10 children – 26%) in the study group. Most of the children in the study group did not take any medications. Only 4 children with hypertension were successfully treated with antihypertensive drugs. In 15 children from the study group, we showed a positive family history of ADPKD. Body mass, height, BP measurement and routine biochemical tests were performed in the study group – assessment of sodium, potassium, creatinine, urea, and uric acid serum concentration. Blood pressure measurements were made using an oscillometric pressure device, with a cuff placed on the arm. The tests were performed 3 times, in the sitting position, after 5–10 min rest, according to the recommended standards, and the average value of the measurements was calculated. The size of the cuff of the oscillometric pressure device was appropriately matched to the circumference and length of the child's arm in accordance with the recommended measurement principles. Hypertension was diagnosed if the mean of measured systolic blood pressure (SBP) or diastolic blood pressure (DBP) was equal to or exceeding 95.cc for age, sex and height according to the Polish pediatric population.[29–31] Estimated glomerular filtration rate (eGFR) was calculated using the Schwartz formula [mL/min/1.73 m^2].[14]

The control group included 20 healthy children (10 girls and 10 boys). These were ambulatory patients diagnosed due to bedwetting or qualified for "one-day" surgical procedures, who additionally agreed to participate in the study. All subjects were in good clinical condition and had no symptoms of acute infection.

We obtained the consent of the Bioethics Committee of the Silesian Medical University in Katowice, Poland (resolution No. KNW/0022/KB1/21/15). Prior to the examination, written consent was obtained for participation in the project from parents or legal guardians and from children over 16 years of age.

Laboratory tests

Blood samples (3–5 mL) for laboratory tests were collected in the morning (8.00–9.00 am) into Eppendorf tubes, during routine tests related to periodic outpatient supervision. After centrifugation at 1,000 × g for 15 min at 4°C, the serum was stored at –20°C until laboratory tests were performed. Urine samples (50–100 mL) were also collected in the morning and stored at –20°C until testing. The standard BioVendor kit (BioVendor, Brno, Czech Republic) was used to determine the concentration of L-FABP in serum and urine according to the manufacturer's protocol (sensitivity 0.08 ng/mL). The concentration of IL-6 in serum and urine was tested with enzyme-linked immunosorbent assay (ELISA) using a standard kit from Diaclone (Besançon, France) according to the manufacturer's protocol (sensitivity 0.81 pg/mL).

Statistical analysis

The Excel spreadsheet from Microsoft Office package v. 16.0 (Microsoft Corp., Armonk, USA) was used to prepare the database. The calculations were performed using STATISTICA v. 12.0 software (StatSoft Inc., Tulsa, USA). In statistical calculations, the level of significance was $p < 0.05$. As parameters of descriptive statistics, the following were assumed: arithmetic mean, median, minimum and maximum value, lower and upper quartiles, and standard deviation (SD). For all parameters, their distribution was checked for compatibility with the normal distribution using the Shapiro–Wilk test. We tested the homogeneity of variance using Levene's test. For comparison of variables with a normal distribution, parametric tests with a separate variance assessment were used. For comparative analysis of variables with distribution deviated from the normal distribution, nonparametric Mann–Whitney U test was used. We performed the correlation analysis using the Pearson's test or Spearman's rank correlation test – according to the distribution of the variables studied.

Results

Table 1 presents the characteristics of the entire study group of children with renal cysts and the derived subgroups (ADPKD and non-ADPKD, number of cysts and gender) and the control group. The average age of children and anthropometric parameters did not differ in comparison with the group with renal cysts and control group. We showed significantly higher values of SBP, DBP and mean arterial pressure (MAP), as well as SBP and DBP

Table 1. Characteristics of examined children with renal cysts and controls

Parameter	Children with kidney cysts							Control group (n = 20)
	whole group (n = 39)	ADPKD (n = 20	non-ADPKD (n = 19)	single cysts (n = 29)	multiple cysts (n = 10)	girls (n = 23)	boys (n = 16)	
Age [years]	10.9 ±4.9 (1.9–19.8)	10.9 ±5.1 (3.4–19.8)	11.0 ±5.0 (1.9–18.7)	10.5 ±4.9 (1.9–19.8)	12.3 ±5.2 (5.6–18.9)	10.8 ±4.6 (3.4–18.7)	11.1 ±5.6 (1.9–19.8)	8.8 ±3.9 (1.8–17.2)
Height [cm]	142.3 ±24.9 (80.0–184.5)	141.7 ±26.0 (97.0–184.5)	142.9 ±24.3 (80–176)	140.0 ±25.7 (80.0–184.5)	148.8 ±22.2 (115–176)	142.1 ±22.5 (97–173)	142.5 ±28.7 (80.0–184.5)	130.8 ±22.7 (82–172)
SDS for height	−0.03 ±1.12 (−2.97–2.24)	−0.05 ±1.00 (−2.97–1.80)	−0.02 ±1.2 (−1.9–2.2)	−0.16 ±1.20 (−2.97–1.80)	0.3 ±1.0 (−1.0–2.2)	0.2 ±1.2 (−2.97–1.81)	−0.3 ±1.0 (−1.9–2.2)	−0.4 ±0.9 (−1.9–2.0)
Body weight [kg]	40.7 ±17.8 (11–78)	41.7 ±19.8 (13–78)	39.6 ±16.0 (11–69)	38.5 ±17.3 (11–70)	47.2 ±18.7 (21–78)	40.5 ±17.6 (13–78)	41.0 ±18.8 (11–70)	33.0 ±16.1 (9.7–63.0)
SDS for BW	0.13 ±1.09 (−3.20–2.07)	0.2 ±1.2 (−3.2–1.9)	0.05 ±1.0 (−1.3–2.1)	−0.04 ±1.00 (−3.2–1.7)	0.6 ±1.1 (−1.4–2.1)	0.2 ±1.2 (−3.20–1.91)	−0.06 ±1.0 (−1.30–2.07)	−0.003 ±1.000 (−1.6–1.8)
BMI [kg/m^2]	18.90 ±3.29 (13.5–28.7)	19.3 ±4.0 (13.5–28.7)	18.4 ±2.4 (14.4–22.3)	18.3 ±2.9 (13.5–25.0)	20.4 ±4.0 (13.9–28.7)	18.9 ±3.7 (13.5–28.7)	18.9 ±2.7 (14.8–23.4)	18.0 ±3.4 (14.2–26.6)
SDS for BMI	0.23 ±0.93 (−1.38–2.02)	0.3 ±1.1 (−1.40–2.02)	0.2 ±0.8 (−1.3–1.7)	0.1 ±0.8 (−1.4–1.8)	0.6 ±1.2 (−1.2–2.0)	0.3 ±1.0 (−1.38–2.02)	0.2 ±0.9 (−1.3–1.7)	0.7 ±2.1 (−1.5–8.8)
SBP	109.8 ±13.3 (90–137)	111.6 ±14.0 (90–137)	107.9 ±12.6 (90–130)	106.4 ±12.0[a] (90–130)	119.5 ±12.7 (90–137)	111.4 ±13.3 (90–137)	107.4 ±13.4 (90–130)	
DBP	64.9 ±8.9 (45–84)	66.7 ±10.5 (45–84)	63.1 ±6.8 (55–75)	62.3 ±7.1[a] (45–75)	72.7 ±9.6 (55–84)	66.5 ±9.2 (50–84)	62.8 ±8.3 (45–77)	
MAP	79.9 ±9.8 (61.7–98.3)	81.7 ±11.1 (61.7–98.3)	78.0 ±8.2 (66.7–93.3)	77.0 ±8.1[a] (61.7–93.3)	88.3 ±9.8 (73.3–98.3)	81.5 ±10.0 (63.3–98.3)	77.7 ±9.3 (61.7–93.3)	
SDS for SBP	0.58 ±1.00 (−1.22–2.63)	0.8 ±1.1 (−0.8–2.6)	0.4 ±0.9 (−1.2–1.6)	0.34 ±0.9[a] (−1.2–2.6)	1.2 ±09 (−0.6–2.2)	0.8 ±1.0 (−0.84–2.63)	0.3 ±0.9 (−1.2–1.8)	
SDS for DBP	0.39 ±0.70 (−0.95–2.07)	0.5 ±0.8 (−0.9–2.07)	0.2 ±0.7 (−0.8–2.0)	0.2 ±0.7[a] (−0.9–2.0)	0.9 ±0.6 (−0.2–2.1)	0.5 ±0.7 (−0.6–2.07)	0.2 ±0.8 (−0.9–2.0)	

Data is presented as: mean ± standard deviation (SD) (minimum–maximum); [a] $p < 0.05$ children with single cysts vs children with multiple cysts; BW SDS – SDS body weight, BMI – body mass index; SBP – systolic blood pressure, DBP – diastolic blood pressure, MAP – mean arterial pressure; ADPKD – autosomal dominant polycystic kidney disease.

Table 2. Laboratory tests and eGFR value in children with renal cysts

Parameter	Whole group (n = 39)	ADPKD (n = 20)	Non–ADPKD (n = 19)	Single cysts (n = 29)	Multiple cysts (n = 10)	Girls (n = 23)	Boys (n = 16)
Na [mmol/L]	140.1 ±2.2 (134–143)	140.0 ±2.5 (134–143)	140.2 ±1.7 (136–143)	140.2 ±1.8 (136–143)	139.9 ±3.1 (134–143)	140.3 ±1.7 (136–143)	139.8 ±2.8 (134–143)
Creatinine [umol/L]	48.0 ±15.6 (22–77)	48.3 ±17.5 (22–77)	47.8 ±13.7 (29–73)	47.6 ±14.9 (22–77)	49.4 ±18.1 (24–76)	45.8 ±13.7 (22–69)	51.25 ±17.90 (27–77)
Uric acid [umol/L]	266.2 ±67.8 (134–370)	267.4 ±66.5 (150–368)	264.9 ±71.0 (134–370)	276.6 ±69.0 (134–370)	235.7 ±56.7 (150–347)	253.4 ±65.0 (134–351)	284.4 ±69.7 (151–370)
Urea [mmol/L]	4.3 ±1.3 (2.4–6.8)	4.4 ±1.4 (2.4–6.8)	4.2 ±1.2 (2.5–6.1)	4.4 ±1.2 (2.4–6.8)	4.0 ±1.4 (2.5–6.6)	4.16 ±1.25 (2.4–6.6)	4.4 ±1.3 (2.5–6.8)
eGFR [mL/min/1.73 m^2]	119.8 ±32.7 (38.2–179.3)	121.5 ±35.0 (38.2–176.0)	117.9 ±30.8 (47.8–179.3)	115.1 ±35.2 (38.2–179.3)	133.3 ±19.9 (103–162)	115.90 ±28.25 (38.2–156.2)	125.3 ±38.5 (47.8–179.3)

Data is presented as: mean ± standard deviation (SD) (minimum–maximum). For all comparisons $p > 0.05$. eGFR – estimated glomerular filtration rate; ADPKD – autosomal dominant polycystic kidney disease.

SDS in a subgroup of children with multiple cysts compared to subgroups of subjects with single cysts. The results of laboratory tests in the study group and in separate subgroups are presented in Table 2.

The mean values of basic laboratory tests in the group of ADPKD and non-ADPKD children as well as single and multiple cysts did not differ significantly. The mean value of eGFR in the study group was 119.8 ±32.7 mL/min/1.73 m^2; in 5 children in the group with cystic kidney disease the value of eGFR was reduced. Moreover, in 4 children in the study group, we diagnosed hypertension (all of them belonged to the ADPKD subgroup).

The concentrations of the tested markers (L-FABP, IL-6) in serum and urine in children from the study and control groups are presented in Table 3. The concentration of L-FABP and IL-6 in serum and urine was significantly higher in children with cystic kidney disease compared to the healthy children. In contrast, serum and urinary

Table 3. Concentration of the examined parameters in serum and in urine in children with kidney cysts (divided into subgroups) and in controls

Parameter	Children with kidney cysts							Control group (n = 20)
	whole group (n = 39)	ADPKD (n = 20)	non-ADPKD (n = 19)	girls (n = 23)	boys (n = 16)	single cysts (n = 29)	multiple cysts (n = 10)	
L-FABP (S) [ng/mL]	70.2 ±17.1* (44.3–100.1)	68.5 ±17.3 (44.3–96.5)	71.9 ±17.3 (46.8–100.0)	69,0 ±15.8 (45.8–95.7)	71.9 ±19.3 (44.3–100.0)	72.9 ±17.3 (44.3–100.0)	62.1 ±14.7 (45.8–96.5)	2.6 ±0.77 (1.1–3.7)
L-FABP (U) [ng/mL]	12.2 ±4.1* (4.7–19.6)	11.0 ±3.3 (4.7–16.4)	13.5 ±4.5 (5.8–19.5)	11.9 ±4.1 (5.8–19.6)	12.6 ±4.2 (4.7–18.8)	13.3 ±4.0 (4.7–19.6)	9.1 ±2.5 (5.9–14.6)	2.76 ±0.6 (1.86–4.10)
L-FABP (S)/BMI	3.8 ±1.1* (2.1–6.7)	3.63 ±0.90 (2.1–5.8)	4.0 ±1.3 (2.5–6.7)	3.8 ±1.1 (2.1–6.5)	3.9 ±1.2 (2.6–6.7)	4.0 ±1.2 (2.5–6.7)	3.1 ±0.8 (2.1–4.8)	0.15 ±0.06 (0.06–0.26)
L-FABP/creat (U)	64.7 ±24.7 (14.6–123.1)	59.8 ±22.4 (14.6–92.1)	69.8 ±26.5 (23.9–123.0)	64.3 ±23.3 (16.8–108.7)	65.2 ±27.3 (14.6–123.0)	68.3 ±24.2 (14.6–123)	54.1 ±24.1 (16.8–92.1)	
IL-6 (S) [ng/mL]	23.4 ±4.6* (11.3–33.7)	23.3 ±5.3 (11.3–31.8)	23.5 ±3.9 (18.8–33.7)	22.0 ±4.0 (11.3–30.2)	25.4 ±4.8 (17.3–33.7)	23.9 ±4.3 (17.9–33.7)	22.1 ±5.5 (11.3–30.2)	7.4 ±1.4 (4.8–9.6)
IL-6 (U) [ng/mL]	90.3 ±15.7* (63.8–135.7)	93.5 ±18.4 (63.8–135.7)	86.9 ±11.8 (69.9–114.8)	85.6 ±12.4 (63.8–116.1)	97.0 ±17.9 (69.9–135.7)	90.0 ±15.4 (63.8–135.7)	91.0 ±17.2 (69.8–123.0)	36.9 ±12.3 (18.6–55.7)
IL-6 (S)/BMI	1.3 ±0.4* (0.7–2.2)	1.3 ±0.4 (0.7–2.2)	1.3 ±0.3 (0.8–2.0)	1.2 ±0.4 (0.7–2.2)	1.4 ±0.4 (0.8–2.0)	1.3 ±0.3 (0.8–2.0)	1.1 ±0.4 (0.7–2.2)	0.42 ±0.1 (0.3–0.6)
IL-6/creat (U)	477.9 ±157.6 (246.0–997.7)	504.5 ±186.1 (246.0–997.7)	450 ±119.4 (325–774)	460.7 ±112.6 (246.6–773.9)	502.7 ±207.8 (300.0–997.7)	460.6 ±142.1 (300–932)	528.1 ±195.5 (246.6–997.7)	

Data is presented as: mean ± standard deviation (SD) (minimum–maximum); p *, $p < 0.05$ the whole group of children with kidney cystic disease vs control group; L-FABP – liver fatty acid binding protein; IL-6 – interleukin 6; S – serum; U – urine; ADPKD – autosomal dominant polycystic kidney disease; BMI – body mass index.

Table 4. Analysis of correlation between blood pressure, eGFR values and the tested markers concentration

Parameter	Children with kidney cysts – whole group
SBP [mm Hg]	serum IL-6 r = –0.485, $p < 0.01$
DBP [mm Hg]	serum IL-6 r = –0.425, $p < 0.01$
MAP [mm Hg]	serum IL-6 r = –0.477, $p < 0.01$
SBP SDS	serum IL-6 r = –0.565, $p < 0.0001$ urine IL-6 r = –0.452, $p < 0.01$
DBP SDS	serum L-FABP r = –0.356, $p < 0.05$ serum IL-6 r = –0.417, $p < 0.01$ urine IL-6 r = –0.379, $p < 0.05$
eGFR [mL/min/1.73 m^2]	urine IL-6 r = 0.400, $p < 0.05$

SBP – systolic blood pressure; DBP – diastolic blood pressure; MAP – mean arterial pressure; L-FABP – liver fatty acid binding protein; IL-6 – interleukin 6; eGFR – estimated glomerular filtration rate.

concentrations of L-FABP and IL-6 in individual subgroups of children with renal cysts were comparable.

When analyzing the correlation of L-FABP and IL-6 concentrations in both serum and urine, and anthropometric measurements, we did not show any significant relationships in the whole group of children with renal cysts.

We showed a significant negative correlation between serum L-FABP concentration and SDS for DBP in the whole study group (Table 4). In children with cystic kidney disease, we observed a significant negative correlation between IL-6 serum concentration and absolute values and SDS for SBP, DBP and MAP. There was also a significant negative correlation between urinary IL-6 concentration and SDS for SBP and DBP. In addition, a significant positive correlation was found between urinary IL-6 concentration and eGFR. Similar correlations were observed in the study group by analyzing the correlation of IL-6 with body mass index (BMI) (data not shown). However, in the whole group with cystic renal changes, we found a negative correlation between L-FABP/BMI ratio and SBP ($r = -0.460$, $p < 0.01$), DBP ($r = -0.378$, $p < 0.05$), MAP ($r = -437$, $p < 0.01$), SDS for SBP ($r = -0.373$, $p < 0.05$), and eGFR ($r = -0.398$, $p < 0.05$), and positive correlation between L-FABP/BMI ratio and serum urea concentration ($r = 0.343$, $p < 0.05$). We also analyzed correlations occurring in subgroups, divided into ADPKD and non-ADPKD (Table 5). We have demonstrated in children with ADPKD a positive correlation between serum L-FABP concentration and serum creatinine concentration and serum uric acid concentration. In addition, in children with ADPKD, we found a positive correlation between the excretion of L-FABP in the urine and the concentration of serum uric acid. In children from the non-ADPKD subgroup, we found a negative correlation between serum L-FABP concentration, SDS for BMI and SDS for DBP and DBP absolute values. In the whole study group with renal cysts, we found a negative correlation between L-FABP/BMI ratio and SBP ($r = -0.460$, $p < 0.005$), DBP ($r = -0.378$, $p < 0.02$), MAP ($r = -0.437$, $p < 0.005$), SDS for SBP ($r = -0.377$, $p < 0.02$), and eGFR ($r = -0.398$, $p < 0.02$), and a positive correlation between L-FABP/BMI ratio and serum urea ($r = 0.343$, $p < 0.05$). However, after normalizing the concentration of L-FABP in urine to the concentration of creatinine, we did not observe the above relationships.

When analyzing the correlation of serum and urine IL-6 concentrations with the results of anthropometric measurements and the IL-6/BMI ratio with BP values, we demonstrated a similar relationship in ADPKD children as in the whole study group, and a significant positive

Table 5. Evaluation of the correlation between the tested markers and biochemical parameters and blood pressure values

Parameter	Children with kidney cysts							
	L-FABP (S)		L-FABP (U)		IL-6 (S)		IL-6 (U)	
	ADPKD	non-ADPKD	ADPKD	non-ADPKD	ADPKD	non-ADPKD	ADPKD	non-ADPKD
SBP	r = −0.038 p = 0.874	r = −0.254 p = 0.294	r = −0.293 p = 0.210	r = −0.092 p = 0.709	r = −0.485 p < 0.05	r = −0.497 p < 0.05	r = −0.245 p = 0.297	r = −0.298 p = 0.216
DBP	r = 0.021 p = 0.930	r = −0.493 p < 0.05	r = −0.186 p = 0.433	r = −0.300 p = 0.212	r = −0.469 p < 0.05	r = −0.350 p = 0.142	r = −0.228 p = 0.333	r = −0.392 p = 0.097
MAP	r = −0.003 p = 0.991	r = −0.404 p = 0.086	r = −0.240 p = 0.307	r = −0.213 p = 0.381	r = −0.500 p < 0.05	r = −0.450 p = 0.053	r = −0.247 p = 0.293	r = −0.370 p = 0.119
SDS for SBP	r = −0.206 p = 0.384	r = −0.393 p = 0.096	r = −0.221 p = 0.349	r = −0.128 p = 0.600	r = −0.556 p < 0.05	r = −0.603 p < 0.01	r = −0.572 p < 0.01	r = −0.417 p = 0.076
SDS for DBP	r = −0.167 p = 0.481	r = −0.570 p < 0.05	r = −0.158 p = 0.505	r = −0.316 p = 0.187	r = −0.505 p < 0.05	r = −0.286 p = 0.235	r = −0.453 p < 0.05	r = −0.445 p = 0.056
Creatinine [umol/L]	r = 0.497 p < 0.05	r = −0.131 p = 0.592	r = 0.237 p = 0.314	r = 0.019 p = 0.939	r = −0.053 p = 0.824	r = −0.324 p = 0.176	r = 0.047 p = 0.844	r = −0.367 p = 0.122
Urea [umol/L]	r = −0.088 p = 0.712	r = 0.340 p = 0.154	r = 0.022 p = 0.925	r = 0.377 p = 0.112	r = 0.259 p = 0.270	r = 0.300 p = 0.212	r = −0.222 p = 0.346	r = 0.132 p = 0.589
Uric acid [mmol/L]	r = 0.572 p < 0.01	r = −0.120 p = 0.624	r = 0.586 p < 0.01	r = 0.086 p = 0.727	r = 0.028 p = 0.907	r = 0.203 p = 0.403	r = 0.084 p = 0.725	r = 0.152 p = 0.535
Na [mmol/L]	r = −0.163 p = 0.493	r = 0.147 p = 0.548	r = −0.331 p = 0.154	r = 0.376 p = 0.112	r = 0.124 p = 0.602	r = −0.020 p = 0.934	r = −0.041 p = 0.865	r = −0.243 p = 0.315
K [mmol/L]	r = −0.100 p = 0.676	r = 0.431 p = 0.065	r = −0.004 p = 0.986	r = 0.435 p = 0.063	r = 0.457 p < 0.05	r = 0.025 p = 0.920	r = 0.078 p = 0.744	r = 0.024 p = 0.923
eGFR [mL/min/1.73 m^2]	r = −0.060 p = 0.802	r = 0.047 p = 0.846	r = −0.284 p = 0.224	r = −0.177 p = 0.469	r = 0.174 p = 0.463	r = 0.240 p = 0.321	r = 0.404 p = 0.077	r = 0.398 p = 0.091

SBP – systolic blood pressure; DBP – diastolic blood pressure; MAP – mean arterial pressure; L-FABP – liver fatty acid binding protein; IL-6 – interleukin 6; S – serum; U – urine; eGFR – estimated glomerular filtration rate; ADPKD – autosomal dominant polycystic kidney disease.

correlation between serum IL-6 concentration and serum potassium concentration. Also in children with ADPKD, we found a negative correlation between urinary IL-6 excretion and SDS for SBP and SDS for DBP and DBP absolute values. In the subgroup with non-ADPKD, we observed only a negative correlation between serum IL-6 concentration and SBP values and SDS for SBP.

In the subgroup of children with single cysts, we observed a significant negative correlation between IL-6 serum concentration and SBP ($r = -0.404$, $p < 0.05$), MAP ($r = -0.368$, $p < 0.05$), and SDS for SBP and SDS for DBP ($r = -0.633$, $p < 0.0001$, $r = -0.381$, $p < 0.05$, respectively). Also, in children with single cysts, we showed a negative correlation between urinary IL-6 excretion and SDS for SBP and SDS for DBP ($r = -0.528$, $p < 0.01$, $r = -0.523$, $p < 0.01$), and a positive correlation between IL-6 excretion in the urine and eGFR ($r = 0.451$, $p < 0.05$). Similar correlations were observed by analyzing the correlation between IL-6 and BMI (data not shown). However, we observed a significant positive correlation between IL-6/creatinine ratio and the age of the examined children ($r = 0.388$, $p < 0.05$), height ($r = 0.391$, $p < 0.05$) and body weight ($r = 0.387$, $p < 0.05$). In a subgroup with multiple cysts, we observed a significant negative correlation between L-FABP/BMI ratio and SDS for SBP ($r = -0.769$, $p < 0.01$). However, we did not observe similar correlations in the subgroup of children with single cysts. In the subgroup of children with multiple cysts, we observed a negative correlation between serum IL-6 concentration and MAP ($r = -0.642$, $p < 0.05$). We also recorded a significant negative correlation between IL-6 and BMI and SBP ($r = -0.873$, $p < 0.01$), MAP ($r = -0.758$, $p < 0.05$), and serum creatinine ($r = -0.708$, $p < 0.05$).

Discussion

Numerous clinical studies have confirmed the increased urinary excretion of L-FABP in kidney diseases in both children and adults. Many studies indicate the usefulness of the L-FABP assay as a biomarker for kidney disease, and L-FABP has also been shown to be able to relieve the occurrence of kidney damage.[19,22,32] Oxidative stress and damage to the proximal renal tubules due to ischemia lead to increased urinary excretion of L-FABP, as shown by Małyszko et al.[21] This was also confirmed by a meta-analysis carried out by Susantitaphong et al., which concluded that L-FABP provides adequate data to diagnose AKI and predict the necessity of renal replacement therapy and acute mortality.[23]

Khatir et al. evaluated the concentration of L-FABP in the group of adult patients with CKD stage 3–4, from which, however, patients with polycystic kidney disease were excluded. These authors showed that elevated L-FABP

concentration in the urine correlates with the loss of renal function only in the absence of significant albuminuria.[33]

Matsui et al. followed 244 adult CKD patients for 3 years and confirmed that elevated urinary L-FABP concentration was associated with progression to ESRD and the incidence of severe cardiovascular events in these patients.[34] In literature, no one before conducted research on the evaluation of L-FABP in a selected group of children with cystic kidney disease, nor did anyone make comparisons between groups of children with single and multiple renal cysts.

In our study, we showed a higher L-FABP concentration both in serum and in urine in children with cystic kidney disease, regardless of the underlying cysts etiology, which may indicate early damage of the proximal tubules even before the occurrence of renal impairment. McMahon et al. reviewed the usefulness of biomarkers in the diagnosis of kidney disease and indicated that increased urinary L-FABP excretion in patients with CKD correlated with the severity of proteinuria.[22] When analyzing the correlation of serum and urine L-FABP concentrations by subgroup division, we showed a positive correlation between serum L-FABP concentration and serum creatinine and uric acid concentration in ADPKD children, which may indicate that L-FABP may be an early marker of CKD development.

Ichikawa et al. performed a study on experimental animals of the *RAS*-activated mouse model to evaluate the renoprotective effect of renal hL-FABP (human L-FABP). This study suggested that the increased expression of renal hL-FABP, known an antioxidant, together with the suppression of angiotensin II type 1 receptor appearance, blocked the production of pro-inflammatory cytokines and diminished the tubulointerstitial damage.[35] In our previous work in the same group of children with renal cysts, we also demonstrated the activation of intrarenal RAAS.[36] Ichikawa et al. concluded that agents that amplify the expression of renal L-FABP in the proximal tubules might be useful as therapeutic agents in future.[37] In our study, a group of children with cystic kidney disease showed a significant negative correlation between serum L-FABP concentration and SDS for DBP. The above results may indicate the beneficial effect of L-FABP and the contribution of this antioxidant in inhibiting the development of hypertension in children with renal cystic changes. The pilot studies conducted by us also indicate the need for further research in a larger group of children with kidney cysts.

Many clinical trials in adults and children have confirmed the association of elevated IL-6 levels with kidney disease, especially CKD progression. It is believed that the cause of this phenomenon is chronic inflammation in the kidney parenchyma, which is a common feature, characteristic for kidney damage due to various reasons. Determination of serum IL-6 concentration may be useful in predicting the risk of end-stage renal disease.[38] Nakamura et al., similarly to our results, found elevated IL-6 concentration in ADPKD adults, where the mean age of the study group was 57 years. In addition, these authors confirmed that IL-6 levels decreased as a result of the renoprotective treatment with angiotensin converting enzyme inhibitor and/or angiotensin receptor blockade.[39] In our study, we found in children with cystic renal changes significantly higher IL-6 concentration in serum and urine, both in subgroups with ADPKD and non-ADPKD as well as with the division due to the number of cysts and gender, in comparison with healthy children, with no difference between individual subgroups. In addition, we have demonstrated a significant positive correlation between urinary IL-6 concentration and eGFR, which indicates IL-6 contribution in the deterioration of renal function. Menon et al. also showed increased levels of IL-6 in the serum of adolescents and adult patients with ADPKD. In this study, they divided the group of patients into 3 subgroups: ADPKD with normal BP and normal eGFR, ADPKD with hypertension but with normal eGFR and ADPKD with hypertension and reduced eGFR. The highest IL-6 concentrations occurred in the subgroup with ADPKD with hypertension and depressed eGFR.[40] In contrast, Soleimani et al. showed higher levels of L-FABP in urine in patients with ADPKD, but not in serum, compared to the healthy group, which would suggest only the local presence of inflammation in the renal parenchyma.[41] Ma et al. confirmed the association of 572C> GG IL-6 polymorphism with the development of hypertension in the Asian population.[28] However, in our study, we showed a significant negative correlation between the serum IL-6 concentration and absolute values and SDS for SBP and DBP, and the value of MAP. There was also a significant negative correlation between urinary IL-6 concentration and SDS for SBP and DBP. Perhaps this is due to the other polymorphisms of the IL-6 gene in the Polish population. Also, the mechanism of activation via binding of IL-6 to its membrane-bound receptor IL-6R, which is named classic signaling (anti-inflammatory action) or binding via the trans-signaling with pro-inflammatory features, could play a role.[17] These results indicate the need for further studies on a larger group of children with renal cysts to more accurately assess the role of this cytokine in the course of cystic changes in children and its contribution to the pathogenesis of hypertension.

In summary, we can conclude that higher concentrations of L-FABP and IL-6 in both serum and urine in children with various types of kidney cysts indicate the development of chronic inflammatory processes and damage to the renal parenchyma even before the occurrence of other organ damage and hypertension. The L-FABP concentration seems to be a good biomarker for an increased risk of hypertension and kidney damage. A negative correlation of serum IL-6 concentration with BP values requires further studies on a larger number of patients with renal cysts, with the determination of the type of IL-6 gene polymorphism. Both L-FABP and IL-6 appear to be useful biomarkers of CKD.

ORCID iDs

Krzysztof Plesiński https://orcid.org/0000-0002-0783-5620
Piotr Adamczyk https://orcid.org/0000-0001-9557-221X
Elżbieta Świętochowska https://orcid.org/0000-0001-5787-7880
Aurelia Morawiec-Knysak https://orcid.org/0000-0003-4914-6513
Aleksandra Gliwińska https://orcid.org/0000-0002-4473-6840
Wojciech Korlacki https://orcid.org/0000-0002-2632-3567
Maria Szczepańska https://orcid.org/0000-0002-6772-1983

References

1. Osathanondh V, Potter EL. Pathogenesis of polycystic kidneys: Survey of results of microdissection. *Arch Pathol*. 1964;77:510–512.
2. Kim B, King BF, Vrtiska TJ, Irazabal MV, Torres VE, Harris PC. Inherited renal cystic diseases. *Abdom Radiol (NY)*. 2016;41(6):1035–1051.
3. Audrezet MP, Corbiere C, Lebbah S, et al. Comprehensive PKD1 and PKD2 mutation analysis in prenatal autosomal dominant polycystic kidney disease. *J Am Soc Nephrol*. 2016;27(3):722–729.
4. Norman J. Fibrosis and progression of autosomal dominant polycystic kidney disease (ADPKD). *Biochim Biophys Acta*. 2011;1812(10): 1327–1336.
5. Nowak KL, Chonchol M, You Z, Gupta M, Gitomer B. Affected parent sex and severity of autosomal dominant polycystic kidney disease: A retrospective cohort study. *Clin Nephrol*. 2018;89(3):196–204.
6. Ravine D, Gibson RN, Donlan J, Sheffield LJ. An ultrasound renal cyst prevalence survey: Specificity data for inherited renal cystic diseases. *Am J Kidney Dis*. 1993;22(6):803–807.
7. Turco D, Severi S, Mignani R, Aiello V, Magistroni R, Corsi C. Reliability of total renal volume computation in polycystic kidney disease from magnetic resonance imaging. *Acad Radiol*. 2015;22(11):1376–1384.
8. Ravine D, Gibson RN, Walker RG, Sheffield LJ, Kincaid-Smith P, Danks DM. Evaluation of ultrasonographic diagnostics criteria for autosomal dominant polycystic kidney disease 1. *Lancet*. 1994;343(8903): 824–827.
9. Müller RU, Benzing T. Cystic kidney diseases from the adult nephrologist's point of view. *Front Pediatr*. 2018;6:1–8.
10. Simms RJ. Autosomal dominant polycystic kidney disease. *BMJ*. 2016; 352:1–10.
11. Pinto CS, Raman A, Reif GA, et al. Phosphodiesterase isoform regulation of cell proliferation and fluid secretion in autosomal dominant polycystic kidney disease. *J Am Soc Nephrol*. 2016;27(4):1124–1134.
12. Niemczyk M, Pilecki T, Gradzik M, Bujko M, Niemczyk S, Pączek L. Blood pressure and intracranial aneurysms in autosomal dominant polycystic kidney disease. *Kidney Blood Press Res*. 2014;39(6):630–635.
13. Dembowska M, Nieszporek T, Więcek A. Zwyrodnienie wielotorbielowate nerek jako przyczyna nadciśnienia tętniczego. *Terapia*. 2011; 19(7–8):14–18.
14. Schwartz GJ, Munoz A, Schneider MF, et al. New equations to estimate GFR in children with CKD. *J Am Soc Nephrol*. 2009;20(3):629–637.
15. Cornec-Le Gall E, Audrezet MP, Rousseau A, et al. The PROPKD Score: A new algorithm to predict renal survival in autosomal dominant polycystic kidney disease. *J Am Soc Nephrol*. 2016;27(3):942–951.
16. Marlais M, Cuthell O, Langan D, Dudley J, Sinha MD, Winyard PJ. Hypertension in autosomal dominant polycystic kidney disease: A meta-analysis. *Arch Dis Child*. 2016;101(12):1142–1147.
17. Hogan MC, Abebe K, Torres VE, et al. Liver involvement in early autosomal-dominant polycystic kidney disease. *Clin Gastroenterol Hepatol*. 2015;13(1):155–164.
18. Glatz JF, Van der Vusse GJ. Cellular fatty acid-binding proteins: Their function and physiological significance. *Prog Lipid Res*. 1996;35(3): 243–282.
19. Xu Y, Xie Y, Shao X, Ni Z, Mou S. L-FABP: A novel biomarker of kidney disease. *Clin Chim Acta*. 2015;445:85–90.
20. Smathers RL, Petersen DR. The human fatty acid-binding protein family: Divergences and functions. *Hum Genom*. 2011;5(3):170–191.
21. Małyszko J, Bachorzewska-Gajewska H, Dobrzycki S. Biomarkers of contrast-induced nephropathy: Which ones and what is their clinical relevance? *Interv Cardiol Clin*. 2014;3(3):379–391.
22. McMahon GM, Waikar SS. Biomarkers in nephrology: Core Curriculum 2013. *Am J Kidney Dis*. 2013;62(1):165–178.
23. Susantitaphong P, Siribamrungwong M, Doi K, Noiri E, Terrin N, Jaber BL. Performance of urinary liver-type fatty acid-binding protein in acute kidney injury: A meta-analysis. *Am J Kidney Dis*. 2013;61(3): 430–439.
24. Schaper F, Rose-John S. Interleukin 6: Biology, signaling and strategies of blockade. *Cytokine Growth Factor Rev*. 2015;26(5):475–487.
25. Wolf J, Rose-John S, Garbers C. Interleukin-6 and its receptors: A highly regulated and dynamic system. *Cytokine*. 2014;70(1):11–20.
26. Tanaka T, Kishimoto T. The biology and medical implications of interleukin 6. *Cancer Immunol Res*. 2014;2(4):288–294.
27. Chiesa C, Pacifico L, Natale F, Hofer N, Osborn JF, Resch B. Fetal and early neonatal interleukin 6 response. *Cytokine*. 2015;76(1):1–12.
28. Ma H, Sun G, Wang W, et al. Association between interleukin-6 -572 C> G and -174- G> C polymorphisms and hypertension: A meta-analysis of case-control studies. *Medicine*. 2016;95(2):e2416. doi: 10.1097/MD.0000000000002416
29. Litwin M. Nadciśnienie tętnicze pierwotne u dzieci i młodzieży – patofizjologia. [In:]. Litwin M, Januszewicz A, Prejbisz A. ed. *Nadciśnienie tętnicze u młodzieży i młodych dorosłych. Zapobieganie, diagnostyka i leczenie*. Kraków, Poland: Medycyna Praktyczna; 2011:289–315.
30. Kułaga Z, Litwin M, Grajda A, Gurzkowska B, Napieralska E, Kułaga K. Rozkłady wartości ciśnienia krwi w populacji referencyjnej dzieci i młodzieży w wieku szkolnym. Standardy medyczne. *Pediatria*. 2010; 7:100–111.
31. Kułaga Z, Rożdżyńska A, Palczewska I, Grajda A, Gurzkowska B, Napieralska E. Siatki centylowe wysokości, masy ciała i wskaźnika masy ciała dzieci i młodzieży w Polsce – wyniki badania OLAF. Standardy medyczne. *Pediatria*. 2010;7:690–700.
32. Sato R, Suzuki Y, Takahashi G, Kojika M, Inoue Y, Endo S. A newly developed kit for the measurement of urinary liver-type fatty acid-binding protein as a biomarker for acute kidney injury in patients with critical care. *J Infect Chemother*. 2015;21(3):165–169.
33. Khatir DS, Bendtsen MD, Birn H, et al. Urine liver fatty acid binding protein and chronic kidney disease progression. *Scand J Clin Lab Invest*. 2017;77(7):549–554.
34. Matsui K, Kamijo-Ikemori A, Imai N, et al. Clinical significance of urinary liver-type fatty acid-binding protein as a predictor of ESRD and CVD in patients with CKD. *Clin Exp Nephrol*. 2016;20(2):195–203.
35. Ichikawa D, Kamijo-Ikemori A, Sugaya T, et al. Renoprotective effect of renal liver-type fatty acid binding protein and angiotensin II type 1a receptor loss in renal injury caused by RAS activation. *Am J Physiol Renal Physiol*. 2014;306(6):F655–F663.
36. Plesiński K, Adamczyk P, Świętochowska E, et al. Angiotensinogen and interleukin 18 in serum and urine of children with kidney cysts. *J Renin Angiotensin Aldosterone Syst*. 2019;20(3):1470320319862662. doi:10.1177/1470320319862662
37. Ichikawa D, Kamijo-Ikemori A, Sugaya T, et al. Renal liver-type fatty acid binding protein attenuates angiotensin II-induced renal injury. *Hypertension*. 2012;60(4):973–980.
38. Jones SA, Fraser DJ, Fielding CA, Jones GW. Interleukin 6 in renal disease and therapy. *Nephrol Dial Transplant*. 2015;30(4):564–574.
39. Nakamura T, Sato E, Fujiwara N, et al. Changes in urinary albumin excretion, inflammatory and oxidative stress markers in ADPKD patients with hypertension. *Am J Med Sci*. 2012;343(1):46–51.
40. Menon V, Rudym D, Chandra P, Miskulin D, Perrone R, Sarnak M. Inflammation, oxidative stress, and insulin resistance in polycystic kidney disease. *Clin J Am Soc Nephrol*. 2011;6(1):7–13.
41. Soleimani A, Adabavazeh R, Nikoueinejad H, Sharif MR, Faraji S, Shahreza BO. T helper 17 lymphocyte pathway in the diagnosis of autosomal dominant polycystic kidney disease. *Iran J Kidney Dis*. 2015;9(2):105–112.

Effects of ozone preconditioning on recovery of rat colon anastomosis after preoperative radiotherapy

İlhan Taşdöven[1,A–F], Ali Uğur Emre[2,B,C,E], Fatma Ayça Gültekin[2,A–C], Muzaffer Önder Öner[3,B,C], Bekir Hakan Bakkal[4,B,C], Ümmühani Özel Türkcü[5,C,E,F], Banu Doğan Gün[6,C], Gülin Ergun Taşdöven[6,D–F]

[1] Department of General Surgery, Van Training and Research Hospital, Turkey
[2] Department of General Surgery, Bülent Ecevit University, Zonguldak, Turkey
[3] Department of Radiation Oncology, Bülent Ecevit University, Zonguldak, Turkey
[4] Department of Medical Biochemistry, Faculty of Medicine, Muğla Sıtkı Koçman University, Turkey
[5] Department of Pathology, Bülent Ecevit University, Zonguldak, Turkey
[6] Department of Otolaryngology, Van Training and Research Hospital, Turkey

A – research concept and design; B – collection and/or assembly of data; C – data analysis and interpretation; D – writing the article; E – critical revision of the article; F – final approval of the article

Advances in Clinical and Experimental Medicine, ISSN 1899–5276 (print), ISSN 2451–2680 (online) *Adv Clin Exp Med*. 2019;28(12):1683–1689

Address for correspondence
İlhan Taşdöven
E-mail: ilhantasdoven1@gmail.com

Funding sources
None declared

Conflict of interest
None declared

Received on April 24, 2017
Reviewed on August 7, 2017
Accepted on June 27, 2019

Abstract

Background. Anastomotic leakage is a devastating complication of colorectal surgery. Neoadjuvant radiotherapy for colorectal cancer can affect the mechanical and biochemical parameters of anastomotic healing. It has been reported that ozone increases antioxidant enzyme activity and stimulates adaptive processes to oppose the pathophysiologic conditions mediated by reactive oxygen species (ROS).

Objectives. The objective of this study was to investigate the effect of controlled administration of ozone on the healing of anastomosis and the activation of antioxidant enzymes in the colon after radiotherapy.

Material and methods. Rats (n = 48) were randomly assigned to the following groups: control groups (1 and 2), saline-treated and irradiated (IR) groups (3 and 4) and ozone oxidative preconditioning (OOP) and IR groups (5 and 6). Rats were exposed to whole-body IR (6 Gy) after pretreatment with either saline or ozone. Rats in groups 1, 3 and 5 were euthanized on postoperative day 3, whereas those in groups 2, 4 and 6 were euthanized on postoperative day 7. The anastomoses were performed on day 7 post-IR. The anastomotic segment was resected to measure hydroxyproline (HPO) content, myeloperoxidase (MPO) activity and malondialdehyde (MDA) concentration and for histopathological evaluation.

Results. The mean bursting pressure of the groups that underwent radiotherapy was lower than that of the control groups ($p < 0.001$). In groups 5 and 6, the tissue HPO concentrations were higher than those in groups 3 and 4. Although mean values for MPO activity in groups 5 and 6 were higher than those in groups 3 and 4, the differences were not significant. Regarding oxidative damage markers, MDA concentrations were significantly lower in group 5 than those in group 3.

Conclusions. In this experimental model, OOP exerted favorable effects on colon anastomotic healing after radiation exposure.

Key words: colon anastomosis, ozone oxidative preconditioning, radiotherapy, anastomotic leakage

Cite as
Taşdöven İ, Emre AU, Gültekin FA, et al. Effects of ozone preconditioning on recovery of rat colon anastomosis after preoperative radiotherapy. *Adv Clin Exp Med*. 2019;28(12):1683–1689. doi:10.17219/acem/110329

DOI
10.17219/acem/110329

Introduction

Anastomotic leakage after colorectal surgery is a dreaded complication, as it greatly increases morbidity and mortality and has been associated with high local recurrence and diminished survival after colorectal cancer surgery.[1] Preoperative radiotherapy is being successfully used as an adjuvant in rectal cancer therapy, but the ionized beams used in radiotherapy can potentially damage organs by increasing the cellular oxidative stress as a result of molecular ionization, leading to the overproduction of reactive oxygen species (ROS).[2,3] Ozone (O_3) therapy is widely used in medicine for its antioxidant, anti-inflammatory and antimicrobial effects.[4] The therapeutic effect of O_3 particularly targets reactive oxygen products, hydrogen peroxide and lipid oxidation products (LOPs).[5] Thus, it has been hypothesized that O_3 is effective in preventing ischemia–reperfusion damage and has been used as a therapeutic option in ischemia–reperfusion studies.[6,7] The term 'O_3 oxidative preconditioning' (OOP) implies the triggering of an adaptation to oxidative stress through the application of O_3 at repeated non-toxic doses. The claimed efficacy of OOP therapy in preventing ischemia–reperfusion damage in various organs, such as the liver, heart and kidneys, has been demonstrated in experimental studies.[6–8] We aimed to determine whether the antioxidant capacity of the O_3 applied would ameliorate any damage after radiotherapy as well as suppress the anti-inflammatory process at the anastomotic site and to obtain histopathological evidence of this effect.

Material and methods

This experimental study was conducted after receiving approval from the Animal Research Committee in the Bülent Ecevit University (Zonguldak, Turkey). All animals were handled in accordance with the recommendations of the National Institute of Health Guidelines for the Care and Use of Laboratory Animals (Ankara, Turkey).

Animals and groups

Forty-eight female Wistar albino rats aged 10–12 weeks and weighing 200–250 g were fed with standard rat feed and fresh potable water ad libitum throughout the study period. They were kept under constant environmental conditions at an average temperature of 21 ±1°C and humidity of 50–60% in transparent plastic cages lined with wood shavings. The rats were randomized in a blinded manner to 6 groups comprising 8 rats each.

In control groups (groups 1 and 2), rats were administered 0.5 mL of intraperitoneal saline for 5 consecutive days. After the administration of the final dose, left colon anastomosis was performed on the rats. On days 3 and 7 following the anastomosis procedure, the rats in group 1 and 2 were euthanized.

In saline-treated and irradiated (IR) groups (groups 3 and 4), rats were administered 0.5 mL of intraperitoneal saline for 5 consecutive days. A single-dose pelvic IR with 500 cGy was performed 1 h after the final dose was administered. On day 7 post-IR, left colon anastomosis was performed. After the procedure, the rats were euthanized on day 3 (group 3) and day 7 (group 4).

OOP and IR groups (groups 5 and 6)

An intraperitoneal injection containing a mixture of 0.7 mg/kg of O_2/O_3 gas was administered each day for 5 consecutive days. A single-dose pelvic IR with 500 cGy was performed 1 h after the final dose was administered. On day 7 post-IR, left colon anastomosis was performed. The rats were euthanized on day 3 (group 5) and day 7 (group 6) after the procedure. The presence/absence of any complications related to the wounded area in rats and any intra-abdominal abscess, anastomotic leakage or stenosis was also noted. Evaluations of the bursting (blast) pressure and hydroxyproline (HPO) concentration during the anastomosis as well as those of the histopathological and biochemical aspects were performed. During the biochemical examination, malondialdehyde (MDA), myeloperoxidase (MPO) and superoxide dismutase (SOD) concentrations were examined as the oxidative markers in the tissue.

Surgical procedure

No bowel preparation was preoperatively applied to the rats. To induce dissociative anesthesia, 80 mg/kg of ketamine HCl (Ketalar® vial; Eczacıbaşı Pharmaceutical Industry and Trade Inc., Lüleburgaz, Turkey) and 10 mg/kg of xylazine HCl (Rompun® 2%; Bayer, Leverkusen, Germany) were intramuscularly injected into each rat. The laparotomy procedure was performed through a 4-centimeter standard mid-line incision. Left colon is transected with a scalpel to perform an anastomosis. Vascular supply of colonic edges is preserved. Colonic contents were cleaned up 2 cm proximally and distally using the stripping method. To minimize the effect of the suturing material on anastomotic healing, 6/0 non-absorbable monofilament round-needle polypropylene sutures were used. An edge-to-edge anastomosis procedure was performed, with approx. 6–8 pieces of primary interrupted sutures.

O_3 production

Ozone was generated by an O_3 generator (Bozon N; Econica, Odessa, Ukraine), allowing control of the gas flow rate and O_3 concentration in real time, using a built-in ultraviolet spectrometer; it was immediately administered at a dose of 1.2 mg/kg daily via an intraperitoneal route. The volume of the injected mixture was approx. 1 mL.

The OOP was performed with 5 applications (once daily) of the O_3/O_2 mixture. The O_3 flow rate was kept constant at 3 L/min, representing a concentration of 60 mg/mL and a gas mixture of 97% O_2 + 3% O_3. Tygon polymer tubes and single-use silicon-treated polypropylene syringes (O_3 resistant) were used throughout the experiment to ensure containment of O_3 and consistency of concentration.[9]

Euthanasia

Groups 1, 3 and 5 were euthanized on postoperative day 3, while groups 2, 4 and 6 were euthanized on postoperative day 7 using the intra-cardiac blood collection method. After the bursting (blast) pressure was measured, the colon segment was resected, including 2 cm of the proximal and 2 cm of the distal part of the anastomotic line. Then, it was divided into 2 equal parts vertically passing through the middle of the anastomosis. For the histopathological examination, a section of tissue, including the anastomosis, was placed in 10% formaldehyde solution. Another section was frozen at –80°C for measuring HPO, MPO, SOD, and MDA concentrations.

Measurement of the bursting (blast) pressure

To measure the bursting pressure, an infusion pump (Infusion pump Hospira Plum A+; Abbott, Irving, USA), a pressure transducer (Transpac IV, Abbott) and a monitor (Petas KMA 460-R; Petas, Ankara, Turkey) were provided. The proximal end of the anastomosis was transected, and the fecal content within (if any) was removed. A 6-Fr catheter that was connected to the monitor along with the pressure transducer was placed within the anastomosis. To avoid any air or fluid leakage, the catheter was fixed with a 2/0 silk suture, and a closed system was established. Fluid was transferred from the catheter placed in the proximal part of the colon by means of a perfusion pump at a speed of 50 mL/h, and the pressure was tracked on the monitor. Fluid leakage or a sudden decline in pressure in the course of the blast at the anastomosis site was determined, and the monitor indicator at that moment was recorded as the bursting (blast) pressure of anastomosis.

Radiation procedure

A single pelvic IR with 500 cGy was applied to the rats while they were in the prone position by a masked investigator. A computed tomography (CT) simulation of a rat anatomy was performed in 1-millimeter slices, and a dose calculation was performed with the help of Eclipse Treatment Planning System v. 8.9 (Varian Medical Systems, Palo Alto, USA). The animals were brought back to their cages in the post-IR period. The animals in the group 1 and 2. were anesthetized but not exposed to radiation.

Biochemical examinations

Biochemical analyses were performed in the Research Laboratory of Nutrition and Dietetics in Muğla Health College, Muğla Sıtkı Koçman University, Turkey. Hydroxyproline concentrations in the tissue were measured according to a modification of the method of Jamall et al.[10] After being weighed, the samples were hydrolyzed with 6 N HCl in an autoclave (Nüve OT4060; Nüve Sanayi Malzemeleri, Izmir, Turkey) at 121°C for 15 min. Twenty-five microliter of hydrolysate were taken and lyophilized and then were dissolved in 1 mL 50% (v/v) isopropyl alcohol. Chloramine-T was added to these samples 10 min later. Then, 1 mL of Ehrlich solution was added, and the samples were incubated at 50°C for 90 min.

Under the same circumstances, 0.4-, 0.8-, 1.2-, and 1.6-microgram L-HPO standards were studied. The color change that occurred during the reaction was spectrophotometrically measured at a 560-nanometer wavelength (PG Instruments T80+; PG Instruments Limited, Leicestershire, UK). Hydroxyproline levels were calculated from a standard curve prepared from L-HPO and expressed as microgram per gram tissue (μg/g tissue).[10,11]

Tissue MDA concentrations was measured in a 96-well microliter plate using an enzyme-linked immunosorbent assay (ELISA) kit (Cusabio Biotech Co., LTD., Newark, USA) according to the manufacturer's guidelines. Tissues were homogenized (Pro-Scientific 200; Pro-Scientific, Oxford, USA) in phosphate-buffered saline (PBS). The homogenates were centrifuged for 5 min at 5,000 × g (Eppendorf 5804R; Eppendorf, Hamburg, Germany). The supernatants were used for the determination of MDA levels. Optical density of each well was measured with a microplate plate reader at 450 nm absorbance (Biorad Model 680 microplate reader; Biorad, Hercules, USA). The sensitivity of the assay was 7.81 pmol/mL and the linear range of the standard was 31.25–2,000 pmol/mL. The intra-assay and inter-assay coefficients of variation were <8% and <10%, respectively. The concentrations of MDA were represented as nanomoles per milligram protein (nmol/mg protein).

Tissue MPO concentrations were measured in a 96-well microliter plate, using an ELISA kit (USCN Life Science, Wuhan, China) according to the manufacturer's guidelines. Tissues were homogenized (Pro-Scientific 200; Pro-Scientific Oxford, USA) in ice-cold PBS. The homogenates were centrifuged for 5 min at 5,000 × g (Eppendorf 5804R). The supernatants were used to determine MPO concentrations. Optical density of each well was measured with a microplate plate reader at 450 nm absorbance (Biorad Model 680 microplate reader). The concentrations of MPO were represented as nanogram per milligram protein (ng/mg protein).

Tissue SOD activity was measured using the spectrophotometric method developed by Sun et al.[12] Tissues were homogenized (Pro-Scientific 200) in PBS were centrifuged for 5 min at 5,000 × g (Eppendorf 5804R). Supernatant were

mixed to equal volume chloroform/ethanol (3:5 ratio) and centrifuged (Eppendorf 5804R) at 5000 × g for 2 h at 4°C. Then, SOD activity and protein levels were measured in supernatants. One unit of SOD was defined as the amount of enzyme causing 50% inhibition of the reduction rate of nitroblue tetrazolium. Superoxide dismutase activity was given as units (U)/mg protein.

Total protein content of tissues was measured using the method of Lowry et al.[13] with BSA as a standard.

Histopathological evaluation

From the tissue samples in 10% formaldehyde solution, paraffin-embedded blocks were prepared and sections of 4–5-micron thickness were stained with hematoxylin and eosin (H&E). The sections were then evaluated under light microscopy (Leica DMLS; Leica Camera AG, Wetzlar, Germany) by a single pathologist in a blinded manner. Mucosal wound recovery was scored according to the scale proposed by Houdart et al.[14] Granulocyte infiltration, mononuclear cell infiltration, fibroblastic proliferation, focal necrosis, and exudate formation pertaining to the anastomotic wound recovery were evaluated and scored according to the modified parameters[14,15] as: 0 – none, 1 – mild, 2 – moderate, and 3 – severe.

Statistical analysis

Statistical analyses were performed using SPSS v. 13.0 (SPSS, Inc., Chicago, USA) statistical software. For continuous variables with the normal distribution, the Shapiro–Wilk test was used, whereas in 3 or more group comparisons of the variables showing non-normal distribution, the Kruskal–Wallis test was used. For group comparisons, the Mann–Whitney U test was used. P-values ≤0.05 were considered statistically significant.

Results

When the groups were evaluated in terms of the bursting pressure, the bursting pressure of the groups that underwent radiotherapy (groups 3–6) was lower than that of the control groups (groups 1 and 2) ($p < 0.001$). The bursting pressures in the group that received OOP prior to IR were significantly higher than those in the groups treated with saline prior to IR ($p < 0.001$). The distribution of the bursting pressure values of anastomosis according to the groups is shown in Fig. 1 and Table 1.

The tissue HPO concentrations in the groups that were treated with saline prior to irradiation were lower than those in the control groups ($p < 0.05$). Conversely, the HPO values of groups 5 and 6 were statistically higher than those of groups 3 and 4 (Fig. 2).

The MDA concentrations of the groups that underwent radiotherapy (groups 3–6) were higher than those of the control groups (groups 1 and 2); however, the difference was statistically significant only in the comparison between group 3 and the control groups ($p = 0.014$). Similarly, although a decrease in the MDA concentrations of groups 5 and 6 was maintained, a statistically significant decline was observed in the MDA concentrations of group 5 ($p = 0.014$) in comparison with those of groups 3 and 4 (Fig. 3).

The MPO concentrations in the groups that underwent radiotherapy (groups 3–6) were lower than those in the control groups (groups 1 and 2). The increase in the MPO concentrations in the group that underwent

Table 1. Distribution of the bursting (blast) pressure and standard deviation (SD). Values of anastomosis by group

Groups	Average bursting (blast) pressure (mm Hg) ±SD	Median	Minimum	Maximum
Group 1	145.38 ±12.716	144.5	123	162
Group 2	149.63 ±37.489	157.5	90	192
Group 3	50.75 ±18.722	52.5	15	75
Group 4	74.13 ±25.737	84.0	40	104
Group 5	86.00 ±19.479	82.5	60	118
Group 6	140.88 ±31.832	142.5	90	185

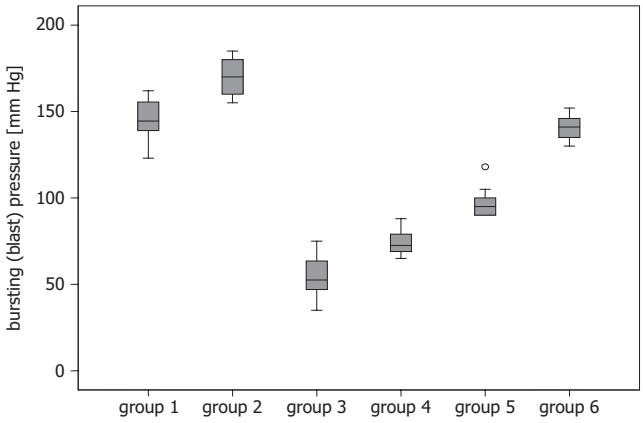

Fig. 1. Distribution of the bursting (blast) pressure values of anastomosis by group

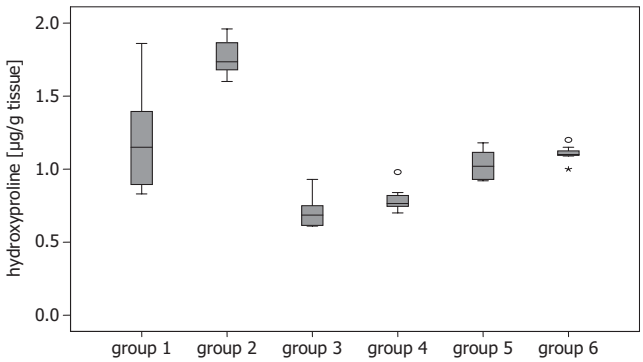

Fig. 2. Hydroxyproline (HPO) concentrations in the anastomotic tissue by group [µg/g tissue]

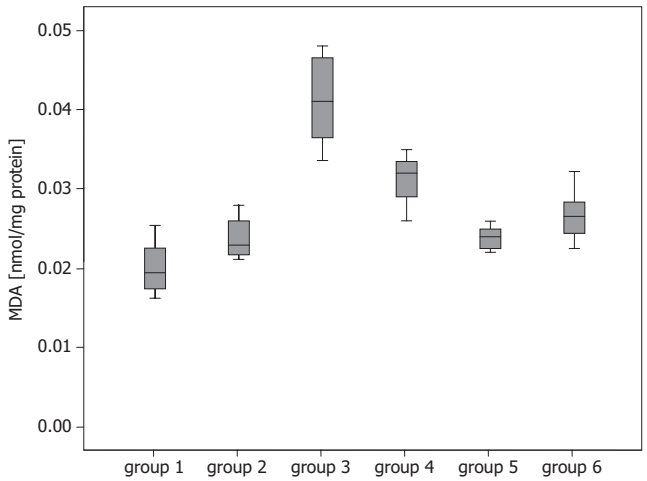

Fig. 3. Malondialdehyde (MDA) levels in the anastomotic tissue by group [nmol/mg protein]

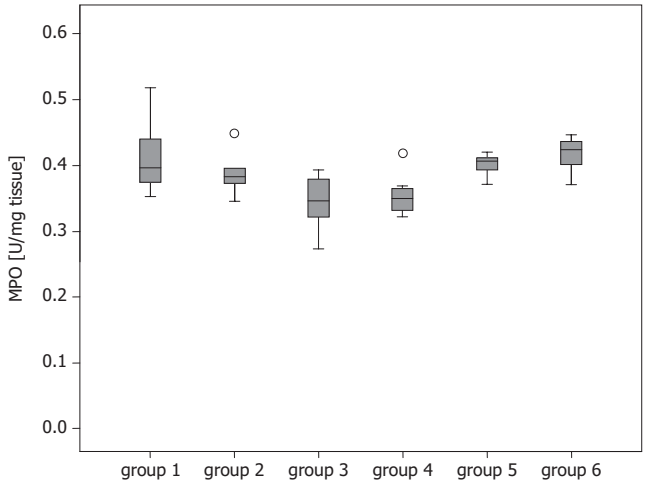

Fig. 4. Myeloperoxidase (MPO) concentrations in the anastomotic tissue by group [ng/mg protein]

OOP (groups 5 and 6) compared with those in the groups treated with saline was only clinically significant. There were no statistically significant differences between the groups (Fig. 4).

The tissue SOD concentrations of groups 3 and 4 were lower than those of groups 1 and 2 ($p < 0.05$). Conversely,

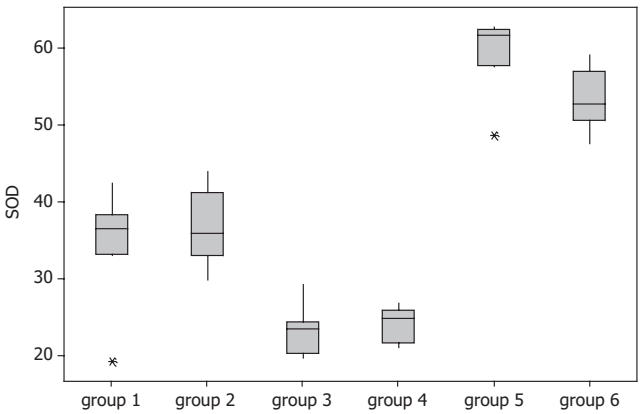

Fig. 5. Superoxide dismutase (SOD) activities in the anastomotic tissue by group [U/mg protein]

the SOD concentrations of groups 5 and 6 were statistically higher than those of groups 3 and 4 ($p < 0.05$) (Fig. 5). Table 2 shows the HPO, MDA, MPO, and SOD concentrations in the anastomotic tissues in control and saline- or O_3-treated irradiated groups euthanized on day 3 or day 7 after IR.

Upon examining the anastomotic wound healing, granulation tissue development and histological changes corresponding to the local inflammatory response of the study groups (scored from 0 to 4), we observed that the inflammatory cell infiltration in all groups was more intense than in the control groups. The fibroblastic proliferation between the groups was similar; however, it was not statistically significant (Table 3).

Discussion

Anastomotic leakage is one of the major and devastating complication of colorectal surgery. The occurrence of postoperative anastomotic leakage can vary between 10% and 20%.[16] Ischemia is regarded as one of the causes of anastomotic leakage. Wound recovery is negatively affected by hypoxia.[17]

Cronin et al. reported that during the measurements of bursting pressure of the anastomosis, the force to be

Table 2. HPO [µg/g], MDA [nmol/g], MPO [nmol/mg], and SOD [U/g] concentrations in the anastomotic tissue by group in control, and saline- or ozone-treated irradiated groups euthanized on day 3 or day 7 after IR. Each group consisted of 6 rats

Oxidative stress markers	Control		IR			
	day 3	day 7	day 3		day 7	
	group 1	group 2	saline-treated group 3	ozone-treated group 5	saline-treated group 4	ozone-treated group 6
HPO [µg/g]	1.071 ±0.241	0.912 ±0.100	0.786 ±0.129	0.942 ±0.165	0.896 ±0.158	1.025 ±0.098
MDA [nmol/mg]	0.021 ±0.111	0.296 ±0.092	0.396 ±0.093	0.442 ±0.076	0.422 ±0.135	0.496 ±0.090
MPO [nmol/mg]	0.357 ±0.111	0.296 ±0.092	0.396 ±0.093	0.442 ±0.076	0.422 ±0.135	0.496 ±0.090
SOD [U/g]	34.66 ±6.86	36.86 ±4.83	23.22 ±3.07	59.36 ±4.75	24.16 ±2.18	53.24 ±3.84

HPO – hydroxyproline; MDA – malondialdehyde; MPO – myeloperoxidase; SOD –superoxide dismutase; IR – irradiation.

Table 3. Histological changes in the anastomotic tissue by group in control, and saline- or ozone-treated irradiated groups euthanized on day 3 or day 7 after irradiation (IR). Each group consisted of 6 rats

	Score	Group 1	Group 2	Group 3	Group 4	Group 5	Group 6
Granulocyte infiltration	0	0	0	1 (12.5%)	2 (25.0%)	4 (50.0%)	3 (37.5%)
	1	3 (37.5%)	4 (50.0%)	4 (50.0%)	5 (62.5%)	4 (50.0%)	5 (62.5%)
	2	1 (12.5%)	3 (37.5%)	2 (25.0%)	1 (12.5%)	0	0
	3	4 (50.0%)	1 (12.5%)	1 (12.5%)	0	0	0
	Score	Group 1	Group 2	Group 3	Group 4	Group 5	Group 6
Mononuclear cell infiltration	0	0	0	2 (25.0%)	1 (12.5%)	0	0
	1	6 (75.0%)	2 (25.0%)	4 (50.0%)	5 (62.5%)	7 (87.5%)	7 (87.5%)
	2	2 (25.0%)	3 (37.5%)	1 (12.5%)	2 (25.0%)	1 (12.5%)	1 (12.5%)
	3	0	3 (37.5%)	1 (12.5%)	0	0	0
	Score	Group 1	Group 2	Group 3	Group 4	Group 5	Group 6
Fibroblastic proliferation	0	0	0	2 (25.0%)	1 (12.5%)	0	0
	1	7 (87.5%)	1 (12.5%)	4 (50.0%)	4 (50.0%)	6 (75.0%)	4 (50.0%)
	2	1 (12.5%)	3 (37.5%)	2 (25.0%)	3 (37.5%)	2 (25.0%)	3 (37.5%)
	3	0	4 (50.0%)	0	0	0	1 (12.5%)
	Score	Group 1	Group 2	Group 3	Group 4	Group 5	Group 6
Focal necrosis	0	8 (100%)	6 (75.0%)	7 (87.5%)	8 (100%)	7 (87.5%)	8 (100%)
	1	0	2 (25.0%)	0	0	1 (12.5%)	0
	2	0	0	1 (12.5%)	0	0	0
	3	0	0	0	0	0	0
	Score	Group 1	Group 2	Group 3	Group 4	Group 5	Group 6
Exudate formation	0	1 (12.5%)	3 (37.5%)	7 (87.5%)	5 (62.5%)	6 (75.0%)	5 (62.5%)
	1	3 (37.5%)	4 (50.0%)	1 (12.5%)	3 (37.5%)	0	2 (25.0%)
	2	1 (12.5%)	0	0	0	2 (25.0%)	1 (12.5%)
	3	3 (37.5%)	1 (12.5%)	0	0	0	0

exerted postoperative day 3 onwards tended to increase until it reached its maximum pressure on days 7–10.[18]

It was shown that there was an increase in the re-infusion of the blood mixed with O_3 and in the nitric oxide (NO) levels, which caused vasodilatation in the ischemic areas, and that oxidative stress was minimized along with decreased hypoxia, SOD activation and decreased glutathione levels.[19,20] It has currently been reported that antioxidant enzymes, NO pathways and other cellular activities could be regulated by low doses of O_3.[21] Controlled administration of O_3 can minimize the damage induced by ROS by maintaining the adaptation to OOP or stress.[20,22] It was reported that O_3 would enhance healing in ischemic and ulcerous wounds by promoting expression, secretion and activation of growth factors from the activated thrombocytes.[23]

Stevens et al. compared the cases of anterior resection performed after radiotherapy with 5,000 rad and a group that did not undergo radiotherapy.[24] They found a significantly higher anastomotic leakage in the radiotherapy group than in the control group; this was consistent with the findings of some other experimental studies reporting negative effect of radiation on anastomotic healing depending on the applied dose and duration.[25–27]

We performed a colon anastomosis on rats on day 7 following the administration of 6 Gy total body IR. During the measurements performed on postoperative days 3 and 7, it was observed that the bursting pressure was lower in the radiotherapy groups than in the control groups ($p < 0.001$). It was also determined that OOP caused an increase in the bursting pressure, which was significantly higher than that in the saline-treated and IR groups ($p < 0.001$). It was observed that the tissue HPO concentration in the saline-treated and IR groups (groups 3 and 4) was low compared with that in the control groups ($p < 0.05$). The HPO concentrations of groups 5 and 6 were significantly higher than those of groups 3 and 4. Along with these findings, we ascertained that a single, low-dose irradiation performed on preoperative day 7 affected the anastomosis recovery in our rat model.

Our findings regarding the low bursting pressure and HPO concentrations in an experimental rodent model suggest that O_3 exposure prior to radiotherapy contributes to a decrease in the incidence of anastomotic leakage after colorectal surgery during the early stage. Although radiotherapy-based damage occurred as the result of oxidative stress, the MDA concentration of group 3 was a significant indicator of oxidative stress among the study groups.

In other groups, the differences in MDA and MPO values were not significant.

Here, OOP caused the bursting pressure and HPO values to increase in rats during the colon anastomosis procedure. The effect of O_3 exposure on the oxidative indicators/markers in the anastomotic tissue was evidenced by a significant decline in MDA concentrations in group 5. In other groups, the differences in MDA and MPO values were not significant.

Our findings reveal that radiation negatively affected recovery after colonic anastomosis surgery and this is concordant with the results of previous reports. Conversely, based on HPO, SOD and MDA measurements and histopathological examinations, we found that OOP had a positive effect on the recovery of anastomoses performed after radiotherapy. These findings in an experimental rodent model suggest that O_3 exposure prior to radiotherapy contributes to a decrease in the incidence of anastomotic leakage after colorectal surgery. However, there is need for further studies to assess the effects and antioxidant capacity of O_3.

References

1. Buchs NC, Gervaz P, Secic M, Bucher P, Mugnier-Konrad B, Morel P. Incidence, consequences, and risk factors for anastomotic dehiscence after colorectal surgery: A prospective monocentric study. *Int J Colorectal Dis*. 2008;23(3):265–270.
2. Mettler FA, Jr, Voelz GL. Major radiation exposure: What to expect and how to respond. *N Engl J Med*. 2002;346(20):1554–1561.
3. Coleman CN, Blakely WF, Fike JR, et al. Molecular and cellular biology of moderate-dose (1–10 Gy) radiation and potential mechanisms of radiation protection: Report of a workshop at Bethesda, Maryland, 17–18 December 2001. *Radiat Res*. 2003;159(6):812–834.
4. Bocci V. Physical-chemical properties of ozone. Natural production of ozone. The toxicology of ozone. In: Bocci V, ed. *Ozone. A New Medical Drug*. Dordrecht, the Netherlands: Springer; 2005:5–8.
5. Bocci V. How does ozone act? How and why can we avoid ozone toxicity? In: Bocci V, ed. *Ozone. A New Medical Drug*. Dordrecht, the Netherlands: Springer; 2005:19–28.
6. Ajamieh HH, Menéndez S, Merino N, Martínez-Sánchez G, Re L, León O. Ischemic and ozone oxidative preconditioning in the protection against hepatic ischemic-reperfusion injury. *Ozone Sci Eng*. 2003;25(3):241–250.
7. Barber E, Menéndez S, Leon OS, et al. Prevention of renal injury after induction of ozone tolerance in rats submitted to warm ischaemia. *Mediators Inflamm*. 1999;8(1):37–41.
8. Berson EL, Remulla JF, Rosner B, Sandberg MA, Weigel-DiFranco C. Evaluation of patients with retinitis pigmentosa receiving electric stimulation, ozonated blood, and ocular surgery in Cuba. *Arch Ophthalmol*. 1996;114(5):560–563.
9. Gultekin FA, Bakkal HB, Guven B, et al. Effects of ozone oxidative preconditioning on radiation-induced organ damage in rats. *J Radiat Res*. 2013;54(1):36–44.
10. Jamall IS, Finelli UN, Que Hee SS. A simple method to determine nanogram levels of 4-hydroxyproline in biological tissues. *Anal Biochem*. 1981;112(1):70–75.
11. Kivirikko KI, Laitinen O, Prockop DJ. Modifications of a specific assay for hydroxyproline in urine. *Anal Biochem*. 1967;19(2):249–255.
12. Sun Y, Oberley LW, Li Y. A Simple method for clinical assay of superoxide dismutase. *Clin Chem*. 1988:34(13):497–500.
13. Lowry OH, Rosebrough NJ, Farr AL, Randall RJ. Protein measurement with the folin phenol reagent. *J Biol Chem*. 1951;193(1):145–157.
14. Houdart, R, Lavergne, A, Galian, A, Hautefeuille, P. Anatomo-pathological evolution of single-layer end-to-end intestinal anastomoses. A study of 210 colonic anastomoses in the rat, from the 2nd to 180th days [in French]. *Gastroenterol Clin Biol*. 1983;7(5):465–473.
15. Kuzu MA, Kuzu J, Köksoy C, Aksoy FH, Uzal D. Histological evaluation of colonic anastomotic healing in the rat following preoperative 5-fluorouracil, fractionated irradiation and combined treatment. *Int J Colorectal Dis*. 1998;13(5–6):235–240.
16. Phillips JD, Kim CS, Fonkalsrud EW, Zeng H, Dindar H. Effects of chronic corticosteroids and vitamin A on the healing of intestinal anastomoses. *Am J Surg*. 1992;163(1):71–77.
17. Witte MB, Barbul A. Repair of full-thickness bowel injury. *Cri Care Med*. 2003; 31(8 Suppl):538–546.
18. Cronin K, Jackson DS, Dunphy JE. Specific activity of hydroxyproline-tritium in the healing colon. *Surg Gyn Obst*. 1968;126(5):1061–1065.
19. Ajamieh HH, Menéndez S, Martínez-Sánchez G, et al. Effects of ozone oxidative preconditioning on nitric oxide generation and cellular redox balance in a rat model of hepatic ischaemia reperfusion. *Liver Int*. 2004;24(1):55–62.
20. Peralta C, Leon OS, Xaus C, et al. Protective effect of ozone treatment on the injury associated with hepatic ischemia reperfusion: Antioxidant-prooxidant balance. *Free Radic Res*. 1999;31(3):191–196.
21. Re L, Mawsouf MN, Menendez S, Leon OS, Sanchez GM, Hernandez F. Ozone therapy: Clinical and basic evidence of it's therapeutic potential. *Arch Med Res*. 2008;39(1):17–26.
22. Leon OS, Menendez S, Merino N, et al. Ozone oxidative preconditioning: A protection against cellular damage by free radicals. *Mediators Inflamm*. 1998;7(4):289–294.
23. Di Paolo N, Bocci V, Gaggiotti E. Ozone therapy. *Int J Artif Organs*. 2004;27(3):168–175.
24. Stevens KR, Fletcher WS, Allen CV. Anterior resection and primary anastomosis following high dose preoperative irradiation for adenocarcinoma of the recto-sigmoid. *Cancer*. 1978;41(5):2065–2071.
25. Pleskovic A, Zorc-Pleskovic R, Vraspir-Porenta O. Colon mucosal cells after combined radiotherapy and chemotherapy. *Folia Biol (Praha)*. 2001;47(5):156–162.
26. Blake DP, Bubrick MP, Kochsiek GG. Low anterior anastomotic dehiscence following preoperative irradiation with 6000 rads. *Dis Colon Rectum*. 1984;27(3):176.
27. Winsey K, Simon RJ, Levenson S. Effect of supplemental vit-A on colon anastomotic healing in rats given preoperative irradiation. *Am J Surg*. 1987;153(2):153–156.

Echocardiographic ultrasound screening assessment of the circulatory system of newborns delivered at basic level perinatal care centers

Joanna Kukawczynska-Noczynska[1,A,C,D], Rita Suchanska[2,B], Marta Berghausen-Mazur[2,B,E]

[1] 1st Department and Clinic of Pediatrics, Allergology and Cardiology, Wroclaw Medical University, Poland
[2] 1st Department and Clinic of Gynaecology and Obstetrics, Wroclaw Medical University, Poland

A – research concept and design; B – collection and/or assembly of data; C – data analysis and interpretation; D – writing the article; E – critical revision of the article; F – final approval of the article

Advances in Clinical and Experimental Medicine, ISSN 1899–5276 (print), ISSN 2451–2680 (online) *Adv Clin Exp Med*. 2019;28(12):1691–1695

Address for correspondence
Joanna Kukawczynska-Noczynska
E-mail: jo.ku@wp.pl

Funding sources
None declared

Conflict of interest
None declared

Received on May 31, 2018
Reviewed on August 30, 2018
Accepted on September 27, 2019

Published online on December 17, 2019

Abstract

Background. For many years standards of medical care for newborns have been created and perfected with the goal of improving care, including early detection of congenital defects.

Objectives. The objective of the study was to assess the circulatory system in newborns born at basic level of perinatal care centers and the comparison of specific parameters of cardiac function and structure according to the method of birth, body mass, sex, Apgar score, pulse oximetry results, and presence of other pathologies.

Material and methods. The study was carried out in 255 newborns aged 3–14 days. The children were assessed according to Apgar score, were weighed and pulse oximetry testing was carried out, and symptoms of neonatal jaundice or infection were taken into account. Each child was subjected to a physical examination and echocardiographic examination.

Results. Among the group studied, 3.5% of children had defects of the circulatory system and functional disorders.

Conclusions. Pulse oximetry testing, due to its low level of invasiveness, high sensitivity and specificity, low cost and repeatability, should be used as the primary screening test, allowing for early detection of critical congenital heart defects (CHDs). It should be stressed that the test should be repeated before discharge of newborns from the neonatology department so as to avoid missing CHDs which are asymptomatic or mute at birth. Morphological and functional assessment of specific structures of the heart in delivered newborns showed correlation of the size of the left ventricle (LV) with body mass. The remaining factors, such as method of delivery, sex, neonatal jaundice, and audible murmur, were irrelevant. Routine cardiological assessment of healthy newborns is therefore not necessary.

Key words: congenital heart defect, echocardiography, newborn

Cite as
Kukawczynska-Noczynska J, Suchanska S, Berghausen-Mazur M. Echocardiographic ultrasound screening assessment of the circulatory system of newborns delivered at basic level perinatal care centers. *Adv Clin Exp Med*. 2019;28(12):1691–1695. doi:10.17219/acem/110327

DOI
10.17219/acem/110327

For many years standards of medical care for newborns have been created and perfected with the goal of improving such care, including early detection of congenital defects. Currently, according to the newest guidelines of care, each newborn is to be assessed along a schedule of screening tests carried out in the neonatology department. Screening tests are a form of prophylaxis, allowing for early diagnosis of congenital diseases before they become symptomatic. Currently, the number of prophylactic screening tests in Poland stands at 27 in addition to auditory assessment and pulse oximetry.[1] The social and economic benefits of screening tests are unquestionable. Between the year 2009 and 2013 in Poland, according to data presented by the Ministry of Health, on the basis of screening tests, 1,394 congenital diseases were diagnosed.[1] The frequency of congenital heart defects (CHDs) in the population is around 0.8–1%, of which 25% can be considered critical defects requiring urgent surgical or hemodynamic intervention.[2,3] Newborns with serious complex heart defects may at first present atypically, without any obvious symptoms of cardiac insufficiency. Typically, the stay for neonates in the neonatology department is short and as a result newborns with undiagnosed cardiac defects are at high risk of death after discharge from the hospital.[4] The advances in ultrasonography, including fetal echocardiography, have resulted in increased early detection of many fetal defects and the referral of pregnant women to deliver in the 3rd highest level of perinatal care units, assuring optimal medical care for such newborns.[5]

It is assumed that newborns delivered in basic level perinatal care units lack prenatal diagnoses indicating potential complications. From the source data it can be concluded that, despite intense improvements and advances in ultrasonography techniques, many heart defects are still not diagnosed until after delivery.[6,7] Pulse oximetry in neonatal units, which currently is regarded as a valuable tool in the early diagnosis of CHD, has been recommended and implemented for several years.[8] According to Thangaratinam et al., the sensitivity of the test is estimated at 76.5% with a specificity of 99.9%.[9] The percentage of false positive results is only 0.14%.

Objectives

The objective of the study was an assessment of the circulatory system in newborns born at basic level of regional perinatal care centers through physical as well as echocardiographic testing, and determination of the number and types of heart defects as well as other circulatory system abnormalities detected in the population studied.

Additionally, another goal of the study was to compare specific parameters of cardiac function and structure taking into account the method of birth, body mass of the newborn, sex, Apgar score, pulse oximetry results, and presence of other pathologies associated with the neonatal phase, such as congenital infection, heart murmur or neonatal jaundice.

Material and methods

The study was carried out on 255 newborns aged 3–14 days, born in a basic level of perinatal care unit during a 12-month period in 2014–2015. Children born in a regional hospital in Środa Śląska were assessed in the neonatology department according to Apgar score at 1 min, 3 min, 5 min, and 10 min of life. The newborns were weighed and pulse oximetry testing was carried out 2–24 h after birth as well as on the day of discharge. When symptoms of neonatal jaundice presented, levels of bilirubin were monitored and with symptoms of infection, the appropriate therapeutic treatment was administered.

The examination assessing the circulatory system was carried out in an ambulatory setting in the cardiology clinic 3–14 days after birth. Each child was subjected to a physical examination which assessed the heart tones, rhythm and rate of the heart as well as the peripheral pulse. Each subject also received an echocardiographic examination which assessed the specific parameters of heart function and structure as well as the morphology of the heart and the presence of structures from prenatal life – patent foramen ovale (PFO) and patent ductus arteriosus (PDA). In the M-Mode, measurements of the right ventricle in diastole (RVED) as well as the left ventricle in diastole (LVED) and systole (LVES) were carried out. The shortening fraction (FS) and ejection fraction for the left ventricle (LVEF) were measured, and the contractile function of the right ventricle (RV) was assessed through tricuspid annular plane systolic excursion (TAPSE); the velocity of flow on the aortic (AoV) and pulmonary valve (PV) as well as flow acceleration time (pulmAT – pulmonary acceleration time) were measured to assess the characteristics of diastolic flow on the mitral valve (MVE – mitral valve velocity flow in early diastole and MVA – mitral valve velocity flow in late diastole).

The statistical analysis was carried out utilizing quantity as well as quality parameters of statistical description. In our work, we used quantitative variables such as mean and standard deviation (SD) and quality variables such as populations of chosen subgroups and percentages showing prevalence of specific characters in subgroups. Correlations between cardiological parameters and quantitative parameters were specified using Spearman's correlation coefficient, while quality parameters were examined with Wilcoxon's test or Fisher's exact test.

Results

Characteristics of the population studied

Briefly, 47.4% of children studied were male while 52.6% were female. Those born naturally comprised 51.4% while those born through caesarean section were 48.6% of the population. The birth weight varied from

2,110 g to 6,000 g with the average being 3,578 g. Broken down by sex, the average mass of females was 3,678 g while for males it was 3,482 g. The registered Apgar scores after 1 min and 5 min showed a great deal of uniformity. Average Apgar score after 1 min was 9 (min. 2 points, max. 10 points). Assessed at 5 min, the Apgar score for nearly all newborns was 10.

Pulse oximetry was carried out twice, with a score of equal to or below 95% considered abnormal. Only in 4 (1.6%) of children was an abnormal result recorded. Neonatal jaundice (above 12 mg%), requiring phototherapy, was detected in 40 (15.7%) patients examined. Congenital infection was diagnosed and treated in 10% of newborns examined (in 25 patients). Various heart murmurs were auscultated in 15% of children (38 newborns). In 1 case, arrhythmia was detected and diagnosed as supraventricular extrasystoles. This data is presented in Table 1.

Results of cardiological testing

Among the group studied, there were 3.5% (9 patients) with defects of the circulatory system diagnosed, such as intra-atrial septal defect (ASD) in 1 newborn (<1%), intraventricular septal defect (VSD) in 4 patients (1.6%), patent ductus arteriosus (PDA) in 3 newborns (1.1%), and complex defect consisting of coarctation of the aorta with bicuspid aortic valve and mitral valve insufficiency in 1 patient (<1%).

In 38 newborns with loud systolic murmur detected over the heart, only 5 were diagnosed with heart defects – VSD and complex defect consisting of coarctation of the aorta with bicuspid aortic valve and mitral valve insufficiency. The complex heart defect was hemodynamically significant and the child was referred for cardiosurgical intervention.

Moreover, among the group studied, mild hypokinesis of the heart muscle was found in 2 newborns (<1%), tricuspid valve insufficiency in 8 newborns (3.1%), decreased acceleration time of pulmonary flow in 7 newborns (2.7%), mild hypertrophy of the intraventricular septum in 3 newborns (1.1%), and single supraventricular arrhythmia in 1 newborn (<1%). Patent foramen ovale was found in 140 newborns (55.0%) of which in 50% of the PFO cases the PFO was 4.0 mm and in 25% of cases the PFO was larger than 5 mm. In 14 additional newborns, other small irregularities of the cardiovascular system were detected and assessed as transient in nature.

The assessment of the selected echocardiographic parameters is presented in Table 2.

In the group studied, the correlation between the measured echocardiographic parameters and body mass, sex, Apgar score, and delivery method and coexistence of neonatal jaundice was analyzed. Infants born naturally and those born through caesarean section presented no difference in measured echocardiographic parameters.

The correlation between Apgar scores at 1 min and 5 min and dimensions of RV and LV were likewise irrelevant; similarly, functional parameters of the circulatory system did not show relevant correlation with Apgar score in newborns. It may be that this is due to the uniformity of the group assessed (overwhelmingly assessed at 8–10 points). A relevant weak negative correlation was observed between pulmonary acceleration time and Apgar score after the 1st min of life (lower level of pulmonary acceleration results in an insignificantly lower Apgar score) while after 5 min of life this correlation disappears, which may be linked to therapeutic efforts (i.e., oxygen therapy) in patients with lower Apgar scores.

Statistical analysis of the size of cavities of RV and LV in dependence on the overall mass of the newborn and sex expressed a weak relevant correlation between the mass of the infant and the dimensions of LV; newborns with a greater body mass had larger dimensions of LV. Little correlation was found between the body mass and the dimensions of RV. The sex of the child has no influence on the size of the LV or RV. A relevant correlation was found between body mass and TAPSE in that its increased value was linked with higher body mass. No effect of neonatal jaundice or the use of phototherapy to treat it was found on the parameters studied on echocardiographic assessment of heart size and function.

The characteristics of mitral influx in the first 2 weeks of life was the same as during fetal life. Mitral valve velocity flow in early diastole was lower than mitral valve velocity flow in late diastole (MVE < A). In almost half

Table 1. Schedule of abnormalities in infant group examined

Physical examination		Echocardiographic examination	
type	quantity	morphological	functional
Jaundice > 12 mg%	15.7% (40 patients)	PDA < 1% (1 patient)	hypokinesis LV <1% (2 patients)
Pulse oximetry ≤95	1.6% (4 patients)	multiASD 1.1% (3 patient)	hypokinesis RV <1% (1 patient)
Congenital infection	10% (25 patients)	mVSD 1.6% (4 patient)	ITV 3.1% (8 patients)
Heart murmur	15% (38 patients)	CoAo < 1% (1 patient)	supraventricle arrhythmia <1% (1 patient)
Arrhythmia	<1% (1 patient)	IVS hypertrophy 1.1% (3 patients)	PulmAT 2.7% (7 patients)
Apgar score 10 points at 5 min	99.2% (253 patients)	PFO 55.0% (140 patients)	MVE < A 41.6% (106 patients)

PDA – patent ductus arteriosus; multiASD – multi atrial septal defect; mVSD – muscular ventricle septal defect; CoAo – coarctation of aorta; IVS – hypertrophy intraventricle septum hypertrophy; PFO – patent foramen ovale; LV – left ventricle; RV – right ventricle; ITV – tricuspid valve insufficiency; pulmAT – pulmonar acceleration time; MVE – mitral valve velocity flow in early diastole; MVA – mitral valve velocity flow in late diastole.

Table 2. Schedule of results of morphological and functional parameters examined

Echocardiographic parameters	Medium	Min	n < 25	n = 50%	n > 25%	Max
RVED [mm]	8.5	5	7	8	9	19
LVED [mm]	18.3	13	17	18	19	27
LVES [mm]	12.2	8	11	12	13	18
PV [m/s]	0.9	0.5	0.8	0.9	1	1.68
PulmAT [ms]	76.8	37	67	74	89	133
AoV [m/s]	0.98	0.16	0.8	1	1	1.90
FS > 28%	33.7	22	31	33	36	70
EF > 55%	65	47	61	65	68	80
TAPSE	10.1	5	9	10	11	22

RVED – right ventricle in diastole; LVED – left ventricle in diastole; LVES – left ventricle in systole; PV – pulmonary valve; PulmAT – pulmonar acceleration time; AoV – velocity of flow on the aortic; FS – fractional shortening; EF – ejection fraction; TAPSE – tricuspid annular plane systolic excursion.

of the subjects examined but also in a large portion of cases in which mitral valve velocity flow in early diastole was the same as mitral valve velocity flow in late diastole (MVE = A) or was higher (MVE > A). No correlation was found between the presence of PFO and Apgar score assessed after 1 min of life. Additionally, the presence of PFO and incidence of neonatal jaundice and body mass showed no relevant correlation.

Due to the small sample size of neonates with congenital infections, correlation with the functional parameters assessed was not analyzed.

Discussion

The literature puts an emphasis on the relevance of screening tests in newborns, which help to diagnose diseases which do not present symptomatically directly after birth or whose symptoms are masked. Recently, the test used to screen for CHDs has been pulse oximetry. From the available data gathered through the POLKARD program in the years 2006–2008, assessing the usefulness of pulse oximetry in the diagnosis of CHD in newborns, we can conclude that the sensitivity of this method is 78% while specificity is 99.9% and negative predictive value is almost 100%.[10] These findings are very similar to the data published by Thangaratinam et al. in 2012 which estimated the sensitivity of the test at 76.5% and specificity at 99.9% with the fraction of false positive results being only 0.14%.[9]

In 1.6% of patients (4 patients), pulse oximetry testing gave false positive results because irregularities in the circulatory system were not confirmed upon further testing. In the population studied, 1 case of hemodynamically relevant CHD was diagnosed, consisting of a coarctation of the aorta with a bicuspid aortic valve necessitating surgical intervention while the test gave a normal result in the child. Pulse oximetry may not reveal coarctation of the aorta unless the defect is of critical intensity, as in the mentioned case.[11]

In the group of newborns examined, 7 cases (2.7%) of simple heart defects were diagnosed with correct pulse oximetry results: 4 cases of muscular ventricle septal defect (mVSD) and 3 cases of patent ductus arteriosus (PDA) which did not require further intervention and in most cases resolved spontaneously. Two children (0.7%) had defects which required surgical intervention despite proper pulse oximetry test results.

In the group analyzed, the most common finding was patent foramen ovale (PFO); such defect with a diameter of less than 4 mm was found in 54.9% of newborns (140 patients), while in only 5% of patients the size of the PFO was above 5 mm in diameter and in 1 newborn – of 8 mm.

Fukazawa et al. in their study of the spontaneous closure of defects in the intra-atrial septum, qualified PFO with a diameter greater than 5–6 mm as an atrial septal defect type II (ASD II).[12] Newborns with a borderline-sized PFO (5 mm) were not qualified as having a congenital heart defect (CHD). Diagnosis of ASD II in newborns seems to be controversial due to the fact that this is a physiological structure in the first days of newborn life.[13] From cardiological observation we know that PFO and the method of its closure varies from patient to patient and may occur gradually or quickly through the PFO valve closure.

Intraventricular septal defect is the most common CHD diagnosed in children and, according to many authors, it makes up from 5% to even 20% of all CHDs.[14] In the analyzed group, 4 incidents of VSD with typical, auscultatable murmurs over the heart with a 3/6 in the Levine scale and proper pulse oximetry test results. Muscular type VSD is a mild form of this heart defect which in most cases does not require intervention, may close spontaneously as the child grows and generally does not produce significant hemodynamic dysfunction.[15]

According to various source data, PDA is recognized as a CHD if its patency is maintained beyond the 4th day of life or, more commonly, beyond the 7th day of life.[13,15,16] In this study, PDA was diagnosed in only 1.1% (3) of patients and in all of those the duct closed spontaneously. Other functional dysfunctions visible in echocardiographic

assessment such as shortened pulmonary flow time, mild tricuspid valve insufficiency and decreased contractility of the cardiac muscle were all transient in nature and may be attributed to the acclimation of newborns to postnatal life.

In the available literature, the data concerning echocardiographic norms of selected structures of the heart and functional parameters come from the 1980s.[17] Currently, analysis of echocardiographic parameters is carried out based on foreign literature[17–23] as well as, more often, calculation of the Z-score.[20,24,25]

On the basis of the group studied, we can create norms of selected parameters of the structure and function of the circulatory system in healthy delivered newborns, which may be useful for physicians conducting heart echocardiography in clinics with limited access to cardiological consult.

Conclusions

Pulse oximetry testing, due to its low level of invasiveness, high sensitivity and specificity, low cost, and repeatability, should be used as the primary screening test allowing for early detection of critical CHDs. It should be stressed that the test should be repeated before discharge of newborns from the neonatology department so as to avoid missing CHDs which are asymptomatic or mute at birth.

Morphological and functional assessment of specific structures of the heart in delivered newborns born in basic level perinatal care centers showed correlation of the size of LV with body mass. The remaining factors, such as method of delivery, sex, neonatal jaundice, and audible murmur, were irrelevant.

Routine cardiological assessment of healthy newborns is not necessary. Cardiological testing as a screening method for newborns should not be recommended.

References

1. Ministerstwo Zdrowia. Program polityki zdrowotnej. Program badań przesiewowych noworodków w Polsce na lata 2015–2018. Warszawa, Poland: Ministerstwo Zdrowia; 2017.
2. Stanek B, Binikowska J, Moll J, Sysa A. Wrodzone nieprawidłowości układu krążenia u noworodków urodzonych w Instytucie Zdrowia Matki Polki w Łodzi w latach 1998–2004. *Post Neonatol*. 2004;Suppl 2: 14–17.
3. Kirshnamurthy G, Ratner V, Levasseur S, Rubenstein D. *Wrodzone wady serca w okresie noworodkowym. Neonatologia w praktyce*. Warszawa, Poland: MediPage; 2015:256.
4. Peterson C, Grosse SD, Glidewell J, et al. A public health economic assessment of hospitals' cost to screen newborns for critical congenital heart disease. *Public Health Rep*. 2014;129(1):86–93.
5. Gadzinowski J, Gruszfeld D, Czech-Kowalska J. *Organizacja opieki nad noworodkiem w skali regionalnej. Standardy opieki medycznej nad noworodkiem w Polsce. Zalecenia Polskiego Towarzystwa Neonatologicznego*. 2nd ed. Warszawa, Poland: Media-Press; 2017:12–16.
6. Brand A, Alves MC, Saraiva CL. Fetus in fetu: Diagnostic criteria and differential diagnosis. A case report and literature review. *J Pediatr Surg*. 2004;39(4):616–618.
7. Mroziński B, Siwińska A, Sobkowski W, Maciejewski J. Wrodzone wady układu krążenia u noworodków i niemowląt diagnozowanych w pracowni echokardiograficznej Kliniki Chorób Dzieci Instytutu Pediatrii Akademii Medycznej im. Karola Marcinkowskiego w Poznaniu w latach 1995–1999. *Post Neonatol*. 2000;Suppl 1;119–123.
8. Rozporządzenie Ministra Zdrowia z dnia 20 września 2012 r. (Dz. U. z dnia 4.10.2012 r. Nr 189, poz. 1100).
9. Thangaratinam S, Brown K, Zamora J, Khan KS, Ewer AK. Pulse oximetry screening for critical congenital heart defects in asymptomatic newborn babies: A systematic review and meta-analysis. *Lancet*. 2012; 379(9835):245–264.
10. Kawalec W, Turska-Kmieć A, Żuk M, et al. Poprawa opieki kardiologicznej nad dzieckiem z patologią układu krążenia ze szczególnym uwzględnieniem oceny wyników leczenia i lepszej jakości życia dzieci z wrodzonymi wadami serca. Ogólnopolski program wielozadaniowy i wieloośrodkowy realizowany w ramach programu POLKARD 2006–2008. *Stand Med Pediatr*. 2009;6:614–622.
11. Błaż W, Turska–Kmieć A. Pulsoksymetria jako metoda wykrywania wad wrodzonych serca u bezobjawowych noworodków. *Pediatr Dypl*. 2010;14(4):107–112.
12. Fukazawa M, Fukushige J, Veda K. Atrial septal defect in neonates with references to spontaneous closure. *Am Heart J*. 1988;116(1 Pt 1): 123–127.
13. Sachdeva R. Congenital cardiovascular malformations; Atrial septal defects. In: Allen HD, Driscoll DJ, Shaddy RE, Feltes TF, eds. *Moss and Adams' Heart Disease in Infants, Children, and Adolescents: Including the Fetus and Young Adult*. Vol 1. 8th ed, Philadelphia, PA; Lippincott Williams & Wilkins. 2013:683–688.
14. Soto B, Becker AE, Moulaert AJ, Lie JT, Anderson RH. Classification of ventricular septal defects. *Br Heart J*. 1980;43(3):332–343.
15. Kubicka K, Kawalec W, Bernatowska E. *Pediatria*. Warszawa, Poland: Wydawnictwo Lekarskie PZWL; 2004:311–317.
16. Andreson RH, Macartney FJ, Shinebourne EA, et al. *Paediatric Cardiology*. 2nd ed. London, UK: Churchill Livingstone; 2002:278–284.
17. Biamino G, Lange L. *Echokardiographie- Stellenwert in der kardiologischen Diagnostik*. Frankfurt am Main, Germany: Hoechst Verlag; 1983:134–138.
18. Cantinotti M, Scalese M, Murzi B, Murzi B, Passino C. Echocardiographic nomograms for chamber diameters and areas in Caucasian children. *J Am Soc Echocardiogr*. 2014;27(12):1279–1292.e2.
19. Cantinotti M, Scalese M, Molinaro S, Murzi B, Passino C. Limitations of current echocardiographic nomograms for left ventricular, valvular, and arterial dimensions in children: A critical review. *J Am Soc Echocardiogr*. 2012;25(2):142–152.
20. Siwińska A, Werner B, Rudziński A, et al; Echocardiography Working Group of the Polish Cardiology Society. Paediatric echocardiography in clinical practice. 2012 Recommendations of the Echocardiography Working Group of the Polish Cardiac Society [in Polish]. *Kardiol Pol*. 2012;70(6):632–640.
21. Kampmann C, Wiethoff CM, Wenzel A, et al. Normal values of M mode echocardiographic measurements of more than 2000 healthy infants and children in central Europe. *Heart*. 2000;83(6):667–672.
22. Lopez L, Colan SD, Frommelt PC, et al. Recommendations for quantification methods during the performance of a pediatric echocardiogram: A report from the Pediatric Measurements Writing Group of the American Society of Echocardiography Pediatric and Congenital Heart Disease Council. *J Am Soc Echocardiogr*. 2010;23(5):465–95
23. Mawad W, Drolet C, Dahdah N, Dallaire F. A review and critique of the statistical methods used to generate reference values in pediatric echocardiography. *J Am Soc Echocardiogr*. 2013;26(1):29–37.
24. Colan SD. The why and how of Z-scores. *J Am Soc Echocardiogr*. 2013; 26(1):38–40.
25. Gokhroo RK, Anantharaj A, Bisht D, Kishor K, Plakkal N, Mondal N. A pediatric echocardiographic Z-score nomogram for a developing country. Indian pediatric echocardiography study: The Z-score. *Ann Pediatr Cardiol*. 2017;11(1):109–111.

Protective effects of dantrolene and methylprednisolone against spinal cord injury-induced early oxidative damage in rabbit bladder: A comparative experimental study

Ibrahim Keles[1,A,B,D], Mehmet Fatih Bozkurt[2,A,D], Erdogan Aglamis[3,C,D], Abdurrahman Fatih Fidan[4,C,F], Cavit Ceylan[5,D,E], Mustafa Karalar[1,D,F], Soner Coban[6,B,C], Baris Denk[4,B,C], Mehmet Emin Buyukokuroglu[7,E,F]

[1] Department of Urology, Faculty of Medicine, Afyon Kocatepe University, Afyonkarahisar, Turkey
[2] Department of Pathology, Faculty of Veterinary, Afyon Kocatepe University, Afyonkarahisar, Turkey
[3] Clinics of Urology, Elazig Training and Research Hospital, Saglik Bilimleri University, Turkey
[4] Department of Biochemistry, Faculty of Veterinary, Afyon Kocatepe University, Afyonkarahisar, Turkey
[5] Clinics of Urology, Turkey Yuksek Ihtisas Training and Research Hospital, Saglik Bilimleri University, Ankara, Turkey
[6] Clinics of Urology, Sevket Yilmaz Training and Research Hospital, Saglik Bilimleri University, Bursa, Turkey
[7] Department of Pharmacology, School of Medicine, Sakarya University, Turkey

A – research concept and design; B – collection and/or assembly of data; C – data analysis and interpretation; D – writing the article; E – critical revision of the article; F – final approval of the article

Advances in Clinical and Experimental Medicine, ISSN 1899–5276 (print), ISSN 2451–2680 (online) *Adv Clin Exp Med.* 2019;28(12):1697–1704

Address for correspondence
Ibrahim Keles
E-mail: drkeles@hotmail.com

Funding sources
This study was supported by the Afyon Kocatepe University Scientific Research Projects Coordination Unit (Project No. 14.TIP.09).

Conflict of interest
None declared

Received on March 8, 2018
Reviewed on October 8, 2018
Accepted on June 27, 2019

Published online on December 18, 2019

Cite as
Keles I, Bozkurt MF, Aglamis E, et al. Protective effects of dantrolene and methylprednisolone against spinal cord injury-induced early oxidative damage in rabbit bladder: A comparative experimental study. *Adv Clin Exp Med*. 2019;28(12):1697–1704. doi:10.17219/acem/110326

DOI
10.17219/acem/110326

Abstract

Background. Spinal cord injury (SCI) may cause dysfunction in the bladder and many distal organs due to systemic inflammatory response and oxidative stress-related injury.

Objectives. We investigated the preventive effects of dantrolene (DNT) and methylprednisolone (MP) on stress-induced tissue damage in rabbit bladder with SCI.

Material and methods. A total of 35 rabbits were included in this study and they were divided into 5 groups: group 1 – control, group 2 – SCI only, group 3 – SCI and DNT, group 4 – SCI and MP, and group 5 – SCI and DNT+MP. Twenty-four hours after SCI, the bladders of these rabbits were removed and the histopathologic changes in the bladder were examined under a light microscope. Additionally, malondialdehyde (MDA), glutathione (GSH), and nitric oxide (NO) levels were evaluated as antioxidant agents both in bladder tissue and in blood.

Results. Compared to the control group, there was an increase in edema and congestion in all groups. The least amount of edema was observed in the group receiving DNT and the least amount of congestion was observed in the group receiving combined treatment (group 5). No superiority was found between the drug-receiving groups in terms of reducing MDA level in blood and tissue after SCI. The most successful group was the group receiving combined drug therapy in terms of increasing the blood GSH level, which was significantly decreased after SCI. After SCI, blood NO level increased significantly in all groups. Nitric oxide levels in the bladder tissue significantly decreased in the groups receiving DNT and combination therapy and fell in the control group.

Conclusions. Dantrolene and MP may have potential benefits against oxidative damage in the bladder after SCIs because of their anti-inflammatory and antioxidant effects. In particular, the combined use of DNT and MP at different doses can be considered a treatment strategy.

Key words: antioxidant, anti-inflammatory, spinal cord injury, methylprednisolone, dantrolene

Introduction

Based on several regional studies, the annual incidence of spinal cord injury (SCI) in the USA is estimated to be roughly 12,000 new cases per year.[1] Spinal cord injuries are mostly caused by traumatic incidents such as traffic accidents, firearm injuries, falls and sports injuries, but non-traumatic causes such as intraspinal infection, vascular ischemia and tumor may also cause SCIs.[2] Traumatic SCI can cause serious neurological damage and multiple organ dysfunction in patients.[2,3] Traumatic SCI is a 2-phase pathological process defined as primary injury and secondary injury.[2,4] Physical compression and mechanical injury of the spinal cord after trauma is defined as primary injury.[4,5] Primary injury causes spinal deformation and narrowing of the spinal canal, resulting in intraspinal hemorrhage and decreased blood circulation due to mechanical damage of nerve tissue and blood vessels.[2] Primary injury occurs in a short period of time and in a restricted area. Hemorrhage is a process characterized by ischemia and edema.[2] Primary injury triggers secondary injury that may occur within hours or days.[6]

Major pathophysiological changes observed in the secondary injury phase include: reduction in glutathione levels, ischemia, oxidative damage, Ca^{2+}-dependent nitric oxide (NO) production, excitotoxicity, free radical damage, lipid peroxidation in cell membranes, increased malondialdehyde level, which is the end product of membrane lipid peroxidation, neurodegeneration, gliosis, and inflammation.[2,7–9] The purpose of medical treatment of traumatic SCIs is to prevent the effects of these secondary mechanisms.[10] In addition to intraspinal inflammation, SCI can trigger systemic inflammatory response syndrome (SIRS), which can lead to failure and dysfunction in multiple organs.[2] After SCI, in the urinary system, complications such as neurogenic bladder, kidney damage and urinary tract infection can be observed.[2] Loss of neuronal stimulation and inflammation play a role in the pathogenesis of urinary system dysfunction.[2]

The inhibition of inflammatory responses can contribute to the recovery from neurogenic depression.[2] Antioxidant and anti-inflammatory agents such as dantrolene (DNT) and methylprednisolone (MP) are used for this purpose.[11] Dantrolene is a ryanodine receptor antagonist that blocks the intracellular release of Ca^{2+}, and is used as an anti-inflammatory and neuroprotective agent.[11] Methylprednisolone acts as a steroidal anti-inflammatory agent, reducing the number of inflammatory cells and oligodentrocytic apoptosis.[11]

The purpose of our work is to comparatively demonstrate the protective effect of DNT and MP, individually or in combination, on stress tissue damage in rabbit bladder in experimental SCI.

Material and methods

The study was conducted in accordance with the Guide for the Care and Use of Laboratory Animals published by the US National Institutes of Health (NIH Publication No. 85-23, revised 1996) and was approved by the Afyon Kocatepe University Animal Experiment Ethics Committee, Afyonkarahisar, Turkey (approval No. AKUHADYEK-49533702/59).

Animals

A total of 35 New Zealand male rabbits weighing 2.5–3 kg were included in the study. The animals were kept in individual cages, under a circadian cycle and temperature control in addition to standard feeding, at the laboratory animals center.

Drugs and chemicals

The drugs and chemicals used were the following: DNT sodium (Ryanodex vial 250 mg/20 mL, Eagle Pharmaceuticals, Woodcliff Lake, USA), MP sodium succinate (Prednol-L amp. 250 mg/4 mL, Mustafa Nevzat Pharmaceuticals, Istanbul, Turkey), ketamine hydrochloride (Ketalar 50 mg/mL; Pfizer, New York, USA) 25 mg/kg, and xylazine (Rompun 100 mg/mL, Bayer AG, Leverkusen, Germany) 5 mg/kg injection. All drugs were diluted in 0.9% sterile saline.

Experimental design and administration of drugs

The animals were randomly divided into 5 groups consisting of 7 rabbits each, as follows: group 1 (control group) rabbits did not receive any drugs and no operation was applied; in group 2 rabbits (SCI+no drug treatment group) a single dose of 2 mL saline was given intraperitoneally (i.p.) 1 h after SCI; group 3 rabbits (SCI+DNT group) were administered 10 mg/kg DNT i.p. 1 h after SCI; group 4 rabbits (SCI+MP group) were given 30 mg/kg MP i.p. 1 h after SCI; and group 5 rabbits (SCI+DNT+MP group) were administered 10 mg/kg DNT+30 mg/kg MP 1 h after SCI.

Surgical procedures for the SCI model

An appropriate disinfection and sterilization environment was established. All rabbits were anesthetized with intramuscular (i.m.) ketamine hydrochloride 25 mg/kg and xylazine 5 mg/kg injection. If necessary, the dose was repeated at 25 mg/kg ketamine and 5 mg/kg xylazine. During ketamine anesthesia, spontaneous breathing of the animals was observed. After back-shaving and field treatment, the rabbits were placed in prone position on the operation table. A midline dorsal incision was performed. The laminae and transverse processes of T6–L2 were exposed with gentle blunt dissection of the paravertebral muscles.

A self-retaining retractor was placed in the operation area, and then laminectomy was performed at T10; then a balloon angioplasty catheter (Medtronic-146.671, 2.0×20 mm; Medtronic plc, Dublin, Ireland) placed extradurally and sublaminary on thorasic spinal cord, upwards below T9 and inflated under 2 atm pressure for 5 min with standby. Following the careful removal of the balloon catheter, the paravertebral fascia and skin were sutured with non-absorbable sutures. Paraparesia developed in all groups, constituting traumatic injury. Twenty-four hours after SCI, the rabbits in all groups were anesthetized with 25 mg/kg ketamine and 5 mg/kg xylazine. The bladder was removed after an abdominal incision. Blood samples from each group were collected with cardiac puncture into heparinized and non-heparinized tubes under anesthesia at the end of the study protocol. At the end of these procedures, all rabbits were sacrificed under deep anesthesia.

Biochemical analysis

Malondialdehyde (MDA), glutathione (GSH) and NO levels were assessed as antioxidant agents in both bladder tissue and blood in all experimental groups.

Blood sample collection

Two milliliters of blood were immediately pipetted into a separate tube to measure MDA and GSH. The remaining blood was centrifuged at 3,000 rpm for 10 min for plasma separation. Plasma samples were stored at –30°C for the analysis of NO.

Tissue homogenate

At the end of the study protocol, the urinary bladder tissues were washed immediately with ice-cold 0.9% NaCl. The urinary bladder was trimmed free of extraneous tissue and rinsed in chilled 0.15 M Tris–HCl buffer (pH 7.4). These tissues were blotted dry and homogenized in 0.15 M Tris–HCl buffer (pH 7.4) to yield a 10% (w/v) homogenate. Then, they were centrifuged at 2,100 g for 10 min at 4°C. The pellets represented the nuclear fraction and the supernatants were subjected to centrifugation at 18,600 g for 20 min at 4°C. Reactive oxygen species (ROS) generation was observed in all the fractions as well as the whole homogenate.

Measurement of malondialdehyde, reduced glutathione and nitric oxide in blood and tissue homogenates

Malondialdehyde levels, as an index of lipid peroxidation, were assayed using the thiobarbituric acid test as described by Ohkawa et al.[12] The principle of the method is based on spectrophotometric measurement of the color produced during the reaction of thiobarbituric acid with MDA and its absorbance was measured spectrophotometrically at 532 nm. Reduced GSH concentration was measured using the method described by Beutler et al. in whole blood and tissue homogenates.[13] The optical density was measured at 412 nm in the spectrophotometer. Results were expressed as nmol/mL in blood and nmol/g in tissue. Plasma NO levels were analyzed with the vanadium (III) chloride Griess reaction method of Miranda et al. that can simultaneously determine the nitrite and nitrate levels in the sample.[14,15]

Histologic analysis

The histopathological changes were assessed with light microscopy by the same pathologist in the bladders removed 24 h after SCI. Urinary bladders were collected and divided into 2 equal parts. One of them was stored at –20°C until biochemical examination. The other part was fixed in buffered 10% formalin solution for pathological examinations. After routine processing, the tissues were embedded in paraffin, sectioned and stained with hematoxylin & eosin (H&E). Stained sections were blindly analyzed under a light microscope (Olympus CX41 attached with Kameram® Digital Image Analyze System; Olympus, Tokyo, Japan) for inflammation, edema and congestion, and scored from 0 to 6. The absence of these findings was evaluated as 0, and the presence as mild to severe (1–6).

Statistical analysis

Statistical tests were performed using SPSS for Windows v. 20.0 software package (SPSS IBM, Armonk, USA). Variables were investigated using visual (histogram and probability plots) and analytical methods (Kolmogorov–Smirnov test) to determine whether or not they were normally distributed. The results are reported as mean ± standard deviation (SD) or as median (min–max). Data with normal distribution was analyzed using one-way analysis of variance (ANOVA) and Tukey's post hoc test. We used statistical evaluation with a nonparametric Kruskal–Wallis test for data with abnormal distribution. The Mann–Whitney U test was performed to analyze the 2 groups. P-value < 0.05 was assessed as statistically significant.

Results

Histological observations

Within the first 24 h in terms of inflammation, no difference was observed between all groups ($p = 0.3$). This may be because inflammation is not fully developed in the first 24 h (Table 1). When edema was assessed, there was a significant increase in edema in all groups compared to the control group ($p < 0.001$). There was no difference between groups 4 and 5, whereas edema was less pronounced in the group receiving DNT 10 mg alone. The edema-dissolving property is higher in the DNT-treated group.

Table 1. Histopathological and biochemical values of blood and tissue for MDA, GSH and NO in experimental groups (mean ±SD)

Examination	Parameter	Control	SCI	SCI+DNT	SCI+MP	SCI+DNT+MP
Pathology	inflammation	0.14 ±0.37	0.14 ±0.37	0.29 ±0.75	0.29 ±0.48	0.71 ±0.75
	edema	0.0 ±0.0	3.29 ±0.75[c]	1.71 ±0.75[b]	2.43 ±1.13[c]	2.43 ±0.53[c]
	congestion	0.71 ±0.95	4.0 ±0.0[c]	4.14 ±0.37[c]	4.0 ±1.15[c]	3.43 ±0.53[c]
Blood biochemistry	MDA [nmol/mL]	3.88 ±0.29	8.86 ±1.81[b]	4.08 ±0.49	4.59 ±0.84	4.32 ±0.58
	GSH [mg/dL]	15.11 ±1.56	10.7 ±0.75[b]	11.15 ±0.42[b]	11.33 ±0.62[b]	12.92 ±0.91[a]
	NO [µmol/L]	10.01 ±1.79	13.03 ±0.87[a]	25.11 ±4.01[b]	28.68 ±2.49[b]	25.26 ±2.84[b]
Tissue biochemistry (urinary bladder)	MDA [nmol/mg]	1.97 ±0.43	3.98 ±1.82[a]	1.63 ±0.45	1.67 ±0.58	1.57 ±0.26
	GSH [nmol/mg]	7.58 ±0.39	7.12 ±0.34	7.54 ±0.42	7.25 ±0.58	6.56 ±2.04
	NO [µmol/mg]	4.55 ±0.29	3.53 ±1.42	1.62 ±0.31[a]	3.71 ±0.83	2.94 ±0.41[a]

[a] $p < 0.05$ with respect to control; [b] $p < 0.01$ with respect to control, [c] $p \leq 0.001$ with respect to control. SD – standard deviation; SCI – spinal cord injury; DNT – dantrolene; MP – methylprednisolone; MDA – malondialdehyde; GSH – glutathione; NO – nitric oxide.

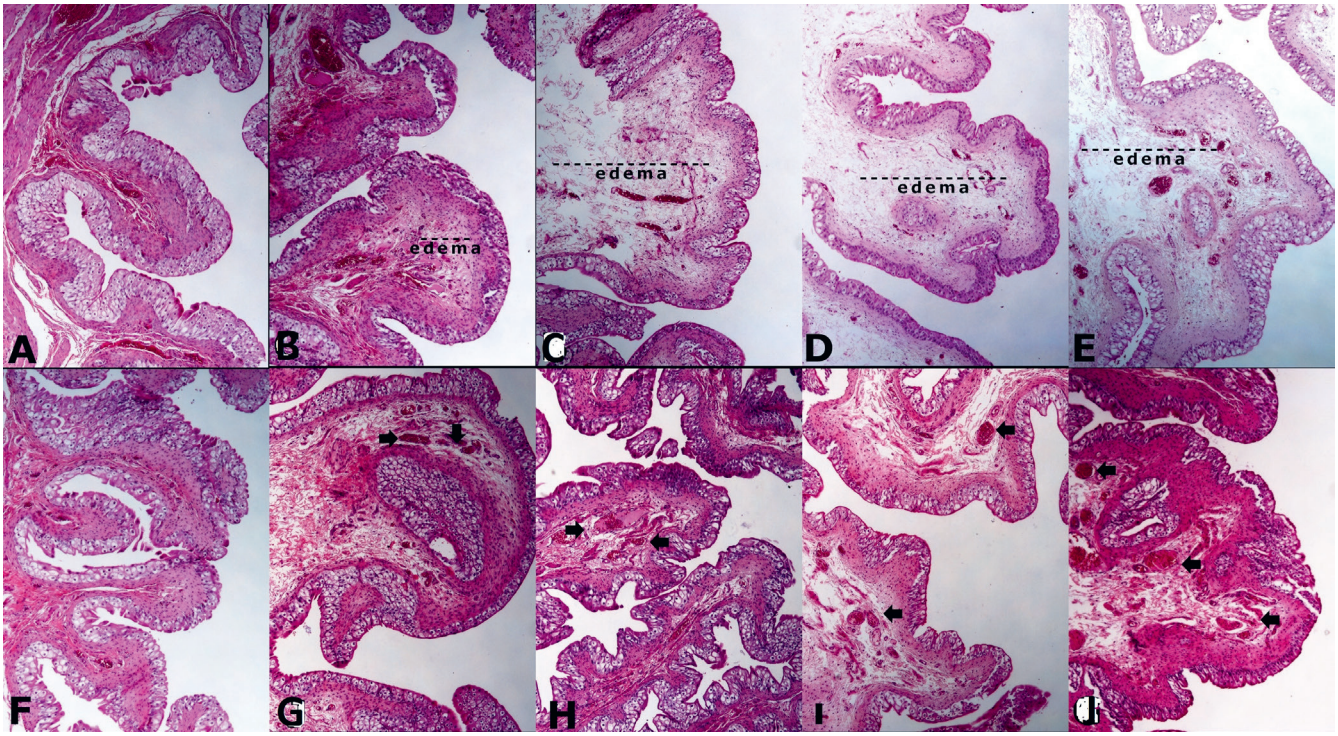

Fig. 1. Histopathological view of group in terms of edema and congestion. A. Control group with no edema (group 1). B. Mild–moderate edema (group 3). C, D, E. Severe edema (groups 2, 4 and 5). F. Control group no congestion (group 1). G. Mild congestion (group 5). H, I, J. Moderate congestion (groups 2, 3 and 4) (arrows). Hematoxylin & eosin (H&E) staining, magnification ×40

However, compared to the control group (comparison of groups 1 and 3), edema was still significantly higher ($p < 0.01$) (Table 1, Fig. 1). There was a statistically significant increase in congestion in groups 3, 4 and 5 compared to the control group ($p < 0.001$). When compared to the other groups with SCI, in group 5, the congestion was less pronounced, but there was not statistically significant difference ($p = 0.02$) (Table 1, Fig. 1).

As a result, combined treatment were found to be slightly more effective than MP alone in reducing edema while no significant effect was observed in preventing early inflammation in the early (early 24 h) period after SCI. Congestion was slightly less observed in the DNT+MP group (Fig. 2C).

Biochemical findings

Biochemical findings in blood

The blood MDA level after SCI was significantly increased compared to the control group ($p < 0.01$). All 3 drugs showed similar efficacy for lowering the elevated MDA levels after SCI and made blood MDA levels similar to the control group (Table 1, Fig. 3A).

When the blood GSH level after SCI was compared with the control group, it fell significantly in all groups ($p < 0.01$ and $p < 0.05$). Dantrolene and MP alone did not have a significant effect on increasing the lowered

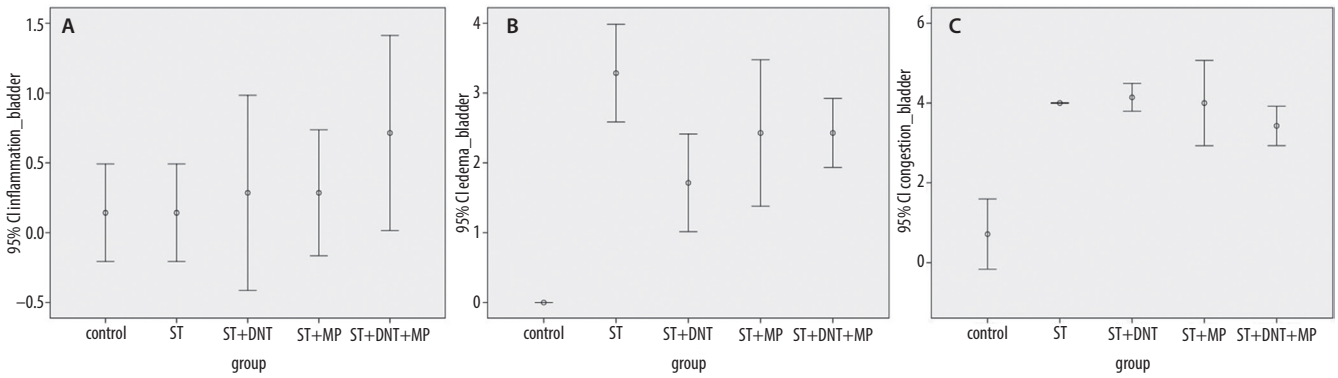

Fig. 2. Comparison of inflammation, edema and congestion in experimental groups. A. There was no difference among all the groups in terms of inflammation. B. Compared to the control group, there was a significant increase in edema in all other groups (p = 0.000). There was no difference between groups 4 and 5. Edema was less observed in the group in which DNT was administered alone. C. There was a significant increase in congestion in the SCI and drug-administered groups (p < 0.001), congestion was less observed in the DNT+MP group

ST – spinal trauma; DNT – dantrolene; MP – methylprednisolone.

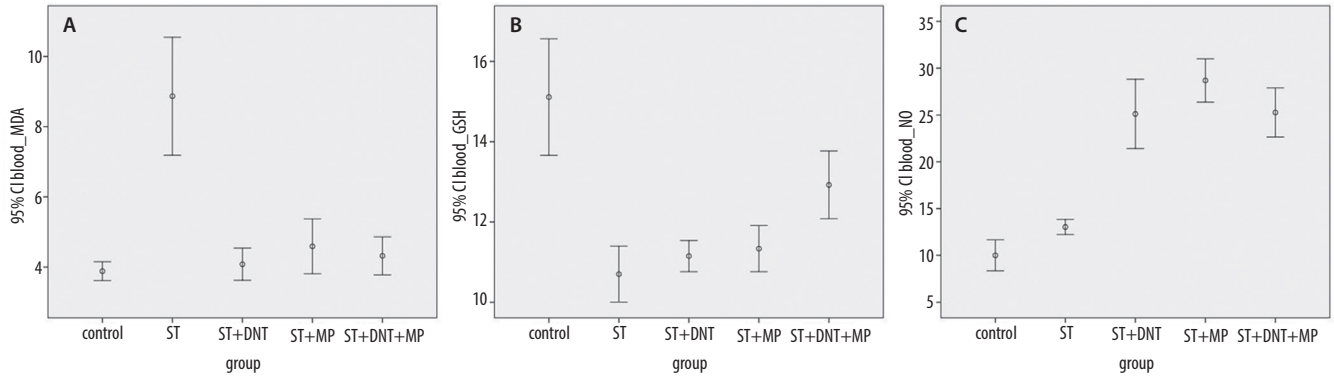

Fig. 3. Comparison of blood MDA, GSH and NO levels in experimental groups. A. Blood MDA levels fell in all 3 drug-treated groups, reaching the same level as in the control group. B. Blood GSH values were decreased after SCI, and neither DNT nor MP did not have a statistically significant effect; GSH levels were highest in DNT+MP group. C. Blood NO values were significantly increased in all 3 drug-administered groups, but the increase was most observed in the MP-administered group

ST – spinal trauma; DNT – dantrolene; MP – methylprednisolone; GSH – glutathione.

blood GSH level (p = 0.22 and p = 0.13, respectively). When the groups treated with DNT and MP alone were compared to the control group, the blood GSH level was significantly lower (p < 0.01). After SCI, the increase in blood GSH levels was observed most prominently in the DNT+MP group, but nevertheless it could not reach the blood GSH level in the control group (p < 0.05) (Table 1, Fig. 3B).

After SCI, the blood NO level was significantly higher in comparison to the control group (p < 0.005), and all 3 groups which received drug therapy had significantly raised levels of NO in comparison to the control group as well as the SCI group. When compared to the control group, blood NO levels were highest in the group which received only MP among the 3 groups which received drugs (p < 0.01) (Table 1, Fig. 3C).

As a result, use of DNT and MP alone or in combination was successful in lowering blood MDA levels and the most successful group for increasing GSH level after SCI was the DNT+MP group. Blood NO levels were highest in the group which received only MP.

Biochemical findings in bladder tissue

When MDA levels in the bladder were examined, the level of MDA after SCI was significantly increased in the bladder tissue. Similar efficacy was observed in all 3 treated groups in decreasing MDA levels which were increased after SCI. Malondialdehyde levels in the bladder tissue decreased to the level of the control group in each of the 3 drug-administered groups (Table 1, Fig. 4A). For the level of GSH in the bladder tissue, no significant change was observed between the experiment groups (Table 1, Fig. 4B). The NO level in bladder tissue was significantly decreased in the DNT and DNT+MP groups and fell below the values of the control group (p < 0.05) (Table 1, Fig. 4C).

Discussion

The aim of this study was to compare the protective efficacy of DNT and MP alone and in combination in preventing early sequelae associated with oxidative stress

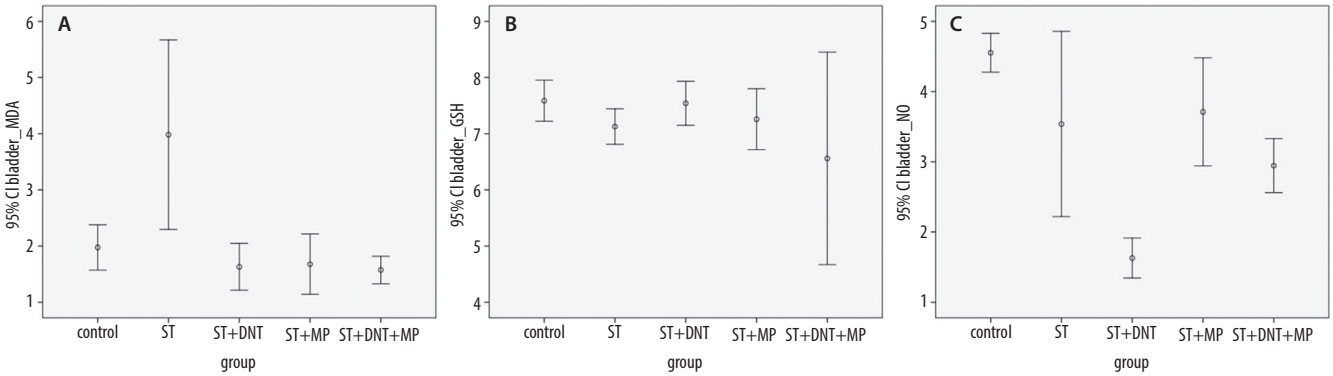

Fig. 4. Comparison of bladder tissue MDA, GSH and NO levels in experimental groups. A. After SCI, bladder MDA levels were significantly increased, and tissue MDA levels decreased in each of the 3 drug-administered groups when compared to the control group. B. There was no significant change in bladder tissue GSH levels among the experimental groups. C. In the group receiving DNT and DNT+MP, bladder tissue NO levels were significantly decreased after SCI and fell below the values of the control group ($p < 0.05$)

ST – spinal trauma; DNT – dantrolene; MP – methylprednisolone; GSH – glutathione.

secondary to traumatic SCI. For this reason, their effects in the first 24 h after trauma were investigated.

Spinal cord injury remains an important clinical problem that can still lead to persistent neurological deficits and secondary complications.[5] In patients with SCI, multiple organ dysfunction and failure may develop.[2] These disorders include neurogenic pain and depression in the nervous system, orthostatic hypotension and autonomic dysreflexia in the cardiovascular system, spleen atrophy and leukopenia, pulmonary edema in the lungs, muscle spasticity and atrophy in the skeletal system, osteoporosis in the bone, neurogenic bowel dysfunction in the gastrointestinal system, renal damage in the urinary system, neurogenic bladder and urinary tract infection, and sexual dysfunction.[2] In addition, SCI can trigger a systemic inflammatory response syndrome, which can be life-threatening by affecting the distal organs.[2] Significant structural, molecular and physiological changes have been reported to develop in SCI animal model studies. In these animal models, hemorrhage due to cellular inflammatory response, rupture of the bladder uroepithelium and inflammation were observed.[16–20] Primary injury in SCI is unavoidable. However, measures against the development of secondary injury can be taken while the treatments are applied. Research and treatments performed for this reason are aimed to prevent secondary injury.[5] Reduction of oxidative stress leading to membrane and cellular damage can provide a potential treatment to prevent secondary injury.[21] A number of studies have been conducted for the treatment of secondary injuries and some therapeutic agents have been used in SCI. Some of the therapeutic agents used for this purpose are DNT and MP. However, there is still no effective treatment to prevent the effects of secondary injury.[4]

After SCI, changes in antioxidant enzyme activities such as superoxide dismutase (SOD), catalase (CAT) and glutathione peroxidase (GPx) can be observed. Decreased SOD and GPx activities in rats after SCI have been reported in the literature.[22,23] In contrast, Nishibe et al., reported no change in total SOD activity in SCI-induced dogs, but a significant reduction in CAT activity was reported.[24] In an experimental study by Cavus et al., in which SCI was induced in rats, it was found that SOD levels were significantly higher in the trauma group and no significant difference was found in GPx and CAT levels between the groups.[10] In our experimental study, GSH, MDA and NO levels were investigated through a biochemical analysis of blood and bladder tissue.

After SCI, systemic inflammation may be triggered and inflammation may develop in distal organs.[2] Irregularities in the neuroendocrine system and changes in neuroimmune regulation are the determining factors in the onset and progression of systemic inflammation after SCI.[2] Spinal cord injury activates the hypothalamic–pituitary–adrenal axis, leading to an increase in the macrophage migration inhibitory factor produced by the pituitary gland. Macrophage migration inhibitory factor is thought to play an important role in the progression of systemic inflammation.[2] Acute treatment after SCI may contribute to healing by suppressing neuroinflammation.[25,26] Studies of SCI in animal models have reported that hemorrhage and inflammatory changes occur in the post-SCI period. Torres et al. found in their study about bladder morphology in SCI rabbits that there was a significant increase in hemorrhage and inflammation in the bladder after 32 h of SCI, and inflammatory infiltration in the bladder was reported to be significantly less pronounced in the DNT group on day 8.[16] Anti-inflammatory treatment may be beneficial in the treatment of neurogenic bladder by inhibiting the inflammatory response.[2,27] Studies have reported that antioxidants such as DNT after SCI contribute to healing of mesenteric lesions by reducing hemorrhage and immunocyte infiltration in the bladder.[2,16,20] In our current study, unlike the literature, there was no difference between the experimental groups in terms of inflammation in the bladder. This may be due to the inadequate development of inflammation in the first 24 h. If more than 24 h of changes had been investigated, perhaps different results could be obtained in terms of edema and inflammation. When compared to the control group,

it was observed that all groups had increased bladder tissue edema. Edema in the DNT group was less pronounced than in other groups which received other drugs. When compared to the control group, it was observed that all groups had increased bladder congestion. Among the drug-administered groups, the DNT+MP combination group was found to be the group with the least congestion.

In traumatic SCI, lipid peroxidation is one of the important trigger components of neuronal degeneration. The increase in lipid peroxidation may be due to an insufficiency of enzymatic and non-enzymatic defense mechanisms. For this reason, the prevention of lipid peroxidation may be important for neurological recovery. Malondialdehyde results from the effect of reactive oxygen radicals on membrane lipids. It is one of the most important indicators of lipid peroxidation and its blood and tissue levels increases after oxidative stress.[4,20,28] In studies conducted, it has been reported that MDA levels in the blood and tissues are increased in animal models with traumatic SCI. In the study of Aslan et al., it was reported that blood MDA levels were significantly increased, and after using DNT blood MDA levels significantly decreased in animal models of SCI. In the same study, it was reported that the MDA level in cerebrospinal fluid significantly increased after DNT treatment but there was no significant change of MDA level in spinal cord tissue.[5] In another study of animal models of SCI, increased MDA levels were reported to be significantly reduced in MP-treated groups.[28] In our study, an increase in MDA levels was also detected in the bladder tissue along with the increase in the levels of the corresponding MDA levels in blood. Reducing the level of MDA, an oxidative stress indicator, may be effective in reducing oxidative stress-related damage. Single or combined use of DNT, which has anti-lipid peroxidative and neuroprotective properties, or MP, which is a glucocorticoid agent with anti-inflammatory properties, reduced MDA levels both in blood and bladder tissue. These findings are evidence supporting the clinical utility of DNT and MP in preventing oxidative damage in post-traumatic SCI.

Glutathione, an important cellular antioxidant, is a thiol-containing tripeptide. It has important biological functions in the defense against the potential damage of oxidative stress. Glutathione protects the cells from possible damage by reacting with free radicals.[5,28,29] Decreased levels of GSH during increased oxidative stress have been reported. A significant increase in GSH levels was observed after MP treatment in experimental animal models of SCI designed by Ates et al.[28] In another study, GSH levels decreased significantly after DNT therapy in animal models of SCI. However, spinal fluid and spinal cord tissue GSH levels were not reported to increase significantly in response to DNT therapy.[5] Cevik et al. investigated the effect of quercetin on rat bladder after SCI and found a significant decrease in GSH levels after SCI in the bladder tissue.[20] In our present work, there was a significant decrease in blood GSH levels after SCI, but there was no significant change in GSH levels in bladder tissue after SCI. The decrease in blood GSH levels in SCI animal models is consistent with the results reported in the literature. No significant change in GSH levels in the bladder tissue of the experimental groups was a similar result as in the literature in which no change in GSH levels was reported in cerebrospinal fluid and the spinal cord. However, the decrease in GSH level in the bladder tissue was not found to be significant compared to the literature. These results suggest that the evaluation of post-SCI levels of GSH in blood is more valuable than evaluating tissue samples. In our study, it was found that DNT and MP had no effect on increasing blood GSH levels when used as single therapy, but showed a significant effect when combined, increasing blood GSH levels. Therefore, combined treatment of DNT and MP at different doses should be investigated as a new therapeutic alternative to increase the level of GSH, which is an important antioxidant.

Nitric oxide is an inorganic free radical gas molecule produced from L-arginine under the influence of NO synthase isoenzymes (iNOS, nNOS and eNOS).[28,30] Nitric oxide is a molecule with both antioxidant and pro-oxidant properties. It is a chain-breaking antioxidant in free radical-mediated lipid peroxidation.[4,31,32] It is involved in some physiological processes, such as regulation of blood vessel walls and neurotransmission, when within physiological limits. However, in situations such as oxidative stress, excessive elevations in NO levels may be detrimental to tissues.[28,33] In non-pathological situations, the NO concentration is in the nanomolar range, but in oxidative damage situations – in the micromolar range.[31,32] In SCI animal models, there was a significant increase in NO levels in the spinal cord after trauma, and there was a significant decrease in tissue NO levels in the MP group.[28] In another study, NO levels were assessed in experimental rabbits with SCI which were given DNT, and there was no difference between the experimental groups in terms of blood and cerebrospinal fluid NO levels.[5] Similar to studies that reported an increase in NO levels after oxidative stress, we also observed a significant increase in blood NO levels in all rabbits after SCI compared to the control group. In experimental groups receiving DNT and DNT+MP, NO levels in bladder tissue also decreased significantly. In our study, DNT and MP were observed to cause a decrease in NO levels in the bladder tissue. This result supports studies that reported a decrease in NO levels in spinal cord and bladder tissue in response to anti-inflammatory treatment in SCI animal models.

In summary, there was no significant increase of inflammation in the bladder tissue at the early stage after traumatic SCI, but there was a significant increase in edema and congestion. There was a significant increase in MDA levels in both blood and bladder tissue. On the other hand, for GSH levels, there was a significant decline in blood, but there was no significant change in bladder tissue. A significant increase was observed in NO levels after traumatic SCI. For reducing edema, use of DNT only was significantly effective, and for reducing congestion, combined

use of DNT and MP was found to be effective. The blood NO level was highest in the MP group. In bladder tissue, the DNT and DNT+MP groups showed a significant decrease in NO level. While single or combined use of DNT and MP was successful in reducing blood MDA levels and no superiority was observed between them, it was observed that DNT+MP was more effective in increasing the level of GSH after oxidative stress.

Such experimental studies are very important in the development of treatment strategies aimed at improving human health after post-traumatic SCI. Potential therapeutic benefits of single or combined use of DNT and MP, along with other treatment approaches, may be seen in reducing the effects of oxidative stress and secondary damage in the bladder following traumatic SCI. The results obtained in our experimental study suggest that combined use of DNT and MP after SCI can be more effective and beneficial in preventing the formation of damage due to oxidative stress in the bladder, providing additional protection. For this reason, the combined use of DNT and MP can be considered as a promising therapeutic strategy. Human clinical trials with an extensive series of treatment strategies in different doses and combined use of DNT and MP are needed in preventing post-SCI damage in the bladder after SCI. In the future, with well-designed experimental studies, it will be a more realistic approach to apply the results of DNT and MP in different doses and combined administration in clinical practice.

References

1. Lasfargues JE, Custis D, Morrone F, et al. A model for estimating spinal cord injury prevalence in the United States. *Paraplegia*. 1995;33(2): 62–68.
2. Sun X, Jones ZB, Chen XM, Zhou L, So KF, Ren Y. Multiple organ dysfunction and systemic inflammation after spinal cord injury: A complex relationship. *J Neuroinflammation*. 2016;3(1):260.
3. Wu J, Yang H, Qiu Z, Zhang Q, Ding T, Geng D. Effect of combined treatment with methylprednisolone and Nogo-A monoclonal antibody after rat spinal cord injury. *J Int Med Res*. 2010;38(2):570–582.
4. Anwar MA, Al Shehabi TS, Eid AH. Inflammogenesis of secondary spinal cord injury. *Front Cell Neurosci.* 2016;10:98.
5. Aslan A, Cemek M, Buyukokuroglu ME, et al. Dantrolene can reduce secondary damage after spinal cord injury. *Eur Spine J*. 2009;18(10): 1442–1451.
6. Tator CH. Review of experimental spinal cord injury with emphasis on the local and systemic circulatory effects. *Neurochirurgie*. 1991; 37(5):291–302.
7. Eaton MJ. Cell and molecular approaches to the attenuation of pain after spinal cord injury. *J Neurotrauma*. 2006;23(3–4):549–559.
8. Tator CH, Fehlings MG. Review of the secondary injury theory of acute spinal cord trauma with emphasis on vascular mechanisms. *J Neurosurg*. 1991;75(1):15–26.
9. Liu D, Li L, Augustus L. Prostaglandin release by spinal cord injury mediates production of hydroxyl radical, malondialdehyde and cell death: A site of the neuroprotective action of methylprednisolone. *J Neurochem*. 2001;77(4):1036–1047.
10. Cavus G, Altas M, Aras M, et al. Effects of montelukast and methylprednisolone on experimental spinal cord injury in rats. *Eur Rev Med Pharmacol Sci*. 2014;18(12):1770–1777.
11. Rosado IR, Lavor MSL, Alves EGL, et al. Effects of methylprednisolone, dantrolene, and their combination on experimental spinal cord injury. *Int J Clin Exp Pathol*. 2014;7(8):4617–4626.
12. Ohkawa H, Ohishi N, Yagi K. Assay for lipid peroxides in animal tissues by Thiobarbituric acid reaction. *Anal Biochem*. 1979;95(2):351–358.
13. Beutler E, Dubon OB, Kelly M. Improved method for the determination of blood glutathione. *J Lab Clin Med*. 1963;61:882–888.
14. Somogyi M. A method for the preparation of blood filtrates for the determination of sugar. *J Biol Chem*. 1930;86:55.
15. Miranda KM, Espey MG, Wink DA. A rapid, simple spectrophotometric method for simultaneous detection of nitrate and nitrite. *Nitric Oxide*. 2001;5(1):62–71.
16. Torres B, Serakides R, Caldeira F, Gomes M, Melo E. The ameliorating effect of dantrolene on the morphology of urinary bladder in spinal cord injured rats. *Pathol Res Pract*. 2011;207(12):775–779.
17. Apodaca G, Kiss S, Ruiz W, Meyers S, Zeidel M, Birder L. Disruption of bladder epithelium barrier function after spinal cord injury. *Am J Physiol Renal Physiol*. 2003;284(5):966–976.
18. Herrera JJ, Haywood-Watson RJ 2nd, Grill RJ. Acute and chronic deficits in the urinary bladder after spinal contusion injury in the adult rat. *J Neurotrauma*. 2010;27(2):423–431.
19. Leung PY, Johnson CS, Wrathall JR. Comparison of the effects of complete and incomplete spinal cord injury on lower urinary tract function as evaluated in unanesthetized rats. *Exp Neurol*. 2007;208(1):80–91.
20. Cevik O, Ersahin M, Sener TE, et al. Beneficial effects of quercetin on rat urinary bladder after spinal cord injury. *J Surg Res*. 2013;183(2): 695–703.
21. Chen X, Cui J, Zhai X, et al. Inhalation of hydrogen of different concentrations ameliorates spinal cord injury in mice by protecting spinal cord neurons from apoptosis, oxidative injury and mitochondrial structure damages. *Cell Physiol Biochem*. 2018;47(1):176–190.
22. Kanter M, Coskun O, Kalayci M, Buyukbas S, Cagavi F. Neuroprotective effects of Nigellasativa on experimental spinal cord injury in rats. *Hum Exp Toxicol.* 2006;25(3):127–133.
23. Erol FS, Kaplan M, Tiftikci M, et al. Comparison of the effects of octreotide and melatonin in preventing nerve injury in rats with experimental spinal cord injury. *J Clin Neurosci.* 2008;15(7):784–790.
24. Nishibe M. Experimental studies on the mechanism of spinal cord ischemia the state of free radical scavengers [in Japanese]. *Hokkaido Igaku Zasshi.* 1989;64(3):301–308.
25. Patel SP, Cox DH, Gollihue JL, et al. Pioglitazone treatment following spinal cord injury maintains acute mitochondrial integrity and increases chronic tissues paring and functional recovery. *Exp Neurol*. 2017;293:74–82.
26. Cabrera Aldana EE, Ruelas F, Aranda C, et al. Methylprednisolone administration following spinal cord injury reduces aquaporin 4 expression and exacerbates edema. *Mediators Inflamm*. 2017;2017: 4792932.
27. Shunmugavel A, Khan M, Hughes Jr FM, Purves JT, Singh A, Singh I. S-Nitroso glutathione protects the spinal bladder: Novel therapeutic approach to post-spinal cord injury bladder remodeling. *Neurourol Urodyn*. 2015;34(6):519–526.
28. Ates O, Cayli S, Altinoz E, et al. Effects of resveratrol and methylprednisolone on biochemical, neurobehavioral and histopathological recovery after experimental spinal cord injury. *Acta Pharmacol Sin*. 2006;27(10):1317–1325.
29. Meister A, Anderson ME. Glutathione. *Annu Rev Biochem*. 1983;52: 711–760.
30. Moncada S, Higgs A. The L-arginine-nitric oxide pathway. *N Engl J Med*. 1993;329(27):2002–2012.
31. Taysi S, Koc M, Büyükokuroğlu ME, Altinkaynak K, Sahin YN. Melatonin reduces lipid peroxidation and nitric oxide during irradiation-induced oxidative injury in the rat liver. *J Pineal Res*. 2003;34(3):173–177.
32. Joshi MS, Ponthier JL, Lancaster JR Jr. Cellular antioxidant and pro-oxidant actions of nitric oxide. *Free Radic Biol Med*. 1999;27(11–12): 1357–1366.
33. Von Euler M, Akesson E, Samuelsson EB, Seiger A, Sundstrom E. Motor performance score: A new algorithm for accurate behavioral testing of spinal cord injury in rats. *Exp Neurol*. 1996;137(2):242–254.

Cognitive features of white matter lesions accompanied by different risk factors of cerebrovascular diseases

Yafei Shangguan[A,C–F], Tao Xiong[B,C,F], Changwei Jiang[C,F], Wei Chen[C,F], Yan Zhang[B,F], Yongpin Zhao[B,F], Guiyin Zhou[C,F], Yulan Fan[C,F], Weimin Liu[E,F]

First People's Hospital of Guiyang, China

A – research concept and design; B – collection and/or assembly of data; C – data analysis and interpretation; D – writing the article; E – critical revision of the article; F – final approval of the article

Advances in Clinical and Experimental Medicine, ISSN 1899–5276 (print), ISSN 2451–2680 (online) *Adv Clin Exp Med*. 2019;28(12):1705–1710

Address for correspondence
Weimin Liu
E-mail: weiminliu7@163.com

Funding sources
This study was supported by Guiyang High-level Innovative Talents Project, project No. 27 ZWKJHTZDC [2013].

Conflict of interest
None declared

Received on June 4, 2018
Reviewed on January 8, 2019
Accepted on June 27, 2019

Published online on November 28, 2019

Abstract

Background. The relationship between different risk factors and the cognitive impairment of white matter lesions (WML) remains poorly understood.

Objectives. To investigate the features of cognitive impairment of patients diagnosed with WML accompanied by different risk factors of cerebrovascular diseases.

Material and methods. A total of 157 cases of WML patients were divided into no risk factor group (n = 26), hypertension group (n = 35), diabetes mellitus group (n = 27), dyslipidemia group (n = 30), and mixed factors group (n = 39).

Results. The severity of WML (Fazekas score) in the hypertension and mixed factors groups was higher than in the non-risk factors group. The Montreal Cognitive Assessment (MoCA) scores in the hypertension and mixed factors groups were lower than in the non-risk factors group. The scores of MoCA, immediate memory and delayed recall in the hypertension and mixed factors groups with Fazekas score ≥3 were lower than in the peer group with Fazekas score <3. The scores of MoCA and immediate memory in the hypertension and mixed factors groups with Fazekas score ≥3 were lower than in the non-risk factors group with Fazekas score ≥3.

Conclusions. Hypertension aggravates the severity of WML and cognitive impairment. The severity of WML is positively correlated with the severity of cognitive impairment accompanied by these risk factors.

Key words: cerebrovascular disease, cognitive impairment, atherosclerosis risk factors, white matter lesions

Cite as
Shangguan Y, Xiong T, Jiang C, et al. Cognitive features of white matter lesions accompanied by different risk factors of cerebrovascular diseases. *Adv Clin Exp Med*. 2019;28(12):1705–1710. doi:10.17219/acem/110324

DOI
10.17219/acem/110324

Introduction

White matter lesions (WML), also known as leukoaraiosis (LA), are common imaging results and are correlated with the incidence of stroke, cognitive impairment, gait disorder, falls, depression, and death.[1,2] They are associated with multiple pathologies, which include apoptosis, edema, widening of perivascular space, demyelination, axonal damage, gliocyte proliferation, and infarction. They are also accompanied by changes of the small blood vessels, such as fibrohyalinosis and venous collagenosis. The primary cause of WML is thought to be chronic ischemia.[2] Hypertension, diabetes mellitus and hyperlipidemia, as well as WML itself, are risk factors for vascular cognitive impairment (VCI).[3,4] Different risk factors can cause the formation of cognitive impairment with different mechanisms[5–7] and may also exert different effects on cognitive function. However, the relationship between different risk factors and cognitive impairment of WML remains poorly understood. Therefore, this research focuses on WML patients presenting different risk factors of cerebrovascular diseases. Cranial imaging scale of cognitive function was used to analyze the features of cognitive functional impairment and determine the factors relevant for identifying and preventing cognitive impairment caused by WML during the early stage of cognitive impairment.

Material and methods

Patients

The general clinical characteristics of the patients and the related data of each group are presented in Table 1. There were no statistical differences in terms of sex ratio, age, years of education, activities of daily living (ADL) scale, or Hamilton Depression (HAMD) scale among the different risk factor groups.

A total of 157 patients were enrolled, including 57 males and 100 females, aged 70.4 ±9.1 years on average (range: 41–87 years), with a mean education level of 9.8 ±4.2 years (range: 0–16 years), from the Department of Neurology in the First People's Hospital of Guiyang, China, from January 2014 to December 2015. This study was approved by the Ethics Committee of the First People's Hospital of Guiyang. Written informed consents were obtained from all participants.

Inclusion criteria were as follows: older than 40 years; magnetic resonance imaging (MRI) of brains indicating WML (varying degrees); no history of cerebrovascular diseases (including hemorrhagic and ischemic cerebrovascular diseases); and no specific diseases causing central nervous injury and related medical history, such as tumor, infection, carbon monoxide poisoning, demyelinating disease of the central nervous system, and degenerative diseases.

Exclusion criteria were the following: previously confirmed cognitive impairment; factors that affect the results of measuring cognitive function (patients with related neuropsychiatric history or depression, taking antidepressant drugs, with hypothyroidism, visual and hearing disorder, and with hemiplegia, hemidysesthesia, aphasia, and other physical signs of focal central nervous system disorders and/or cerebral hemorrhage or cerebral infarction verified with related imaging evidence); other diseases or medical history causing central nervous injuries; excessive drinking; heart, liver and kidney failure.

Grouping

All WML patients included were grouped according to different risk factors and divided into 5 groups: a no risk factor group, a hypertension group, a diabetes mellitus group, a dyslipidemia group, and a mixed factor group (including 2 or more types of the above risk factors). Hypertension referred to the patients who currently took orally antihypertensive drugs or whose multiple blood pressure values were higher than 140/90 mm Hg, but they were not taking medication; diabetes mellitus referred to the patients who had been diagnosed previously and/or who were currently taking insulin or oral hypoglycemic drugs for treatment; dyslipidemia referred to the patients whose total cholesterol was higher than 5.7 mmol/L, low-density lipoprotein (LDL) was higher than 3.12 mmol/L, high-density lipoprotein was lower than 1.20 mmol/L, and triglyceride was higher than 1.88 mmol/L.

Table 1. Clinical qualitative characteristics of different risk factor groups

Variables	No risk factor group	Hypertension group	Diabetes group	Dyslipidemia group	Mixed factors group
Cases, n	26	35	27	30	39
Male/female	10/16	13/22	10/17	10/20	14/25
Age [years]	69.73 (12.58)	72.03 (6.95)	63.55 (6.15)	70.33 (8.88)	71.36 (8.337)
Education [years]	9.31 (4.35)	10.86 (3.66)	11.82 (3.25)	9.53 (4.23)	8.85 (4.68)
ADL [points]	21.12 (3.39)	21.83 (3.27)	20.63 (1.03)	20.70 (1.32)	21.41 (3.24)
HAMD [points]	4.09 (1.64)	4.94 (1.19)	5.09 (1.38)	5.30 (1.47)	5.15 (1.25)

ADL – activities of daily living scale; HAMD – Hamilton Depression scale.

Imaging evaluation

The degree of WML could be quantified and evaluated using MRI adopting the Fazekas scale (the lowest total score is 0, the highest – 6).[8] The changes of periventricular and deep cerebral white matter were evaluated and the total scores was obtained through generalizing the scores of the 2 parts. The respective scores meant for periventricular white matter hyperintense signals: 0 – absence; 1 – cap shape or pencil-thin lining; 2 – smooth halo; 3 – irregular periventricular hyperintense signals spreading into deep white matter. For deep white matter hyperintense signals the scores meant: 0 – absence; 1 – point-like foci; 2 – starting confluence of point-like foci; 3 – large confluent areas. Cranial MRI was jointly judged by clinical neurologists and radiologists.

Neuropsychological assessment

The Montreal Cognitive Assessment (MoCA) scale and auditory verbal memory test (including immediate word recall, delayed word recall and word recognition) were used to evaluate the cognitive function. Blind operation and judgment of results were carried out by well-trained neurologists. The ADL scale was used to evaluate the general conditions of patients, while the HAMD scale was used for exclusion of patients with depression.

Blood biochemical test

Fasting venous blood was collected from the patients (fast for 8 h) for analysis of liver function, renal function, blood lipids, blood glucose, uric acid, and thyroid function to monitor the general conditions of the patients.

Statistical analysis

Data analysis was performed using SPSS v. 18.0 software (SPSS Inc., Chicago, USA). The data was presented as mean ± standard deviation (SD). Enumeration data was compared with a χ^2 test. The comparison for quantitative data among multiple groups was assessed with one-way analysis of variance (ANOVA) followed by the post-hoc Bonferroni test. A p-value of less than 0.05 was considered as statistical significance.

Results

Comparison of WML and cognition in different risk factor groups

White matter lesions severity (Fazekas score) in the hypertension and mixed factors groups was higher than that in the no risk factor group (p = 0.022; Fig. 1A); there was no statistical difference among other groups. The MoCA scores of the hypertension group and mixed factors group were lower than in the no risk factor group (p = 0.018; Fig. 1B) without statistical difference among the other groups. In addition, there were no statistical differences regarding the comparisons of immediate word recall, delayed word recall and word recognition among all groups (Fig. 1C–E).

The effect of WML degree on cognition

According to Fazekas scoring, WML severity can be divided into a Fazekas score <3 group and the studied population. Comparing the association of different WML severities with cognitive impairment in all groups, we found that the MoCA score, immediate word recall score and delayed word recall score of patients with a Fazekas score ≥3 in the hypertension group and mixed factor group were lower than of those with a Fazekas score <3 in the same groups (p = 0.031; Table 2). In addition, we found that the MoCA score and immediate word recall score of patients with a Fazekas score ≥3 in the hypertension group and mixed factor group were lower than of those with a Fazekas score ≥3 in the no risk factor group (p = 0.022; Table 2). There were no statistical significances for the comparison of the MoCA score, immediate word

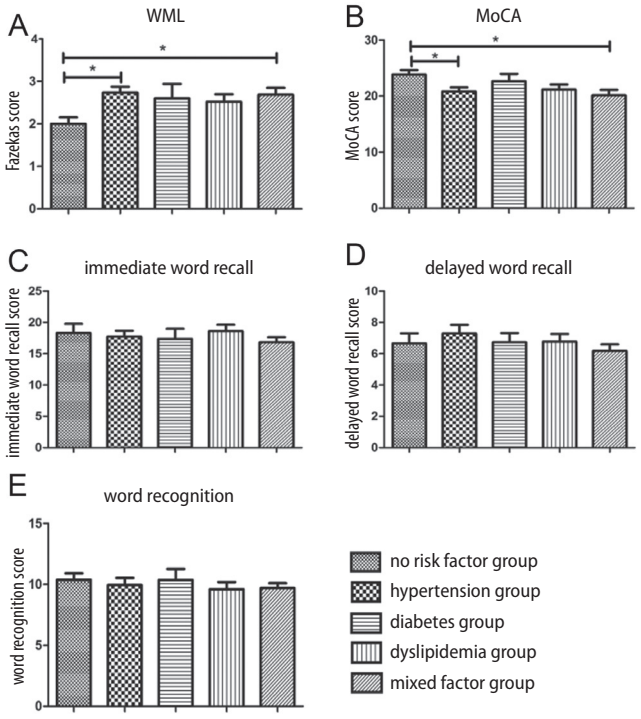

Fig. 1. Comparison of WML and cognitive scores among different risk factor groups. A. Fazekas score indicated that the WML severity of the hypertension group and mixed factors group was higher than that of the no risk factor group, and there was no statistical difference among other groups. B. MoCA scores of the hypertension group and mixed factor group were lower than that of the no risk factor group, without statistical difference among other groups. C–E. There were no statistical differences in terms of the comparisons of immediate word recall, delayed word recall and word recognition among these groups

* p < 0.05 – statistical significance.

Table 2. Quantitative comparisons of different WML severities on cognition in each risk factor group

Group	Fazekas score	Cases (%)	MoCA	Immediate word recall	Delayed word recall	Word recognition
No risk factor group	<3	20 (76.9)	24.05 (4.26)	19.64 (7.09)	10.88 (6.96)	10.77 (2.37)
	≥3	6 (23.1)	22.30 (7.53)	18.10 (4.00)	5.50 (1.73)	8.25 (3.59)
Hypertension group	<3	15 (42.9)	23.26 (4.38)	19.48 (6.62)	12.94 (8.06)	10.74 (3.32)
	≥3	20 (57.1)	18.50 (3.48)*#	14.67 (5.10)*#	5.17 (2.69)*	8.42 (3.32)
Diabetes group	<3	13 (48.1)	22.63 (4.75)	18.50 (5.32)	11.56 (6.42)	10.25 (2.31)
	≥3	14 (51.9)	22.67 (4.04)	18.67 (5.67)	7.00 (2.00)	10.67 (5.13)
Dyslipidemia group	<3	18 (60.0)	22.05 (3.64)	19.42 (6.25)	11.67 (7.68)	9.42 (3.39)
	≥3	12 (40.0)	19.64 (6.39)	17.18 (4.54)	6.00 (2.00)	9.91 (3.21)
Mixed factor group	<3	18 (46.1)	23.05 (4.26)	18.55 (5.59)	10.68 (5.83)	10.09 (2.86)
	≥3	21 (53.9)	17.00 (7.00)*#	14.59 (3.08)*#	5.00 (2.34)*	9.18 (1.81)

* MoCA score, immediate word recall score and delayed word recall score in the hypertension group and mixed factor group with Fazekas ≥3 are lower than those in the same groups with Fazekas score <3, $p < 0.05$.
# MoCA score and immediate word recall score of the hypertension group and mixed factor group with Fazekas score ≥3 are lower than those of the no risk factor group with Fazekas score ≥3, $p < 0.05$. There was no statistical significance on the comparisons of MoCA, immediate word recall, delayed word recall, and word recognition among all risk factor groups with Fazekas score <3.

recall score, delayed word recall score, and word recognition score among all risk factor groups when patients with Fazekas score <3 were concerned (Table 2).

Discussion

With the continuous development of neuroimaging technology, the detection rate of WML is significantly improved. The imaging description of WML is manifested with symmetricly speckled or patchy changes of periventricular and centrum ovale white matter. Magnetic resonance T2-weighted image shows high signal intensity, whereas T1-weighted image reveals equal or low signal intensity. In clinical practice, WML is a prevalent disease associated with multiple neurologic disorders,[1] especially with cognitive impairment.[9,10] Some risk factors of cerebrovascular diseases, such as hypertension and diabetes mellitus, can lead to the development of WML.[5–7] However, the relationship between the different risk factors and cognitive impairment in consequence of WML remains unclear. This study aimed to investigate the cognitive impairment features of WML accompanied with different risk factors of cerebrovascular diseases.

The influence of severity of WML on cognition

Scott et al.[3] found that in aged people with normal cognition, WML is widely thought to be the sign of cerebral small vessel disease, which is associated with vascular injury caused by vascular risk factors, including hypertension, high cholesterol and diabetes mellitus. Medical history of hypertension is independently associated with WML capacity. Our study has also found that the WML (measured with Fazekas scoring) in the hypertension and mixed factor groups is more severe than in the no risk factor group. Some scholars have found that MoCA is more sensitive than Mini-Mental State Examination (MMSE) in detecting the cognitive impairment in WML patients.[11] Therefore, we evaluated the patients' congnition by using MoCA scale and auditory verbal memory, and found that MoCA scores in the hypertension and mixed factor groups were lower than in the no risk factor group, and there was no statistical significance in immediate word recall, delayed word recall and word recognition among all groups. Sierra[12] found that hypertensive patients are more prone to WML than normotensive people, and that arteriosclerosis of the cerebral perforator vessel is the primary cause of ischemic WML. In patients with declining cognition and dementia, chronic ischemia of white matter is associated with arteriosclerosis and/or the lipohyalinosis of small perforating artery hypertension, and antihypertensive treatment can reduce the risk of dementia.[13] In the elderly populations, excessive variation of self-measured systolic blood pressure aggravates the progress of cognitive functional impairment and WML.[14] The study of Peng et al.[15] found that systolic blood pressure controlled within 140–160 mm Hg and systolic blood pressure reduced by 15–35 mm Hg are beneficial in delaying the progression of cognitive impairment and WML. Our study found that the severity of WML and MoCA score in the hypertension and mixed factor groups were statistically different from those in the no risk factor group, and there were no statistical differences between the diabetes mellitus group/dyslipidemia group and no risk factor group. However, some scholars have found that diabetes mellitus and dyslipidemia were associated with WML,[4,16] leading to declined cognition[17] and increased risk of vascular dementia.[6] Considering the effect of diabetes mellitus and dyslipidemia in the mixed factor group, the sample size should be increased to further investigate the independent effect of diabetes mellitus and dyslipidemia on WML and cognition in subsequent research.

Fazekas score and severe WML

The MoCA score, immediate word recall score and delayed word recall score of patients from the hypertension group and mixed factor group with Fazekas score ≥3 were lower than of those from the same groups with Fazekas score <3. The MoCA score and immediate word recall score of patients from the hypertension group and mixed factor group with Fazekas score ≥3 were lower than of those from the no risk factor group with Fazekas score ≥3, but there were no statistical differences in the comparisons of those from all risk factor groups with Fazekas score <3. Therefore, we speculate that the severity of WML in the hypertension group and mixed factors group is positively correlated with cognitive functional impairment, and that the cognitive impairment in WML with risk factors is more severe than that in WML with no risk factors. Defrancesco et al.[18] have found that patients with mild cognitive impairment (MCI) converting to Alzheimer's disease (AD) obtain higher periventricular Fazekas scores and present more severe WML. Periventricular WML is associated with low cognitive function of MCI patients, which is consistent with the findings of our study. The severity of WML accelerates the progression of MCI.[19] Maillard et al.[20] found that increased WML is obviously related to the decline of episodic memory and executive function, and the progression of WML is related to cognition. Some studies have shown that the more severe the damage to periventricular white matter is, the higher the risk of dementia,[21] and cognitive impairment of WML is associated with the severity of WML.[22] The white matter is mainly supplied by the vertical short branch of the terminal artery with less anastomotic branches and poor collateral circulation.[16] Therefore, the blood flow volume in the white matter is lower than in the grey matter. In addition, the risk factors of cerebrovascular diseases cause damage in small cerebral blood vessels, so less cerebral blood flow and insufficient cerebral perfusion will lead to ischemic injury in the white matter. Therefore, the cognitive impairment of WML accompanied with the risk factors of cerebrovascular diseases may be more severe than in WML with no risk factors.

Effect of risk factors on severity of WML

The MoCA scale includes the detection of multiple aspects of cognitive impairment such as memory, execution, language, attention, and orientation. Auditory verbal memory is an extension of the memory test. Our study found that MoCA, immediate word recall and delayed word recall were influenced by the WML severity in the hypertension group and mixed factor group, and MoCA and immediate word recall in the hypertension group and mixed factor group were statistically different than in no risk factor group, suggesting that WML had comprehensive effects on cognition. Te et al.[23] believed that WML patients with MCI obviously presented the declining of memory and attention, damage of executive function and close connection with dementia in the early days. Zi et al.[24] found out that a cognitive test for patients with periventricular high signal lesion shows obvious declining of word fluency and executive function. In addition, Vasquez et al.[25] found that the processing speed and executive function in VCI are poorer. White matter lesions are an early predictive index of dementia risk, but this association is dependent on cognitive reserve, age and spatial distribution of the lesions.[26] Some studies have shown that the brain white matter of the elderly was obviously less smaller in volume than that of a middle-aged group, and the brain white matter of the middle-aged was obviously less smaller in volume than that of a youth group.[7] A low education level group (≤8 years of education) presented increased risk of severe WML developing into MCI and dementia, but there were no such risks in a high education level group (>8 years of education).[27] In our study, there were no significant differences in age and years of education among all the groups, and the effect of these factors upon the study results was not considered.

Effect of WML on automatic activity

Severe WML results in a more than twofold increase of the risk of transition from automatic activities to activity dependence. White matter lesions are associated with a decline of cognitive and athletic ability, depressive symptoms related to aging and vascular diseases, dysfunction of the urinary system, and various abnormities of the nervous system.[28] Such lesions are the primary cause of falls.[29,30] Al-Mashhadi et al.[31] found that the dysfunction of WML is not confined to lesions, and that the normal white matter is also damaged. In view of the perniciousness of WML, we need to identify and impede the risk factors, aiming to prevent the progression and improve cognitive prognosis. A study found that L-carnitine can improve WML and prevent cognitive impairment of a chronic hypo-perfusion model,[32] and another study found that supplementation of 6-g L-arginine in diet is beneficial to improving the cognition and preventing gait disorders of WML patients.[33]

Study limitation

In this study, the interaction between variables was not considered and analyzed, which might affect the statistical results. We will consider and analyze this point in further investigation.

Conclusions

Hypertension and multiple risk factors of cerebrovascular diseases will aggravate the severity of WML and cognitive impairment, and the severity of WML accompanied

with these risk factors is positively correlated with the degree of cognitive impairment. However, the damage of cognitive domains of WML affected with WML accompanied by different risk factors of cerebrovascular diseases may be different. Therefore, we plan to expand the sample size to compare execution, attention, language, orientation, and other cognitive domains in the future. We need to further investigate the cognitive features of WML accompanied by diabetes mellitus and dyslipidemia, aiming to comprehensively understand the features of cognitive impairment in WML accompanied by different risk factors of cerebrovascular diseases.

ORCID iDs

Yafei Shangguan https://orcid.org/0000-0002-5272-1972
Tao Xiong https://orcid.org/0000-0001-8247-8582
Changwei Jiang https://orcid.org/0000-0001-9728-6209
Wei Chen https://orcid.org/0000-0003-0171-194X
Yan Zhang https://orcid.org/0000-0002-3566-2907
Yongpin Zhao https://orcid.org/0000-0003-2979-1478
Guiyin Zhou https://orcid.org/0000-0003-2870-1178
Yulan Fan https://orcid.org/0000-0002-7021-0770
Weimin Liu https://orcid.org/0000-0001-6966-0101

References

1. O'Brien JT. Clinical significance of white matter changes. *Am J Geriatr Psychiatry*. 2014;22(2):133–137.
2. Miki Y, Sakamoto S. Age-related white matter lesions (leukoaraiosis): An update [in Japanese]. *Brain Nerve*. 2013;65(7):789–799.
3. Scott JA, Braskie MN, Tosun D, et al; Alzheimer's Disease Neuroimaging Initiative. Cerebral amyloid and hypertension are independently associated with white matter lesions in elderly. *Front Aging Neurosci*. 2015;7:221.
4. Bowler JV. The concept of vascular cognitive impairment. *J Neurol Sci*. 2002;203–204:11–15.
5. Akiguchi I, Yamamoto Y. Vascular mechanisms of cognitive impairment: Roles of hypertension and subsequent small vessel disease under sympathetic influences. *Hypertens Res*. 2010;33(1):29–31.
6. Xu W, Qiu C, Gatz M, Pedersen NL, Johansson B, Fratiglioni L. Mid- and late-life diabetes in relation to the risk of dementia: A population-based twin study. *Diabetes*. 2009;58(1):71–77.
7. Brickman AM, Zimmerman ME, Paul RH, et al. Regional white matter and neuropsychological functioning across the adult lifespan. *Biol Psychiatry*. 2006;60(5):444–453.
8. Fazekas F, Chawluk JB, Alavi A, Hurtig HI, Zimmerman RA. MR signal abnormalities at 1.5 T in Alzheimer's dementia and normal aging. *AJR Am J Roentgenol*. 1987;149(2):351–356.
9. Prins ND, van Dijk EJ, den Heijer T, et al. Cerebral small-vessel disease and decline in information processing speed, executive function and memory. *Brain*. 2005;128(Pt 9):2034–2041.
10. Benedictus MR, van Harten AC, Leeuwis AE, et al. White matter hyperintensities relate to clinical progression in subjective cognitive decline. *Stroke*. 2015;46(9):2661–2664.
11. Li J, Hu W. Glucose metabolism measured by positron emission tomography is reduced in patients with white matter presumably ischemic lesions. *Med Sci Monit*. 2014;20:1525–1530.
12. Sierra C. Essential hypertension, cerebral white matter pathology and ischemic stroke. *Curr Med Chem*. 2014;21(19):2156–2164.
13. Hanon O. Hypertension and dementia [in French]. *Ann Cardiol Angeiol (Paris)*. 2014;63(3):204–208.
14. Liu Z, Zhao Y, Zhang H, et al. Excessive variability in systolic blood pressure that is self-measured at home exacerbates the progression of brain white matter lesions and cognitive impairment in the oldest old. *Hypertens Res*. 2016;39(4):245–253.
15. Peng J, Lu F, Wang Z, et al. Excessive lowering of blood pressure is not beneficial for progression of brain white matter hyperintensive and cognitive impairment in elderly hypertensive patients: 4-year follow-up study. *J Am Med Dir Assoc*. 2014;15(12):904–910.
16. Tullberg M, Fletcher E, DeCarli C, et al. White matter lesions impair frontal lobe function regardless of their location. *Neurology*. 2004;63(2):246–253.
17. Williamson JD, Launer LJ, Bryan RN, et al; Action to Control Cardiovascular Risk in Diabetes Memory in Diabetes Investigators. Cognitive function and brain structure in persons with type 2 diabetes mellitus after intensive lowering of blood pressure and lipid levels: A randomized clinical trial. *JAMA Intern Med*. 2014;174(3):324–333.
18. Defrancesco M, Marksteiner J, Deisenhammer E, Kemmler G, Djurdjevic T, Schocke M. Impact of white matter lesions and cognitive deficits on conversion from mild cognitive impairment to Alzheimer's disease. *J Alzheimers Dis*. 2013;34(3):665–672.
19. Devine ME, Fonseca JA, Walker Z. Do cerebral white matter lesions influence the rate of progression from mild cognitive impairment to dementia? *Int Psychogeriatr*. 2013;25(1):120–127.
20. Maillard P, Carmichael O, Fletcher E, Reed B, Mungas D, DeCarli C. Coevolution of white matter hyperintensities and cognition in the elderly. *Neurology*. 2012;79(5):442–448.
21. Prins ND, van Dijk EJ, den Heijer T, et al. Cerebral white matter lesions and the risk of dementia. *Arch Neurol*. 2004;61(10):1531–1534.
22. Loeb C, Gandolfo C, Croce R, Conti M. Dementia associated with lacunar infarction. *Stroke*. 1992;23(9):1225–1229.
23. Te M, Zhao E, Zheng X, Sun Q, Qu C. Leukoaraiosis with mild cognitive impairment. *Neurol Res*. 2015;37(5):410–414.
24. Zi W, Duan D, Zheng J. Cognitive impairments associated with periventricular white matter hyperintensities are mediated by cortical atrophy. *Acta Neurol Scand*. 2014;130(3):178–187.
25. Vasquez BP, Zakzanis KK. The neuropsychological profile of vascular cognitive impairment not demented: A meta-analysis. *J Neuropsychol*. 2015;9(1):109–136.
26. Mortamais M, Artero S, Ritchie K. Cerebral white matter hyperintensities in the prediction of cognitive decline and incident dementia. *Int Rev Psychiatry*. 2013;25(6):686–698.
27. Mortamais M, Portet F, Brickman AM, et al. Education modulates the impact of white matter lesions on the risk of mild cognitive impairment and dementia. *Am J Geriatr Psychiatry*. 2014;22(11):1336–1345.
28. Pantoni L, Fierini F, Poggesi A. Impact of cerebral white matter changes on functionality in older adults: An overview of the LADIS Study results and future directions. *Geriatr Gerontol Int*. 2015;15(Suppl 1):10–16.
29. Morley JE. White matter lesions (leukoaraiosis): A major cause of falls. *J Am Med Dir Assoc*. 2015;16(6):441–443.
30. Ogama N, Sakurai T, Shimizu A, Toba K. Regional white matter lesions predict falls in patients with amnestic mild cognitive impairment and Alzheimer's disease. *J Am Med Dir Assoc*. 2014;15(1):36–41.
31. Al-Mashhadi S, Simpson JE, Heath PR, et al; Medical Research Council Cognitive Function and Ageing Study. Oxidative glial cell damage associated with white matter lesions in the aging human brain. *Brain Pathol*. 2015;25(5):565–574.
32. Ueno Y, Koike M, Shimada Y, et al. L-carnitine enhances axonal plasticity and improves white-matter lesions after chronic hypoperfusion in rat brain. *J Cereb Blood Flow Metab*. 2015;35(3):382–391.
33. Calabro RS, Gervasi G, Baglieri A, Furnari A, Marino S, Bramanti P. Is high oral dose L-arginine intake effective in leukoaraiosis? Preliminary data, study protocol and expert's opinion. *Curr Aging Sci*. 2013;6(2):170–177.

Glomerular podocytes in diabetic renal disease

Paweł Podgórski[1,A–E], Andrzej Konieczny[3,A,D–F], Łukasz Lis[1,A,C,E], Wojciech Witkiewicz[1,E,F], Zbigniew Hruby[1,2,A–F]

[1] Voivodeship Specialty Hospital, Center for Research and Development, Wrocław, Poland
[2] Faculty of Health Sciences, Wroclaw Medical University, Poland
[3] Department of Nephrology and Transplantation Medicine, Wroclaw Medical University, Poland

A – research concept and design; B – collection and/or assembly of data; C – data analysis and interpretation;
D – writing the article; E – critical revision of the article; F – final approval of the article

Advances in Clinical and Experimental Medicine, ISSN 1899–5276 (print), ISSN 2451–2680 (online) *Adv Clin Exp Med*. 2019;28(12):1711–1715

Address for correspondence
Zbigniew Hruby
E-mail: z.hruby@wp.pl

Funding sources
None declared

Conflict of interest
None declared

Received on August 17, 2018
Reviewed on October 26, 2018
Accepted on February 18, 2019

Published online on December 18, 2019

Abstract

Diabetic nephropathy (DN) is the most common cause of end-stage renal disease (ESRD), both in the USA and in Europe; moreover, its incidence is rising worldwide. The main laboratory markers of DN progression are albuminuria and a reduction in glomerular filtration rates, although progression of the disease has been observed even in the absence of these biomarkers. Renal impairment, associated with diabetes, results from damage to the glomerular filtration barrier, at the level of highly differentiated glomerular epithelial cells: podocytes. These cells regulate glomerular filtration and many immunological processes occurring at this level. The earliest possible diagnosis of diabetic kidney disease (DKD) and implementation of intensive treatment offers the possibility of preventing or substantially delaying the onset of ESRD. In this article, we review various urinary biomarkers linked with glomerular podocyte cytophysiology as potentially sensitive diagnostic tools for the early detection of DKD. These biomarkers have predictive potential for assessing the progression toward end-stage nephropathy.

Key words: pathogenesis, diabetic kidney disease, podocytes

Cite as
Podgórski P, Konieczny A, Lis Ł, Witkiewicz W, Hruby Z. Glomerular podocytes in diabetic renal disease. *Adv Clin Exp Med*. 2019;28(12):1711–1715. doi:10.17219/acem/104534

DOI
10.17219/acem/104534

Diabetic kidney disease (DKD) or diabetic nephropathy (DN) is a clinical entity developing in patients suffering from diabetes mellitus type 1 or 2, defined as albuminuria (30–300 mg/1 g creatinine in the morning urine sample), worsening of glomerular filtration and arterial hypertension. The prevalence of DN has grown steadily in recent years due to a massive increase of the incidence of diabetes type 2. The International Diabetes Federation forecasts an increase in the number of patients with diabetes mellitus from 285 million worldwide in 2010 to 385 million in 2030.[1] Diabetic kidney disease is the most frequent cause of end-stage renal disease (ESRD), both in Europe[2] and in the USA.[3] In the next decade, the increase is expected to continue. In 2025 the prevalence of diabetic ESRD is predicted to amount to 3.2% per year.[4]

Early diagnosis of DN enables the implementation of strategies preventing progression of chronic renal disease and reducing the risk of potentially lethal cardiovascular injury. Moreover, Fioretto et al. have demonstrated that even established histopathological changes are reversible by normoglycemia following successful pancreatic transplantation in DKD patients.[5]

Currently, the main laboratory markers of DKD progression are albuminuria and glomerular filtration rate (GFR). Nevertheless, at the early stages of DN albuminuria is absent and GFR is elevated. Perkins et al. reported that during a 6-year follow-up of 386 patients with diabetes type 1, regression to normal albumin excretion levels was observed in the majority of patients (58%).[6] The classical model of DN proposed by Mogensen has been modified: In the new DN phenotype, deterioration of GFR is not related to rise of albuminuria, and can even be seen in its absence.[7]

The weakness of albuminuria as a biomarker of DN progression is underscored by observations of significant histopathological alterations in DN with a virtual absence of albuminuria. Therefore, it is not advisable to rely solely on albuminuria and GFR in monitoring disease activity or establishing a prognosis in DKD. At present, no alternative biomarkers of the disease are available. Alternative biomarkers should be sufficiently specific and sensitive for DN without being invasive and expensive. Establishing such markers would permit a significant cohort of patients to be identified at a very early stage of the disease, when albuminuria and GFR are normal, yet the probability of developing full-blown DN is imminent.

This manuscript presents alternative biomarkers of DKD linked with glomerular visceral epithelial cells: podocytes.

The role of podocytes in diabetic kidney disease

Podocytes are differentiated cells lining the external surface of the glomerular basement membrane (GBM). They consist of 3 distinct parts: the cell body, major processes and foot processes (FPs). The FPs of neighboring podocytes interdigitate, forming a meshwork called a slit diaphragm (SD), an ultimate barrier to prevent urinary protein loss.[8–10] The main function of podocytes is therefore to participate in the formation of the filtration barrier and to regulate glomerular filtration, along with the GBM and the endothelium. Podocytes also mechanically support the glomerular vascular bud, participate in the metabolic turnover of the GBM and take part in the immunological processes at the glomerular level.

The development of DN is highlighted by the accumulation of extracellular matrix, the proliferation of mesangial cells and damage to the GBM. These changes are followed by alterations in the renal tubules, interstitium and arterioles. The ultimate changes include sclerotization of the glomerular tufts and fibrosis of the interstitium.[11]

Damage to the podocytes leads to a loss of their adhesive properties and is a principal cause of DN progression.[12,13] It has been demonstrated that the number of glomerular visceral epithelial cells is reduced in diabetes type 1, even after a short disease duration.[14] Moreover, an analysis of the histopathological results of renal biopsies in Pima Indians with diabetes type 2 revealed widening of the FPs, coupled with reductions in the number of podocytes.[15] A morphometric study performed by Dalla Vestra et al. among type 2 diabetes patients determined that diminishment of podocyte density is a more adequate correlate of albuminuria than reduction in the total podocyte number.[16]

Mature podocytes have limited proliferative capacities in situ.[17] Losses of up to 20% of podocytes result in proliferation of the mesangial cells, whereas more substantial losses cause denudation of the GBM with subsequent glomerular fibrosis and increased proteinuria.[18]

Another compensatory mechanism of podocyte injury is their ability to regenerate from progenitor cells, namely glomerular parietal epithelial cells (PEC) and renin-secreting arteriolar wall cells.[19]

It has been demonstrated that podocytes are being excreted in the urine of patients with glomerulopathies, and that the magnitude of podocyturia correlates with the disease activity.[20,21]

Podocyte-dependent pathogenic pathways leading to glomerular injury in DN

Podocyte loss initiating glomerular hypertrophy and subsequent sclerosis may result from hyperglycemia-induced generation of reactive oxygen species (ROS) causing podocyte apoptosis.[22] Changes in glomerular cells are interrelated: endothelial nitric oxide (NO) synthase deficiency may be responsible for podocyte loss resulting in glomerulosclerosis.[23]

Autophagy in podocytes is a homeostatic process enabling lysosomal degradation of obsolete proteins and cell organelles. Chronic exposure to high glucose

concentrations leads to impairment in autophagy with subsequent lysosome insufficiency and podocyte apoptosis, causing development of DN.[24] Thus, activation of autophagy in podocytes may serve as a therapeutic intervention to prevent the progression of DKD.

Poor control of diabetes results in a constant elevation of circulating growth hormone (GH) concentrations, and functional GH receptors are expressed on podocyte cell membranes. As a result, podocyte hypertrophy ensues, accounting for progressive podocyte aberrations leading to the detachment of the GBM[25] with consequent glomerulosclerosis. High levels of GH are equally implicated in kidney hypertrophy and proteinuria during early DN.[26] Growth hormone contributes to renal sclerosis by promoting the synthesis and accumulation of extracellular matrix components.[27] Yet another mechanism of podocyte depletion due to GH activity in early DN is programmed cell death, or apoptosis. Its pathogenesis is linked to 2 possible mechanisms: GH-induced generation of ROS,[28] or exposure to transforming growth factor beta (TGF-β), also resulting from high GH levels.[29]

Epithelial-to-mesenchymal transition (EMT) consists of the acquisition of mesenchymal characteristics by epithelial cells, specifically by proximal tubular cells and podocytes. As a result, these cells undergo transformation to extracellular matrix protein-generating myofibroblasts that initiate and perpetuate fibrosis of renal tissue. Epithelial-to-mesenchymal transition in podocytes results in abnormalities of their functioning, leading to impairment of glomerular filtration.[30] Studies in experimental diabetes have demonstrated phenotypical changes in podocytes: the replacement of an epithelial marker (nephrin) by a mesenchymal marker (desmin).[31] In human studies of podocytes secreted in the urine and renal biopsy specimens of type 2 diabetes patients, it has been demonstrated that a rise in podocyte EMT markers is directly correlated with the clinical and pathological severity of the disease.[32]

Sphingolipid accumulation occurs in glomerular diseases, including DN. Sphingomyelin phosphodiesterase acid-like C3b (SMPDL3b) is expressed in podocytes, where it modulates danger signaling[33] and is linked with the pathogenesis of DN. The intracellular composition of sphingolipids in podocytes impacts the progression of the disease. It has been determined that there is a link between sphingolipid accumulation and glomerular proliferation and hypertrophy in DKD.[34] The accumulation of ceramide seen in apoptotic cells is related to the podocytopenia observed in DKD.

Methods of quantitative and qualitative assessment of podocyturia

Methods for evaluating podocyte injury include histopathological examination of renal biopsy specimens or cytological assessment of podocytes excreted in the urine, taking into account the number, membrane protein expression, mRNA, exosomes, and microRNA.[22] Kidney biopsy is still regarded as the "gold standard" in diagnosing renal parenchymal diseases. Although percutaneous biopsy is widely utilized and relatively safe, certain complications may ensue, such as bleeding from the puncture site or fistula formation. Therefore, attempts have been made to employ the evaluation of urinary podocytes as a diagnostic tool in DKD, since it is a method that is safe, widely available and fully reproducible. The initial approach to the evaluation of urinary podocytes was to establish a culture of podocytes recovered from urinary sediment, with the aim of assessing the expression of their membrane proteins using immunofluorescent visualization.[35,36] It was soon demonstrated that assessment of podocyte antigen expression immediately after the recovery of the cells from urinary sediment by adhesion to a plastic surface provides a useful tool to investigate the importance of podocytes in the progression of glomerular diseases.[37]

The concentration of proteins secreted to the urinary space by damaged podocytes can be measured using the western blot technique. In patients with diabetes, the urinary podocalyxin concentration is higher than the cut-off value in patients at the normoalbuminuric, microalbuminuric and macroalbuminuric stage.[38]

Another way of identifying biomarkers specific to podocytes is to assess mRNA for proteins derived from podocytes in the urine with the real-time polymerase chain reaction (RT-PCR) method.[39] Wang et al. in a study based on 21 biopsy-proven cases of DN, showed a correlation between glomerular podocyte number and intra-renal expression of nephrin, podocin and synaptopodin. The number of glomerular podocytes was also significantly correlated with the urinary expression of synaptopodin, but not with other targets.[39]

In another study, expressions of nephrin, podocin, synaptopodin, WT-1, and alpha actinin-4 were higher in patients with DN than in the normal controls. Urinary nephrin and synaptopodin expressions were correlated with baseline proteinuria or renal function, while WT-1 expression was related to the degree of histological damage.[40]

In recent years, new diagnostic methods like proteomics and peptidomics have gained importance. Rossing et al. used a panel of biomarkers that allowed them to distinguish diabetes subjects with nephropathy with 97% sensitivity and specificity.[41] This panel of biomarkers also identified patients who had microalbuminuria and diabetes and progressed toward overt DN over 3 years. In another study, collagen fragments were shown to be prominent biomarkers 3–5 years before the onset of macroalbuminuria.[42]

Summary

Despite notable improvements in treatment efficacy in recent years and constant broadening of knowledge on the pathogenesis of DKD, end-stage renal failure in the course of DN still remains a challenging problem.

As described in this article, the widely employed, noninvasive biomarkers of DKD such as albuminuria and impairment of glomerular filtration may be insufficient for early diagnosis of diabetic renal injury. More adequate information can be provided by the histopathological features of percutaneous renal biopsies, although the indications for this procedure in the early phase of DN are disputable; moreover, biopsies are invasive and impose the risk of potential complications. As result, alternative diagnostic methods are being evaluated. Growing evidence of the pivotal role of podocytes in the pathogenesis of DN has attracted attention to markers of injury to these cells. The biomarkers of podocytopathy can be quite easily assessed in urine sediment. The expression of proteins linked with podocyte injury or mRNA can be determined using currently available methods such as western blot or RT-PCR.

Future clinical research should focus on validating and confirming the importance of urinary DKD biomarkers with particular emphasis on the early clinical stages of the disease. Up-to-date therapeutic strategies do not bring about complete remission of DN and concentrate on stopping or slowing down the progression of the disease. The earliest possible diagnosis of this entity and implementation of intensive treatment has the potential to prevent or substantially delay the onset of ESRD.

ORCID iDs

Andrzej Konieczny https://orcid.org/0000-0002-4966-9771
Paweł Podgórski https://orcid.org/0000-0002-2225-3469
Łukasz Lis https://orcid.org/0000-0002-4075-6924
Wojciech Witkiewicz https://orcid.org/0000-0002-4194-1160
Zbigniew Hruby https://orcid.org/0000-0002-1369-4705

References

1. Shaw JE, Sicree RA, Zimmet PZ. Global estimates of the prevalence of diabetes for 2010 and 2030. *Diabetes Res Clin Pract*. 2010;87(1):4–14.
2. Kramer A, Pippias M, Noordzij M, et al. The European Renal Association – European Dialysis and Transplant Association (ERA-EDTA) Registry Annual Report 2015: A summary. *Clin Kidney J*. 2018;11(1):108–122.
3. Saran R, Robinson B, Abbott KC, et al. US Renal Data System 2017 Annual Data Report: Epidemiology of kidney disease in the United States. *Am J Kidney Dis*. 2018;71(3 Suppl 1):A7.
4. Kainz A, Hronsky M, Stel VS, et al. Prediction of prevalence of chronic kidney disease in diabetic patients in countries of the European Union up to 2025. *Nephrol Dial Transplant*. 2015;30(Suppl 4):iv113–118.
5. Fioretto P, Steffes MW, Sutherland DE, Goetz FC, Mauer M. Reversal of lesions of diabetic nephropathy after pancreas transplantation. *N Engl J Med*. 1998;339(2):69–75.
6. Perkins BA, Ficociello LH, Silva KH, Finkelstein DM, Warram JH, Krolewski AS. Regression of microalbuminuria in type 1 diabetes. *N Engl J Med*. 2003;348(23):2285–2293.
7. Pugliese G. Updating the natural history of diabetic nephropathy. *Acta Diabetol*. 2014;51(6):905–915.
8. Greka A, Mundel P. Cell biology and pathology of podocytes. *Annu Rev Physiol*. 2012;74:299–323.
9. Mundel P, Shankland SJ. Podocyte biology and response to injury. *J Am Soc Nephrol*. 2002;13(12):3005–3015.
10. Mundel P, Kriz W. Structure and function of podocytes: An update. *Anat Embryol (Berl)*. 1995;192(5):385–397.
11. Hayden MR, Whaley-Connell A, Sowers JR. Renal redox stress and remodeling in metabolic syndrome, type 2 diabetes mellitus, and diabetic nephropathy: Paying homage to the podocyte. *Am J Nephrol*. 2005;25(6):553–569.
12. Steffes MW, Schmidt D, McCrery R, Basgen JM; International Diabetic Nephropathy Study Group. Glomerular cell number in normal subjects and in type 1 diabetic patients. *Kidney Int*. 2001;59(6):2104–2113.
13. Pagtalunan ME, Miller PL, Jumping-Eagle S, et al. Podocyte loss and progressive glomerular injury in type II diabetes. *J Clin Invest*. 1997;99(2):342–348.
14. Kriz W. Podocyte is the major culprit accounting for the progression of chronic renal disease. *Microsc Res Tech*. 2002;57(4):189–195.
15. Lemley KV. A basis for accelerated progression of diabetic nephropathy in Pima Indians. *Kidney Int Suppl*. 2003;83:S38–42.
16. Dalla Vestra M, Masiero A, Roiter AM, Saller A, Crepaldi G, Fioretto P. Is podocyte injury relevant in diabetic nephropathy? Studies in patients with type 2 diabetes. *Diabetes*. 2003;52(4):1031–1035.
17. Griffin SV, Petermann AT, Durvasula RV, Shankland SJ. Podocyte proliferation and differentiation in glomerular disease: Role of cell-cycle regulatory proteins. *Nephrol Dial Transplant*. 2003;18(Suppl 6):vi8–13.
18. Wharram BL, Goyal M, Wiggins JE, et al. Podocyte depletion causes glomerulosclerosis: Diphtheria toxin-induced podocyte depletion in rats expressing human diphtheria toxin receptor transgene. *J Am Soc Nephrol*. 2005;16(10):2941–2952.
19. Shankland SJ, Pippin JW, Duffield JS. Progenitor cells and podocyte regeneration. *Semin Nephrol*. 2014;34(4):418–428.
20. Vogelmann SU, Nelson WJ, Myers BD, Lemley KV. Urinary excretion of viable podocytes in health and renal disease. *Am J Physiol Renal Physiol*. 2003;285(1):F40–48.
21. Petermann AT, Krofft R, Blonski M, et al. Podocytes that detach in experimental membranous nephropathy are viable. *Kidney Int*. 2003;64(4):1222–1231.
22. Susztak K, Raff AC, Schiffer M, Bottinger EP. Glucose-induced reactive oxygen species cause apoptosis of podocytes and podocyte depletion at the onset of diabetic nephropathy. *Diabetes*. 2006;55(1):225–233.
23. Eremina V, Quaggin SE. The role of VEGF-A in glomerular development and function. *Curr Opin Nephrol Hypertens*. 2004;13(1):9–15.
24. Fang L, Zhou Y, Cao H, et al. Autophagy attenuates diabetic glomerular damage through protection of hyperglycemia-induced podocyte injury. *PLoS One*. 2013;8(4):e60546.
25. Kriz W, Lemley KV. A potential role for mechanical forces in the detachment of podocytes and the progression of CKD. *J Am Soc Nephrol*. 2015;26(2):258–269.
26. Landau D, Israel E, Rivkis I, et al. The effect of growth hormone on the development of diabetic kidney disease in rats. *Nephrol Dial Transplant*. 2003;18(4):694–702.
27. Herbach N, Schairer I, Blutke A, et al. Diabetic kidney lesions of GIPRdn transgenic mice: Podocyte hypertrophy and thickening of the GBM precede glomerular hypertrophy and glomerulosclerosis. *Am J Physiol Renal Physiol*. 2009;296(4):F819–829.
28. Reddy GR, Pushpanathan MJ, Ransom RF, et al. Identification of the glomerular podocyte as a target for growth hormone action. *Endocrinology*. 2007;148(5):2045–2055.
29. Chitra PS, Swathi T, Sahay R, Reddy GB, Menon RK, Kumar PA. Growth hormone induces transforming growth factor-beta-induced protein in podocytes: Implications for podocyte depletion and proteinuria. *J Cell Biochem*. 2015;116(9):1947–1956.
30. Loeffler I, Wolf G. Epithelial-to-mesenchymal transition in diabetic nephropathy: Fact or fiction? *Cells*. 2015;4(4):631–652.
31. Dai HY, Zheng M, Tang RN, et al. Effects of angiotensin receptor blocker on phenotypic alterations of podocytes in early diabetic nephropathy. *Am J Med Sci*. 2011;341(3):207–214.
32. Yamaguchi Y, Iwano M, Suzuki D, et al. Epithelial-mesenchymal transition as a potential explanation for podocyte depletion in diabetic nephropathy. *Am J Kidney Dis*. 2009;54(4):653–664.
33. Merscher S, Fornoni A. Podocyte pathology and nephropathy: Sphingolipids in glomerular diseases. *Front Endocrinol (Lausanne)*. 2014;5:127.
34. Ishizawa S, Takahashi-Fujigasaki J, Kanazawa Y, et al. Sphingosine-1-phosphate induces differentiation of cultured renal tubular epithelial cells under Rho kinase activation via the S1P2 receptor. *Clin Exp Nephrol*. 2014;18(6):844–852.
35. Czyżewska-Buczyńska A, Konieczny A, Ryba M, et al. Zastosowanie nowych markerów wydalanych z moczem w diagnostyce wczesnego uszkodzenia nerek. *Diagn Lab*. 2013;49:239–245.

36. Yu D, Petermann A, Kunter U, Rong S, Shankland SJ, Floege J. Urinary podocyte loss is a more specific marker of ongoing glomerular damage than proteinuria. *J Am Soc Nephrol*. 2005;16(6):1733–1741.
37. Konieczny A, Czyzewska-Buczynska A, Ryba M, et al. Expression of cell membrane antigens in cells excreted in the urinary sediment predicts progression of renal disease in patients with focal segmental glomerulosclerosis. *Am J Nephrol*. 2015;42(1):35–41.
38. Hara M, Yamagata K, Tomino Y, et al. Urinary podocalyxin is an early marker for podocyte injury in patients with diabetes: Establishment of a highly sensitive ELISA to detect urinary podocalyxin. *Diabetologia*. 2012;55(11):2913–2919.
39. Wang G, Lai FM, Lai KB, et al. Intra-renal and urinary mRNA expression of podocyte-associated molecules for the estimation of glomerular podocyte loss. *Ren Fail*. 2010;32(3):372–379.
40. Wang G, Lai FM, Lai KB, Chow KM, Li KT, Szeto CC. Messenger RNA expression of podocyte-associated molecules in the urinary sediment of patients with diabetic nephropathy. *Nephron Clin Pract*. 2007;106(4):c169–179.
41. Rossing K, Mischak H, Dakna M, et al. Urinary proteomics in diabetes and CKD. *J Am Soc Nephrol*. 2008;19(7):1283–1290.
42. Zurbig P, Jerums G, Hovind P, et al. Urinary proteomics for early diagnosis in diabetic nephropathy. *Diabetes*. 2012;61(12):3304–3313.

Matrix metalloproteinase-3 in brain physiology and neurodegeneration

Anna Maria Lech[1,2,D–F], Grzegorz Wiera[2,D–F], Jerzy Władysław Mozrzymas[2,D–F]

[1] Department of Molecular Physiology and Neurobiology, University of Wrocław, Poland
[2] Laboratory of Neuroscience, Department of Biophysics, Wroclaw Medical University, Poland

A – research concept and design; B – collection and/or assembly of data; C – data analysis and interpretation;
D – writing the article; E – critical revision of the article; F – final approval of the article

Advances in Clinical and Experimental Medicine, ISSN 1899–5276 (print), ISSN 2451–2680 (online) *Adv Clin Exp Med*. 2019;28(12):1717–1722

Address for correspondence
Anna Maria Lech
E-mail: anna.lech@uwr.edu.pl

Funding sources
National Science Centre, Poland,
grant No. 2017/26/D/NZ4/00450

Conflict of interest
None declared

Received on January 28, 2019
Reviewed on February 28, 2019
Accepted on June 27, 2019

Published online on December 16, 2019

Abstract

Structural and functional synapse reorganization is one of the key issues of learning and memory mechanisms. Specific proteases, called matrix metalloproteinases (MMPs), play a pivotal role during learning-related modification of neural circuits. Different types of MMPs modify the extracellular perisynaptic environment, leading to the plastic changes in the synapses. In recent years, there has been an increasing interest in the role played by matrix metalloproteinase-3 (MMP-3) in various processes occurring in the mammalian brain, both in physiological and pathological conditions. In this review, we discuss a crucial function of MMP-3 in synaptic plasticity, learning, neuronal development, as well as in neuroregeneration. We discuss the involvement of MMP-3 in synaptic long-term potentiation, which is likely to have a profound impact on experience-dependent learning. On the other hand, we also provide examples of deleterious actions of uncontrolled MMP-3 activity on the central nervous system (CNS) and its contribution to Alzheimer's and Parkinson's diseases (AD and PD). Since the molecular mechanisms controlled by MMP-3 have a profound and diverse impact on physiological and pathological brain functioning, their deep understanding may be crucial for the development of more specific methods for the treatment of neuropsychiatric diseases.

Key words: neuroplasticity, MMP-3, neurodegenerative diseases, learning and memory, long-term potentiation

Cite as
Lech AM, Wiera G, Mozrzymas JW. Matrix metalloproteinase-3 in brain physiology and neurodegeneration. *Adv Clin Exp Med*. 2019;28 1717–1722. doi:10.17219/acem/110319

DOI
10.17219/acem/110319

Introduction

Learning and memory are contingent on a continuous modification of neural connectivity and circuitry by means of mechanisms that depend on network activity. This ability to change the synaptic strength in an experience-dependent manner is called synaptic plasticity and is considered as a substrate of learning, memory and behavior.[1] As a result of synaptic plasticity, the strength of synaptic transmission can be either enhanced or depressed. The plasticity that leads to the stable amplification of synaptic transmission is called long-term potentiation (LTP). Conversely, in the process of long-term depression (LTD) synaptic strength is reduced. Upon learning, both inhibitory and excitatory synapses undergo synaptic plasticity.[1] Furthermore, the balance between excitation and inhibition is a key feature in the proper functioning of the brain and the disruption in this dynamic "equilibrium" may underlie different neurological diseases such as autism[2,3]; schizophrenia[3] or epilepsy.[4]

Both structural and functional reorganization of the synapse starts to occur at early stages of central nervous system (CNS) development and continue to take place in the adult learning brain in the form of complex processes of neuroplasticity. It is well established that synapses are surrounded by a complex network of extracellular matrix (ECM) constituents,[5,6] including structural proteins, proteoglycans, glycosaminoglycans, adhesion molecules as well as growth factors. A growing body of experimental evidence suggests that diverse molecules in the ECM play crucial physiological roles in synaptogenesis,[7,8] synaptic plasticity[9,10] and regeneration of CNS after injury.[11] Moreover, the structure of brain ECM is not static as it is continuously remodeled, e.g., by proteolysis of ECM proteins that leads to the modifications in the synapse proteome and its interaction with the extracellular environment. Degradation of ECM proteins and peptides is catalyzed, in particular, by serine proteases (such as tPA or neuropsin) and matrix metalloproteinases (MMPs). In recent years, numerous studies described the crucial role played by MMPs-dependent ECM proteolysis in physiological processes such as synaptic plasticity, learning and memory.[12,13] Nonetheless, abnormal expression, localization and activity of MMPs could have a detrimental impact on brain functioning,[6,14,15] and, in physiological conditions, MMPs activity is kept under strict control at both the transcriptional and cellular levels by controlling the synthesis, release, activation, inhibition, and degradation.

The main purpose of this review is to discuss recent research into the matrix metalloproteinase-3 (MMP-3), one of the crucial brain proteases engaged both in physiological brain functions and in pathogenesis of neurological diseases. In the first section, we present a brief description of the MMP family. Then, we discuss the beneficial involvement of MMP-3 in key physiological and regenerative processes in CNS. We highlight the specific MMP-3-dependent proteolysis of ECM components and its role in development, synaptic plasticity, learning and memory, as well as in neuroregeneration after CNS injury. In the final chapter, we focus on the role of MMP-3 in pathophysiological conditions.

Matrix metalloproteinases and MMP-3

Matrix metalloproteinase-3 and, in general, MMPs have been identified as the major brain proteases affecting numerous processes. Because of the broad substrate spectrum, MMP-3 initially was considered primarily in relation to its role in pathophysiology. More recently, however, several physiological functions of this MMP have been revealed. Indeed, as we outline in the present review, MMP-3 plays a crucial role in the mammalian brain development, synaptic plasticity, learning, and memory.

Matrix metalloproteinases constitute a part of the larger family of proteases called metzincin clan. These multidomain, proteolytic enzymes, with a zinc ion (Zn^{2+}) in their catalytic site, can degrade ECM components, growth factors and adhesion molecules. Therefore, they are characterized by the ability to modify the extracellular environment and to modulate cell-to-cell signaling. In humans, MMP family consists of 24 distinct members, which are expressed either as soluble or transmembrane proteins.[16] Based on ECM substrate specificity and domain composition, MMPs are organized into 6 groups: collagenases, gelatinases, stromelysins, matrilysins, transmembrane MMPs, and "others".[16] Numerous studies have shown that the proteolytic activity of MMPs is extracellular, but their intracellular action was also suggested (MMP-3,[17] MMP-12[18]).

A number of studies have found that MMPs in CNS play a fundamental role in synaptic plasticity[19,20] and dendritic spine morphology.[21] Furthermore, MMPs are able to regulate cell proliferation and differentiation,[22] migration,[23] inflammation,[24] and apoptosis.[25,26] Thus, not surprisingly, MMPs are precisely controlled. In the CNS, MMPs are expressed and secreted both by neurons and glial cells[13] but their activity in normal conditions is low. The level of MMP activity significantly increases only in specific time windows, for example, during the induction of synaptic plasticity or repairing processes. Because MMPs are secreted mainly in their inactive form called zymogen, proMMPs in the extracellular space are inactive until the interaction between catalytic zinc ion and the cysteine residue at pro-peptide domain is disturbed. Matrix metalloproteinases can be activated by other proteases or, e.g., by reactive oxygen species (ROS). To block MMP activity, proteases are degraded or inhibited. Tissue inhibitors of metalloproteinases (TIMPs) bind noncovalently to MMP (in 1:1 ratio), which blocks its activity.

It has been shown that a precisely balanced level of TIMP activity is essential, as its alterations may lead to various pathologies, including different types of cancer.[27]

Matrix metalloproteinase-3 belongs to stromelysin group of MMPs. Numerous studies have shown that MMP-3 can function both extra- and intracellularly. Extracellularly, proMMP-3 may be activated by the serine proteinases like plasmin or other MMPs.[28] Matrix metalloproteinase-3 cleaves ECM components such as aggrecan, tenascins, fibronectin, laminin[29]; tumor necrosis factor α (TNF-α) precursor; interleukin 1b (IL-1b) and pro-forms of other MMPs like proMMP-1, proMMP-3 and proMMP-9.[29] As already mentioned, MMP-3 proteolytic activity was also reported inside the cells. Choi et al. described proMMP-3 activation inside the dopaminergic neurons that undergo cellular stress, in which pro-MMP-3 zymogen was activated by serine proteases.[25] Furthermore, there are several studies showing that exogenous MMP-3 can enter the cytoplasm, probably through clathrin-dependent endocytosis,[30] and may even translocate into the nucleus.[17,31] The proper balance of MMP-3 activity is regulated by TIMP-1 and altered MMP-3 activity connected with lower level of TIMP-1 plays an important role, e.g., in neuronal apoptosis during oxidative stress.[32]

Matrix metalloproteinase-3 in the developing CNS

Among others, Vaillant et al. described increased expression of MMP-3 and MMP-9 in dividing granular precursor cells in the developing cerebellum.[33] During this period MMP-3 and other MMPs are crucial for cell migration and neurite outgrowth through the degradation or activation of cell surface proteins and ECM components.[33] Moreover, MMP-3 has also been shown to play a crucial role in dendritogenesis. Reduction in dendritic tree size of Purkinje cells in the cerebellum was described both in postnatal, juvenile and adult *mmp-3*-deficient mice (MMP-3$^{-/-}$).[34] These findings can be explained by the interaction of MMP-3 with repellent or attractive signaling molecules in the extracellular environment. Likewise, studies conducted on MMP-3-deficient mice shed light on the effects of MMP-3 on the morphology of pyramidal neurons in cortex and hippocampus. The Golgi-stained MMP-3$^{-/-}$ pyramidal cells from layer V of the visual cortex exhibit significantly shorter apical dendrites compared to the wild-type controls.[35] On the contrary, Nowak et al. have shown that there are no significant differences between morphology of MMP-3$^{-/-}$ pyramidal neurons in the CA1 hippocampal field in comparison to the wild-type group.[36] Collectively, these studies suggest that the functioning of the MMP-3 in developing CNS is more complex and may depend on the region of the brain.

Matrix metalloproteinase-3 in synaptic plasticity, learning and memory

The architecture of the synapse is determined by both cell–cell and cell–ECM interactions. The coordinated, activity-dependent remodeling of the perisynaptic extracellular environment regulates synaptic transmission and synaptic plasticity.[14] Over the past decade or so, the growing body of evidence has indicated that MMP-9 is a key player in neuroplasticity mechanisms. Although the functioning of MMP-9 in neural circuits has been extensively described,[19,37] more recent works also highlighted the impact of MMP-3 on CNS plasticity. In the hippocampal Schaffer collaterals-CA1 pathway, one can distinguish 2 different LTP components: 1) dependent on NMDA receptors (nmdaLTP); 2) dependent on L-type voltage-dependent Ca^{2+} channels (VDCCs, vdccLTP). In 2002, Evers et al. have described an impairment of vdccLTP in the hippocampus of tenascin-C deficient mice.[10] Because tenascin-C is a well-known MMP-3 substrate,[38] it may suggest the involvement of MMP-3 in vdccLTP. Additionally, Kochlamazashvili et al. demonstrated that vdccLTP is dependent on the presence of hyaluronic acid in ECM in the vicinity of synapses, because enzymatic digestion of hyaluronan impaired specifically vdccLTP.[39] These results reveal a new "dimension" of the synaptic plasticity, namely that enzymatic modification (such as proteolysis) of ECM constituents plays a pivotal role in regulating plastic phenomena at a variety of synapses. Moreover, recent studies have confirmed that MMP-3 activity is indeed crucial in regulating vdcc-dependent form of LTP in hippocampus, but not for nmdaLTP (that is regulated, e.g., by MMP-9).[13] Nevertheless, there is also some evidence that MMP-3 can affect NMDA receptors. In cultured spinal cord neurons, chronic NMDAR overstimulation leads to an increase in MMP-3 activity which, in turn, cleaves GluN1 subunit of NMDA receptor to constrain calcium influx and prevent neuron apoptosis.[40] The activity of MMP-3 is also crucial for the plasticity of neuronal excitability. Brzdak et al.[41] have suggested that potentiation of neuronal spiking requires short-term activation of MMP-3, which, in turn, increases calcium influx into neurons through NMDA receptors. Additionally, Brzdak et al. clearly demonstrated that MMP-3 activity differs between basal and apical dendrites of pyramidal neurons from the CA1 region of the hippocampus and the plasticity of synapses located in apical dendrites are MMP-3-dependent in contrast to those in basal dendrites.[42] Finally, contrary to LTP, the role of MMP-3 on LTD is still unknown.

The impact of MMP-3 on learning and memory has not been studied in detail. There is limited evidence that during hippocampus-dependent learning (e.g., in Morris water maze), the level of MMP-3 activity and mRNA are increased

within the first days after experiment.[43] This could indicate that a higher level of MMP-3 as well as MMP-9 is important over a relatively short period, in which plasticity phenomena are induced. So far, however, the exact role of MMP-3 in learning remains unknown. To understand the broader aspect of MMP-3 functioning in behavior, experiments using MMP-3$^{-/-}$ mice are necessary. Although the physiological role of MMP-3 still awaits a thorough and extensive investigation, the available evidence points to its key role in neural plasticity and development.

Matrix metalloproteinase-3 in CNS after injury

Several studies have reported the involvement of MMP-3 in neurite outgrowth and remyelinisation. Gonthier et al. have noted that MMP-3 can be engaged in the elongation of axons in response to specific attractor molecules.[44] More recent studies have reported that MMP-3 as well as others MMPs can overcome chondroitin sulphate proteoglycans (CSPGs)-dependent inhibition of neurite regeneration.[45] Chondroitin sulphate proteoglycans are produced and secreted during glial scar formation to effectively slow down or even block the axonal regeneration. Importantly, almost all CSPGs constituents are putative substrates of MMP-3. Cua et al. have observed that local expression of MMP-3 in the vicinity of glial scar is increased and MMP-3 activity promotes axonal outgrowth.[45] Furthermore, a few years earlier Pizzi and Crowe have reported that the application of fibroblasts overexpressing MMP-3 into the injured spinal cord augments axon regrowth.[46] They have additionally observed transient progression in motor functions recovery, what could have been related to axonal regeneration. Another aspect of beneficial functions of MMP-3 is related to remyelination. Cuprizone-induced demyelination is the most often examined model in which remyelination process can be assessed. Immunohistochemical investigation showed a significant increase in the expression level of MMP-3 during remyelination in the corpus callosum induced by cuprizone.[47] Altogether, these studies provide important insights into the protective roles played by the MMP-3 activity after injury and are likely to indicate promising avenues for future therapeutic developments.

The role of MMP-3 in neuronal pathologies

Besides crucial role played by MMP-3 in brain physiology, its excessive uncontrolled activity often correlates with numerous neurodegenerative disorders. In several pathologies, MMP-3 appears to have a causative role, which may be related to the disruption of the blood–brain barrier (BBB), role in demyelination, cell apoptosis or initiation of the inflammatory response. In subsequent sections, we describe the role played by MMP-3 in the pathophysiology of Alzheimer's and Parkinson's diseases (AD and PD).

MMP-3 in Parkinson's disease

Numerous reports indicate the involvement of MMP-3 in the pathophysiology of PD, which is characterized by a progressive loss of dopaminergic neurons in the *substantia nigra* of the midbrain, leading to cognitive and motor disorders. The increase in the level of MMP-3 protein and activity has been observed in various experimental models of PD such as in animals injected with 6-hydroxydopamine or lipopolysaccharide.[48] In the case of MPTP (1-methyl-4-phenyl-1,2,3,6-tetrahydropyridine)-induced PD, a significant reduction in the degeneration of the *substantia nigra* neurons has been observed in mice deficient in MMP-3 compared to wild-type controls.[49] Similarly, studies on tissue cultures also have shown that cell death of dopaminergic neurons may be limited by inhibition of MMP-3 or by MMP-3 knock-out.[50] *Substantia nigra* is particularly rich in microglial cells; therefore, the role of MMP-3 in the pathophysiology of PD may be related to the activation of microglia and inflammatory processes in response to cellular stress.[51] Additionally, changes in the permeability of the blood–brain barrier were observed both in PD patients and in animal PD models.[52] Tight junction proteins are among MMP-3 putative substrates, thus the MMP-3-dependent increase in BBB permeability is considered as one of PD pathomechanisms.

Additionally, it is also worth noting that cellular proteins whose mutations correlates with PD are also MMP-3 substrates. The dysfunction of α-synuclein, which is a component of Lewy bodies, is a well-known player in PD pathogenesis. Matrix metalloproteinase-3 cleaves the C-terminal part of α-synuclein, exposing a hydrophobic patch on the protein surface, which contributes to the increased formation of protein aggregates.[51] It has also been shown that mutations in the α-synuclein, which are associated with early onset of PD, lead to an increased occurrence of α-synuclein in Lewy bodies. This, in turn, suggests that the mutant protein may be more prone to proteolysis mediated by MMP-3. Another aspect of MMP-3 engagement in PD pathogenesis is related to protein DJ-1 that protects from oxidative proteasomal and mitochondrial stress. Mutations in DJ-1 protein and its loss of activity have been observed in PD patients. Therefore, because DJ-1 is a substrate for MMP-3, the decreased activity of DJ-1 in PD may be a result of increased uncontrolled MMP-3 proteolytic activity.[53] In conclusion, the role of MMP-3 in the pathophysiology of PD is manifested through the contribution of protease to the formation of α-synuclein aggregates and by the interference of the MMP-3 protease with the protective functions of DJ-1 protein against oxidative stress.

MMP-3 in Alzheimer's disease

Matrix metalloproteinase-3 contributes also to the development of AD, which is one of the most common neurodegenerative disorders and the main cause of dementia. The main characteristic features of AD are a widespread degeneration of neurons, the formation of so-called plaques that contain amyloid-β (Aβ) peptide and deposition of neurofibrillary tangles abnormally rich in hyperphosphorylated tau protein.[14] Amyloid-β is the product of proteolytic cleavage of amyloid precursor protein (APP). The involvement of MMP-3 in AD pathogenesis is complex. Firstly, it was shown that patients suffering from AD have an elevated level of MMP-3 in the brain, especially in the white matter and senile plaques.[54] It is suggested that the expression of MMP-3 in microglial cells and astrocytes can be induced by the Aβ peptide.[55] Secondly, the analysis of *mmp-3* gene polymorphisms has linked the 6A allele of the *mmp-3* gene promoter (-1612 5A/6A) to the higher susceptibility to AD.[56] This result was; however, contested by others.[57] Finally, it was reported that in the human cerebrospinal fluid the reduction of MMP-3 level goes hand in hand with a lower level of Aβ.[58] Additionally, in patients with risk markers for AD, a higher MMP-3 levels and a higher MMP-3/TIMP-1 ratio were reported in comparison to those without risk markers.[59] Moreover, it was proposed that MMP-3 plasma levels could be a biomarker for early diagnosis of AD.[60]

Conclusions

The examples discussed above underscore many roles played by MMP-3 in the developing and adult CNS. Although, over the years, more attention has been directed to the function of MMP-3 in pathophysiological processes, recent research suggests that, in the hippocampus and cortex, MMP-3 regulates also synaptic plasticity and takes part in the processes of CNS recovery after injury. In particular, the activation of MMP-3 is essential for the induction of long-term potentiation dependent on voltage-gated calcium channels.[10,13,41] Additionally, plastic changes at synapses correlate with short-term window of MMP-3 activity in hippocampus.[43] Consistently, the activity of MMP-3 is also important in the developing brain,[33] and has been shown to play a pivotal role in the dendritogenesis of pyramidal neurons in the cortex and Purkinje cells in the cerebellum.[34]

On the other hand, uncontrolled MMP-3 activity is often associated with neurodegenerative disorders. As was mentioned before, numerous authors described the involvement of MMP-3 in PD and AD. Matrix metalloproteinase-3 has been found to be engaged in the pathological process of dopaminergic neurons loss in the *substantia nigra*.[49] In addition, MMP-3 contributes to the increased formation of α-synuclein aggregates in PD patients.[52] In the same way, recent research reported an elevated level of MMP-3 in brains of AD patients,[55,56,60] and proposed the use of MMP-3 as a promising biomarker for AD diagnosis.[60] Taking into consideration the involvement of excessive MMP-3 activity in CNS pathophysiology, the MMP-3 inhibitors may have potential clinical applications. Overall, it should be noted that increasing our knowledge about precise brain molecular mechanisms dependent on MMP-3 and its specific substrates can consequently lead to the development of new methods for the treatment of PD and AD.

ORCID iDs

Anna Maria Lech https://orcid.org/0000-0001-8550-4803
Grzegorz Wiera https://orcid.org/0000-0003-2489-4451
Jerzy Władysław Mozrzymas https://orcid.org/0000-0003-1674-1818

References

1. Citri A, Malenka RC. Synaptic plasticity: Multiple forms, functions, and mechanisms. *Neuropsychopharmacology.* 2008;33(1):18–41.
2. Uzunova G, Pallanti S, Hollander E. Excitatory/inhibitory imbalance in autism spectrum disorders: Implications for interventions and therapeutics. *World J Biol Psychiatry.* 2016;17(3):174–186.
3. Canitano R, Pallagrosi M. Autism spectrum disorders and schizophrenia spectrum disorders: Excitation/inhibition imbalance and developmental trajectories. *Front Psychiatry.* 2017;8:1–7.
4. Buckley AH, Holmes GL. Epilepsy and autism. *Cold Spring Harb Perspect Med.* 2016;6(4):a022749.
5. Dityatev A, Schachner M. Extracellular matrix molecules and synaptic plasticity. *Nat Rev Neurosci.* 2003;4(6):456–468.
6. Huntley GW. Synaptic circuit remodelling by matrix metalloproteinases in health and disease. *Nat Rev Neurosci.* 2012;13(11):743–757.
7. Allen NJ, Bennett ML, Foo LC, et al. Astrocyte glypicans 4 and 6 promote formation of excitatory synapses via GluA1 AMPA receptors. *Nature.* 2012;486(7403):410–414.
8. Dityatev A. Polysialylated neural cell adhesion molecule promotes remodeling and formation of hippocampal synapses. *J Neurosci.* 2004;24(42):9372–9382.
9. Albiñana E, Gutierrez-Luengo J, Hernández-Juarez N, et al. Chondroitin sulfate induces depression of synaptic transmission and modulation of neuronal plasticity in rat hippocampal slices. *Neural Plast.* 2015;2015:463854.
10. Evers MR, Salmen B, Bukalo O, et al. Impairment of L-type Ca2 channel-dependent forms of hippocampal synaptic plasticity in mice deficient in the extracellular matrix glycoprotein tenascin-C. *J Neurosci.* 2002;22(16):7117–7194.
11. Wang D, Ichiyama RM, Zhao R, Andrews MR, Fawcett JW. Chondroitinase combined with rehabilitation promotes recovery of forelimb function in rats with chronic spinal cord injury. *J Neurosci.* 2011;31(25):9332–9344.
12. Al-Muhtasib N, Forcelli PA, Conant KE, Vicini S. MMP-1 overexpression selectively alters inhibition in D1 spiny projection neurons in the mouse nucleus accumbens core. *Sci Rep.* 2018;8(1):16230.
13. Wiera G, Nowak D, van Hove I, Dziegiel P, Moons L, Mozrzymas JW. Mechanisms of NMDA receptor- and voltage-gated L-type calcium channel-dependent hippocampal LTP critically rely on proteolysis that is mediated by distinct metalloproteinases. *J Neurosci.* 2017;37(5):1240–1256.
14. Brzdak P, Nowak D, Wiera G, Mozrzymas JW. Multifaceted roles of metzincins in CNS physiology and pathology: From synaptic plasticity and cognition to neurodegenerative disorders. *Front Cell Neurosci.* 2017;11:1–22.
15. Dubey D, McRae PA, Rankin-Gee EK, et al. Increased metalloproteinase activity in the hippocampus following status epilepticus. *Epilepsy Res.* 2017;132:50–58.
16. Nagase H, Visse R, Murphy G. Structure and function of matrix metalloproteinases and TIMPs. *Cardiovasc Res.* 2006;69(3):562–573.

17. Si-Tayeb K, Monvoisin A, Mazzocco C, et al. Matrix metalloproteinase 3 is present in the cell nucleus and is involved in apoptosis. *Am J Pathol.* 2006;169(4):1390–1401.
18. Dandachi NG, Shapiro SD. A protean protease: MMP-12 fights viruses as a protease and a transcription factor. *Nat Med.* 2014;20(5):470–472.
19. Nagy V. Matrix metalloproteinase-9 is required for hippocampal late-phase long-term potentiation and memory. *J Neurosci.* 2006;26(7): 1923–1934.
20. Brzdąk P, Włodarczyk J, Mozrzymas JW, Wójtowicz T. Matrix metalloprotease 3 activity supports hippocampal EPSP-to-Spike plasticity following patterned neuronal activity via the regulation of NMDAR function and calcium flux. *Mol Neurobiol.* 2017;54(1):804–816.
21. Magnowska M, Gorkiewicz T, Suska A, et al. Transient ECM protease activity promotes synaptic plasticity. *Sci Rep.* 2016;6:27757.
22. Valente MM, Allen M, Bortolotto V, Lim ST, Conant K, Grilli M. The MMP-1/PAR-1 axis enhances proliferation and neuronal differentiation of adult hippocampal neural progenitor cells. *Neural Plast.* 2015;2015:646595.
23. Endo K, Takino T, Miyamori H, et al. Cleavage of syndecan-1 by membrane type matrix metalloproteinase-1 stimulates cell migration. *J Biol Chem.* 2003;278(42):40764–40770.
24. Marchant DJ, Bellac CL, Moraes TJ, et al. A new transcriptional role for matrix metalloproteinase-12 in antiviral immunity. *Nat Med.* 2014; 20(5):493–502.
25. Choi DH, Kim E-M, Son HJ, et al. A novel intracellular role of matrix metalloproteinase-3 during apoptosis of dopaminergic cells. *J Neurochem.* 2008;106(1):405–415.
26. Biswas MHU, Almeida S, Lopez-Gonzalez R, et al. MMP-9 and MMP-2 contribute to neuronal cell death in iPSC models of frontotemporal dementia with MAPT mutations. *Stem Cell Rep.* 2016;7(3):316–324.
27. Jackson HW, Defamie V, Waterhouse P, Khokha R. TIMPs: Versatile extracellular regulators in cancer. *Nat Rev Cancer.* 2017;17(1):38–53.
28. Nagase H, Enghild JJ, Suzuki K, Salvesen G. Stepwise activation mechanisms of the precursor of matrix metalloproteinase 3 (stromelysin) by proteinases and (4-aminophenyl)mercuric acetate. *Biochemistry.* 1990;29(24):5783–5789.
29. Nagase H, Fields CG, Fields GB. Design and characterization of a fluorogenic substrate selectively hydrolyzed by stromelysin 1 (matrix metalloproteinase-3). *J Biol Chem.* 1994;269(33):20952–20957.
30. Traub LM. Tickets to ride: Selecting cargo for clathrin-regulated internalization. *Nat Rev Mol Cell Biol.* 2009;10(9):583–596.
31. Eguchi T, Kubota S, Kawata K, et al. Novel transcription factor-like function of human matrix metalloproteinase 3 regulating the CTGF/CCN2 gene. *Mol Cell Biol.* 2008;28(7):2391–2413.
32. Choi D-H, Kim J-H, Seo J-H, Lee J, Choi WS, Kim Y-S. Matrix metalloproteinase-3 causes dopaminergic neuronal death through nox1-regenerated oxidative stress. *PLoS One.* 2014;9(12):e115954.
33. Vaillant C, Didier-Bazès M, Hutter A, Belin M-F, Thomasset N. Spatiotemporal expression patterns of metalloproteinases and their inhibitors in the postnatal developing rat cerebellum. *J Neurosci.* 1999; 19(12):4994–5004.
34. Van Hove I, Verslegers M, Buyens T, et al. An aberrant cerebellar development in mice lacking matrix metalloproteinase-3. *Mol Neurobiol.* 2012;45(1):17–29.
35. Aerts J, Nys J, Moons L, Hu T-T, Arckens L. Altered neuronal architecture and plasticity in the visual cortex of adult MMP-3-deficient mice. *Brain Struct Funct.* 2015;220(5):2675–2689.
36. Nowak D, De Groef L, Moons L, Mozrzymas JW. MMP-3 deficiency does not influence the length and number of CA1 dendrites of hippocampus of adult mice. *Acta Neurobiol Exp (Wars).* 2018;78(3):281–286.
37. Wiera G, Wozniak G, Bajor M, Kaczmarek L, Mozrzymas JW. Maintenance of long-term potentiation in hippocampal mossy fiber-CA3 pathway requires fine-tuned MMP-9 proteolytic activity. *Hippocampus.* 2013;23(6):529–543.
38. Imai K, Kusakabe M, Sakakura T, Nakanishi I, Okada Y. Susceptibility of tenascin to degradation by matrix metalloproteinases and serine proteinases. *FEBS Lett.* 1994;352(2):216–218.
39. Kochlamazashvili G, Henneberger C, Bukalo O, et al. The extracellular matrix molecule hyaluronic acid regulates hippocampal synaptic plasticity by modulating postsynaptic L-type Ca2+channels. *Neuron.* 2010;67(1):116–128.
40. Pauly T, Ratliff M, Pietrowski E, et al. Activity-dependent shedding of the NMDA receptor glycine binding site by matrix metalloproteinase 3: A putative mechanism of postsynaptic plasticity. *PLoS One.* 2008;3:e2681.
41. Brzdak P, Włodarczyk J, Mozrzymas JW, Wójtowicz T. Matrix metalloprotease 3 activity supports hippocampal EPSP-to-spike plasticity following patterned neuronal activity via the regulation of NMDAR function and calcium flux. *Mol Neurobiol.* 2017;54(1):804–816.
42. Brzdak P, Wójcicka O, Zareba-Koziol M, et al. Synaptic potentiation at basal and apical dendrites of hippocampal pyramidal neurons involves activation of a distinct set of extracellular and intracellular molecular cues. *Cereb Cortex.* 2019;29(1):283–304.
43. Meighan SE, Meighan PC, Choudhury P, et al. Effects of extracellular matrix-degrading proteases matrix metalloproteinases 3 and 9 on spatial learning and synaptic plasticity. *J Neurochem.* 2006;96: 1227–1241.
44. Gonthier B, Nasarre C, Roth L, et al. Functional interaction between matrix metalloproteinase-3 and semaphorin-3C during cortical axonal growth and guidance. *Cereb Cortex.* 2007;17:1712–1721.
45. Cua RC, Lau LW, Keough MB, Midha R, Apte SS, Yong VW. Overcoming neurite-inhibitory chondroitin sulfate proteoglycans in the astrocyte matrix. *Glia.* 2013;61:972–984.
46. Pizzi MA, Crowe MJ. Transplantation of fibroblasts that overexpress matrix metalloproteinase-3 into the site of spinal cord injury in rats. *J Neurotrauma.* 2006;23:1750–1765.
47. Hoyos HC, Marder M, Ulrich R, et al. The role of galectin-3: From oligodendroglial differentiation and myelination to demyelination and remyelination processes in a cuprizone-induced demyelination model. *Adv Exp Med Biol.* 2016;949:311–332.
48. McClain JA, Phillips LL, Fillmore HL. Increased MMP-3 and CTGF expression during lipopolysaccharide-induced dopaminergic neurodegeneration. *Neurosci Lett.* 2009;460(1):27–31.
49. Kim YS, Choi DH, Block ML, et al. A pivotal role of matrix metalloproteinase-3 activity in dopaminergic neuronal degeneration via microglial activation. *FASEB J.* 2007;21(1):179–187.
50. Choi DH, Kim EM, Son HJ, et al. A novel intracellular role of matrix metalloproteinase-3 during apoptosis of dopaminergic cells. *J Neurochem.* 2008;106(1):405–415.
51. Kim EM, Hwang O. Role of matrix metalloproteinase-3 in neurodegeneration. *J Neurochem.* 2011;116(1):22–32.
52. Kortekaas R, Leenders KL, van Oostrom JC, et al. Blood-brain barrier dysfunction in parkinsonian midbrain in vivo. *Ann Neurol.* 2005;57(2): 176–179.
53. Choi DH, Kim YJ, Kim YG, Joh TH, Beal MF, Kim YS. Role of matrix metalloproteinase 3-mediated alpha-synuclein cleavage in dopaminergic cell death. *J Biol Chem.* 2011;286(16):14168–14177.
54. Yoshiyama Y, Asahina M, Hattori T. Selective distribution of matrix metalloproteinase-3 (MMP-3) in Alzheimer's disease brain. *Acta Neuropathol.* 2000;99(2):91–95.
55. Deb S, Gottschall PE. Increased production of matrix metalloproteinases in enriched astrocyte and mixed hippocampal cultures treated with beta-amyloid peptides. *J Neurochem.* 1996;66(4):1641–1647.
56. Baig S, Kehoe PG, Love S. MMP-2, -3 and -9 levels and activity are not related to Abeta load in the frontal cortex in Alzheimer's disease. *Neuropathol Appl Neurobiol.* 2008;34(2):205–215.
57. Reitz C, van Rooij FJ, de Maat MP, et al. Matrix metalloproteinase 3 haplotypes and dementia and Alzheimer's disease. The Rotterdam Study. *Neurobiol Aging.* 2008;29(6):874–881.
58. Mlekusch R, Humpel C. Matrix metalloproteinases-2 and -3 are reduced in cerebrospinal fluid with low beta-amyloid1-42 levels. *Neurosci Lett.* 2009;466(3):135–138.
59. Stomrud E, Björkqvist M, Janciauskiene S, Minthon L, Hansson O. Alterations of matrix metalloproteinases in the healthy elderly with increased risk of prodromal Alzheimer's disease. *Alzheimers Res Ther.* 2010;2(3):20–20.
60. Peng M, Jia J, Qin W. Plasma gelsolin and matrix metalloproteinase 3 as potential biomarkers for Alzheimer disease. *Neurosci Lett.* 2015; 595:116–121.

Annual Contents

No. 1 (January)

Original papers

Reviews

No. 2 (February)

Original papers

Reviews

No. 3 (March)

Original papers

Reviews

Letter to the Editor

No. 4 (April)

Original papers

Reviews

No. 5 (May)

Original papers

No. 6 (June)

Original papers

Reviews

No. 7 (July)

Original papers

Reviews

No. 8 (August)

Original papers

Reviews

No. 9 (September)

Original papers

Reviews

No. 10 (October)

Original papers

No. 11 (November)

Original papers

Reviews

No. 12 (December)

Original papers

Reviews

Index of Authors